



**HAL**  
open science

# Impact of control strategies of hybrid heat pumps on the greenhouse gases emissions for space heating and domestic hot water production

Marianne Biéron

## ► To cite this version:

Marianne Biéron. Impact of control strategies of hybrid heat pumps on the greenhouse gases emissions for space heating and domestic hot water production. Thermics [physics.class-ph]. Université de La Rochelle, 2024. English. NNT: 2024LAROS008 . tel-04906693

**HAL Id: tel-04906693**

**<https://theses.hal.science/tel-04906693v1>**

Submitted on 22 Jan 2025

**HAL** is a multi-disciplinary open access archive for the deposit and dissemination of scientific research documents, whether they are published or not. The documents may come from teaching and research institutions in France or abroad, or from public or private research centers.

L'archive ouverte pluridisciplinaire **HAL**, est destinée au dépôt et à la diffusion de documents scientifiques de niveau recherche, publiés ou non, émanant des établissements d'enseignement et de recherche français ou étrangers, des laboratoires publics ou privés.



LA ROCHELLE UNIVERSITE

ÉCOLE DOCTORALE EUCLIDE (618)

Laboratoire LaSIE (UMR CNRS 7356)

THÈSE

présentée par :

Marianne BIERON

soutenue le 11 janvier 2024

pour l'obtention du grade de Docteur de La Rochelle Université

Discipline : Energétique et thermique

**Impact of control strategies of hybrid heat pumps on the GHG emissions for space heating and domestic hot water production**

JURY :

Christian INARD  
Laurent MORA  
Robin GIRARD  
Jérôme LE DREAU  
Monica SIROUX  
Charlotte ROUX

Professeur, La Rochelle Université, Président du jury  
Professeur, IUT de Bordeaux, Rapporteur  
Maître de conférences HDR, MINES Paris PSL, Rapporteur  
Maître de conférences, La Rochelle Université, Directeur de thèse  
Professeur, INSA Strasbourg  
Maître de conférences, ARMINES

INVITE :

Benjamin HAAS

Ingénieur de recherche, ENGIE

## **Acknowledgements**

## Abstract

In France, space heating emits 75 million tons of CO<sub>2</sub> annually, accounting for approximately 15% of total emissions. Hybrid heat pumps (heat pumps coupled with gas boilers) can facilitate the integration of non-dispatchable renewable energies into the power grid and avoid greenhouse gas (GHG) emissions from carbonized electricity production by providing demand-side flexibility without any service interruption. The aim of this thesis was to develop a control strategy for a fleet of hybrid heat pumps to reduce the French GHG emissions for space heating and domestic hot water production. In a first part, a model of the French power system was developed to assess the marginal emission factor of the electricity consumption. The model is based on two calibrated merit-orders to reproduce the daily and intra-daily dynamics and includes the conservation of hydroelectric energy and cross-border exchanges. In addition, the marginal emission factor of the electricity generation in the other European countries was evaluated by linear regression between the hourly variation of the GHG emission and of the dispatchable electricity generation. In a second part, the electricity and gas consumption of a fleet of 3000 hybrid heat pumps, heating 100 000 dwellings spread throughout France was evaluated. A Modelica-model of a district archetype of 300 dwellings was simulated in seven cities representative of the French climatic zones to obtain the national heating demand. The hybrid production, storage and distribution systems were modelled at the building level. Finally, two control strategies and four sizing of the heat pumps (120%, 50%, 35% and 20%) were evaluated. Between July 2018 and June 2019, a strategy prioritizing the heat pumps would have avoided between 8 000 and 26 000 t<sub>CO<sub>2</sub>eq</sub> of GHG emissions. A strategy switching between the heat pump and the boiler based on the marginal emission factor of the electricity consumption would have avoided around 38 000 t<sub>CO<sub>2</sub>eq</sub>, with a limited influence of the sizing of the heat pump.

**Keywords:** Hybrid heat pumps, Fuel switch, Marginal emission factor, Unit-Commitment and Economic Dispatch, Demand Side Management, Space heating, Domestic Hot Water, UBEM

## Résumé

En France, le chauffage émet 75 millions de tonnes de CO<sub>2</sub> par an, ce qui représente environ 15 % des émissions totales. Les pompes à chaleur hybrides (pompes à chaleur couplées à des chaudières gaz) peuvent faciliter l'intégration des énergies renouvelables non pilotables dans le système électrique et éviter les émissions de gaz à effet de serre liées à la production d'électricité carbonée en fournissant un effacement de la consommation électrique tout en maintenant le chauffage. L'objectif de cette thèse est de développer une stratégie de contrôle pour un parc de pompes à chaleur hybrides afin de réduire les émissions de gaz à effet de serre françaises liées au chauffage et à la production d'eau chaude sanitaire des. Dans une première partie, un modèle du système électrique français a été développé pour évaluer le facteur d'émission marginal de la consommation d'électricité. Le modèle est basé sur deux merit-orders calibrés pour reproduire les dynamiques journalières et intra-journalières et inclut la conservation de l'énergie hydroélectrique et les échanges transfrontaliers. En outre, le facteur d'émission marginal de la production d'électricité dans les autres pays européens a été évalué par régression linéaire entre la variation horaire des émissions de gaz à effet de serre et de la production d'électricité pilotable. Dans une deuxième partie, la consommation d'électricité et de gaz d'un parc de 3000 pompes à chaleur hybrides, chauffant 100 000 logements répartis dans toute la France, a été évaluée. Un modèle Modelica d'un archétype de quartier de 300 logements a été simulé dans sept villes représentatives des zones climatiques françaises pour obtenir la demande nationale de chauffage. Les systèmes hybrides de production, de stockage et de distribution ont été modélisés au niveau du bâtiment. Enfin, deux stratégies de contrôle et quatre dimensionnements des pompes à chaleur (120%, 50%, 35% et 20% du dimensionnement du système hybride) ont été évalués. Entre juillet 2018 et juin 2019, une stratégie privilégiant les pompes à chaleur aurait permis d'éviter entre 8 000 et 26 000 tCO<sub>2</sub>eq d'émissions de GES. Une stratégie activant alternativement les pompes à chaleur ou les chaudières en fonction du facteur d'émission marginal de la consommation d'électricité aurait permis d'éviter environ 38 000 tCO<sub>2</sub>eq, le dimensionnement de la pompe à chaleur ayant un impact très faible sur ce résultat.

**Mots-clés :** Pompes à chaleur hybrides, Fuel switch, Facteur d'émission marginal, Unit-Commitment and Economic Dispatch, Gestion active de la demande, Chauffage, Eau chaude sanitaire, Modélisation énergétique quartier

# Nomenclature

## Acronyms

TSO	Transmission System Operator
CCGT	Combined Cycle Gas Turbine
OCGT	Open Cycle Gas Turbine
CHP	Combined Heat and Power
LCA	Life Cycle Assessment
UCED	Unit-Commitment and Economic Dispatch
MEF	Marginal Emission Factor
RC	Residual consumption
DR	Demand Response
DSM	Demand Side Management
NTC	Net transfer Capacity
RMSE	Root Mean square error
R	Correlation coefficient
HP	Heat pump
DHW	Domestic hot water
GB	Gas boiler
SH	Space heating

## Latin letters

Symbol	Definition
1/2d	Half-day
1/2h	Half-hour
A	Surface (m <sup>2</sup> )
C	French consumption (MW)
c	Coefficient for the evaluation of the DHW demand
C <sub>p</sub>	Thermal capacity of the water (J/(kg.K))
d	Day
E	Energy (MWh)
EF	Emission factor (t <sub>co2</sub> /MWh)
exch	Electricity exchanges considered as a technology (MW)
fr	Fraction of radiative heat transfer from the total heat transferred
GHG	GHG emissions (t <sub>co2</sub> )
glazed ratio	Glazed ration of the outside walls
gr	Group (elements from L <sub>gr</sub> )
H	Solar irradiation (W)
h	Heating value (MJ/kg)

HL	Heat losses (W)
hydro	Dispatchable hydroelectric powerplants
indic1(gr)	Indicator setting the position of the group gr in the merit-order MO1
indic2(gr)	Indicator setting the position of the group gr in the merit-order MO2
int	Intercept evaluated after a linear regression
Losses	Losses on the power grid (%)
$\dot{m}$	Mass flow rate (kg/s)
ME	Marginal emissions ( $t_{CO_2}$ )
MEF	Marginal emission factor ( $t_{CO_2}/MWh$ )
mix	Vector of the generation level P of each technology (W)
$n_{gr}$	Length of the list $L_{gr}$
$N_s$	Number of standard dwellings
NTC	Net Transfer Capacity (W)
P	Generated power (W or MW)
Q	Absorbed radiation (W)
q	Air change rate (vol/h)
r	Ratio (between 0 and 1)
RC	Residual Consumption (WM)
RC	Average residual consumption (W)
Rcremain	Remaining power to dispatch or commit during UCED (W)
sl	Slope evaluated after a linear regression
SOC	State of charge of the DHW tank (%)
surf	Surfaces of the dwelling ( $m^2$ )
t	Time (s)
T	Transmitivity
tech	Technology (elements from $L_{tech}$ )
th	Thickness of the material (m)
U	Heat loss coefficient ( $W/(m^2.K)$ )
UA	UA-value ( $W/(m^2.K)$ )
V	Volum ( $m^3$ )
$\gamma$	Load factor (firing rate of the boiler or normalized speed compressor of the heat pump) (between 0 and 1)

### Greek letters

Symbol	Definition
$\alpha$	Thermal diffusivity
$\vartheta$	Temperature ( $^{\circ}C$ )
$\varepsilon$	Emissivity
$\eta$	Efficiency (%)

$\Delta$	Variations
$\rho$	Density of the water (kg/m <sup>3</sup> )

### Subscripts, exponents and indices

Symbol	Definition
7-35	Operating point of the heat pump ( $T_{air}=7^{\circ}C$ , $T_{supply HS}=35^{\circ}C$ )
air	Room air volume
<i>avail</i>	Availability of the powerplants
<i>coil</i>	Coil from the DHW storage tank
<i>cold</i>	Cold temprature in input of the DHW systems
cons	Electricity consumption
<i>conv</i>	Convective
<i>corr</i>	Corrected data
<i>country</i>	Country from the list of the neighboring countries
<i>d</i>	Daily
<i>design</i>	Design temperature of space heating
DHW	Domestic hot water network of the building
<i>diff</i>	Solar diffuse irradiation
<i>dir</i>	Solar direct irradiation
<i>Dis</i>	Distribution
<i>dw</i>	Dwelling
ecoinvent	Evaluated with data from the ecoinvent database
elec	Electricity
<i>eurostat</i>	Evaluated with data from the eurostat database
<i>exch</i>	Electricity exchanges
<i>exp</i>	Export
<i>f</i>	Natural gas combustion
<i>floor</i>	Floor construction of the dwelling
FR	France
GB	Natural gas boiler
<i>gen</i>	Electricity generation
<i>ground floor</i>	Ground floor of the building
<i>h</i>	Hourly
HP	Heat pump
<i>HP off</i>	Minimum time before restart of the heat pump
<i>i, j</i>	Ranks in the lists or section from a disretized component
<i>imp</i>	Import
<i>in</i>	Input
<i>inner</i>	Inner surfaces of the dwelling



<i>LD Tr</i>	Long distance transport
<i>m</i>	Monthly
<i>marginal</i>	Marginal electricity generation
<i>mat</i>	Material constituting a part of a wall
<i>max</i>	Maximum level (resulting from the unit-commitment)
<i>mean</i>	Average (vérifier si on a pas mis average qqpart, ce serait peut etre mieux?)
<i>min</i>	Minimum level (must-run and minimum generation outputs)
<i>NG</i>	Natural gas
<i>nom</i>	Nominal
<i>out</i>	Output
<i>pump radiator</i>	Pump from the primary network of the building
<i>r</i>	Radiative
<i>rad</i>	Radiant
<i>radiator</i>	Radiator of the dwelling
<i>remain</i>	Remaining groups to dispatch or commit during UCED
<i>roof</i>	Top roof of the building
<i>SH</i>	Space heating
<i>size HP</i>	Size of the heat pump
<i>supply DHW</i>	DHW flowing from the DHW tank to the dwellings
<i>surf</i>	Wall surfaces
<i>tan</i>	Stored water in the DHW storage tank
<i>tan HP</i>	Hydroelectric separator
<i>tech</i>	Technology (elements from or non-dispatchable units or dispatchable units)
<i>th</i>	Thermal
<i>Tr</i>	Transport
<i>TSO</i>	Data from French TSO
<i>y</i>	year
<i>valid</i>	Variable used for validation
<i>ventil</i>	Ventillation and infiltration
<i>vpp<sub>exch</sub></i>	Virtual powerplant representing electricity exchanges (included in groups)
<i>w</i>	Week
<i>wall</i>	External wall of the dwelling (elements from $L_{wall\ ext}$ )
<i>water</i>	Water
<i>window</i>	Windows of the dwelling

## Lists

Symbol	Definition
--------	------------

$d_{gr}$	List of days when the group $gr$ is producing electricity
dispatchable units	List of the dispatchable units
$L_{exch}$	List of the countries included in the model
$L_{floor}$	List of the inner surface from a floor construction of the dwelling
$L_{gr}$	List of groups $gr$ after discretization of the technologies from the list $L_{tech}$
$L_{inner}$	List of the inner surfaces of the dwelling
$L_{inner} \setminus L_{floor}$	List of the non-floor inner surfaces of the room
$L_{tech}$	List of technologies considered in the model (including electricity exchanges)
$MO_1$	Merit-order for the unit commitment, corresponding to a sorted version of $L_{gr}$
$MO_2$	Merit-order for the dispatch, corresponding to a sorted version of $L_{gr}$
neighbors	List of the neighboring countries
non-dispatchable units	List of the non-dispatchable units
$L_{wall\ ext}$	List of the external walls of the dwelling

# Table of content

Acknowledgements.....	2
<b>1. General introduction.....</b>	<b>12</b>
1.1. Decarbonization of the energy consumption in France.....	12
1.2. Possible impacts of the electrification of the heating demand .....	14
1.3. Demand-side management through the control of hybrid heat pumps.....	17
1.4. Objectives of the thesis.....	18
<b>2. Review of the methods to evaluate the marginal emission factor of the electricity consumption and first evaluation .....</b>	<b>21</b>
2.1. General overview of the power system organization .....	21
2.2. Life Cycle Assessment methodologies for the GHG emissions of electricity .....	29
2.3. Simplified evaluation of the Marginal Emission Factor of electricity generation and consumption in Europe .....	37
2.4. Overview of Unit Commitment and Economic Dispatch models.....	46
2.5. Conclusions.....	52
<b>3. Development and validation of the French power system model .....</b>	<b>54</b>
3.1. Model for Unit Commitment and Economic Dispatch .....	54
3.2. Methodology to evaluate the marginal emission factor of the electricity consumption .....	63
3.3. Validation of the unit commitment model.....	65
3.4. Application: Marginal mix and MEF assessment.....	72
3.5. Conclusions.....	78
<b>4. Evaluating the space heating and domestic hot water needs of a district..</b>	<b>80</b>
4.1. Case study.....	80
4.2. Method .....	83
4.3. Space heating demand .....	89
4.4. Domestic Hot Water demand.....	100
4.5. First results .....	104
4.6. Conclusion .....	109
<b>5. Evaluation of control strategies for a fleet of hybrid heat pumps .....</b>	<b>110</b>
5.1. Model of the heat generation system.....	110
5.2. Overview of the heating system configurations .....	113
5.3. Reference heating system .....	116
5.4. Control strategy 1: Prioritizing the heat pump .....	122

5.5.	Control strategy 2: MEF-based fuel switch .....	124
5.6.	Evaluation of the impact of the control strategies and heat pump sizing .....	129
5.7.	Conclusion .....	137
<b>6.</b>	<b>Conclusion .....</b>	<b>139</b>
6.1.	Summary.....	139
6.2.	Thesis contribution.....	140
6.3.	Future work .....	140
	<b>References .....</b>	<b>143</b>
	<b>Appendix A: Description and analysis of the French power system.....</b>	<b>152</b>
A)	Nuclear electricity generation.....	152
B)	Hydroelectric powerplants.....	157
C)	Interconnections .....	165
D)	Electricity generation from fossil fuels.....	172
	<b>List of publications .....</b>	<b>181</b>

# 1. General introduction

## 1.1. Decarbonization of the energy consumption in France

Global warming is largely caused by greenhouse gases (GHG) emissions, which are mainly produced by anthropogenic activities (Masson-Delmotte, V., P. Zhai, A. Pirani, Connors, C. Péan, S. Berger, N. Caud, Y. Chen, L. Goldfarb, M.I. Gomis, M. Huang, K. Leitzell, E. Lonnoy, and Matthews, T.K. Maycock, T. Waterfield, O. Yelekçi, R. Yu 2021). In order to limit global warming, the countries of the world committed themselves under the Paris Agreement to reduce their GHG emissions, which are substantially due to the use of fossil fuels. In France, the Low Carbon Strategy (Ministry for the ecological and solidarity transition 2020) drafted the French actions up to 2050 in the building sector, agriculture, forestry, industry, energy production and waste. The associated Multi Year Planning specifies these actions for the years 2019 to 2028 (Ministère de la transition écologique et solidaire 2019). Figure 1 presents the expected and forecasted variations of GHG emissions and sinks for every sector in France between 2005 and 2050. The most significant emission reduction should be in transport (-97% between 2015 and 2050), in the building sector (-95%), and in energy production (-95%) (Ministry for the ecological and solidarity transition 2020).

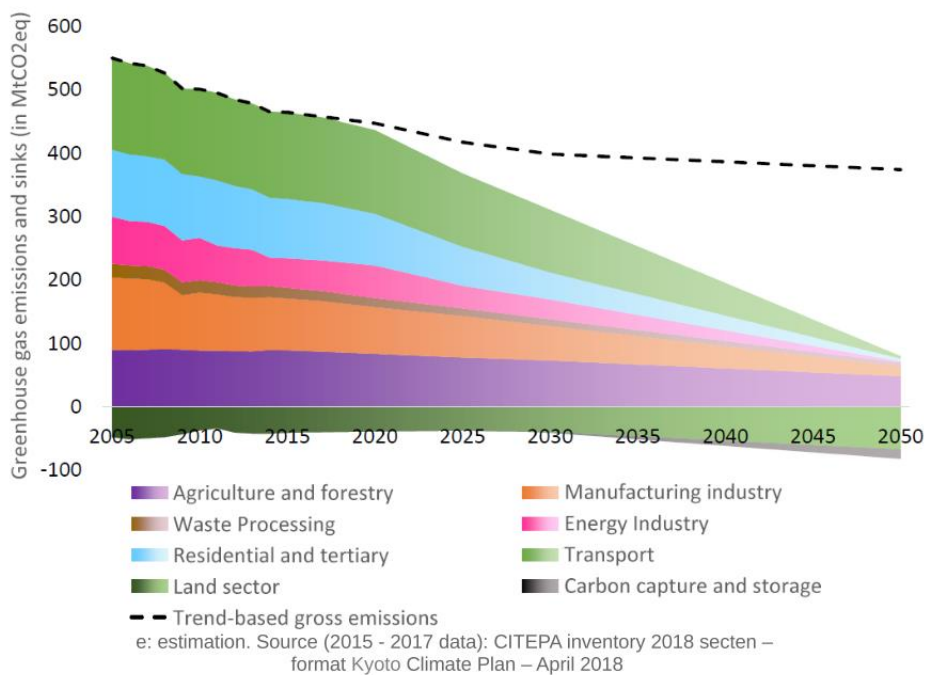


Figure 1: Observed and targeted GHG emissions and sinks for every sector in France between 2005 and 2050

(Ministry for the ecological and solidarity transition 2020)

The actions to reduce GHG emission are mainly related to the energy generation and consumption. Figure 2 shows the variation of the observed and forecasted final energy consumption (electricity and other energy sources) from 1960 to 2050 in France. The French energy consumption increased continuously from the 1960s to the 2000s and decreases since them.

Three main actions shown in Figure 2 should contribute to reducing the GHG emissions related to energy consumption:

- The reduction of the final energy consumption by energy saving measures and an improvement of energy efficiency.
- The increase of the share of electricity in the final energy consumption to substitute fossil fuel. Coal and oil consumption should drastically decrease. Gas consumption, whose emission factor is also expected to decrease due to the replacement of fossil gas with renewable gas, will decrease to a lesser extent.
- The increase of the share of low carbon generation in the electricity mix.

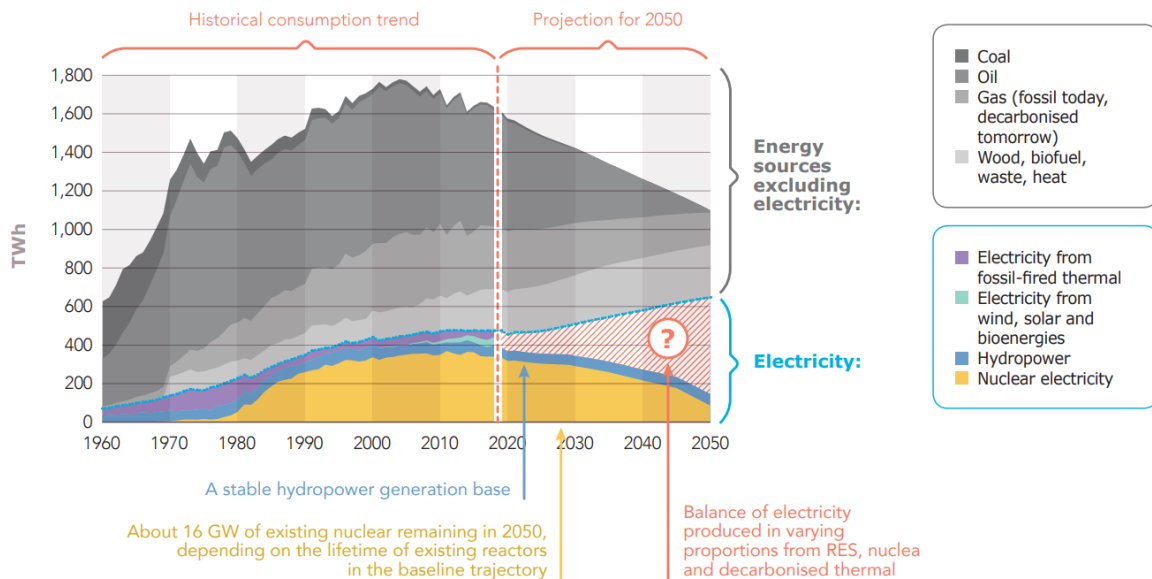


Figure 2: Observed and forecasted total electricity consumption and final energy for other energy sources in France between 1960 and 2050, from (RTE 2021).

In this thesis we will focus on the decarbonisation of the heating and domestic hot water (DHW) demand of the residential sector, which represented 20% of the final energy consumption in France in 2021 (Ministère de la transition énergétique 2023). At the building level, the strategy in France for decreasing the energy demand for space heating by 2028 is based on three principles (Ministère de la transition écologique et solidaire 2019):

- The improvement of the energy performance of the new buildings, with the implementation of a stricter environmental regulation for new buildings (RE2020).
- The refurbishment of existing buildings to decrease the heating demand.
- The deployment of renewable heat in buildings thanks to financial incentives such as subsidies or tax cuts. The renewable heat should come from biomass (including biomethane) boilers, heat pumps, solar energy systems or district heating networks.

Consequently, the share of electricity in the primary energy used for heating should grow with widely spread aérothermal heat over the territory. Figure 3 presents the final energy consumption for buildings according to the French low carbon strategy. The share of oil (used for heating and DHW) and gas (used for heating, DHW but also cooking) should highly decrease by 2050.

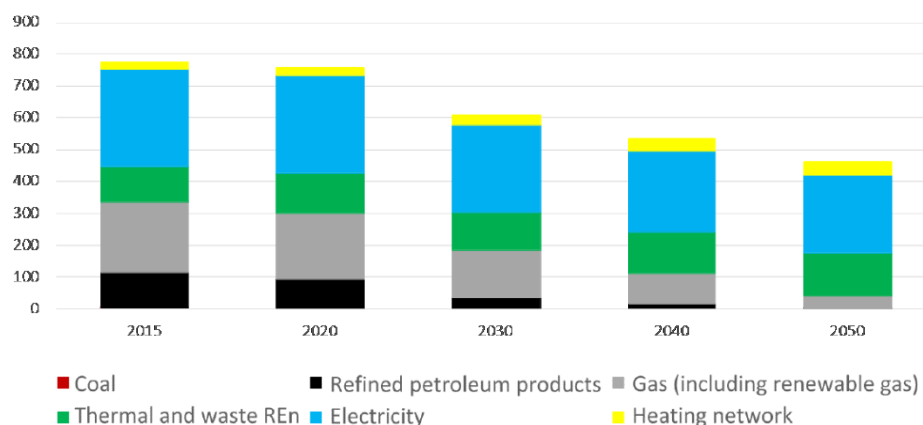


Figure 3: Final energy consumption for buildings in the baseline scenario from the French low carbon strategy, adapted from (Ministry for the ecological and solidarity transition 2020)

## 1.2. Possible impacts of the electrification of the heating demand

Outdoor temperature and electricity consumption are closely related in France. It is referred to as thermal sensitivity. Electricity consumption is higher in winter than in summer, which results in a seasonal peak consumption. Figure 4 presents the daily electricity consumption against the mean outdoor temperature for several European countries between July 2018 and June 2019. In comparison to its neighbors, the French electricity consumption has the strongest increase when the outdoor temperature decreases. The winter thermal sensitivity in France is evaluated to 2.4 GW/°C (RTE 2022c). The high share of electricity in space heating explains this trend. Indeed 36% of households were heated up with electricity in 2017 (ADEME 2018a). Until 2050, this share should increase up to 70% of the households (RTE 2022c). At the same time, the performances of the heating systems will improve as aerothermal heat pumps have a higher efficiency than electric radiators (direct electric heating) although their coefficient of performance (COP) decreases significantly with low outdoor temperatures. In addition, the heating demand should decrease due to the renovation rates and climate change. According to the French TSO, the thermal sensitivity of the electricity grid will be maintained during the first years and then decrease as a result of changes in the building sector. However, this trend depends on renovation rates and assumes an increase up to 700 000 complete renovations per year. This issue is all the more relevant given the low renovation rate currently observed (equivalent to 200 000 complete renovations (RTE ADEME 2020)), which highlights the difficulties of keeping peak demand under control. This explains why the ability of the French electricity system to meet electricity demand during the winter peak should be addressed.

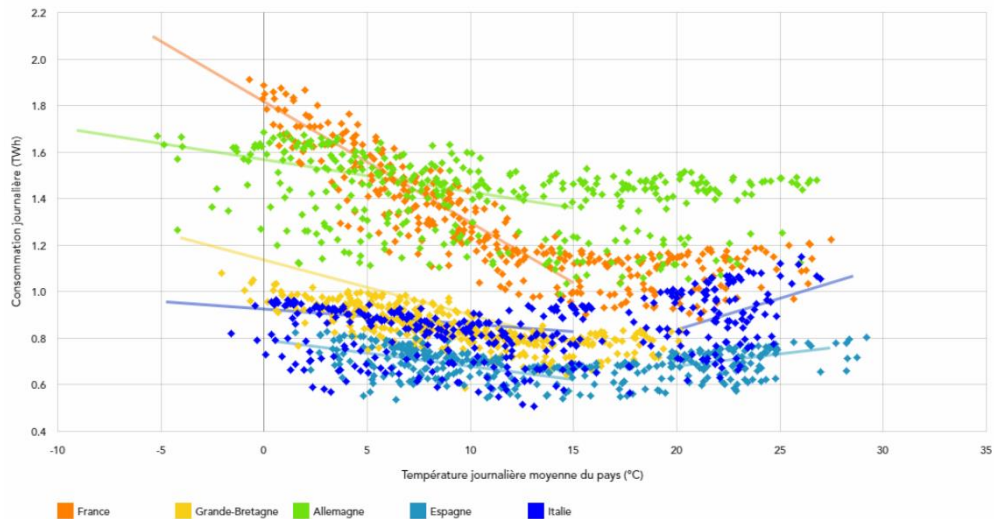


Figure 4: Daily electricity consumption against the mean daily temperature for France, Great Britain, Germany, Spain and Italy between July 2018 and June 2019 (RTE 2019a)

In 2018, 14% of the French installed electricity generation capacity was fossil-based and these units are mostly activated in winter to meet the additional electricity demand. Figure 5 shows the average emission factor for the electricity production in France between July 2017 and June 2018. Although the yearly mean carbon intensity of the French electricity is currently low as it is dominated by the nuclear production, the electricity mix is more carbon intensive during the cold spells. The emission factor of the generation units activated to respond to a variation of the heating demand, referred to as the marginal emission factor, should then be taken into account in order to evaluate the GHG emissions related to the changes of the heating demand pattern. In (Roux, Schalbart, and Peuportier 2017), the authors evaluated the carbon footprint for space heating in a low-energy house in France between 61 to 85  $g_{CO_2eq}/kWh$  with an average method and between 765 and 929  $g_{CO_2eq}/kWh$  with the marginal method. A similar evaluation should be performed for a building heated by a heat pump, taking into account its COP variations. In comparison, the same study evaluates the carbon footprint of a boiler supplied with natural gas between 218 and 284  $g_{CO_2eq}/kWh$ . Therefore, it might be beneficial to switch between energy carriers depending on the emission factor of the electrical grid.

As fossil fuel-fired generation units, which emit significantly more GHG than nuclear plants, are activated in winter to meet the increase in electricity demand due to heating, it could be interesting to couple the heat pumps with another energy carrier to avoid emissions when the marginal electricity becomes too carbon intensive. Installing such hybrid heat pumps (electric heat pumps coupled with a gas boiler) instead of heat pumps and optimizing their regulation could then reduce the GHG emissions due to space heating.



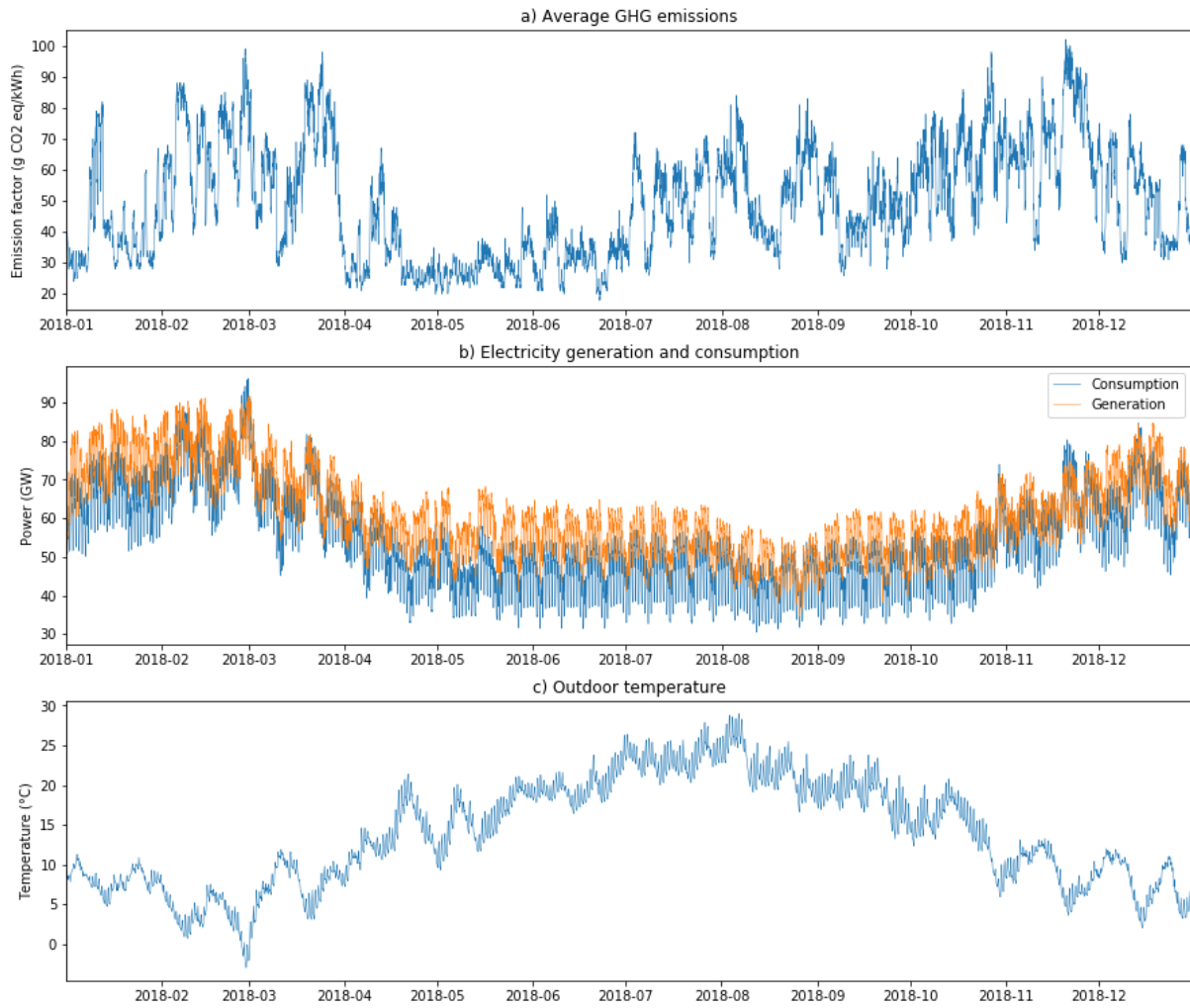


Figure 5: GHG emission factor for the French electricity production, electricity consumption and generation, and outdoor temperature in 2018 (RTE 2022a; ENEDIS 2020).

However, the benefits of hybrid systems are not limited to reducing emissions in the short term. In the future grid, the decarbonized-electricity system will be mainly composed of renewable power plants (with an electricity generation highly related to weather and consequently that cannot follow the demand) and of nuclear units (that are only partly flexible), the shift being planned gradually between 2035 and 2045. Demand-side management in buildings is a way to improve the integration of the non-dispatchable renewable energies in the electrical production system. Fuel-switching using biogas is a way to gain flexibility in the electrical system. As the growth of the capacity for biogas production is limited, it is necessary to address the optimal use of this valuable energy source. The goal for biogas production in 2028 is set at 24 up to 32 TWh (including 14 to 22 TWh injected) (Ministère de la transition écologique et solidaire 2019), and a 50TWh target is foreseen by 2030 in the multi-year planning revision (Secrétariat général à la planification Écologique 2023). According to the French Agency for Ecological Transition and its S3 scenario (the most favorable for renewable gases production), France has a potential of 130 TWh of biomethane, and new production technologies (gaseification and methanation) can provide extra-potentials (ADEME 2021). Supplying part of the heat demand with biogas instead of electricity when needed would be a reasonable usage of this valuable energy source. The biogas supply would compensate intermittently for the lack of flexibility of the electrical system.

### 1.3. Demand-side management through the control of hybrid heat pumps

Different demand-side management strategies can be implemented to control the electric consumption of heating systems. In many studies, a dynamic control of the heating set-point or the addition of an energy storage were proposed to improve the GHG emissions from space heating. (Clauß et al. 2019) demonstrated that curtailment of the electricity consumption driven by GHG emissions had a positive effect only when the daily fluctuation of the emission factor of electricity compensated for the increase in electricity consumption after the interruption, as in this case consumption is only shifted. (T. Péan et al. 2019) implemented control strategies of the set-point temperature for space heating in a dwelling to reduce the primary energy consumption, the operating cost or the marginal emissions. However, such strategies may decrease comfort and are limited by the acceptance of occupants. The electricity use for space heating can also be displaced during the day using a thermal storage. (D’Ettorre et al. 2019) estimated that the addition of an optimally controlled thermal storage to a heating system could reduce the operation cost for space heating of a building in Italy by 8%. However, the amount of displaceable energy is limited by the size of the thermal storage tank, which is also related to the size of the heating system.

Alternatively, hybrid heating systems have been proposed to offer more flexibility between energy carriers. (Beccali et al. 2022) performed a review of 38 journal articles published between 2016 and 2022 studying hybrid heat pumps. The low number of journal articles available on this technology illustrates the need to investigate the possible interactions between hybrid heat pumps and the power system. The main application for hybrid systems coupling a heat pump and a gas boiler was usually the undersizing of the heat pump to improve the performance and reduce the installation costs (Klein, Huchtemann, and Müller 2014). In this case the system is controlled to minimize the primary energy consumption or the fuel cost. More recently, the coupling of different energy carriers for demand-side management, cost reduction or carbon footprint reduction has been examined. Such strategies need to model interactions with the energy system outside the building.

(Vuillecard et al. 2011) investigated the impact at a low-voltage level of demand-side management through hybrid heat pumps. (Heinen and O’Malley 2015; Heinen, Burke, and O’Malley 2016) demonstrated the benefit of hybrid heat pumps in Ireland, where 40% of the energy comes from wind turbines. In Great-Britain, (Clegg and Mancarella 2019) estimated a decrease by 24% of the peak load when hybrid heat pumps are deployed to supply 29% of the heat demand. (Boesten 2018) modeled fuel-switch technologies in heat and electricity smart grids and identified an economical benefit in the Danish case. (Li and Du 2018) also demonstrated economic benefits as well as energy savings through the control of hybrid heat pumps for space heating and DHW production. (Roccatello et al. 2021) investigated the impact of the hybrid heating system design and operation on the primary energy consumption for space heating and DHW. Various building types and locations were considered.

Only a limited number of studies evaluates the impact of hybrid heat pumps on GHG emissions. In the Australian context (Aditya and Narsilio 2020) demonstrated a reduction of the lifetime GHG emissions for space heating supplied by a ground source heat pump coupled with a gas boiler in comparison with the same system without a gas boiler. However, this study is based on an attributional Life Cycle Analysis (LCA) and does not evaluate the impact of the control strategy. (Entchev et al. 2018) developed a control strategy for a hybrid heating system using neural predictive control. They evaluated emission reduction up to around 36% for a single house located in Ottawa. The two studies cited previously considered a single heating system. (Bennett et al. 2022) evaluated different scenarios for the replacement of the gas boilers in England considering single heat pumps or hybrid heat pumps. The study demonstrated the interest of hybrid technologies for mitigating peak electricity demand.

However, the authors considered a constant average emission factor for the electricity consumption. The outdoor temperature affects the heat pump performance and their COP varies much with the climate, so does the GHG emissions of the power system. Moreover, the potential positive impact of hybrid heat pumps depends on the deployment of a large fleet of the technology. Consequently, it is important to evaluate the influence of the local control systems and then upscale the evaluation to an entire fleet of hybrid-heat pumps.

From this review, it can be observed that most studies on hybrid heat pumps are evaluating several indicators (energy consumption, operating or installation cost) but rarely GHG emission. The studies evaluating the GHG emissions from hybrid heat pumps do not always consider the impact of control strategies and often evaluate a single heating system. Moreover, such systems are rarely controlled by a signal providing the marginal GHG emission of the avoided electricity production and few studies inquired this point in details.

By comparing the emission factors of different energy carriers and the efficiency of the production systems, we can get a rough estimation of the activation time of such hybrid heat pumps. In the case of a heating system coupling an aerothermal heat pump with a gas boiler, the gas boiler should be activated to avoid electricity production from high-emission fossil plants. The last French coal-fired powerplants should be decommissioned between 2024 and 2026. However, the French grid is highly interconnected with Europe, especially Germany. The German coal-fired powerplants might produce electricity until 2035 (Fraunhofer ISE 2021). Gas-fired combined cycle gas turbine (CCGT) will continue to operate after 2035. An optimal regulation of hybrid system based on the GHG emissions should then allow to avoid emissions at least until 2035. After 2035 the different technologies allowing centralized flexibility (CCGT and combustion turbines) and decentralized flexibility (boilers, gas heat pumps, micro cogeneration units) using biogas as primary energy source should be compared against each other.

## 1.4.Objectives of the thesis

In order to address the growing need of flexibility for the electrical system, several solutions such as storage, demand-side management or power-to-gas systems can be considered. The objective of this thesis is the evaluation of the impact of the control strategy of a fleet of hybrid heat pumps through France on the GHG emission of space heating and DHW. This study consider the impact of the control strategies for heat pumps at an aggregated level, the climatic diversity of the country and the actual dynamics of the French power system.

Choosing the right energy carrier (electricity or natural gas) will be driven by the GHG emissions of the entire energy system, including the national grid and its connections with neighboring European countries. The activation time of the gas supply depends on both the heating production technology and the local climate conditions. Figure 6 presents the interactions between the buildings, the national electricity grid and the local gas supply.

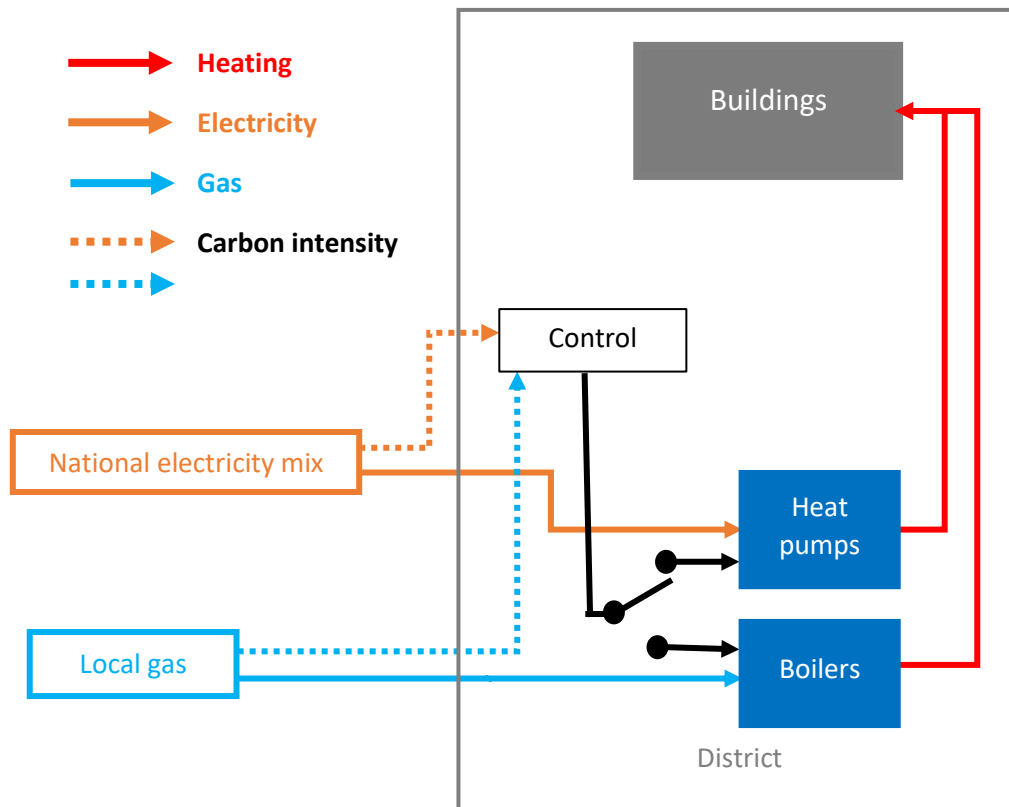


Figure 6: Operation strategy of a building driven by a GHG emissions signal

To control properly hybrid heat-pumps, it is necessary to determine the carbon intensity of the electricity consumption avoided during the entire operating time of hybrid heat pumps. As the reduction of the electricity consumption during the activation of the gas boilers influences the electricity grid and thus the level of the GHG emissions, coupling the supply and the demand models is essential. The electrical system is complex to predict because the decisions influencing the activation of the generation units are made by several operators on different time scales. Therefore, proving the interest of the optimal control strategy for hybrid systems requires an accurate model of the electrical system. The development of an appropriate model to estimate the marginal emission factor of the electricity consumption is the focus of the first half of the thesis. In the second half, simulations of hybrid heat pumps at the building level are carried out to properly model the dynamics of such systems and to evaluate different sizing and control strategies. The potential of such a technology for different climatic zones in France is also considered.

The following research questions will be addressed in the thesis:

- Which level of details is required to model properly the short-term dynamics of power systems? How to validate marginal observations on the power systems?
- How are different demand-side management strategies impacting the power system?
- How should hybrid systems be controlled at the building level? What is the influence of the sizing and of the low-level controllers?
- Can hybrid systems support the decarbonisation of heating?

The manuscript is organized as follows. The methods for assessing GHG emissions from demand-side management strategies are discussed in Chapter 2 and a first estimate for 2018-2019 is made. In Chapter 3, a model of the French power system is developed and validated. Results on the marginal

mix and the emission factor are also discussed in this section. In Chapter 4, the method to model the heating demand for space heating at a district level and the scaling up at the national level are presented. In Chapter 5, the models of hybrid heating systems as well as the different sizing and control strategies are described. The models developed in the previous part are used to evaluate the impact of different control strategies and different sizing of the hybrid heating systems. The conclusions and perspectives are presented in the last section.

## 2. Review of the methods to evaluate the marginal emission factor of the electricity consumption and first evaluation

Consequent to the Paris agreement, objectives for carbon neutrality by 2050 were defined for many countries over the world. A key lever to reduce the greenhouse gas (GHG) emissions resulting from energy consumption is the decarbonization of the energy vectors, mainly by increasing the renewable share of electricity generation (Ministry for the ecological and solidarity transition 2020). Renewable powerplants being poorly flexible, relying on new sources of flexibility such as demand-side management of electricity usage is a critical issue. Such an approach requires an investigation of the impact of demand reductions on the power system, and more specifically in terms of GHG emissions. This means identifying the variation in the GHG emissions, referred to here as the “marginal emission factor” (MEF), consequent to this variation in demand. A good knowledge of the power system response is thus required to evaluate this marginal emission factor.

Methodologies for calculating the MEF are based on different assumptions about the power systems. The operating principles of the electrical system must therefore be well understood in order to select the most appropriate method. Section 2.1 describes the electrical system organization applicable to most of the European countries. With this knowledge, the main decisions concerning the GHG emission calculation will be justified. In Section 2.2, the different methods to assess the MEF will be presented. This emission factor may or may not be calculated using a model of the power system. Despite its limitation, a method of the first category (not based on a model of the power system) will be applied in Section 2.3 to get a first estimate of the benefits of hybrid systems. As only methods based on an explicit model of the power system can replicate the behavior of a power system, such models will be reviewed in Section 2.4 and the selected methodology will be described in the conclusion of this chapter.

### 2.1. General overview of the power system organization

In this section, the general organization of the power systems is described with a focus on the dynamics of the electricity demand, the planning of the power system for the different time horizons and the mechanisms to ensure the balance between supply and demand. The constraints to be included for the evaluation of the MEF for electricity consumption in France will be deduced from this analysis.

#### 2.1.1. Electricity consumption

The yearly electricity consumption of a country depends on many parameters such as the industrialization level, the composition of the building stock, the mean temperature during the winter, etc. The price of electricity and the level of electricity consumption are also interdependent. This is theorized as the price elasticity of demand. Over the course of a year the electricity demand varies depending on:

- the weather: this is the thermal sensitivity. In winter, a temperature decrease below 15°C leads to an increase of the heating need (also depending on the cloud cover ratio). This trend is particularly strong in France where electric heating systems are widely used. In some countries such as Spain or Italy, there is an increase of the cooling need in summer due to the outdoor temperature rise.

- the activity: this is the temporal sensitivity. Due to variations in economic activity, the electricity consumption is higher during the week than at week-ends or holidays, and during working hours than at night. In addition, the residential activities (usages such as lighting or cooking) influence the intraday electrical consumption. In general, two consumption peaks are observed daily: the first one in the morning and the second one around 7 pm. The consumption level is lower during the night.

In addition to the electricity consumption, losses occur during transport and distribution between the generation unit and the end-consumers. These losses mainly depend on the transported power, the distance and the outdoor temperature.

### 2.1.2. Sizing of the electricity generation system

Two types of generation units are installed in order to meet this demand:

- The non-dispatchable generation units: in general and as of today, electricity generation from these plants is not driven by the demand. This is the case for wind turbines and photovoltaic panels, which level of production depends on the weather conditions and can only be adjusted downwards. As the cost of generating electricity from solar and wind is extremely low, a decrease in the production of these units is undesirable. A small share of the run-of-river production is dispatchable. In France, combined heat and power (CHP) systems and biomass plants are not driven by the power need, but by the heating need. As electricity is only a by-product, this type of unit is also considered as non-dispatchable.
- The dispatchable generation units: nuclear, coal, gas, oil, hydropeaking, storage and pumped-storage hydroelectric units can modulate their power output within technical and economical constraints.

In 2018, 40% of the installed French generation capacity was renewable and this percentage should grow in the coming years. Figure 7 presents the distribution of the installed electricity generation capacities and the electricity production in France in 2018.

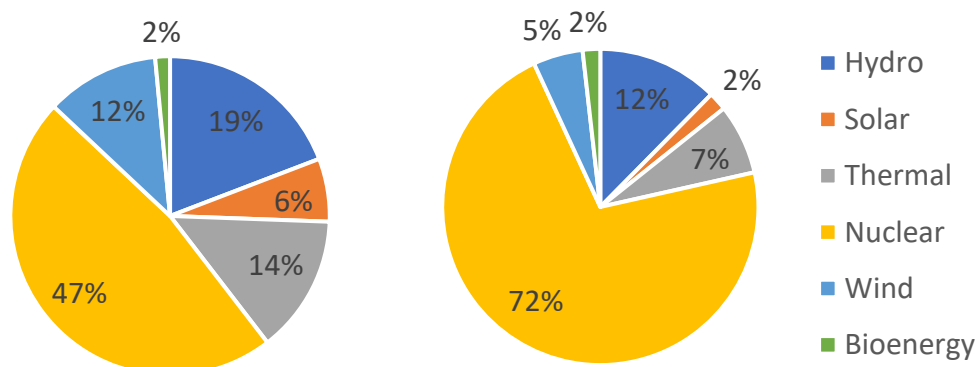


Figure 7: Distribution of the installed capacities (left) and electricity (right) production in France in 2018

The difference between dispatchable and non-dispatchable units enables us to define a first important indicator, the residual consumption (RC). It is defined as the consumption (C), from which the

production of the non-dispatchable units is subtracted (see Equation 1). The electricity production of the dispatchable units and the electricity exchanges with the neighboring countries are then adjusted continuously to this residual consumption to meet the demand (see Equation 2). The planning of electricity generation, also called “unit-commitment and economic dispatch”, is complex and relies on multiple stakeholders that act across various markets and time frames.

$$RC(t) = C(t) - \sum_{tech \in non-dispatchable\ units} P_{tech}(t) \quad 1$$

$$RC(t) = \sum_{tech \in dispatchable\ units} P_{tech}(t) + \sum_{country \in neighbors} P_{country}(t) \quad 2$$

The power system is sized in order to fulfill the electricity supply security criterion, which is set to three hours in France. It means that among all the scenarios modeled by the Transmission System Operator (TSO), RTE in France, the mean duration for inability to meet the demand with the electricity markets should be less than three hours. During this time, the balance is fulfilled by means of post-market utilities.

Using this criterion, the main risk is a cold spell, which can occur every 10 to 20 years. Other risks are due to the unavailability of several nuclear reactors at the same time, or the case of low wind in several European countries or the unavailability of transfer capacities on the European grid. Historically the French electricity system was oversized, but the security margins were reduced during the last years and the electricity supply security is now becoming a critical issue.

### 2.1.3. Organization of the electricity generation

The electricity generation fleet and the interconnection capacities of a country have to be designed to ensure the security of electricity supply. This is the role of the TSO, which is responsible of the national grid. The TSO has to (RTE 2019b):

- Size the electricity generation fleet to ensure than the installed capacity can supply enough power in most of the cases;
- Adjust the grid frequency and ensure enough production capacities and flexibilities in order to compensate the outage of one or more production capacities (this is for example managed at the European level);
- Have control over the voltage plan to ensure the nominal voltage across the country.

During the year, the activable operating generation units are decided on a daily basis. The generation level of these units is then continuously adjusted throughout the day. These last two steps are referred to in this thesis as “scheduling and dispatch”. Although the TSO is responsible for the security of electricity supply, some energy utilities take care of the scheduling and dispatch of their own powerplants. The dispatch is then reported to the TSO and the TSO can send instructions in case of an imbalance between demand and supply. The dispatch of the electricity generation among the several generation units of the fleet is the result of a sequence of decisions taken during different time frames:

- The long-term planning (several years) for the installation of new facilities or the refurbishment of the existing ones (the criteria used for the security of electricity supply was presented in section 2.1.2);



- The seasonal scheduling: planning of the maintenance work on the plants, refueling, managing the water reserves of hydroelectricity, the temporary shut-down of part of the fleet, etc ;
- The day-ahead and intra-day scheduling (discussed in section 2.1.4);
- The frequency services and balancing mechanisms, with reaction time from 30 seconds up to two hours (discussed in section 2.1.5);
- The post-market utilities (discussed in section 2.1.6).

Figure 8 from (Heggarty 2021) summarizes the different sources of variability and uncertainty but also the flexibility solutions to ensure the balance between demand and electricity generation.

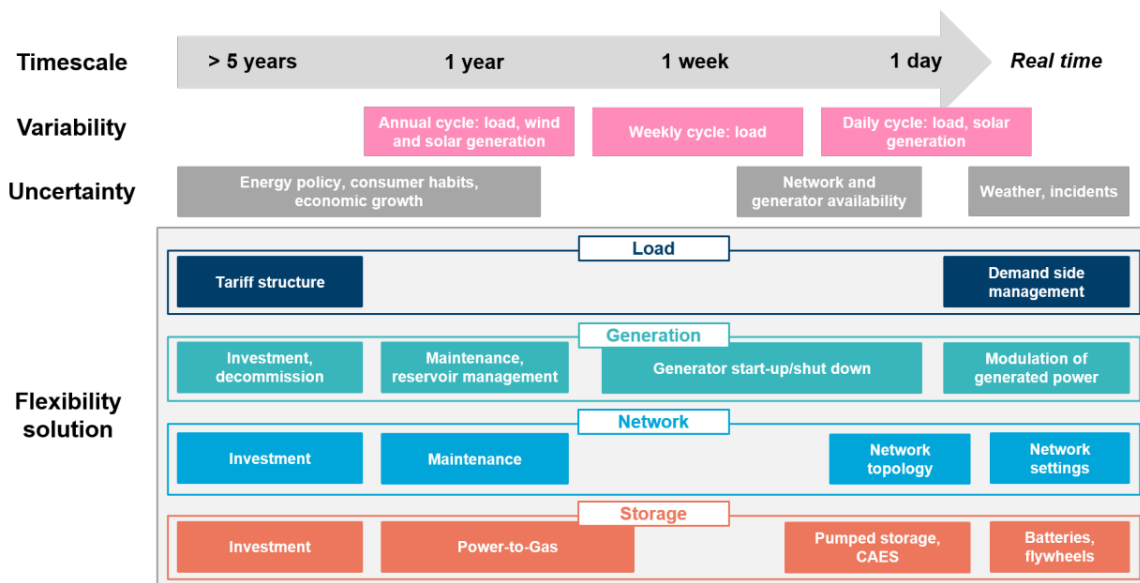


Figure 8: Sources of variability and uncertainty in power system for different time scales (Heggarty 2021)

#### 2.1.4. Day-ahead and intraday planning

The scheduling and the dispatch are daily optimized according to the technical constraints of the different units of the fleet and to the costs of these units. Table 1 summarizes the cold and hot startup times and the maximum ramp rates for the different types of generations units. For all the technologies listed, the maximum time required to reach 100% of the nominal power of the unit is 20 minutes. This means that for an analysis with a time-step greater than 30 minutes, the effect of the ramping restriction will not be visible. Regarding the startup period, the TSO has to plan in advance the activation of the units considering the (sometimes) long startup time. It could also affect the minimum activation duration of the unit.

Table 1: Comparison of the flexibility of different electricity generation technologies in France (Camille Cany 2017; RTE 2015)

	Cold start duration	Hot start duration	Maximum nominal power value for one unit	Maximum power ramp relative to nominal power	Maximum power ramp for one unit
Oil-fired powerplant	15 min	5 min	180 MW	25 %/min	45 MW/min
Open cycle gas turbine (OCGT)	10-20 min	10-20 min	200 MW	20 %/min	40 MW/min
Combined cycle gas	3 h	30-60 min	585 MW	7 %/min	41 MW/min

turbine (CCGT)					
Coal-fired power plant	6 h	2 h	595 MW	5 %/min	30 MW/min
Nuclear reactor	1 to 2 days	2 h	1500 MW	5 %/min	75 MW/min


The dispatch plan depends on the forecasted consumption and the level of non-dispatchable generation. The forecast is performed day-ahead and actualized throughout the day. The dispatchable generation units are activated in order to maximize the profits by minimizing the generation cost of electricity.

The cost of a generation unit can be divided into four parts:

- The investment cost (€/kW) represents all the costs before the electricity generation starts.
- The annual operating costs or fixed costs (€/kW.year) include the maintenance, the management, the labour costs, etc. It does not depend on the amount of electricity produced.
- The proportional operating costs or variable costs (€/MWh) are proportional to the electricity produced and corresponds to the fuel cost, the taxes and also the start up costs.
- The dismantling cost (€/kW) is the cost when the unit does not produce electricity any longer.

The electricity producers were historically paid according to the electricity generated. The profit made over the lifetime of the powerplant should repay the investment and the dismantling costs. Since 2017, the electricity producers can also be paid for their installed capacity through the capacity markets. Variable and fixed costs for some French generation units were evaluated for the year 2020 (Cany 2017) and are reported in Table 2. Although these costs are not constant over time and are based on a number of assumptions, these estimates allow a quick comparison between the different technologies.

Table 2: Fixed and variable costs for different electricity generation technologies (Cany 2017; RTE 2022b; ENTSOE 2022)

Load factor	Units		Load factor (2018-2019) (%)	Variable costs (€/MWh)	Fixed costs per year (€/kW.year)
Load factor depending on the weather	Non-dispatchable production	Wind power	27	0	39
		Solar power	19	0	38
		Non-dispatchable hydro power	14	0	33
Load factor increase 	Baseload generation	Nuclear	95	6	164
	Intermediate load generation	CCGT	49	62	0.06
		OCGT	2	94	0.03
Management of the water reserve	Peak load generation	Dispatchable hydro power	34	0	14

Electricity generation is primarily planned to minimize the total production costs, which include the fixed and variable costs of the activated power plants. The unit-commitment problem can be described using an economic merit-order approach: the different generation units are stacked according to their variable cost. The units with the lowest variable cost are first activated (baseload units), whereas the units with the highest variable cost are activated during the peaks. The marginal cost of the system

corresponds to the electricity generation cost of an additional demand for electricity. In the same way, the marginal generation unit is the unit whose generation level is adjusted consequently to an additional demand for electricity. The marginal cost of electricity is then equal to the variable cost of the marginal generation unit. The units with high fixed costs and low variable costs are then logically activated at their maximum output level most of the time (baseload unit) in order to maximise profit. Consequently, as can be seen in Table 2, the load factor of the technologies increases as the variable costs decrease. The dispatchable hydro units are activated according to their usage cost: they have a low variable cost, are highly flexible but have a limited reserve. That is why they have to be used optimally. Moreover, peak units with both high starting costs and high variable costs are rarely activated, but they generate electricity at their maximum level to compensate their startup costs when activated. These units are consequently poorly contributing to the system intra-daily flexibility. These general observations of the system dynamics are of course an oversimplified representation of an electrical system and both peak and base units can be totally or partially controlled to follow the load. Technical, political and economical constraints can affect the generation mix. Some of them are discussed in the following parts.

The short-term flexibility of the different technologies can be easily represented by plotting the variation in production of each technology between each half-hour over a year, as a function of the variation of the residual consumption. Such a plot is shown in Figure 9 for the French power system for the year 2018. A linear regression was applied on the data obtained for each technology and for the electricity exchanges. The coefficient of determination ( $R^2$ ) and the slope ( $s$ ) are indicated on each figure. The slope can be interpreted as an indicator of the contribution of each technology to the hourly flexibility of the power system. Some conclusions about the hourly flexibility can be drawn from these graphs:

- Hydroelectric power plants are contributing to around half of the hourly flexibility ( $s=0.48$ );
- Electricity exchange with interconnected neighboring countries is the second lever of hourly flexibility ( $s=0.28$ );
- CCGT ( $s=0.08$ ) and nuclear power plants ( $s=0.11$ ) bring a moderate contribution to the short-term power system flexibility;
- Finally peak units such as OCGT, oil- or coal- fired plants bring flexibility only on a very limited timescale ( $s<0.02$ ).

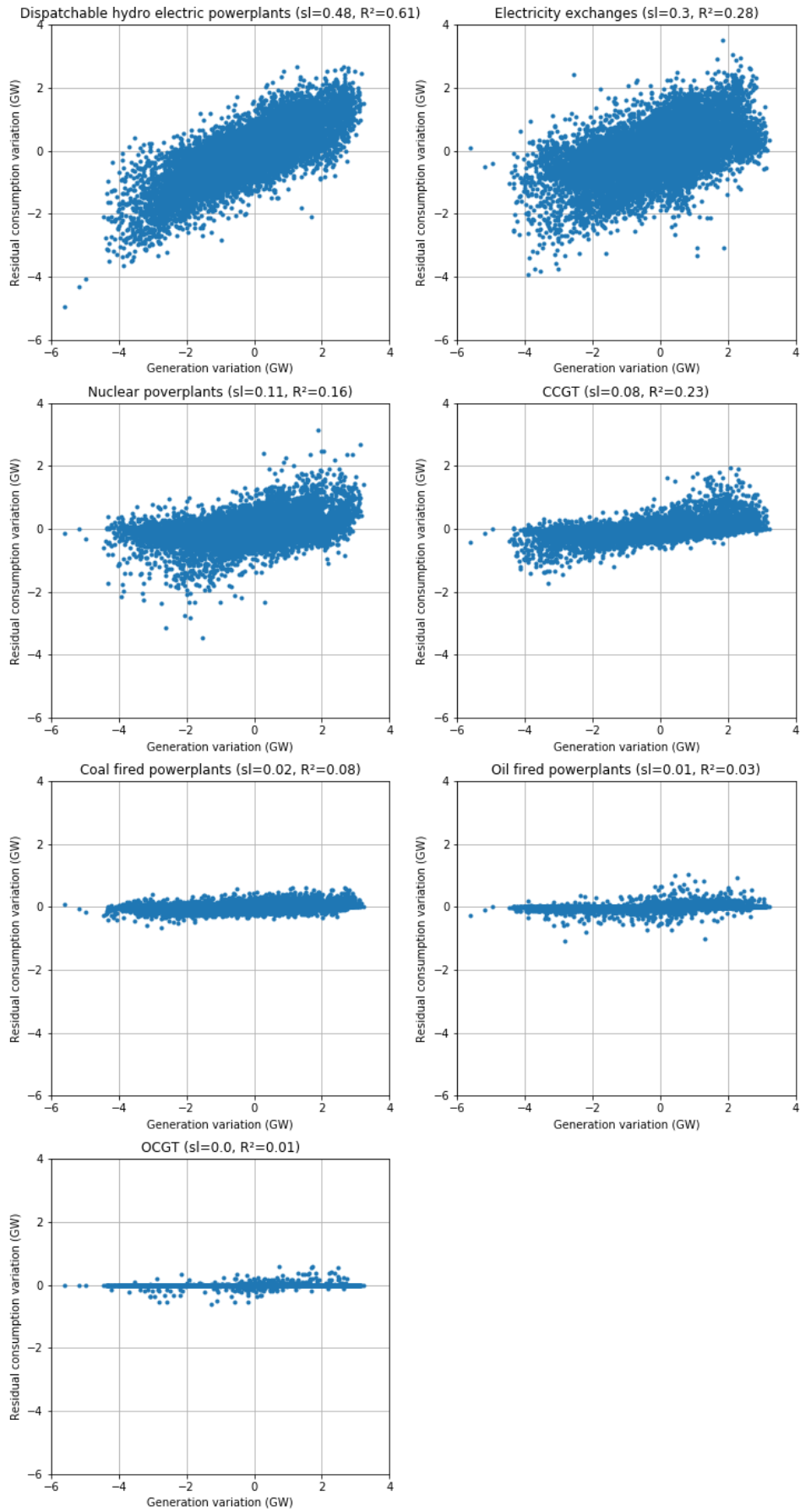


Figure 9: Correlation between the variation of electricity generation and the variation of the residual consumption for the French power system in 2018.

### 2.1.5. System and ancillary services

The balancing of demand and production maintains the frequency of the electricity grid around a reference value, which is 50 Hz in Europe. When the generation power is lower than the demand, the generation units decelerate and the frequency decreases. On the contrary, a generation power above the demand causes a frequency increase. An unbalance between the demand and the production is caused by inaccurate forecast of the consumption, of the generation level of the non-dispatchable units or by unplanned outages of the generation units or of the grid.

The system services are automatically activated in order to ensure this balance. They are divided in two reserves:

- At the European scale, the Frequency Containment Reserve (FCR) has to be able to replace the production of two major generation units (3000 MW in total) in less than 30 seconds. The share of the French grid on these 3000 MW is 600 MW.
- The secondary reserve (automatic Frequency Restoration Reserve: aFRR at the European scale) can be activated in less than 400 seconds and can provide 1000 MW in winter (500 MW in lower consumption periods).

The system services are sometimes not sufficient. Therefore, two tertiary reserves (named ancillary services) can be activated twice a day:

- The rapid tertiary reserve (manual Frequency Restoration Reserve at the European stage) can activate 1000 MW in less than 15 minutes during 2 hours. Coupled with the secondary reserve, the activable power is equivalent to the largest generation unit (1500 MW).
- The additional reserve (Replacement Reserve at the European level) can activate a power of 500 MW in less than 30 minutes during 1h30, in order to recover the reserve.

### 2.1.6. Post-market utilities

When there is no unit available in the intra-day market or that ancillary services are not sufficient to supply the electricity demand, two mechanisms can be activated: the electricity consumption of some large industrial consumers can be interrupted or the voltage of the grid can be decreased. These solutions do not affect private consumers. As a last resort, power can be cut in restricted areas and for a limited duration.

### 2.1.7. Main constraints to be considered in the calculation of marginal emission factors

Considering the general organization of the power systems described previously and the short-term flexibility analysis performed in Figure 9, the following constraints should be included when evaluating a marginal emission factor (MEF):

- Daily and intra-day dynamics: The dynamics of the power plants activation depends on the considered time frame, as illustrated in (Heggarty et al. 2020). For example, French coal-fired powerplants are rarely activated because of the high price of coal. These units, when scheduled, have to produce as much energy as possible to counterbalance the fixed cost of

switching them on. Electricity generation is then generally constant during the days they are activated. In this example, these units are highly flexible at the daily timescale, but provide limited flexibility on the hourly timescale. Consequently, the marginal mix and emission factor also varies with the dynamic of the marginal electricity consumption. A simple economic merit-order model based only on variable costs implies that rarely activated units (with high variable costs) have high flexibility during the day, which is not always the case. The order in which plants will be called up depends on the ratio between combustible and start up costs, and also on additional constraints such as the long-term strategy (for example, using French nuclear powerplants for flexibility) and the geographical or local policy constraints (for example, German protectionism regarding coal).

- Limited water reserves: Highly reactive and with low variable costs, dispatchable hydroelectric powerplants provide a large part of the power system's flexibility, but their water reserves are limited. The hydroelectricity generation being also low carbon, these units contribute to decreasing the MEF of electricity generation. The usage of the hydroelectric powerplants is optimized as a function of electricity consumption and the expected level of water in the reservoirs during the year. If additional electricity consumption is supplied by hydroelectric powerplants, the corresponding water resource is no longer available for future power generation and will thus trigger the activation of other powerplants. Neglecting the limitation of the water reserves would then lead to an underestimation of the MEF.
- Electricity exchange with interconnected countries: The balance between electricity demand and generation is ensured by both national electricity generation and exchanges. European countries being increasingly interconnected, it has become crucial to take into account the interaction with neighboring power systems in order to describe properly the national unit-commitment. The French power system being sized according to the winter peak demand, France exports electricity to the neighboring countries for much of the year, when the French electricity demand is low. If the French marginal powerplant has a lower variable cost than the marginal powerplant of a neighboring power system importing electricity from France, the units adapting their electricity to a change in the French consumption could be in these neighboring countries. The French power system emitting less than most of the European power system, neglecting the electricity exchanges could thus lead to an underestimation of the French MEF.

Regarding the time scale under evaluation, one should have in mind the scope of the thesis, which is the evaluation of control strategies for a fleet of hybrid heat pumps spread throughout France. Considering the reactivity of such hybrid heating systems, it is not possible to address system services. Consequently, the method to calculate the MEF of the electricity consumption should address variation in the demand from 30 minutes up to a week.

## 2.2. Life Cycle Assessment methodologies for the GHG emissions of electricity

Electrical systems are complex to model as they are organized on different time scales and depend on the interaction of several operators. The methodology for the evaluation of GHG emissions cannot

then be simple. In the following section, several Life Cycle Assessment (LCA) methodologies and options will be reviewed in order to make the most relevant choices.

The LCA is a methodology for evaluating the environmental impacts of a manufactured product, process or service at each stage of its life cycle. Four phases in the LCA methodology are described by the ISO 14040 methodology:

- goal and scope definition,
- inventory analysis,
- impact assessment,
- interpretation.

The two main types of LCA are attributional and consequential (Ekvall 2019) and are described in the following sections.

#### 2.2.1. Attributional methods

The attributional methodologies are used to assess the impacts associated to each stage of the life cycle and to estimate the share of the global environmental impact attributable to the product. Different hypothesis can be formulated depending on the consumption type (for all usages or differentiated according to the usage), the boundaries of the electricity production (national or including the international exchanges) and the time step (year, season, month or hour). Consequently, three main types of attributional LCA can be identified:

- The average attributional method assesses the impacts during a time period long enough to give a global estimation of the impact for the consumption of 1 kWh of electricity.
- The attributional dynamic method (seasonal, monthly or hourly) includes the temporal variation of the system.
- The attributional method by usage and seasonally-adjusted evaluates the impact for each usage taking into account the variation in time of the usage.

#### 2.2.2. Consequential methods

The consequential methodologies are used for the evaluation of the impacts due to the production and use of the product and assess the changes on the margin of the system. In the context of power systems evaluation, the short-term consequential LCA (also named “operating margin”) refers to an increase or decrease of electricity demand during a short period and of a restricted amplitude to avoid the modification of the installed electricity generation capacity. Such an approach requires an investigation of the impact of a demand variation on the power system. This means identifying the GHG emissions of a set of generation units, referred to here as the “marginal emissions” and the “marginal mix” that will adapt their generation level consequent to this variation in demand. Long-term consequential LCA (also named “build margin”) is applied to evaluate the impact due, for example, to major changes in the demand patterns leading to variations in the installation of new generation units. Several articles summarized the existing approaches to assess the short-term MEF of power systems and generally identify two main categories (Ryan, Johnson, and Keoleian 2016; Fleschutz et al. 2021; Braeuer, Finck, and McKenna 2020):

- Methods without a model of the electrical system (also named “Empirical Data & Relationship Models” in (Ryan, Johnson, and Keoleian 2016) and (Fleschutz et al. 2021)):

- One method consists in determining a marginal powerplant, and consequently a marginal emission factor for a whole year.
- Another method considers that the current market price of electricity always corresponds to the variable cost of the marginal powerplant and then deduces the marginal emission factor directly from the market price of electricity (Rogers et al. 2013). However, other factors such as grid congestion can also impact the market price.
- A third method consists in reconstructing the economic merit-order of the power system for every hour, the marginal powerplant being the last activated at current load according to this merit-order (Fleschutz et al. 2021). McKenna and Darby (McKenna and Darby 2017) applied this method to evaluate the impact of demand response on power systems. The GHG protocol suggests that power plants from the highest tenth of the merit-order are marginal (Broekhoff 2005).
- (Braeuer, Finck, and McKenna 2020) evaluated the MEF of the electricity generation for each hour of the year 2017 in Germany as the ratio between the change in the dispatchable generation and the change in the GHG emissions related to the dispatchable electricity generation.
- (Hawkes 2010) calculated the MEF using a linear regression between the change in the total GHG emissions and the change in the demand. In order to improve the results, the data can be separated in set depending on parameters and several factors can be used depending on the context.
- More complex machine learning models can also be used in a similar way (Corradi 2018).

These methods are often based on historical data and are relatively easy to implement, but the results might be insufficiently robust and depend on the data used for the calibration. These methods usually do not take into account the duration or the dynamics of the variation, neither the water reserve conservation. Moreover, most of these methods assess the marginal mix of national electricity generation rather than electricity consumption since they do not consider electricity exchanges.

- Methods with a model of the electrical system (also named “Power system optimization” models): In this second approach, the marginal electrical mix can be deduced from the difference between the electricity mix of the national consumption with and without marginal consumption, both mixes being obtained using a model of the power system. Figure 10 describes this method. The economical, technical, geographical and political constraints can be taken into account depending on the power system model complexity. However, this method requires in-depth knowledge of the electrical system and a model with a sufficient level of detail.

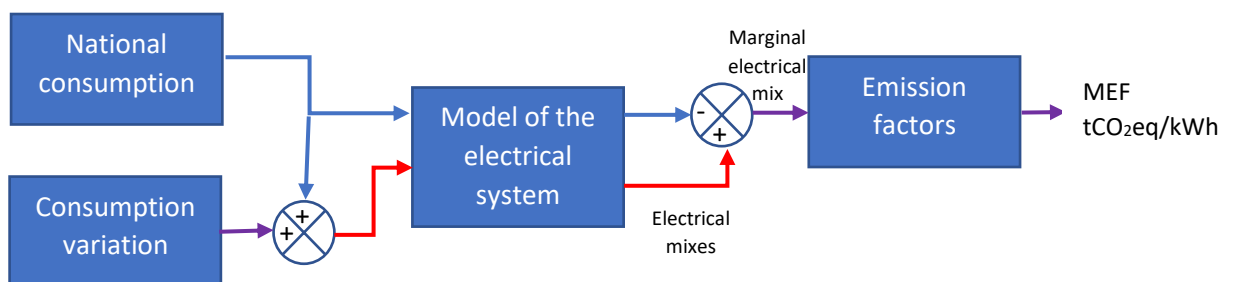


Figure 10: Assessment of the MEF of the electricity consumption using a model of the electrical system



### 2.2.3. Definition of the objectives and scope of the study

The objective of this section is to identify methodologies to assess the GHG emissions avoided consequently to a short-term change of electrical consumption on the demand-side, i.e. a switch between a heat pump and a gas boiler for heating buildings. Several LCA methodologies were presented in the previous section and their strengths and weaknesses are summarized in Table 3. For real-time control of hybrid systems, the attributional methodology is not sufficient because fuel-switching will only affect the electrical system on the margin for a few hours or a few days (i.e. not all power plants will be affected by such a change). This objective corresponds thus to a short-term consequential LCA approach as long as the avoided electricity consumption is in the range of the winter peak consumption (and thus the current installed capacities). Throughout the thesis, a case study is selected that is consistent with the French long-term environmental goal (see Chapter 4). In “*Energy pathways to 2050*”, the French TSO published different targets for electricity demand reduction potential exceeding one hour in residential heating, which should be partly covered by hybrid heat-pumps. In the different scenarios the required maximum flexibility varies from 0 up to 5.6 GW (RTE 2022c).

Table 3: Comparison of the attributional and consequential methodologies for LCA

	Attributional LCA	Consequential LCA
<b>Principle</b>	Assess the overall emissions and sharing them across all electricity consumers in proportion to their demand	Assess the change in emissions due to a change in demand
<b>Advantages</b>	Transparency of the method  Robust	Decision support tool  Provide information on the dynamics of the system
<b>Drawbacks</b>	No indications about the dynamics of the electrical production system  No indications about the usage of a product	Difficulties to evaluate the marginal error of the model  Model accuracy dependent on the number of causalities included in the model  Feasibility  Cost  Uncertainty

Additionally, the consequential approach should fit the following criteria:

- Geographical area: France, including interconnections
- Time-step: 0.5h
- Duration of the variation: short-term (few hours up to few days)
- Type of variation: marginal mix due to a decrease of the electrical consumption from space heating and DHW production in the residential sector
- Target for the model accuracy: uncertainty of the model lower than the avoidable emissions

To ensure the accuracy of the evaluation of the avoided GHG emissions, a method based on a power system model (power system optimization models) should be preferred and will be developed in the next chapter. Figure 11 presents the power system models classification according to their time resolution. The level of detail required for such models decreases when the time resolution of the model increases. In this thesis, the model is used to identify the impact on the power system of the electricity consumption of hybrid-heat pumps from 30 minutes up to a few days. Consequently, Unit-Commitment and Economic Dispatch models are the most appropriate for this type of analysis. Such models will be reviewed in section 2.4.

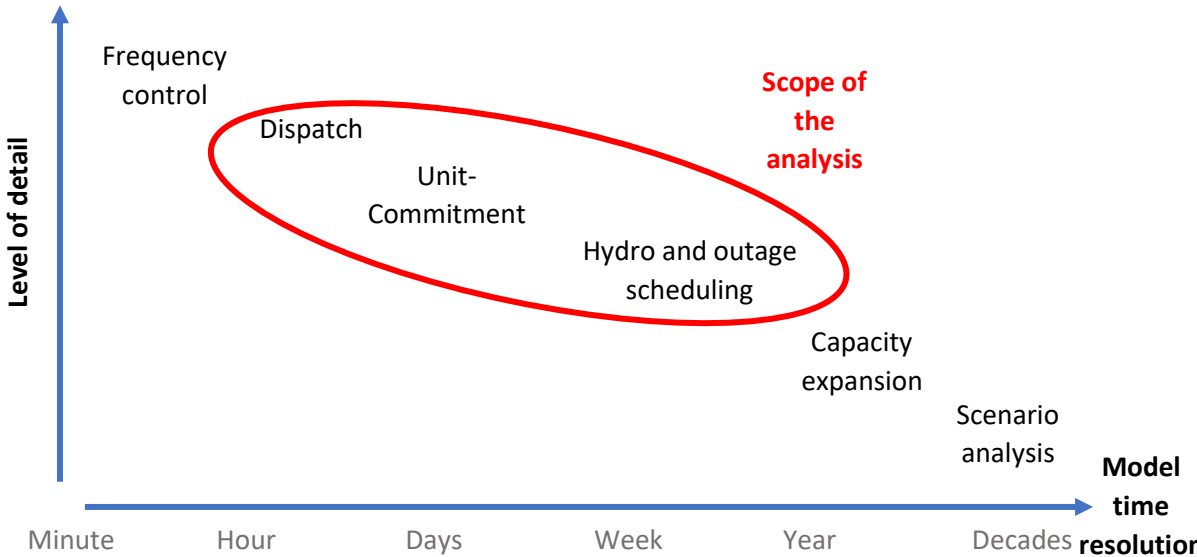


Figure 11: Power system models classification according to their time resolution

2.2.4.Data for the environmental inventory

The choice of data for the environmental inventory has a major impact on the evaluation of the carbon footprint. In order to derive the marginal emission factor from the marginal mix, the impact of the entire process up to the heat generation, as represented in Figure 12, has to be inventoried. In this section, the choice of the emission factors for the electricity generation and the distribution losses are discussed.

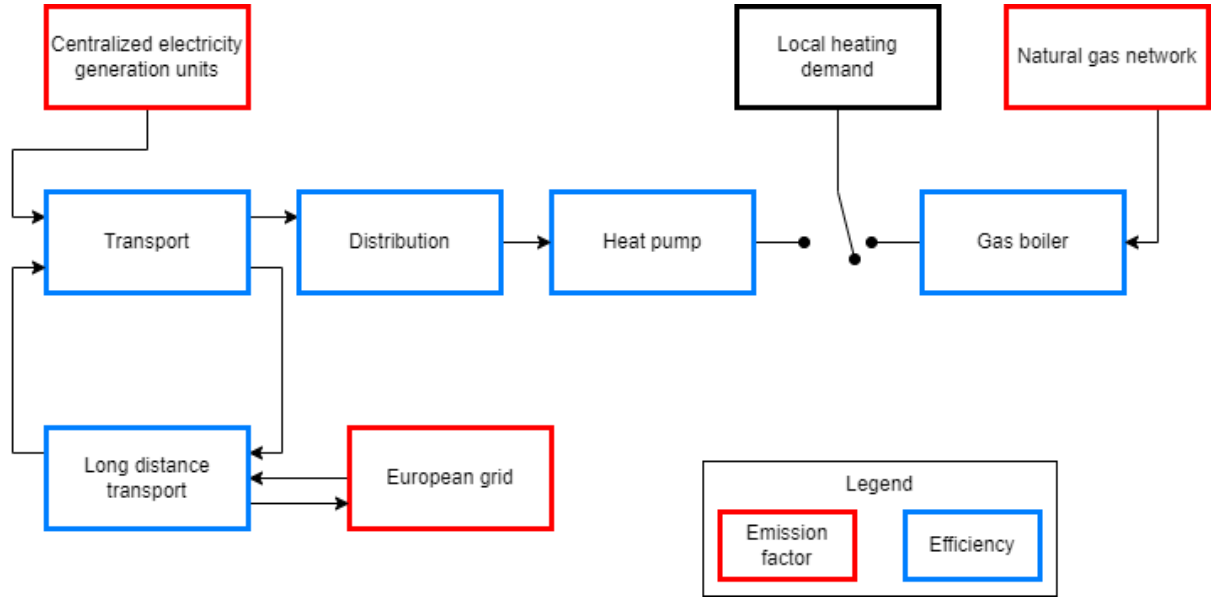


Figure 12: Diagram of the process of heat generation

As the model to evaluate the MEF considers electricity exchanges across Europe, the emission factor applied for the generation units should correspond to a European inventory. In addition, it could be interesting to evaluate the effect of fuel-switching using indicators other than the GHG emissions. Consequently, the emission factors were evaluated using the *ecoinvent 3.0* (Ecoinvent 2013) database for the inventory and adjusted with IPCC 2021 for the global warming potential of GHG (Masson-Delmotte, V., P. Zhai, A. Pirani, Connors, C. Péan, S. Berger, N. Caud, Y. Chen, L. Goldfarb, M.I. Gomis, M. Huang, K. Leitzell, E. Lonnoy, and Matthews, T.K. Maycock, T. Waterfield, O. Yelekçi, R. Yu 2021). As the analysis is marginal, the infrastructure processes were excluded from the inventory.

### Electricity generation

The data from *ecoinvent* could not be used directly to evaluate GHG emissions for the French CCGT power plants due to inconsistencies. The emission factor for French CCGT is  $0.545 \text{ t}_{\text{CO}_2\text{eq}}/\text{MWh}$ , which seems too high. For comparison, according to ADEME, the emission factor (excluding infrastructure emissions) is  $0.352 \text{ t}_{\text{CO}_2\text{eq}}/\text{MWh}$  for electricity generation from gas in France (ADEME 2020). In this thesis, the efficiency of the electricity generation from natural gas in France was evaluated on the basis of the Eurostat data using Equation 3.  $E_{\text{gas powerplants}}^{\text{in}}$  is the primary energy input of the gas-fired powerplants,  $E_{\text{gas powerplants}}^{\text{out}}$  and  $E_{\text{gas grid}}^{\text{in}}$  are respectively the gross electricity generation from natural gas and the energy injected in the gas network. *Losses* are the losses due to gas distribution. The corresponding efficiency assumed in *ecoinvent* is evaluated using Equation 4 with  $V_{\text{NG},\text{ecoinvent}}^{\text{in powerplants}}$  the volume of natural gas consumed to generate 1 MJ of electricity on the French gas fired powerplants.  $35.2 \text{ MJ}/\text{m}^3$  corresponds to the lower heating value of the gas combustion used in *ecoinvent*. The corrected emission used for the French CCGT is calculated using Equation 5.

$$\eta_{\text{eurostat}} = \frac{E_{\text{gas powerplants}}^{\text{out}}}{E_{\text{gas powerplants}}^{\text{in}}} \cdot \frac{E_{\text{gas grid}}^{\text{in}} - \text{Losses}}{E_{\text{gas grid}}^{\text{in}}} \quad 3$$

$$\eta_{\text{ecoinvent}} = \frac{1 \text{ MJ}}{35.2 \text{ MJ}/\text{m}^3 \cdot V_{\text{NG},\text{ecoinvent}}^{\text{in gas powerplants}}} \quad 4$$

$$EF_{corr} = EF_{ecoinvent} \cdot \frac{\eta_{ecoinvent}}{\eta_{eurostat}}$$

5

The emission factors for plants other than "Fossil Gas" (e.g. in OCGT) have been taken directly from the *ecoinvent* database without any additional modification. The emission factors used in this thesis for the other European countries are detailed for each country and each type of combustible in Table 4. The generation sets of the countries interconnected with the French power system is based on the data from the transparency platform (ENTSOE 2020). However, this platform does not detail the specific generation sets for each type of technology using the same fuel. Consequently, it is not possible to differentiate power generation from CCGT and OCGT. In this thesis, the emission factor for the category "Fossil Gas" corresponds to CCGT powerplants to avoid an overestimation of the emissions. The variation of the emission factors between the different countries can be explained by differences in the origin of fuel, in losses during the transportation of gas, and in the efficiency of the plants. According to the information in the documentation, the plant efficiency has the greatest impact on the variation of the emission factor. This variation in the plant efficiency can be explained by the age of the fleet, the maturity of the technology and the load factor of the fleet. Indeed, the efficiency of the process depends on the level of generation.

Table 4: Emission factor of the powerplants for the different countries included in the model

	Emission factor (tCO <sub>2eq</sub> /MWh)					
	Fossil Brown coal/ Lignite	Fossil Gas	Fossil Hard coal	Fossil Oil	Fossil Peat	Nuclear
Austria (AT)		0.514	0.973	1.121		
Denmark (DK)		0.346	0.973	1.205		
Luxembourg (LU)		0.389		0.834		
Spain (ES)		0.472	1.158	0.842		0.006
Sweden (SE)				0.830	1.162	0.006
Belgium (BE)		0.415	1.102	0.887		0.006
Croatia (HR)	1,271	0.723	1.126	0.932		
Czech Republic (CZ)	1.179	0.482	1.202	1.034		0.006
France (FR)		0.327	1.079	0.926		0.006
Germany (DE)	1.227	0.430	1.069	0.850		0.006
Greece (GR)	1.302	0.613		0.965		
Ireland (IE)		0.372	1.038	0.892	1.017	
Italy (IT)	1.117	0.469	1.088	1.0289		
Malta (MT)		0.389		1.186		
Montenegro (ME)						
Netherlands (NL)		0.377	1.014	0.772		0.006
Norway (NO)		0.346		0.471		
Poland (PL)	1.117	0.441	0.973	0.834		
Portugal (PT)		0.444	1.074	0.809		
Slovenia (SI)	1.196	0.389		1.347		0.006
Switzerland (CH)		0.389				0.006
United Kingdom (UK)		0.353	1.074	1.284		0.006

Electricity losses during transport ( $Losses_{Tr}$ ) and distribution ( $Losses_{Dis}$ ) are estimated at 2.16% (RTE 2018) and at 6.02% (Enedis 2019). We also consider that electricity imported or exported suffer additional losses due to transportation beyond the French borders. This long-distance transportation losses ( $Losses_{exch}$ ) are set to 2% of the electricity exchanges. The power losses between the generating unit and the consumer are then dependent on both the location of the plant and of the end-user. Three cases were identified:

- Case 1 : When electricity is produced in France (Figure 13), the losses only include transport ( $Losses_{Tr}$ ) and distribution ( $Losses_{Dis}$ ) (Equation 6).



Figure 13: Transport and distribution of 1 kWh marginal electricity from the national power system

$$(1 - Losses_{FR}) = (1 - Losses_{Tr}) \cdot (1 - Losses_{Dis}) \quad 6$$

- Case 2 (imports) :

When France is a net importer (Figure 14), the losses include long-distance transport ( $Losses_{LD Tr}$ ), transport and distribution (Equation 7).

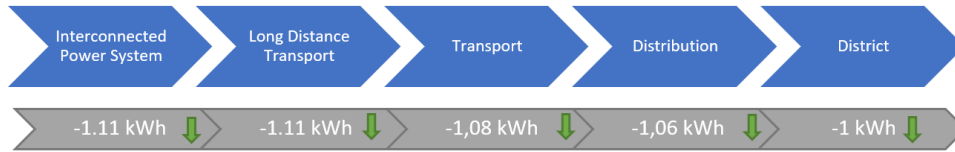


Figure 14: Transport and distribution of 1 kWh marginal electricity from imports

$$(1 - Losses_{imp}) = (1 - Losses_{LD Tr}) \cdot (1 - Losses_{Tr}) \cdot (1 - Losses_{Dis}) \quad 7$$

- Case 3 (exports)

When France is net exporter (Figure 15), the marginal variation of the French exports is compensated by the countries exporting to the same countries as France. It is supposed that the long-distance transport losses are the same in the case of electricity exported from France or from another exporting countries. Consequently, the long-distance transport losses are the same in both cases. The losses only include transport and distribution (Equation 8).

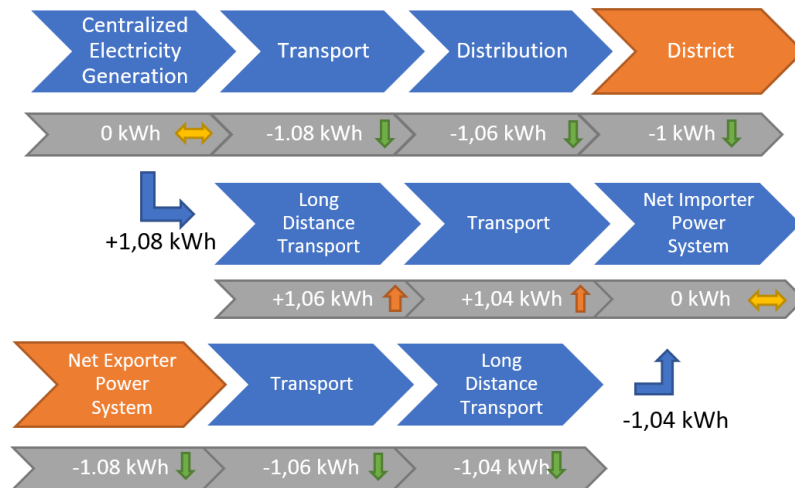


Figure 15: Transport and distribution consequently of the decrease of local heating in case of marginal net exports

$$(1 - Losses_{exp}) = (1 - Losses_{Tr}) \cdot (1 - Losses_{Dis})$$

8

### Gas boiler

The environmental impact of the gas boiler is evaluated using the inventory for “Unit Heat, district or industrial, natural gas” for the location “Europe without Switzerland”. The corresponding emission factor is 0.251 t<sub>CO<sub>2</sub>eq</sub>/MWh.

## 2.3.Simplified evaluation of the Marginal Emission Factor of electricity generation and consumption in Europe

In order to get a rough estimate of the potential of hybrid heat pumps to decarbonize the domestic heating, an evaluation based on a simplified model is performed. A large part of the flexibility of the French power system being provided through cross-border electricity exchanges, the analyze of the power systems of the neighboring countries should be included to evaluate the Marginal emission Factor (MEF) of the electricity consumption in France. Methods for assessing the MEF of electricity consumption that are not based on power system models are easy to implement and suitable for evaluation at European level and potential analysis. Consequently, this section presents a method to estimate the MEF of electricity exchanges and then of electricity consumption in France.

In this section, a simplified method to evaluate the MEF of electricity consumption in France, considering electricity exchanges with other European countries, is developed based on the method proposed by (Hawkes 2010). This model is of the type “Empirical Data & Relationship Models”. Then the method to evaluate the MEF of the electricity generation is applied to European countries. Using these MEF and a flow tracing method, the MEF of French electricity exchanges is evaluated. Finally, a first assessment of the MEF of the French electricity consumption depending on the residual consumption on the French power system is presented. However, to ensure the accuracy of the evaluation of the avoided GHG emission, a method based on a power system model should be preferred and will be developed in the next chapter.

### 2.3.1.Simplified method for the assessment of the marginal emission factor

The best method to assess the MEF of the generated electricity in the interconnected countries would be to use a power system model bounded by the national perimeter for each country. Such a model was not available in the context of this study. Therefore, we used the approach developed by (Hawkes 2010). It allows to calculate the MEF of a power system without the need of a power model. This method is based on the hypothesis that, considering a time interval  $[t - \Delta t ; t]$ , a variation of electricity production ( $\Delta E$  in MWh) always leads to a proportional variation of GHG emissions ( $\Delta GHG$  in  $t_{CO2eq}$ ) during the same time interval. The method is thus based on the following equation:

$$MEF(t, \Delta t) \cdot \Delta E(t, \Delta t) = \Delta GHG(t, \Delta t) \quad 9$$

The variation of the electricity production and of the GHG emissions are derived from the power data from TSO ( $P_{TSO}$  in MW) using Equation 10.

$$MEF(t, \Delta t) \cdot \left( \int_t^{t+\Delta t} P_{TSO}(t) dt - \int_{t-\Delta t}^t P_{TSO}(t) dt \right) = \left( \int_t^{t+\Delta t} P_{TSO}(t) \cdot EF(t) dt - \int_{t-\Delta t}^t P_{TSO}(t) \cdot \overline{EF}(t) dt \right) \quad 10$$

The MEF calculations based on this method and found in the literature differ mainly in two characteristics:

- **The clustering of the variables:** this method is usually applied by grouping the observed variables ( $\Delta GHG$  and  $\Delta E$ ) according to various parameters (electricity generation, week days or weekend, season, hour of the day, amount of renewable in the mix, etc). In (Huber et al. 2021), the variables are grouped according to the load level and in (T. Q. Péan, Salom, and Ortiz 2018) the variables are groups according to both the system load and the share of the renewable generation.
- **The definition of  $\Delta E$ :** The calculation of  $\Delta E$  can be based on different time series  $P_{TSO}$  (in MW) (whole electricity production (T. Q. Péan, Salom, and Ortiz 2018) or dispatchable production only, etc) depending on the assumptions made in the study. (Braeuer, Finck, and McKenna 2020) express the necessity to define the boundaries of the system (consumption or production based approach).

After the calculation of the time series ( $\Delta E$  and  $\Delta GHG$ ) and the clustering of data, a regression is performed between the variation of the GHG emissions and of the electricity production to observe the presence of a trend.

However, several limitations of such models have to be addressed and are listed below:

- The water reserves conservation for the hydroelectric powerplants is usually not considered. Hydroelectric powerplants are the most reactive plants in power systems and are often responsible for a large part of the load following. These powerplants should then have a large impact in the calculation of the MEF. Moreover, these powerplants have a very low emission factor meaning that in countries with a large hydroelectric capacity, a variation of electricity production does not always lead to a proportional variation of the GHG emission. However, the water resources are limited, which means that an additional electricity demand supplied with a hydroelectric plant will affect the availability of the water resource for a later production. This limitation is rarely addressed in the literature. In this thesis, a fictive emission

factor corresponding to the powerplants replaced by the use of the water resources is attributed to the hydroelectric generation. These powerplants should be those that have been marginal during the past 7 days. In this model the fictive emission factor is then chosen as the weekly mean MEF calculated without the hydroelectric powerplants in the electricity production. In reality, electricity exchanges should also be included in the fictive emission factor of the hydroelectric powerplants, which is not the case using this method. In the case of France, this should lead to an underestimation of the emission factor, as the French power system is less carbon-intensive than most of the European countries.

- Many researchers assess the MEF related to electricity generation instead of consumption by neglecting the electricity exchanges. However, in the case of France, electricity exchanges provide flexibility to the power system. In this thesis, the method was applied with a calculation of  $\Delta GHG$  and  $\Delta P$  based on dispatchable powerplants to assess the MEF of the electricity generation in each country. Afterwards, the obtained MEF can be used to evaluate the MEF of the electricity exchanges. To do this, it is necessary to determine the balance of the countries exchanging electricity with France. It should be noted that the real source countries are not necessarily the neighboring countries, as electricity can pass through many countries before reaching its final destination. It is therefore not sufficient to measure the physical exchange of electricity across each French border. Consequently, a model is described in the next section to determine for each time step the source or destination of the electricity exchanges through Europe.
  
- The impact of the dynamics of the marginal demand (e.g. duration) cannot be included in such a model as they are generally built with a time interval between only 30 minutes and one hour. The sensitivity of the method to a change in the considered time interval will be evaluated later. However, a larger time interval should lead to a higher MEF considering the decrease of the impact of the hydroelectric powerplants for larger time intervals. Choosing a short time interval then avoids an overestimation of the MEF. The methodology is thus conservative.

In summary, the method explained previously (Equation 9) is adapted to evaluate the MEF of the electricity consumption at a hourly granularity, considering the limited water reserve of the hydroelectric powerplants and the cross-border electricity exchanges. The methodology follows these four steps:

1. **Evaluation of the fictive emission factor of the hydroelectric powerplants for each European country (rolling average MEF over 7 days) by applying linear regressions:**
  - with  $P_{TSO}$  being the sum of the dispatchable units, hydroelectricity excluded
2. **Evaluation of the MEF of electricity generation for each European country by applying linear regressions (see Section 2.3.2):**
  - with  $P_{TSO}$  being the sum of the dispatchable units
  - and using the fictive emission factor for hydroelectricity for the calculation of  $\Delta GHG$  (see step 1).
3. **Evaluation of the MEF of the electricity exchanges in France (see Section 2.3.3):**
  - tracing the flow of the cross-border exchanges of France with other European countries,



- And summing the MEF of the electricity exchanges for each European country (see step 2) weighted according to the cross-border exchange balance.
- 4. Evaluation of the MEF of the French electricity consumption by applying linear regressions (see Section 2.3.4):**
- with  $P_{TSO}$  being the French residual consumption,
  - using the fictive emission factor for hydroelectricity for the calculation of  $\Delta GHG$  (see step 1),
  - and the MEF of electricity exchanges in France (see step 3).

### 2.3.2. Marginal emission factor of the electricity generation for each European country

The data used to calculate the variation of the dispatchable production  $\Delta P$  and of the GHG emissions  $\Delta GHG$  corresponds to the electricity mix for each country from the European TSO (ENTSOE 2022). The method detailed previously was applied for each country after clustering the yearly time series ( $\Delta GHG$  and  $\Delta P$ ) in 20 groups of similar size according to the level of dispatchable production of the power system. A linear regression was then applied twice: the first one to evaluate the fictive emission factor of the hydroelectric powerplants (step 1), and the second one to evaluate the MEF of the electricity generation in each country (step 2). Figure 16 describes this second linear regression for the German and French power systems.

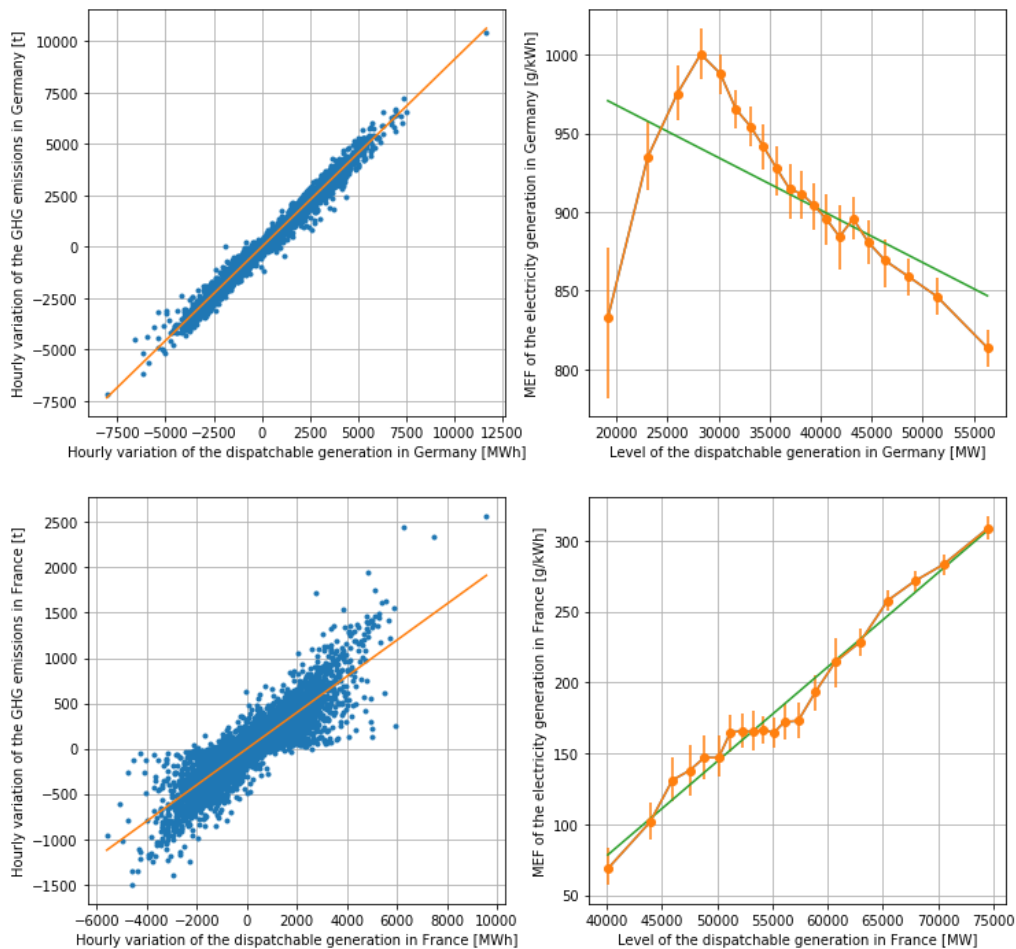


Figure 16: Hourly variation of the GHG emissions depending on the related variation of the dispatchable generation in Germany and France (left) and variation of the MEF across different generation levels generation in Germany and France (right)

Figure 17 presents the MEF for electricity generation obtained for several countries depending on the normalized dispatchable production level and the associated 95% confidence interval. In this figure, the dispatchable production was normalized by scaling the residual consumption between 0 and 1. The ordinate of 0 corresponds to the low consumption level of the country and 1 to the high consumption (typically in winter).

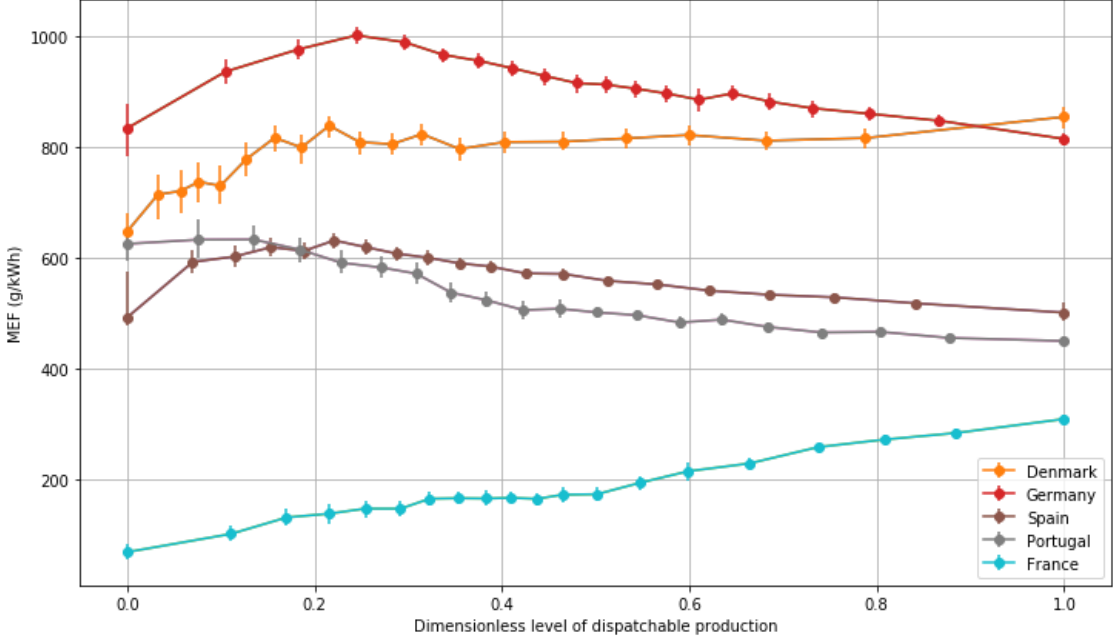


Figure 17: MEF of the electricity generation in several European countries depending in the normalized residual consumption of each country.

In this thesis, the method is considered valid for the countries with a coefficient of determination above 0.8 for the 20 groups of data. Figure 18 shows these coefficients of determination for the different countries. The method is thus not considered as valid for France, Sweden, Switzerland and Norway, which have a large share of low-carbon electricity in their mix. In the case of Sweden, Switzerland and Norway, the average emission factor is near zero. For these three countries, an emission factor of zero is then chosen. Due to a lack of data, the MEF for Luxembourg and Malta cannot be evaluated and is then also set to zero.

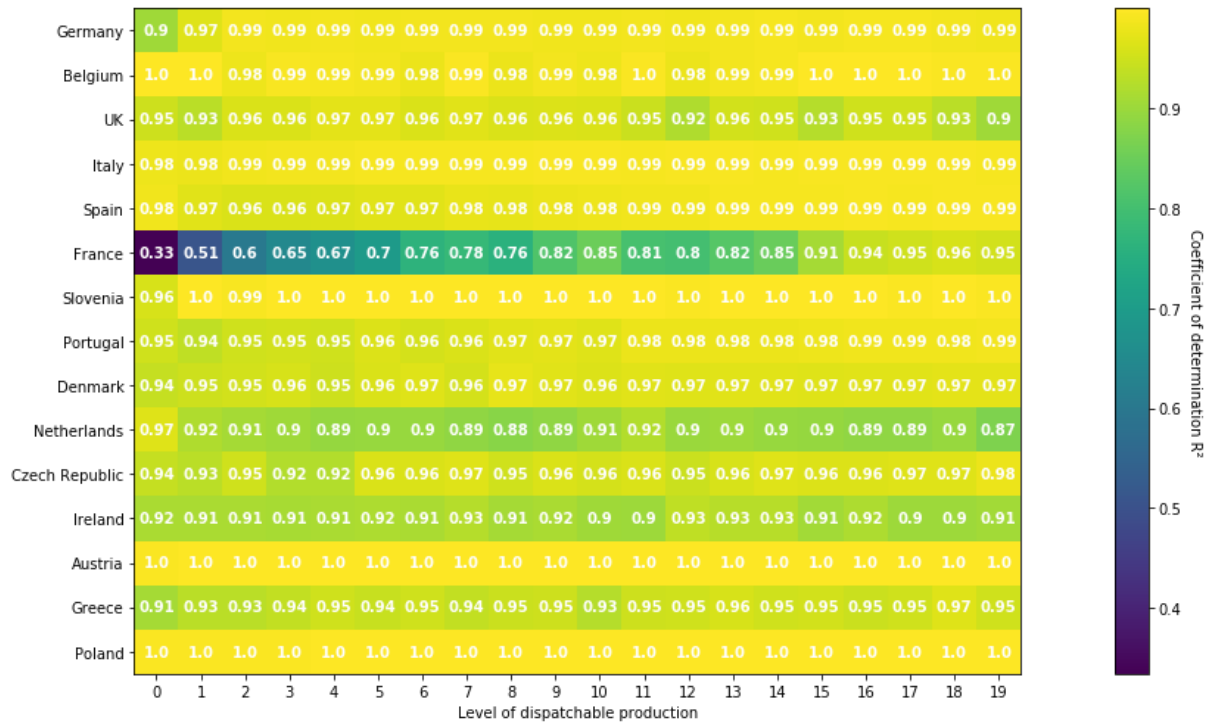


Figure 18: Coefficient of determination of the (second) linear regression for different power systems in Europe

For each country, a third linear regression is applied over the 20 values of MEF and the corresponding residual consumption  $RC_{country}$  in MW (see green line in Figure 16). The resulting slope coefficient  $s_l$  and intercept  $int$  are summarized for each country in Table 5. The MEF for electricity generation (in  $kg_{CO2eq}/MWh$ ) can then be calculated for each country at time step  $t$  using Equation 11.

$$MEF_{gen}(t, country) = s_l_{country} * RC_{country}(t) + int_{country} \tag{11}$$

It can be clearly seen in the previous figures and in Table 5, that, in Germany as in many European countries, the marginal emission factor decreases when the generation level increases (leading to a negative value of  $a$ ). This means that the technologies with the lowest variable production costs emit the most. Germany uses coal for its electricity production, which explains this trend. In (Fleschutz et al. 2021), the MEF and the prices for electricity generation in 20 European countries were calculated for the years 2017-2019. The same effect, named “merit-order dilemma”, was noticed in several European countries including Germany.

Table 5: Coefficients to apply to evaluate the MEF of the electricity production

Country	Slope coefficient $s_l$ [ $kg_{CO2eq}/MWh.MW$ ]	Intercept $int$ [ $kg_{CO2eq}/MWh$ ]
Germany	-0.004	1040
Belgium	-0.001	406
UK	0.006	306
Italy	-0.002	568
Spain	-0.006	696

Country	Slope coefficient $sl$ [ $kg_{CO_2eq}/MWh.MW$ ]	Intercept $int$ [ $kg_{CO_2eq}/MWh$ ]
France	0.005	-148
Slovenia	0.024	1082
Portugal	-0.033	660
Denmark	0.064	730
Netherlands	-0.011	591
Czech Republic	-0.025	1070
Ireland	-0.008	531
Austria	-0.001	541
Greece	0.014	668
Poland	-0.002	1052

### 2.3.3. Marginal emission factor of the exchanged electricity (flow tracing)

The MEF for electricity generation in the different European power systems can be evaluated using the previous method. These MEF can be used to approximate the MEF of the electricity exchanges, which is necessary to evaluate the GHG emissions from electricity consumption in a country. The cross-border physical flows of electricity in Europe are available in the “Transparency Platform” from ENTSOE (ENTSOE 2020) and can be used to evaluate the electricity exchanges. However, this is not sufficient as the source/destination of electricity needs to be identified and, more importantly, the countries whose production level will be impacted by the demand-response (DR) events. For each time step, there is a balance at the European level between the total electricity production, the transmission and distribution losses and the electricity consumption. Some countries (net exporters) thus produce more electricity than they consume, while others (net importers) produce less than they consume and need this excess power. (Bialek 1996) proposed an algorithm based on proportional sharing to trace back the flow of electricity in an electricity grid. It relies on the assumption that each country is considered as a “perfect mixer” for all the imported and exported flows. The amount of electricity consumed by each net-importing country from the national production of each exporting country can then be estimated. This method uses the physical exchange of electricity at the border between countries at each time-step. The list of countries potentially impacted  $L_{exch}$  is built up by including countries successively until the excluded countries have, on average, a total impact lower than 5% on the yearly French exchanges. This results in a list of 22 countries (including France) integrated in the flow-based model. This method indicates, for each time-step, the proportion of French exports consumed by each net-importing country or the proportion of French imports produced by each net-exporting country.

Now that we have identified the drivers of electricity flows in Europe, we need to discuss how these exchanges will vary as French consumption varies. It is assumed that in net importing countries, the power system is either saturated or could produce more electricity but at a price higher than the market price and thus that they will not adapt their electricity generation. Consequently, for each time step, only the net exporters can adapt their electricity generation following a variation in French exchanges that would be caused by DR events. At each time-step  $t$ , two situations can be distinguished:

- When France produces less electricity than its national demand, France is a net importer. The countries adapting their electricity generation are then the countries from which France imports electricity.
- When France produces more electricity than its national consumption, France is a net exporter. As it is considered that only net exporters can adapt their electricity generation, the countries adapting their generation consequent to a change in French exchange are the countries exporting electricity to the same countries as France.

This method does not consider possible congestion issues, which would further reduce the number of countries adapting their production.

Figure 19-a represents, for each hour of 2018, the countries which adapt their electricity generation if the cross-border exchange is marginal. Each color represents a country and the y-axis shows the share of the exchange variation compensated by this country. The country that most compensates the decrease of the French exports is Germany, which seems logical as Germany and France are the biggest exporters in Europe. Most of the time, France and Germany compete for exports to the same countries and when French exports decrease, German electricity production and exports increase. However, during spring Germany is replaced by Switzerland. This observation can be explained by the high share of hydroelectric powerplants in the Swiss power system: as the snow melts the hydroelectric power generation is higher, decreasing the electricity price.

The marginal emission factor of the electricity exchanges  $MEF_{exch}$  is then calculated for each timestep using Equation 12 :

$$MEF_{exch}(t, FR) = \sum_{i \in L_{exch}} r_{exch}(t, i) \cdot MEF_{gen}(t, i), \quad 12$$

where

- $i$  denotes the country potentially affected by the variation of in exchanges, from the list  $L_{exch}$  (i.e. most of the European interconnected countries);
- $MEF_{gen}(t, i)$  is the marginal emission factor in  $t_{CO_2 eq}/MWh$  of the electricity generation in country  $i$  at the timestep  $t$  evaluated using the Equation 11;
- $r_{exch}(t, i)$  is the ratio (between 0 and 1) of the variation of the French exchanges compensated by the country  $i$  at the timestep  $t$ . To ensure power conservation, the sum of all the ratios  $r_{exch}$  is forced to one at each timestep.

In addition, the losses for long distance transport are included in the calculation when France is a net importer as stated in section 2.2.4. Figure 19-b represents the MEF of the electricity exchanges for France in 2018 calculated with the method described above. What is striking in this figure is the high variability of the MEF. These results highlight then the importance of the use of a dynamic MEF for the electricity exchanges.

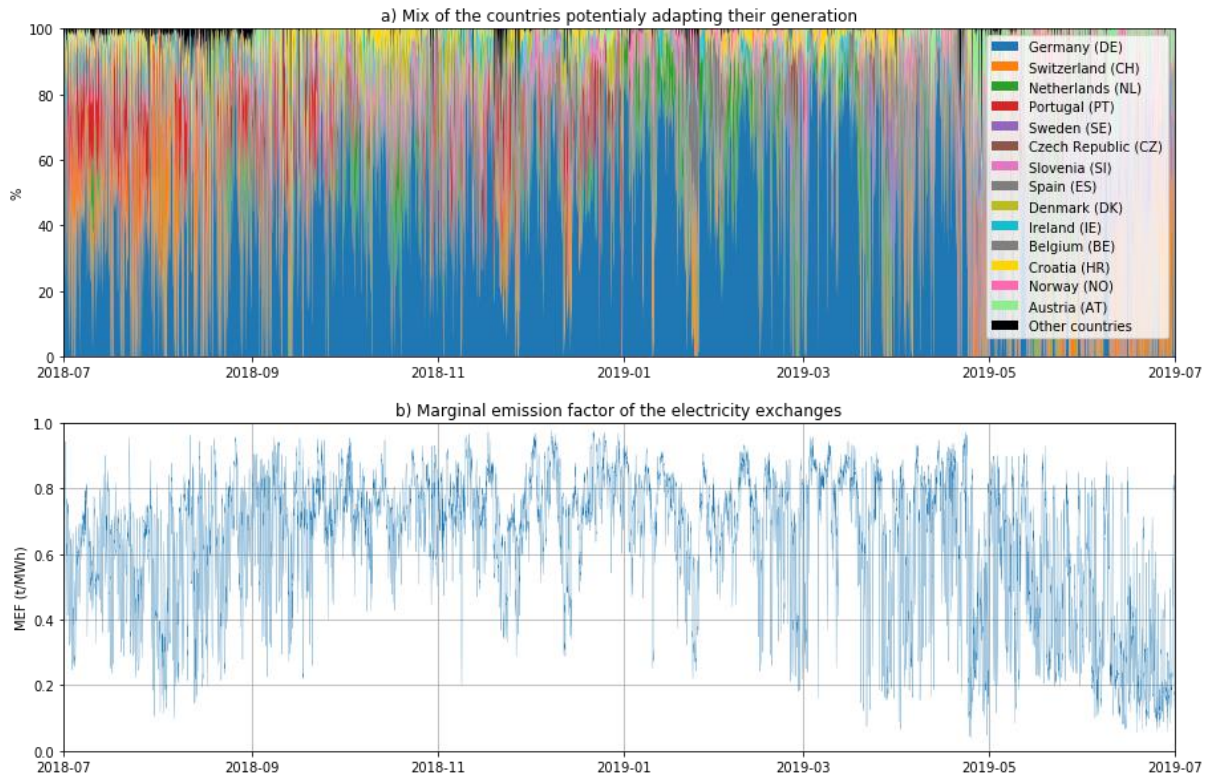


Figure 19: Countries adapting their generation in case of cross-border exchanges being marginal in France (a) and the associated marginal emission factor (b).

#### 2.3.4. First estimation of the marginal emission factor of the electricity consumption in France

The method presented in section 2.3.1 can be used to evaluate the MEF of the electricity consumption in a country. In this case,  $P$  includes the sum of the dispatchable units and also the balance of the physical electricity exchanges (positive for import, negative for export).  $GHG$  includes the sum of emissions from the national power system and from the exchanges (positive for import, negative for export). For the French power system, the resulting  $GHG$  value is thus sometimes negative due to the difference between the French MEF and the one of the cross-border exchanges and the amount of exports. The emission factor corresponding to the electricity exchanges is the one calculated in the previous sections, weighted according to the origin/destination of electricity. Figure 20 presents a first estimation of the French MEF calculated using this method depending on the level of residual consumption. With this method, the MEF for electricity consumption in France in 2018 is estimated between 0.35 and 0.45 t<sub>CO<sub>2</sub>eq</sub>/MWh. In comparison, during the same period, the dynamic average emission factor for the electricity production in France did not exceed 0.10 t<sub>CO<sub>2</sub>eq</sub>/MWh.

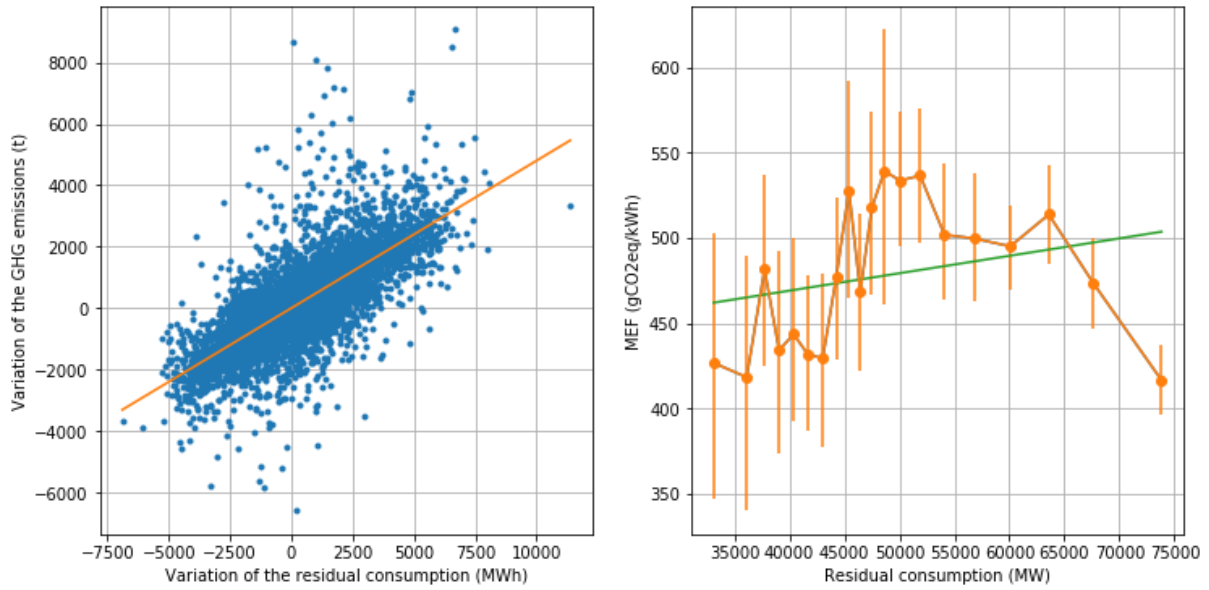


Figure 20: Hourly variation of the GHG emissions depending on the variation of the residual consumption in France (left) and MEF of the electricity consumption depending on the level of the residual consumption (right)

This first estimation shows that there might be a potential in France to decrease the GHG emission of space heating using hybrid heat pumps. In fact, the GHG emissions of a gas boiler (around  $0.251 \text{ tCO}_{2\text{eq}}/\text{MWh}$ ) could be lower than the ones of the heat pump under certain conditions (e.g. high MEF of electricity and low COP of the heat pump). Moreover, the different assumptions made in this evaluation all lead to an underestimation of the MEF.

The MEF of the electricity consumption in France  $MEF_{\text{cons}}(FR, t)$  can be deduced from the residual consumption using Equation 13. However, the coefficients of determination resulting of the application of this method are below 0.8 for low French residual consumption. This is due to the large share of low-carbon dispatchable electricity generation in the French power system. Consequently, this method should not be applied for the evaluation of short-term demand response events and a more complex method, based on a model of the French power system should be applied. However, the correlation coefficients being satisfactory for the countries interconnected with France, the MEF of the electricity exchanges can be used in addition to a model of the French power system.

$$MEF_{\text{cons}}(FR, t) = 0.001 \cdot RC(t) + 428 \quad 13$$

## 2.4. Overview of Unit Commitment and Economic Dispatch models

In this work, we are interested in reproducing the dynamics of power systems on time steps ranging from an hour up to weeks (see Figure 11). Unit-Commitment and Economic Dispatch (UCED) models were identified as the most appropriate for our purposes (see section 2.1.7). Such models are able to “simulate the operation of a given energy-system to supply a given set of energy demands” (Connolly et al. 2010). A detailed state-of-the art is necessary to define the precise methodology that can deal with the three main points of attention concerning these models: the daily and intra-daily dynamics of generation units, the limited water reserves and the electricity exchanges.

### 2.4.1. Overview of methodologies

A review of the existing numerical models of energy systems with a focus on the integration of renewable energies in the energy mixes can be found in (Connolly et al. 2010). In (Delarue 2009) and (Künle 2018), the different methods to solve the unit-commitment problem were addressed. In (Morales-España, Martínez-Gordón, and Sijm 2022) several energy models are proposed to estimate the response of power systems to DR events. However, these models are explicit power system optimization tools such as Balmorel (Elkraft System et al. 2001) (a partial equilibrium model combining the electricity and heat sectors in an international perspective), EnergyPLAN (Department of Development and Planning Aalborg University 2022) (a national multi-energy model including electricity, heating, cooling, industry and transport sectors), or Antares-Simulator (RTE 2020a) (a model from the French TSO evaluating the adequacy or economic performance of power systems). In these models, many parameters are required, such as the start-up and shutdown costs or the minimum on- and off-time of power plants, though they are not readily available. Semi-physical models are a good compromise between model complexity and accuracy. They are based on a minimization (optimal or not) of the costs combined with one or more constraints. Intra-day dynamics of demand and interconnections are frequently neglected, whereas the conservation of the hydroelectric powerplants is integrated into most of the models. Neglecting any of these three constraints would strongly modify the obtained marginal mix and then reduce the accuracy of the model. However, the validation of the marginal mix obtained with such approaches is rarely addressed. For example, (Moradi et al. 2015) or (Staffell and Green 2016) evaluated their models according to performance metrics (cost minimization and computational speed) without verifying that the model output is realistic.

Within this category of semi-physical approaches, two main methodologies for modelling the activation of power plants and solve the UCED problem can usually be found in the literature:

- **Optimization of a cost function:** Most models of electrical systems are based on a cost function minimized using an optimization algorithm constrained by the supply-demand balance (Patteeuw et al. 2015; Roux, Schalbart, and Peuportier 2017; Erik Delarue and D’haeseleer 2008; Yang et al. 2021; Gupta, Davis, and Kumar 2021; Huo, Bouffard, and Joós 2022). The methodologies for solving this problem are various (dynamic programming, Lagrangian relaxation, mixed integer linear programming, etc.) as are the cost-function definitions. Cost-function may contain only the variable cost of the technologies (Roux, Schalbart, and Peuportier 2017; Huo, Bouffard, and Joós 2022) or be more complex and completed with additional constraints for thermal units.
- **Priority-list/merit-order models:** In such models, reviewed by (Zheng et al. 2015), the units or groups of units are started successively in ascending order of variable cost (when cost-based) (Voorspools and William 2003; Voorspools et al. 2000; Zheng et al. 2015) or calibrated indicator (when utilization-based) (Zheng et al. 2015; Bettel, Pout, and Hitchin 2006). These models can also be constrained with additional rules, but do not guarantee the economic optimum. In (Bettel, Pout, and Hitchin 2006), data were grouped according to the weekday/weekend type for the four seasons and the generators were then ranked in height lists according to their percentage of full load operation. There are different ways to constitute a utilization-based merit-order. Unit-decommitment models can be seen as a subsection of the merit-order models. In such models, all or part of the units are considered active and are then successively decommitted to minimize the costs and still meet the demand. As for the models based on a merit-order, these types of models can be integrated into a unit commitment problem or used stand-alone as a unit commitment algorithm (Tseng et al. 1997).



Merit-orders have a quicker calculation time in comparison with models minimizing a cost function (Cebulla and Fichter 2017), especially in the case of a high proportion of renewable energy in the electricity production (E Delarue, Cattrysse, and D’Haeseleer 2013). In (Senjyu et al. 2006), the UCED is solved using a stochastic priority-list method with a better computation time in comparison to genetic algorithms. In (Moradi et al. 2015), the priority-list is also applied, with additional procedure to include minimum up/down times and ramp rates to solve the UCED problem with competitive computation time and results. In (Staffell and Green 2016), a method based on a simple merit-order and a second model based on a merit-order considering start-up costs and the minimum operating point of the units were compared with a model of full constrained minimization of a cost function. The constrained merit-order model and the model based on the minimization had similar results. Hybrid approaches combine the advantages of the two methods as in (Erik Delarue 2009), where a model based on a priority list was used as a complement to a cost-function optimization model to improve the simulation performance.

UCED models can be cost- or utilization-based. Models explicitly using the known costs (Patteeuw et al. 2015; Erik Delarue and D’haeseleer 2008; Yang et al. 2021; Gupta, Davis, and Kumar 2021; Huo, Bouffard, and Joós 2022; Zhou et al. 2019; Voorspools and William 2003; Tseng et al. 1997; Voorspools et al. 2000; Zheng et al. 2015) will be referred to as cost-based. However, when the information relative to cost is not known with sufficient quality, such models can be calibrated with historical data (Roux, Schalbart, and Peuportier 2017; Bettle, Pout, and Hitchin 2006; Zheng et al. 2015) and are referred to as utilization-based. Although cost- and utilization-based models are presented as two distinct categories, some cost-based models use historical data in order to define the constraints of the model (Zheng et al. 2015).

For a more systematic comparison, Table 6 provides an overview of these models and an assessment of the constraints that have been included. In both types of models, electricity production can be dispatched at the level of individual generation units (Zheng et al. 2015; Bettle, Pout, and Hitchin 2006; Tseng et al. 1997; Huo, Bouffard, and Joós 2022; Zhou et al. 2019; Erik Delarue and D’haeseleer 2008; Patteeuw et al. 2015), but generation units can also be aggregated per technology (Roux, Schalbart, and Peuportier 2017; Gupta, Davis, and Kumar 2021). This simplification makes the model faster, but some parameters such as the start-up cost cannot be defined or are more complicated to evaluate for an aggregated group of units. A third approach is to aggregate some units with very similar properties, such as type, fuel and efficiency (Voorspools and William 2003).

Table 6: Model of electrical system reviewed in the thesis

Reference	Geographical area	Cost-based (CB) or utilization-based (UB)	Dispatch on single units or on aggregated technologies	Water reserves conservation	Cross-border exchanges included	Validation against historical data
<b>Models based on the optimization of a cost-function</b>						
(Patteeuw et al. 2015)	Belgium	CB	single	no	no	no
(Roux, Schalbart, and Peuportier 2017)	France	UB	aggregated	yes	yes	yes
(Erik Delarue and D’haeseleer 2008)	Belgium	CB	single	yes	no	no

(Yang et al. 2021)	none	CB		no	no	no
(Gupta, Davis, and Kumar 2021)	Canada	CB	aggregated	no	yes	no
(Huo, Bouffard, and Joós 2022)	none	CB	single	yes		no
(Zhou et al. 2019)	Henan province (China)	CB	single	no	no	no
(Huang and Purvins 2020)	Europe				yes	global validation based on costs
<b>Models based on priority lists/merit-orders</b>						
(Voorspools and William 2003)	Europe	CB	aggregated	yes????	Yes	no
(Voorspools et al. 2000)	Belgium	CB	single	yes	no	no
(Zheng et al. 2015)	England	CB and UB	single		no	
(Bettle, Pout, and Hitchin 2006)	United Kingdom	UB	single	no	no	global validation based on GHG emissions
(Moradi et al. 2015)	Korea	CB	single	no	no	no
(Staffell and Green 2016)	United Kingdom	CB	single	yes	no	no
(Senjyu et al. 2006)		CB	single			

This section presents a detailed state-of-the-art of these models with a focus on their overall structures, the incorporation of hydro energy conservation and the interconnections.

#### 2.4.2. Intraday dynamics

Modelling the daily and intraday dynamics requires accounting for both the unit-commitment and the economic dispatch. The unit-commitment problem (or scheduling) aims to determine which power plants are switched on or off (defined as a discrete variable), while the economic dispatch problem sets the production level of each unit (defined as a continuous variable). If only the variable costs and the availability of the powerplants are considered, both methodologies are similar and lead to a poor representation of the daily and intra-daily dynamics. In most of the models reviewed, it is possible to distinguish the constraints added to consider such intra-daily dynamics of the production system in the model. The implementation differs according to the type of model:

- **In models based on optimization of a cost function:** Researchers use various techniques to model the intra-daily dynamics. One can use constraints on the ramp, constraints on the minimum up- and down-time, or start-up or ramping costs (Patteeuw et al. 2015; Erik Delarue and D’haeseleer 2008; Yang et al. 2021; Zhou et al. 2019). In (Roux 2017), the production units are clustered in groups of generators of similar technology. Only the marginal cost of the technologies is used. Additional constraints are used in the model for the thermal units: maximum and minimum power output, ramp limits, availability and limitation of the nuclear production. The marginal costs and most of these parameters are determined calibrating the model with historical data. Cost calculation and additional constraints for several models based on the optimization of a cost function are detailed in Table 7.

Table 7: Cost calculation and constraints in several models with optimization of a cost function

Model	Discretization	Cost calculation	Additional constraints to demand supply balance
(Roux 2017)	Groups of similar technology	Marginal cost calibrated	Maximum and minimum power output, Maximum and minimum ramp up, Availability limitation of the nuclear production
EnergyPlan (Energy, Analysis, and Model 2019)	Generation unit	Fuel costs Variable operation and maintenance costs	Minimum dispatchable share of the mix
Balmorel (Elkraft System et al. 2001)	Generation unit	Marginal costs for: generation, transmission, distribution taxes	Low and high limitation of capacity, Availability of generation capabilities, Fuel availability, Emission limitations
Antares-Simulator (RTE 2020a)	Generation unit	For the complete system: Transmission cost, generation shortage cost Spillage cost For hydraulic generation: marginal costs For thermal units: fixed cost marginal cost cost for the commissioning or decommissioning	Must-run commitments power availability, Number of running units bounded, Minimum stable power generation maximum capacity thresholds, Minimum running and not-running durations
(Patteeuw et al. 2015)	Generation unit	Fuel costs Start-up costs Ramping costs	Minimum and maximum output, Ramping rates Minimum on and off times of every power plant

In models with detailed generation units such as EnergyPlan (Energy, Analysis, and Model 2019), Balmorel (Elkraft System et al. 2001), Antares-Simulator (RTE 2017) or (Patteeuw et al. 2015), the cost calculation is often more detailed, including variable, fixed, and start-up costs. Scheduling is usually modelled using constraints on the ramp or on minimum up- and down-time, or with start-up or ramping costs (Patteeuw et al. 2015; Erik Delarue and D’haeseleer 2008; Yang et al. 2021; Zhou et al. 2019).

It should be noted that each technology has different power ramp restrictions. However, for each technology, these ramp limits are higher than the nominal power of the plants for a time

step of 30 minutes (Camille Cany 2017). The ramping constraints observed in the data are thus related to economic rather than technical limitations. Using start-up costs (for models with detailed units) or ramping-costs (for models with aggregated technologies) seems then to be the best way to model the intra-day constraints for models based on the optimization of a cost function.

- **In priority-list/merit-order models:** Unit-commitment is generally implemented through additional constraints, such as minimum operating point and minimum up- and down-time (Voorspools and William 2003; Voorspools et al. 2000) or maximum ramp rates (Zheng et al. 2015). In (Delarue, 2009), the *E-simulate* model based on a priority-list is used in addition to a cost-function optimization model to improve the simulation performances. In this model, units are aggregated under groups of similar types, fuel and efficiency. This model considers as additional constraints: the minimum operating point (as a percentage of the rated capacity), the part-load efficiencies (as a percentage of the rated efficiency), the minimum up- and down-times.

Based on the previous observations, Table 8 summarizes the constraints that are usually considered in power system models in addition to the supply-demand balancing. In models with production dispatch on detailed units, the constraints always consider scheduling and dispatch even if the separation between the two is not always explicit. In the case of models aggregating all the units of the same type of technology, the scheduling is never explicit and is not always addressed.

Table 8: Summary of the possible constraints applied to models of the power system

		Type of models	
		Dispatch on units	Dispatch on technologies
Constraints on scheduling	Profit maximization	Marginal + fixed cost	Aggregated marginal cost + sometimes fixed cost
	Available capacity	Detailed for every unit	Aggregated
	Minimum up and down time	Detailed for every unit	Not considered
	Must-run	Detailed for every unit	Aggregated
Constraints on dispatch	Ramp limitation	Detailed for every unit	Aggregated (proportional to the aggregated available power)
	Minimum operating point	Detailed for every unit	Aggregated

#### 2.4.3. Water management models

Hydroelectric powerplants play an important role in regulating power systems and their specificity should be accounted for in UCED problems. However, it requires a special approach compared to other technologies because its marginal production cost is close to zero and water resources are limited. Some authors modeled the hydroelectric power plant fleet as a real-world hydro-power unit-commitment (Flatabø et al. 1998; Sahraoui, Bendotti, and D'Ambrosio 2019). In this case, the different turbines, pumps and reservoirs were explicitly modeled and the water usage was optimized. The models took into account the market price of electricity, the residual consumption, the water level objectives, the rainfall and the water runoff. However, most models use a unique water reservoir

volume, whether power plants are aggregated (Roux, Schalbart, and Peuportier 2017) or modeled independently (RTE 2017).

Hydroelectric powerplant models are commonly incorporated into complete power system models: interactions between hydroelectric powerplants and thermal powerplants are then taken into account. In models minimizing a cost-function, the variable cost of the hydroelectric power plants is generally set to zero and the minimization algorithm is usually constrained on a weekly basis, with a water reservoir conservation condition (RTE 2017; Roux, Schalbart, and Peuportier 2017; Flatabø et al. 1998). However, to the best of our knowledge, the conservation of the water reserves is rarely addressed in empirical (Corradi 2018) or merit-order models (Bettle, Pout, and Hitchin 2006; Zheng et al. 2015). One solution, as in (Staffell and Green 2016), is to model hydroelectricity generation before applying the merit-order and then neglecting the interaction with the other dispatchable power plants without a significant degradation in accuracy. This also facilitates the implementation of a hydroelectric unit model with the conservation of energy.

#### 2.4.4. Interconnection models

Due to the high degree of interconnection of France to the European electricity system, the electricity exchanges between interconnected countries should not be neglected in a UCED model. The models can be sorted according to the geographical area they consider, either focusing on a single-country or modelling explicitly each interconnect country. In the latter case, each interconnected country is usually modelled with a similar level of detail (Voorspools and William 2003; Huang and Purvins 2020). Electricity generation is committed for each country with a profit maximization algorithm or a merit-order, importing electricity from interconnected countries when the local generation is more expensive and when the network is not saturated.

For models focusing on a single country, only a few models consider the flexibility provided by electricity exchanges. In (Roux, Schalbart, and Peuportier 2017), the authors developed a model of the French power system, which assesses the balance of the electricity exchanges using a black-box model, based on a two-layer neural network. In this model, only domestic parameters influenced the electricity exchange, namely: the domestic residual consumption, the domestic solar and wind generation, the availability of the French nuclear powerplants and the average French temperature.

Due to its unique characteristics, the French power system, can be represented with a single-country model and still include cross-border exchanges. Indeed, the French power system is a specific case in Europe as it is designed to supply electricity during winter, when the national demand is high due to the heating demand, which explains why France exports a large amount of electricity during the rest of the year. As nuclear powerplants, with low variable costs, represent a large part of the fleet, French electricity is one of the cheapest in Europe between April and October. Consequently, France usually adjusts its exports following the residual consumption. Indeed, electricity exchange constitutes a high proportion of the balancing mechanism: 42% upwards and 21% downwards (RTE 2018).

## 2.5. Conclusions

The objective of this chapter was to identify the method to evaluate the marginal emission factor (MEF) of electricity consumption, which is needed to control a fleet of hybrid heat pumps. In the first section, the general organization and planning of the power systems were described to identify the main characteristics that should be considered when evaluating MEF. These characteristics are the

consideration of the water reserves of the hydro electric power plants, the daily and intra-daily dynamics and the cross-border electricity exchanges. In the second section, two main categories were identified , one based on a model of the power system and one without. Methods that are not based on models of the power system are easier to implement but less accurate. In the third section, such a method was successfully applied to several European power systems. However, due to the high share of dispatchable low-carbon electricity generation in the French power mix, the method showed a limited accuracy for the French case-study. The power system models solving the UCED problems correspond to the accuracy and the time frame required for this study. In the fourth part, the UCED models are reviewed but none of the existing semi-physical model accounted for the constraints listed above. In conclusion, to describe the UCED problem of a power system, a model with the following features has to be developed:

- Single country model (such models being sufficient to consider electricity exchanges (Roux, Schalbart, and Peuportier 2017));
- utilization-based (cost-based merit-order model would require the detailed costs and the minimum up- and down-time for each power generation, which is a complex task given the level of public information available);
- based on two priority-lists representing respectively the unit-commitment and the dispatch. A model based on the minimization of a cost-function would require the calibration of both the variable and the ramp costs. However, given the number of powerplants constituting the French power system, it seems difficult to calibrate so many parameters. Moreover, as the priority-list method is a good compromise between computation time and accuracy (Staffell and Green 2016), such a method seems to be the most appropriate;
- and applied on aggregated technologies, which are then discretize to reproduce correctly the daily and intra-daily dynamics. Indeed, it was observed from the French TSO data that aggregated technology groups can generally be split into “must-run” and “flexible” parts. The flexibility of an aggregated technology is usually provided by different powerplants during the year, but the flexible capacity is almost always similar. Therefore, it would have been counterproductive to discretize per powerplant.

These choices ensure that the model can reproduce the daily and intra-daily dynamics with a reasonable computation time. In addition:

- national electricity exchanges are considered as virtual power plants integrated in the priority lists;
- hydroelectric dispatch is solved in preprocessing as in (Voorspools and William 2003).

Finally, after calculating the marginal mix, the MEF of the electricity consumption in France can be evaluated from both the MEF of the electricity exchanges and the emission factors for electricity generation from the different power plants in France (see section 2.3).

### 3. Development and validation of the French power system model

In the previous chapter, methods to evaluate short-term MEF of the electricity consumption in France were reviewed. This review showed that an original UCED model based on a semi-physical approach needs to be developed and validated for marginal evaluations. The aim of the current work is then to develop a unit-commitment model, applied to France for instance, that can be used to evaluate the short-term marginal mix of electricity consumption. This model should provide enough information to show how the production mix adapts to a planned interruption in electricity consumption for a period ranging from half an hour up to a few days (i.e. resulting from fuel-switching of hybrid heat pumps). This model could also be used for evaluating key performance indicators such as GHG emissions and cost reductions for curtailment, smart charging, sector coupling or storage. This chapter presents the development and validation of the UCED model. The type of model (single-country model based on two priority lists and accounting for cross-border exchanges) was chosen in the previous chapter. Section 3.1.1 describes the structure and the input data of the developed model details the methodology used for each sub-model of the French power system. Section 3.1 describes the method to evaluate the MEF of the electricity consumption in France using the model developed and the limitations of the methodology. In Section 3.2.3, the model is validated for the year 2018. Finally, in Section 3.3, the model is applied to evaluate the marginal mix for different demand response events and strategies.

#### 3.1. Model for Unit Commitment and Economic Dispatch

This Section describes the UCED model developed to evaluate the MEF of the electricity consumption in France. First, the structure of the model is presented and then the different sub models are successively reviewed.

##### 3.1.1. Input data and structure of the French power system model

The input to the model is the French national consumption, from which is subtracted the non-dispatchable production. This input is called the residual consumption ( $RC$ ). The input of the model can be defined either using historical data (e.g. from the French TSO (RTE 2022b)) or with user-defined time series, at a 30-minute time-step. Renewable generation units such as solar, wind and run-of-river power plants can only be adjusted downward, which is rare as they provide electricity for a very low variable cost. In general and as of today, electricity generation from these plants is not driven by demand and per definition cannot be part of the marginal mix. Consequently, solar, wind and run-of-river power plants were considered to be non-dispatchable and thus were not included in the model.

Furthermore, other time series were needed for the model:

- The Net Transfer Capacities ( $NTC$ ) in the hourly resolution (RTE 2022a), which corresponds to the maximum power that can be exchanged across a border in both export ( $NTC_{exp}$ ) and import ( $NTC_{imp}$ ) directions ( $NTC_{exp}$  and  $NTC_{imp}$  both being positive) in the hourly resolution;
- The availability of the powerplants ( $P_{avail}$ ) in the half-hourly resolution (ENTSO-E Transparency Platform (ENTSOE 2022));

- The weekly energy produced by the hydroelectric powerplants  $E_{\text{TSO}}(\text{hydro}, w)$ , as it is assumed that hydroelectric energy can only be shifted over the week. From the French TSO data, the following types of hydroelectric units were considered “dispatchable” for our study:
  - storage hydroelectric plants (with a storage capacity over 400 hours to exclude run-of-river plants);
  - pumped-storage hydroelectric (PSH) units, which are fitted with reversible turbines located between two water tanks at different levels;
  - non-reversible pumps, used to pump water to reservoirs fitted with non-reversible turbines.
- In some cases, data were not provided, such as the availability of a category of powerplant labeled “Fuel – Others”; this parameter is conventionally set at 460 MW. For a similar reason, the pumping capacity of the pumped storage hydroelectric units was set at 85% of the available capacity for the electricity generation of these units, based on the fact that the installed capacities for electricity generation and for pumping were 5 029 and 4 291 MW respectively in 2015 (RTE 2015).

The half-hourly electricity mix  $mix_{\text{elec}}$  (the vector of the generation level of each technology) is the output of the model. The generation level  $P$  was calculated for each time-step, for each type of powerplant (hydroelectric, nuclear, combined-cycle gas turbine (CCGT), coal-fired, open-cycle gas turbine (OCGT) and fuel-fired power plants), and for the electricity exchange.

Figure 21 represents the structure of the UCED model. The time-step was set to 30 minutes, which fits the resolution of the TSO data. The following notations are used: weeks  $w$  and days  $d$  that refer to periods starting and ending at weekly (resp. daily) minimum residual consumption. The daily minimum residual consumption generally occurs during a time-step between midnight and 6 am. Thus, a week  $w$  indicates a period of time beginning on Monday after this time-step until the following Monday at the daily minimum. A day  $d$  indicates a period of time between two consecutive daily minima. A less deep off-peak can be also noticed daily between 12am and 6pm. Half-days, denoted  $1/2d$ , correspond to the first or second part of the day before or after this mid-day off-peak. Examples of week  $w$ , day  $d$  and half-day  $1/2d$  are illustrated in Figure 22.

It is necessary to use this method to separate the days as there are large variations in residual consumption from day to day, either due to changes in weather conditions, renewable production or type of day (weekdays vs. weekends). For example, at midnight on 10 February the residual consumption is higher than during the rest of the day. Consequently, considering days from midnight to midnight would result in an excessive number of units being committed for the 10 February.



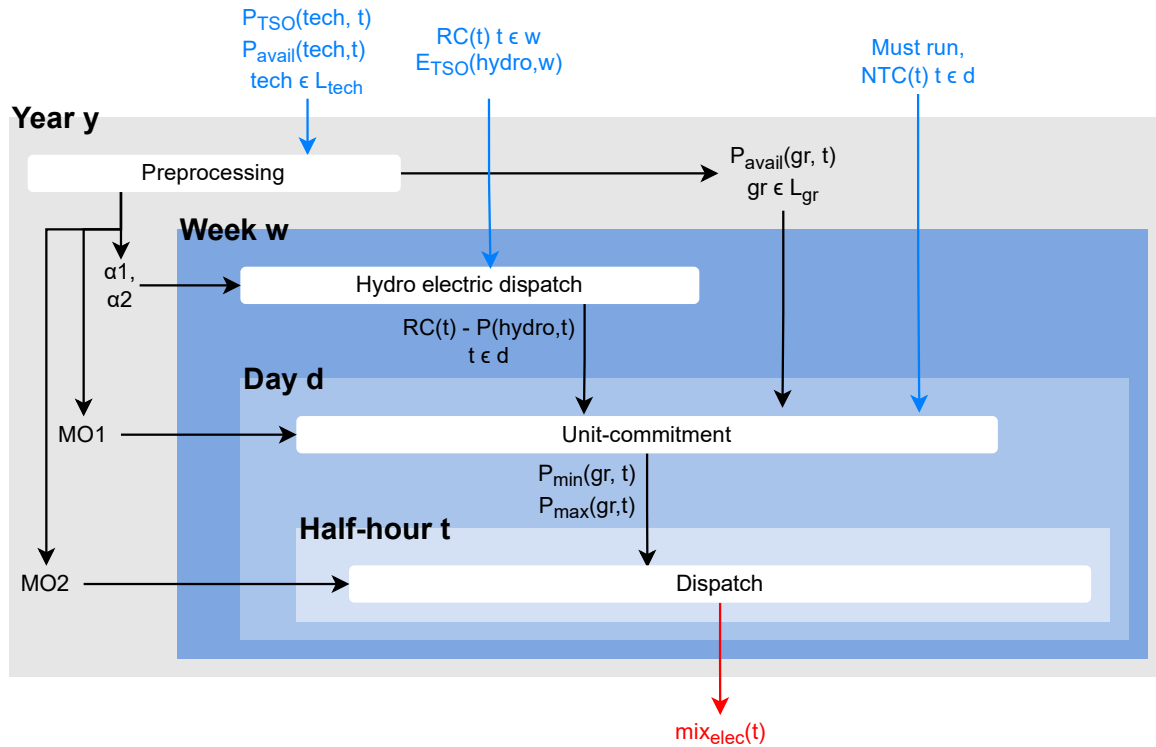


Figure 21: General overview of the French power system model.

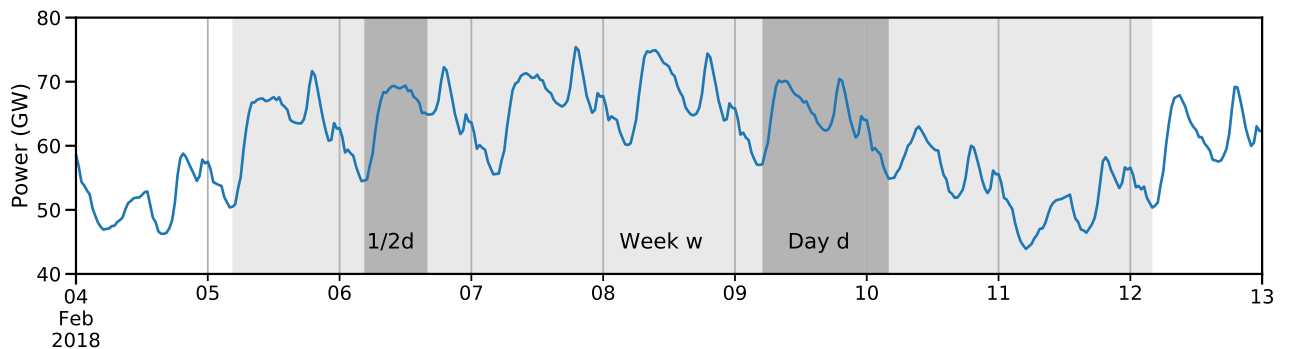


Figure 22: Residual consumption between the 4<sup>th</sup> and 12<sup>th</sup> of February 2018 and definition of the various time-frames.

The first step in the model is data pre-processing which is necessary to:

- Adapt the data related to electricity exchange in order to include them as virtual power plants in the merit-orders;
- Discretize the domestic production technologies and the virtual power plants (referred to as *tech* and listed in  $L_{tech}$ ) into groups (referred to as *gr* and listed in  $L_{gr}$ ), calculate the generation capacity and availability of each group and define the minimum activation power of each group ( $P_{min}$ );
- Generate the two merit-orders *MO1* and *MO2*;
- Calibrate the hydro electric dispatch sub-model.

Once the data are preprocessed, the units can be committed using the three sub-models described in sections 3.1.3, 3.1.4 and 3.1.5:

- In the hydroelectricity dispatch sub-model, the generation level of the hydroelectric powerplants is evaluated;
- In the unit-commitment sub-model, the committed capacity  $P_{max}$  of each group is evaluated daily;
- In the dispatch sub-model, the generation level of each group is defined considering the commitment of the group.

In the following sections, the methodologies applied in the different sub-models presented in Figure 21 (data pre-processing, hydroelectric powerplants, unit-commitment and dispatch) are described.

### 3.1.2. Data pre-processing

#### Including interconnections as virtual dispatchable powerplants

As stated in Section 2.4.4, the national data were considered sufficient to determine the level of electricity exchange and it was thus integrated directly into the unit-commitment and dispatch sub-models. This modelling strategy was chosen to reflect the high correlation between the export and the residual consumption, which is typical of the French power system due to the high installed capacity of nuclear energy. Consequently, cross-border exchanges were modelled as a production from virtual powerplants (named  $vpp_{exch}$ ) representing the level of exchange between the other EU countries and France. To be part of the merit orders, the electricity generation of the corresponding technology must be positive. To achieve this, the residual consumption and the level of the electricity exchanges were rescaled as follows:

- The model assumes that the power to be dispatched between the French power plants and the borders is equal to the sum of the residual consumption and the NTC for exports.
- The production level of this virtual powerplant ranged between 0 and the sum of both transfer capacities ( $NTC_{exp}(t) + NTC_{imp}(t)$ ): France is a net exporter if  $P(vpp_{exch}, t)$  is below  $NTC_{exp}(t)$ , whereas France is a net importer if  $P(vpp_{exch}, t)$  is above  $NTC_{exp}(t)$ . This is illustrated in Figure 23.

This modelling procedure ensures that the production level of exchanges will always be above zero in the merit-order and avoid distinguishing imports from exports.

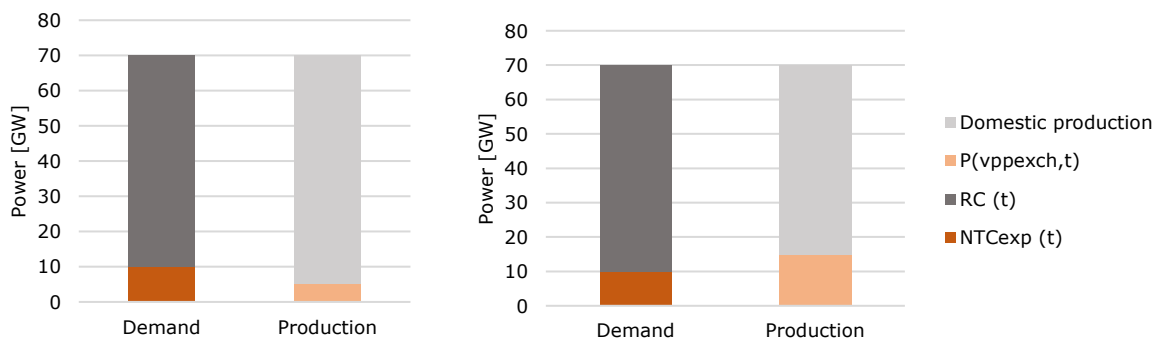


Figure 23: Dispatching principle for exchanges in the case of net exporter (left) and net importer (right)

To calculate the indicators relative to the merit-orders MO1 and MO2 and then generate the two merit orders, the equivalent generation ( $P_{\text{TSO}}(vpp_{\text{exch}}, t)$ ) and availability ( $P_{\text{avail}}(vpp_{\text{exch}}, t)$ ) of the virtual powerplants have to be calculated with Equations 14 and 15 from the net transfer capacity for exports and imports and from the electricity exchanges summed over the borders.  $P_{\text{TSO}}(exch, t)$  is positive for imports and negative for exports.  $P_{\text{TSO}}(vpp_{\text{exch}}, t)$  is thus always positive.

$$P_{\text{TSO}}(vpp_{\text{exch}}, t) = P_{\text{TSO}}(exch, t) + NTC_{\text{exp}}(t) \quad 14$$

$$P_{\text{avail}}(vpp_{\text{exch}}, t) = NTC_{\text{exp}}(t) + NTC_{\text{imp}}(t) \quad 15$$

The level of electricity exchanges, obtained in the output of the model, is transformed by subtracting the  $NTC$  for export (Equation 16).

$$P(exch, t) = P(vpp_{\text{exch}}, t) - NTC_{\text{exp}}(t) \quad 16$$

During national holidays in France and Germany (only a few days per year), the correlation between the French residual consumption and the electricity exchanges seemed to be reduced. Comparing the French exchanges with the German residual consumption showed that the French exports are generally lower when the German residual consumption remains low. As a result, the French exports were limited as a function of the German residual consumption. Indeed, a large part of the variation in electricity exchanges from France has an impact on the German power system. This means that when the German grid is already exporting to the European grid, the European market becomes saturated, leading to limited French exports. Such an assumption should be discussed for the modelling of a future power system with different commercial behavior and installed capacities in Europe.

With the method described above, the electricity exchanges are evaluated aggregating all the borders. To distinguish the electricity flow across the various borders, the countries whose production will be impacted by the change in French electricity consumption are evaluated using the method described section 2.3.3.

## Discretization

Parametrization and calibration of the model would not be possible for individual powerplants. This is why dispatchable units of similar technologies were aggregated. However, in order to improve the dynamics of the model, the virtual powerplant and all the technologies have to be discretized. The virtual power plant obtained from electricity exchanges represents indeed a wide span of power variation. Different discretization strategies were used for each technology in order to constitute groups with properties as homogeneous as possible for daily and intra-day flexibility. The size of each group (from 200 up to 10 000 MW) was defined based on observation and parametric analysis. The observation on the French electricity generation for year 2018, which led to the discretization applied in this thesis, is presented in Annex A. The groups obtained after discretization do not represent real powerplants.

There were five coal-fired power plants producing electricity in France in 2018. Data from the French TSO show that the coal-fired fleet was activated in steps (around 585 MW) and that the daily flexibility was always in a range that was also around 585 MW. Thus the coal-fire fleet was split into five groups of 585 MW in order to have a group with a high activation rate and the largest intra-day flexibility, while the other groups were less activated and had little flexibility. In addition, the minimum power

output of the highly flexible coal group was set to 300 MW only on the days when this group was scheduled, consistently with the observations made on the French TSO data.

As the combined-cycle gas turbines (CCGT) are easily interchangeable with the coal-fired units in terms of dynamics (depending on their combustible cost difference), this technology was also divided into 10 groups of 585 MW following the same logic. The aggregation of all the CCGT units resulted in a minimum power of 200 MW, which was then set as the minimum power output of the first CCGT group to be activated. The fleet of oil-fueled and OCGT technologies were not discretized.

Nuclear powerplants have a high load factor as their variable cost is very low. However, some of the nuclear powerplants (over a maximal span of 15 000 MW) are controlled in load-following mode and a reserve of between 1000 MW and 2000 MW can be observed most of the time. This group was therefore divided into a first reserve group of 10 000 MW and five additional reserve groups of 1000 MW each, and a base group with a capacity corresponding to the total availability from which 15 000 MW was subtracted. The base group always produced at its maximum available value, which was also set as the minimum power output value.

Electricity exchanges at all French borders were aggregated as one virtual generation unit and then discretized into 10 groups of equal size (2.5 GW). This value was chosen using a parametric analysis in order to ensure the error in the model was small enough while maintaining good simulation performance.

### Calibration of the use of powerplants

Two merit-orders were used to reproduce the unit-commitment and dispatch of the electricity generated and thus two priority indicators were developed and calibrated for France with data from the TSO of 2018 (RTE 2022b). In this study, the merit-orders were calibrated before the simulation and the orders remained unchanged throughout the entire simulation.

The unit-commitment merit-order (MO1) was based on a first indicator (Equation 17), which is evaluated on a daily basis and quantifies the activation frequency of the units of a group. The closer the indicator is to 1, the more often the units are activated. The second indicator related to dispatch defines the second merit-order (MO2) (Equation 18) and represents the reactivity of the units. A value close to 1 corresponds to the base units and close to 0 to peak units. The  $d_{gr}$  list indicates the days of the year 2018 when the group  $gr$  was activated (i.e. a daily maximum generation power higher than 20 MW) and  $\text{len}(d_{gr})$  the length of the list  $d_{gr}$ .

$$Indic_{MO1}(gr) = \frac{1}{365} \cdot \sum_{d \in 2018} \frac{\max_{t \in d}(P_{TSO}(gr,t))}{\max_{t \in d}(P_{avail}(gr,t))} \quad 17$$

$$Indic_{MO2}(gr) = \frac{1}{24 \cdot \text{len}(d_{gr})} \sum_{d \in d_{gr}} \int_{t \in d} \frac{P_{TSO}(gr,t)}{\max_{t \in d}(P_{TSO}(gr,t))} \quad 18$$

The two calibrated merit-orders, respectively for the unit commitment and the dispatch of the electricity, are presented in Figure 24 for the French power system in 2018. This can be compared with the parameters usually employed in cost-based methods. The value  $1 - Indic_{MO1}(gr)$  corresponds indeed to the relative fuel cost for each type of power plants and the value  $Indic_{MO2}(gr)$  to the relative ramping cost. The constraints on must-run units can also be identified on the merit-order for unit-commitment and the reserves on the merit-order for dispatch.

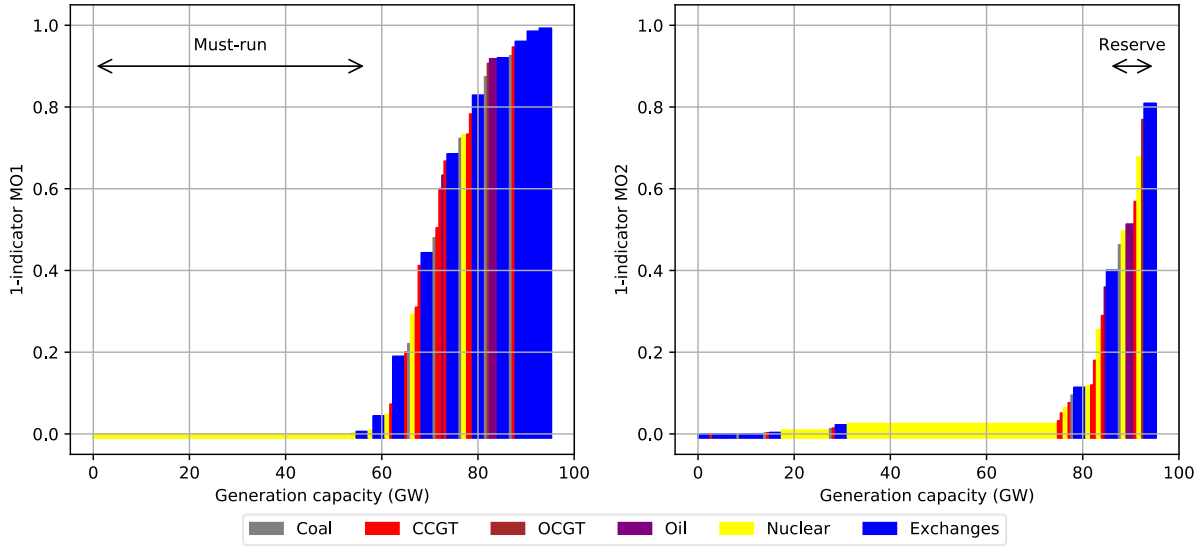


Figure 24: Merit-orders for unit-commitment and dispatch evaluated for the French power system for 2018.

### 3.1.3. Hydroelectric powerplants (week $w$ )

In this study, hydroelectric powerplants were considered as one group of technologies whose generation level was summed over the consumption of the pumps for water storage and the generation of the turbines. The generation level of the hydroelectric group was thus either negative (more pumping for water storage than electricity generation by the turbines) or positive (in the opposite situation).

The use of hydroelectric powerplants being mainly driven by the residual consumption, their activation is processed first in the model. The developed model for the hydroelectric dispatch supposes that:

- hydroelectric energy generation  $E_{\text{TSO}}(\text{hydro}, w)$  is conserved weekly as in (Roux, Schalbart, and Peuportier 2017; RTE 2020a);
- the half-daily and half-hourly variation in residual consumption are partly compensated by hydroelectric power plants.

Indeed, in (Heggarty et al. 2020), the authors showed that pumped storage hydroelectric power plants mostly modulate on the daily and half-daily timescales in Germany. Similar results would have been obtained in most of the countries with pumped storage hydroelectric power plants. Consequently, the hydroelectric dispatch model should compensate for half-daily energy demand variation in addition to half-hourly variation and to weekly energy conservation.

Figure 25 illustrates the breakdown of the residual consumption to isolate the weekly mean (orange in plot a), a half-daily component (orange in plot b, which corresponds to the half daily mean of the residual consumption less the weekly mean) and a half-hourly component (blue in plot b, which corresponds to the residual consumption less the two previous components). In order to account for the half-daily and half-hourly compensations in the UCED model, a function to dispatch the hydroelectric energy is defined in Equation 19 and applied first.  $sl_{1/2d}^{\text{hydro}}$  is constant over the year and equals 0.19 for 2018, while  $sl_{1/2h}^{\text{hydro}}$  has a specific value at the end of winter when the water reserves are discharged in preparation for spring and equals 0.61 at the end of winter and 0.45 the rest of the

year in 2018.  $sl_{1/2h}^{hydro}$  and  $sl_{1/2d}^{hydro}$  are evaluated using a linear regression.  $\overline{RC}(1/2d)$  and  $\overline{RC}(w)$  corresponds to the half-daily and weekly means of residual consumption, respectively.

For  $1/2d \in w$ , for  $t \in 1/2d$ ,

$$f_{hydro}(t) = sl_{1/2h}^{hydro} \cdot (RC(t) - \overline{RC}(1/2d)) + sl_{1/2d}^{hydro} \cdot (\overline{RC}(1/2d) - \overline{RC}(w)) + \frac{E_{TSO}(hydro, w)}{\text{len}(w)} \quad 19$$

However, this function does not guarantee that pumping never exceeds the availability of the pumps. Therefore, in a second step, the output power is saturated with the pumping capacity. Then, another saturation is applied to curtail the extreme low values, which are not consistent with the observed behavior of the hydroelectric fleet. Finally, the curtailed hydroelectric power generation has to be shifted to ensure the conservation of the energy produced. The curtailed energy is allocated between the half-day of the curtailment and the week. Once the hydroelectric dispatch is applied for a week, the different groups of technologies have to be dispatched each day of the week.

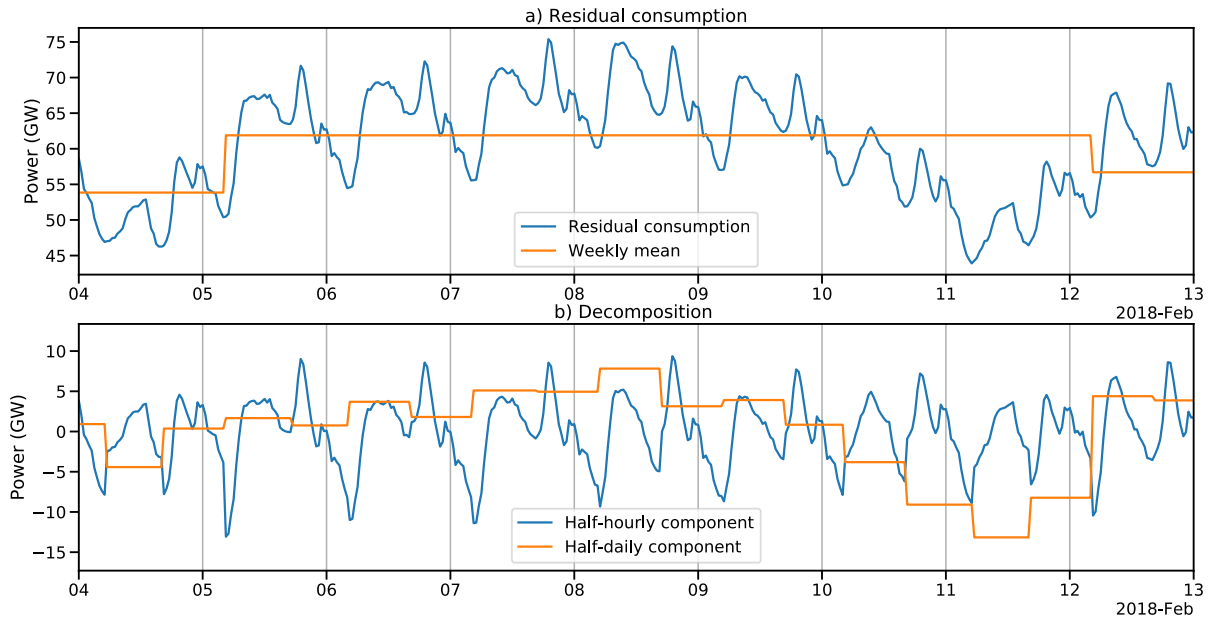


Figure 25: Breakdown of residual consumption into weekly, half-daily and half-hourly components.

### 3.1.4. Unit Commitment (day d)

The different groups  $i$  of power plants were committed everyday, meaning that the daily maximum activable power for each group ( $P_{\max}(MO1[i], t)$ ) was calculated by activating successively the different groups in the order of the first merit-order (MO1). The merit-order method is applied with the following characteristics:

- Ranking: MO1 order defined using the indicator defined in section 3.1.2 (Equation 17).
- Upper boundary: availability of each group
- Lower boundary: must-run units

The following sequence (steps 1 to 3) was applied successively for each group  $i$  of power plants following the ranking of the first merit-order (MO1) of length  $n_{gr}$ :

1. Calculation of the remaining capacity to commit  $RC_{\text{remain}}(i, t)$  with equation 20 for each time step of the day. At each time step, the daily maximum activable power of each already committed group and the minimum activation power  $P_{\text{min}}$  (which correspond to must-run units) of each not-yet committed group have to be subtracted from the power to be provided.

for  $t \in d$ ,

20

$$RC_{\text{remain}}(i, t) = RC(t) + NTC_{\text{exp}}(t) - P(\text{hydro}, t) - \sum_{j \in [1, i-1]} P_{\text{max}}(MO1[j], t) - \sum_{j \in [i+1, n_{gr}]} P_{\text{min}}(MO1[j], t)$$

2. The remaining capacity to be provided is the daily maximum of the time series  $RC_{\text{remain}}(i, t)$ .
3.  $P_{\text{max}}(MO1[i], t)$  is then obtained by saturating this value between 0 and the available capacity of the group  $P_{\text{avail}}(MO1[i], t)$ . As the available capacity varies during the day,  $P_{\text{max}}(MO1[i], t)$  also varies during the day.

All the  $P_{\text{max}}(MO1[i], t)$  are thus obtained for each group  $i$ .  $P_{\text{min}}$  is set for the groups, whose value depend on the commitment (e.g. coal-fired powerplants in the French context).

### 3.1.5. Dispatch (hour $h$ )

Once the maximum and minimum activable powers have been calculated during the Unit-Commitment, the generation level  $P(MO2[i], t)$  of each group  $i$  is calculated successively for each time step of the day  $t$  following the ranking in the merit-order for the dispatch (MO2). The merit-order method is applied with the following characteristics:

- Ranking: MO2 order defined using the indicator defined in section 3.1.2 (Equation 18).
- Upper boundary: committed capacity of each group
- Lower boundary: must-run or minimum output constraints of some units

The following sequence (steps 1 to 2) was applied successively for each group of power plants following the ranking of the second merit-order (MO2) of length  $n_{gr}$ :

1. For the group ranked  $i$  in the merit-order for the dispatch MO2, the remaining electricity to dispatch  $RC_{\text{remain}}(i, t)$  is first calculated with Equation 21. At each time step, the generation level  $P$  of each already dispatched group  $i$  and the minimum activation power  $P_{\text{min}}$  (which corresponds to must-run units minimum output constraints of some units) of each not-yet dispatched group have to be subtracted from the power to be provided.

For  $t \in d$ ,

21

$$RC_{\text{remain}}(i, t) = RC(t) + NTC_{\text{exp}}(t) - P(\text{hydro}, t) - \sum_{j \in [1, i-1]} P(MO2[j], t) - \sum_{j \in [i+1, n_{gr}]} P_{\text{min}}(MO2[j], t)$$

2. The electricity generated at time step  $t$  by the group ranked  $i$  in the merit order for dispatch is then obtained by saturating  $RC_{\text{remain}}$  between the minimum output power  $P_{\text{min}}(MO2[i], t)$  and the committed capacity of the group  $P_{\text{max}}(MO2[i], t)$  at time step  $t$ .

## 3.2. Methodology to evaluate the marginal emission factor of the electricity consumption

### 3.2.1. Evaluation of the marginal mix

Usually, the marginal mix of a power system is defined as the response of the power system to an increase or a decrease in electricity demand during 1 hour. This corresponds to the proportion of the production offset during a Demand-Side Management (DSM) event due to the energy saved. In this section, we will evaluate the marginal mix for a decrease in electricity demand of 100 MW and for a duration between 30 minutes up to one week. For a duration of 6 hours, the demand was decreased between midnight and 6am, 6am and 12am, 12am and 6pm and 6pm and midnight. For the half-day, day and week, the definition given in section 3.1.1 was used.

In practice, the marginal electricity mix can be determined by running the power system model twice, as illustrated in Figure 10. First the actual national residual consumption is used as input in the model to obtain the generation level  $P(\text{tech}, t)$  for each type of technology. Then the marginal demand (positive or negative) is added to the residual consumption to obtain the adapted generation levels. The marginal mix is then identified as the adaptation of generation  $\Delta P_{\text{tech}}(t)$  for each type of power plant  $\text{tech}$ , as well as the adaptation of electricity exchange  $\Delta P_{\text{exch}}(t)$  for each time step  $t$  of the week by comparing the results with and without the marginal demand.

Considering the model structure for hydroelectricity dispatch, these powerplants are part of the marginal mix most of the time for a perturbation in demand of less than one week. The model considers that the energy generated by the hydroelectric powerplants is fixed for each week, the offset hydroelectricity generation during the time-steps with a modified demand is then displaced to the rest of the week. Consequently, for a decrease in the national demand, the difference between the two runs of the UCED model is:

- Negative or null for all the technologies during time-steps of demand response;
- Positive for hydroelectric powerplants and negative or null for the other technologies during the other time-steps of the week.

After integration over one week, the proportion of hydroelectricity in the marginal mix was zero and this was compensated by other technologies. Thus, the perturbations influence the electricity mix for both past and future time-steps. Powerplants compensating over an entire week were considered to be representative of the real behavior with respect to the volume of energy displaced.

The marginal mix was then calculated for each time step  $t_{\Delta t}$  of the year using Equation 22,  $t_{\Delta t}$  corresponding to the beginning of the decrease in demand which was then varied according to the  $\Delta t$  considered.  $E_{\text{marginal}}$  is the energy saved during the demand response event.

For  $\Delta t \in \{30\text{min}, 6\text{h}, 1/2\text{d}, 1\text{d}, 1\text{w}\}$ , for  $\text{tech} \in L_{\text{tech}}$ , for  $t_{\Delta t} \in w_i$

22



$$mix_{\text{marginal}}(t_{\Delta t}, tech) = \frac{\int_{w_i}^{w_{i+1}} \Delta P(tech, t) dt}{E_{\text{marginal}}}$$

### 3.2.2. Evaluation of the marginal emission factor

The marginal emissions  $ME$  (in  $g_{CO_2eq}$ ) related to a marginal demand are evaluated for each time step  $t$  using Equation 23 where the emission factors  $EF_{tech}$  of the domestic production units are provided in section 2.2.4 and the MEF for electricity exchanges  $MEF_{exch}$  in section 2.3.3. The domestic losses  $Losses_{FR}$  and the losses related to electricity exchange  $Losses_{exch}$  (in percentage) were defined in Section 2.2.4.

$$ME(t) = (1 + Losses_{FR}) \cdot \sum_{tech \in L_{tech}} EF_{tech} \cdot \Delta P(tech, t) + (1 + Losses_{exch}) \cdot MEF_{exch}(t) \cdot \Delta P(exch, t) \quad 23$$

The marginal emission factor (in  $g_{CO_2eq}/kWh$ ) related to a marginal demand is evaluated using Equation 24.

$$MEF(t_{\Delta t}) = \frac{\int_{t_{\Delta t}}^{t_{\Delta t} + \Delta t} ME(t) dt}{E_{\text{marginal}}} \quad 24$$

### 3.2.3. Limitations

Various assumptions about the method developed limit the range of validity of the model and should be addressed. The first assumptions relate to some of the inputs to the model:

- The unavailability of the power plants was considered as an input of the model, although planning of nuclear unavailability is known to follow electricity consumption on a monthly basis (Morilhat et al. 2019). A large change in electricity consumption could then change the unavailability forecasts.
- The hydroelectric weekly generation was also considered as an input neglecting the possible impact of the change in the electric demand on seasonal storage.

However, the model was developed in order to evaluate the impact of changes in the electric demand from a few hours to a few days. Such events should have a limited impact on the planned outages of the power plants and on hydroelectric planning.

The second major limitation of the model is that it is based on the current French power system. The model can then be used as long as the change in electricity consumption does not modify the installed capacity of the power system, for example a historical situation in this study. Future power system models could be derived from a model calibrated with historical data considering a few changes:

- Changing the capacity of the groups of power plants to reproduce changes in the installed capacities;
- Changing the order of the groups in the first merit order (MO1) to reproduce the evolution of the variable prices;

- Accounting for new thermal or electrical storages using the method applied for hydroelectric powerplants;
- Implementating power-to-X strategies or electricity curtailment measures following the method for the integration of electricity exchanges in the merit-orders.

### 3.3.Validation of the unit commitment model

We validated our model using data from the French TSO (RTE 2022a) for 2018. In addition, the model was also validated for the year 2019 with calibration for 2018, which confirmed the validity of the model for similar years. The modeled generation level of each group of units was compared to the TSO data and evaluated using two indicators:

- The correlation coefficient ( $R$ ), evaluating the linear dependence between two sets of data. A value near 1 means that the dynamics of the system are correctly modeled but does not give any information about the potential systematic bias between the results and the measured data.
- The root-mean-square error (RMSE), representing the error between the simulation results and the TSO data. This value is absolute and has to be compared with the mean daily range of the residual consumption, which is around 14 GW.

The validation of the model is based on two steps:

- First, a yearly validation of the model in order to evaluate its overall behavior using the correlation coefficient and the RMSE over the whole year;
- A weekly validation in order to check the response of the model during periods corresponding to the marginal analysis;
- Finally, an aggregated indicator is calculated to evaluate the whole model.

#### 3.3.1.First step: yearly validation

The correlation coefficient  $R$  and the  $RMSE$  were calculated for the different technologies using the data from the TSO and the simulation results for 2018 (Table 9). In this table, the different technologies were ranked according to the correlation coefficient. The observed operation time during 2018 is also indicated for each technology. It can be observed that the first powerplants of the merit-order MO1 (that are more often committed) have a higher correlation coefficient, while the peak units suffer from the accumulated errors of the units better ranked in the merit-order. The error on fossil fuel power plants can be partly explained by the price of fossil combustibles, which varies continuously and is not explicitly accounted for in the model. The error on peak units can also be explained by the scope of the model (mentioned in part 2.5), e.g. ancillary services and congestion are not explicitly taken into account.

Table 9: Error metrics of the French power system model for 2018

Technologies	Operation time in 2018 (%)	R	RMSE (GW)

Nuclear	100	0.99	1
Hydroelectric	100	0.90	1
Exchanges	100	0.89	1,9
CCGT	99	0.83	1
Coal	71	0.74	0,4
Oil	31	0.65	0,3
OCGT	3	0.48	0,1

For a more detailed overview of the model, Figure 26 presents the modeled and observed power generation for each type of power plant. The behavior of the model for nuclear, hydroelectric, CCGT powerplants and electricity exchanges matches well with the real power system. Regarding oil turbines and the OCGT, the error on these powerplants can be considered acceptable for the analysis as their activation time (31% and 3%, respectively, in 2018) and their energy generation level were small. Moreover, the values from Table 9 were compared with the validation of other unit commitment models (Roux, Schalbart, and Peuportier 2017; Frapin et al. 2021; Huang and Purvins 2020) and the performances were similar to this model for a yearly validation.

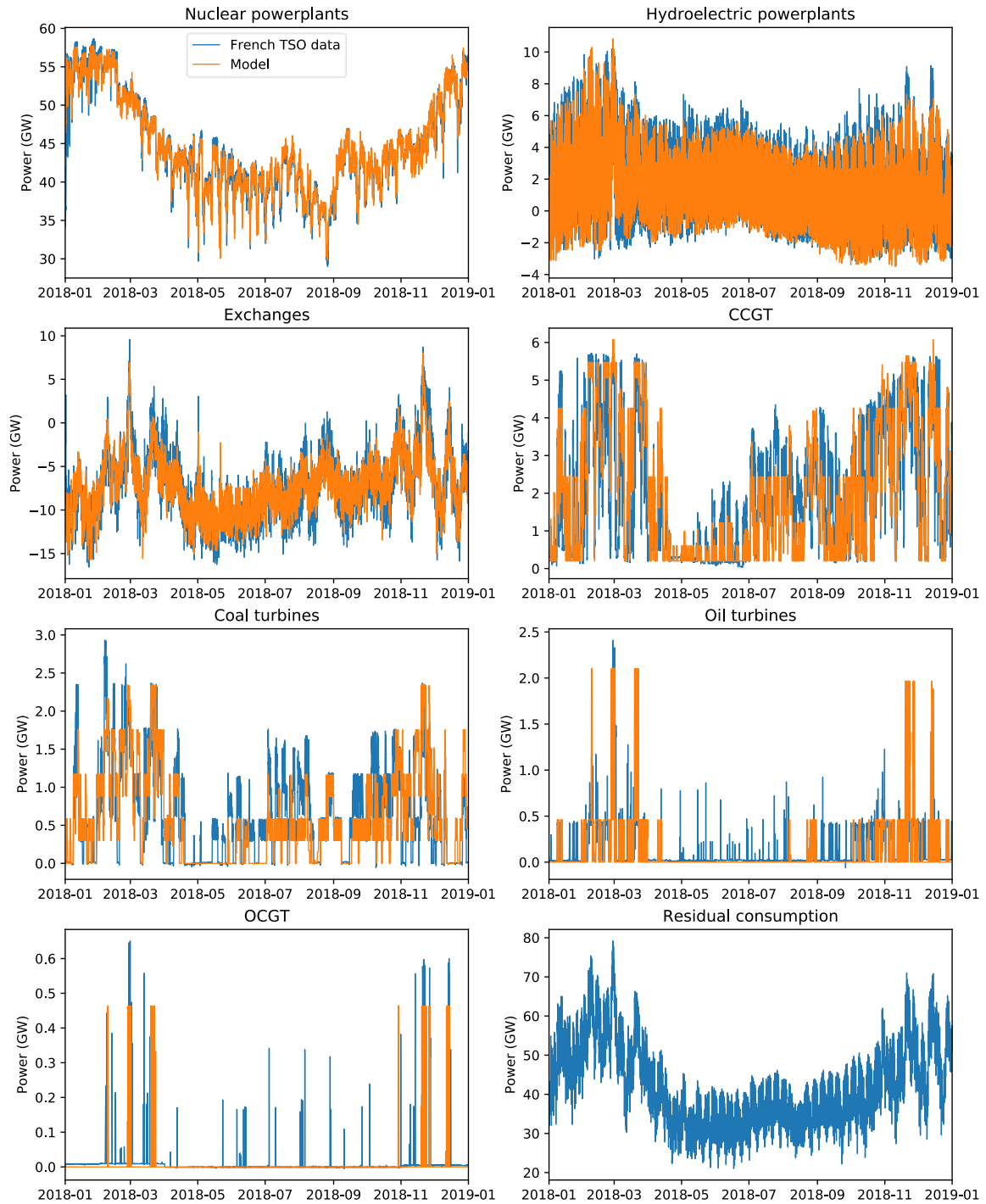


Figure 26: Modeled and observed power generation (RTE 2022b) for each type of powerplant in 2018. The residual consumption at the bottom right is provided for information, being an input of the model.

Such a validation protocol ensures that the model can predict the electricity mix, but, at this stage, does not validate its marginal behavior. Validating models designed for applications such as demand-response requires testing them against the dynamics of the duration of flexibility.

### 3.3.2. Second step: weekly validation

The scope of this thesis being the estimation of the marginal mix for decreases in the electricity consumption ranging between 30 minutes and a few days, the weekly scale also needed to be considered for validation. To that purpose, the correlation coefficient  $R$  and the  $RMSE$  for each type of power plant were calculated for each week, comparing the TSO data to the results of the model. Figure 27 and Figure 28 represent the distribution of the correlation coefficient and the  $RMSE$ , respectively. The  $RMSE$  cannot be calculated if one of the two time series is constant (e.g. equal to 0), which often occurs for the simulation of a power system for OCGT, coal and oil-fired turbines. These values have thus been removed from the analysis.

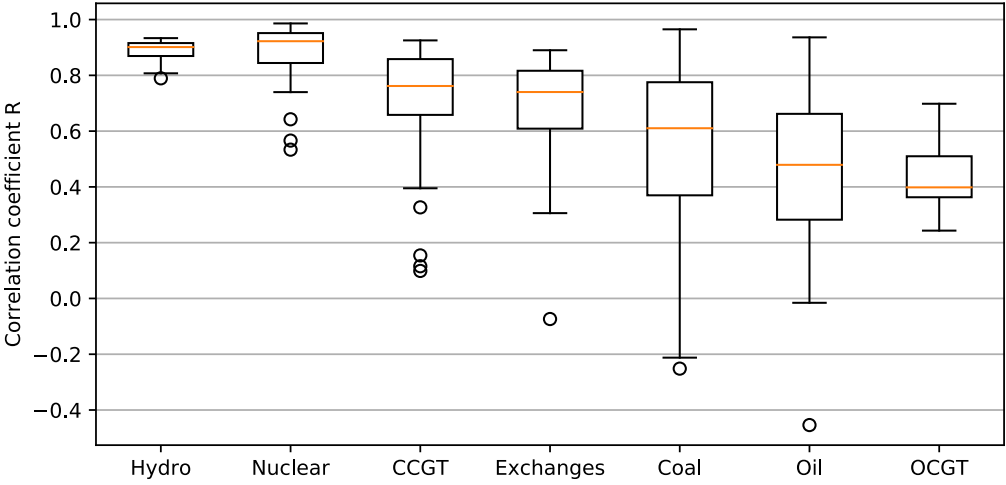


Figure 27: Distribution of the correlation coefficient calculated for each technology during each week of 2018. The orange line represents the median of the values, the box the values between the lower and the upper quartiles of the distribution, the circles the values under the lower quartile and above the upper quartile

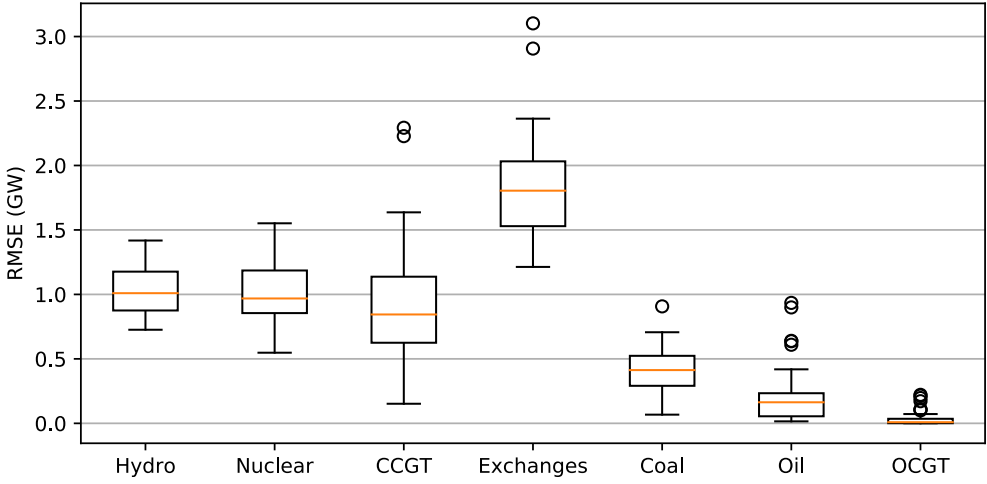


Figure 28: Distribution of the RMSE calculated for each technology during each week of 2018.

For a more detailed understanding of the model dynamics, Figure 29 presents the modeled and observed power generation for each type of power plant detailed for one week of February 2018.

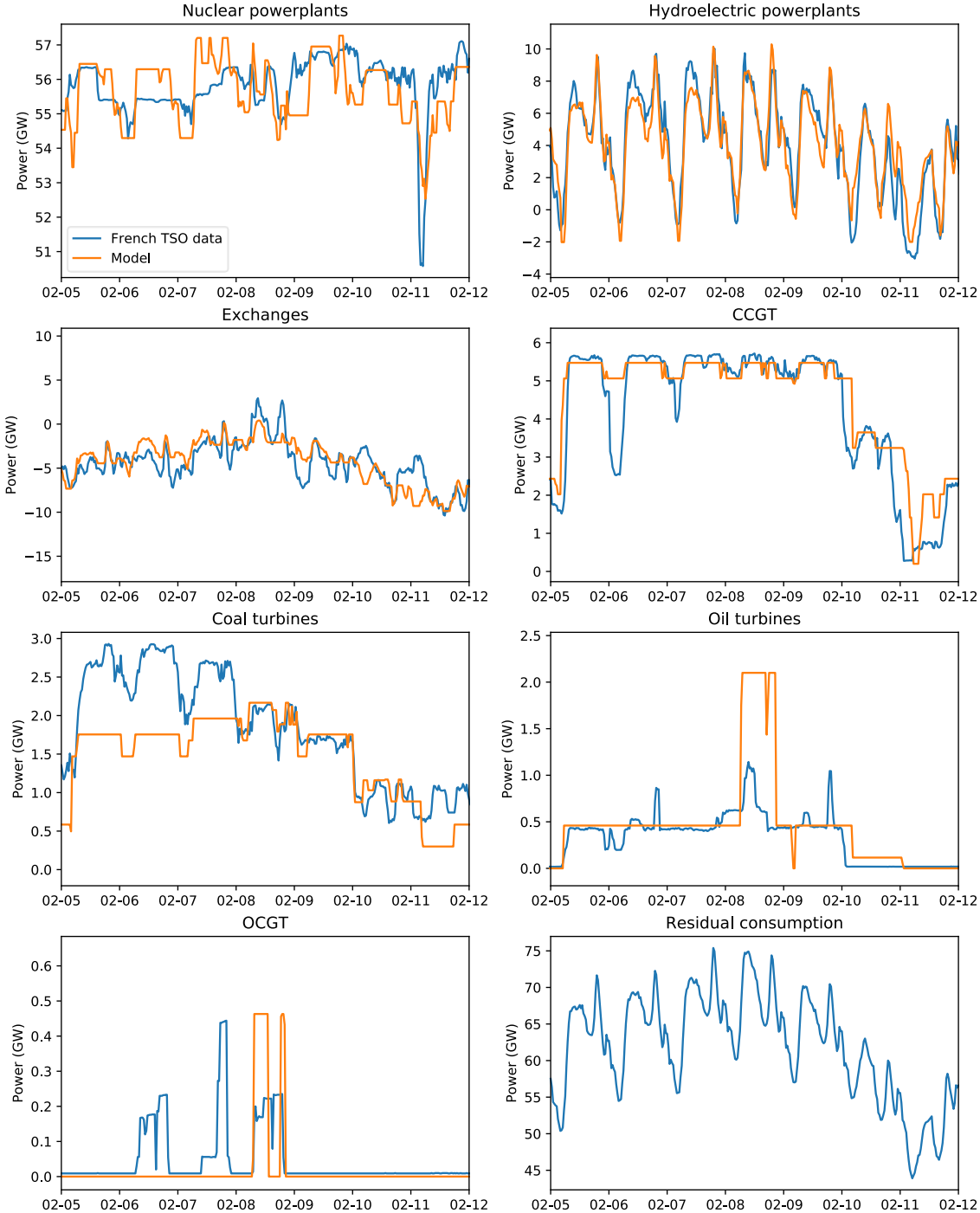


Figure 29: Modeled and observed power generation (RTE 2022b) for each type of powerplant for one week of February 2018.

The weekly validation confirmed the yearly results since the correlation coefficient and the *RMSE* were satisfactory for the frequently activated power plants and worse for the peak units. Although the weekly coefficients of the *RMSE* and the correlation were not as good as the annual validation, especially for electricity exchange and fossil fuel power plants, these indicators validate the model for a marginal usage.

In addition, the weekly analysis highlighted some seasonal effects on the performance of the model for some technologies:

- The coefficient of correlation for CCGT was lower at the beginning of spring but the *RMSE* remained low over the same period;
- Electricity exchanges were better correlated between April and September.

Weekly validations of power system models were not available in the literature to make a comparison with this model.

### 3.3.3. Third step: Aggregated indicator

A global signal aggregating the entire power system is needed in order to validate the global behavior of the model and verify the impact of the error on the peak units on the overall result. (Huang and Purvins 2020) validated their European model by comparing the electricity price obtained using a model with historical data from 2016. (Bettle, Pout, and Hitchin 2006) developed a model to evaluate the impact of energy-savings measures in England and Wales using a merit-order model. This model was validated by comparing the average emission factor of the electricity generation calculated by the model with historical data. The objective of the thesis being the assessment of the change in GHG emissions due to a decrease of the electricity consumption, a validation similar to this second approach seems appropriate. However, the French UCED model developed in this thesis also includes electricity exchanges, which should also be included in the whole validation. Consequently, the real average emission factor of the electricity generation cannot be used for the validation. A global indicator was then developed based on the emission factors of the technologies in the list  $L_{tech}$ . This indicator  $GHG_{valid}$ , (in tCO<sub>2eq</sub>, see Equation 25) is derived from the one used to calculate the marginal emissions ME (see Equation 22) and preserve the weighting between technologies.

$$GHG_{valid}(t) = \sum_{tech \in L_{tech}} EF_{tech} \cdot P_{tech}(t) + MEF_{exch}(t) \cdot P_{exch}(t) \quad 25$$

Figure 30 presents the aggregated indicator calculated with the TSO data and with the model (top figure) and the error between the two signals (lower figure). It should be noted that negative values are obtained for the indicator due to the high level of exports from France. The correlation between the two signals is 0.95 and the *RMSE* is 1114 tons of CO<sub>2eq</sub>, indicating a good overall model behavior. However, a significant error on 1<sup>st</sup> May can be observed. This error is mainly due to an error in the calculation of the electricity exchanges. As this is a non-working day in most European countries, the assumption made for the exchanges is not valid.

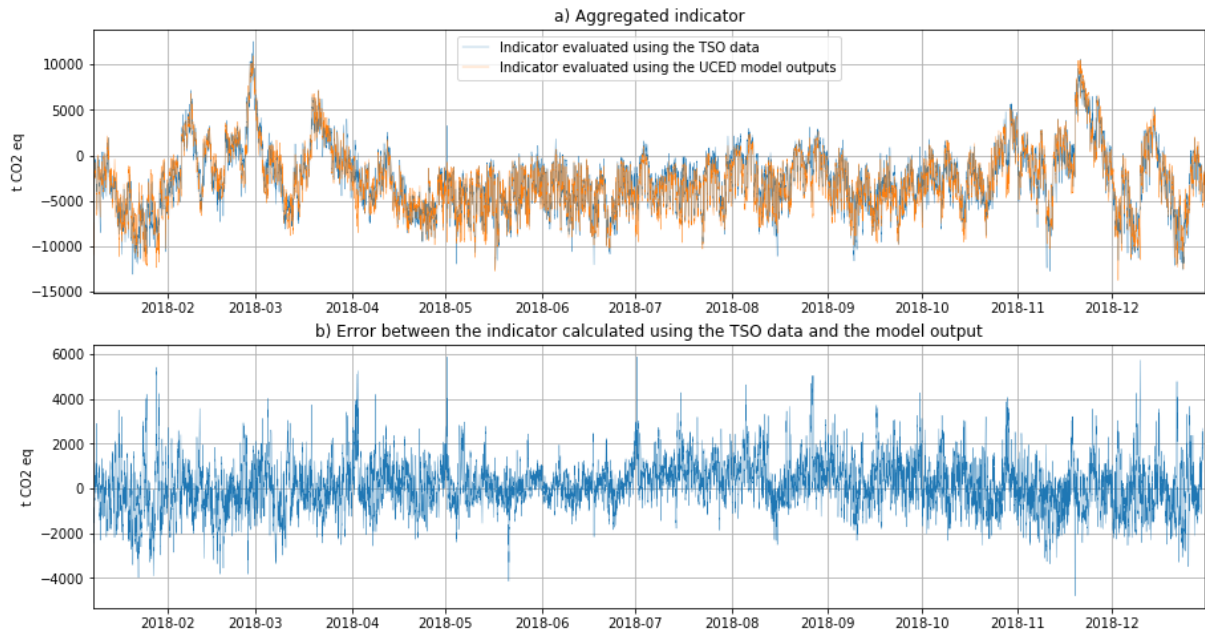


Figure 30: Aggregated indicator calculated with the TSO data and with the model and difference between them

Figure 31 represents the correlation coefficient  $R$  and the  $RMSE$  for the aggregated indicator  $GHG_{valid}$  calculated for each week and each year in 2018. The weekly and daily validations confirm the annual results, the correlation coefficient (in average 0.90 and 0.81) and the  $RMSE$  (in average 1080 and 1017 tons) staying stable during the year.

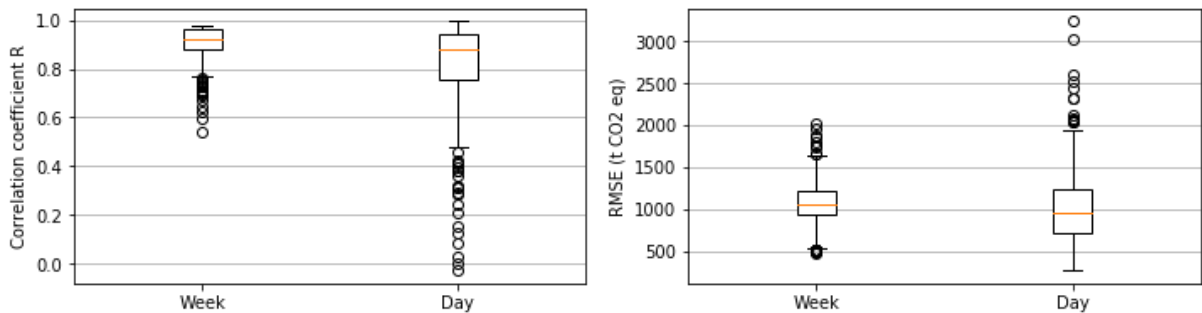


Figure 31: Distribution of the weekly and daily coefficient of correlation and  $RMSE$  for the aggregated indicator  $GHG_{valid}$

Figure 32 shows the duration curve of the correlation coefficient  $R$  for the aggregated indicator  $GHG_{valid}$  calculated for each working and non-working day. The model seems to reproduce better the dynamics of the power system during days with high consumption in France and in Europe. However, the days with low consumption in France and in Europe are not interesting for the electricity consumption interruption. The model should then be valid for DSM applications as the daily correlation coefficient is above 0.8 for 80% of the working days.



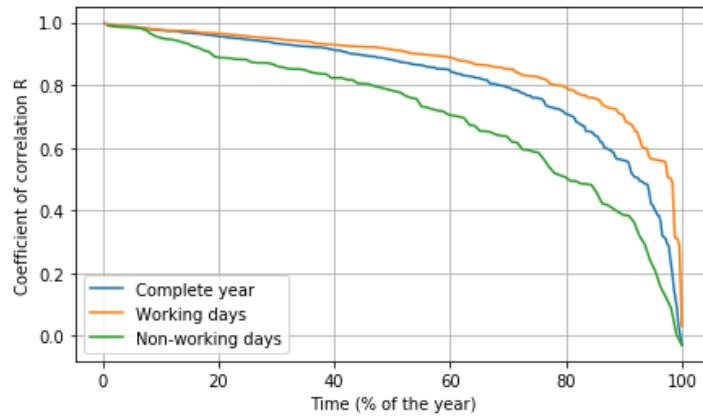


Figure 32: Duration curve of the daily correlation coefficient of the aggregated indicator for validation

### 3.4.Application: Marginal mix and MEF assessment

In this section, first results are obtained using the UCED model described and validated previously to evaluate the impact of different Demand-Side Management (DSM) events on the French power system.

#### 3.4.1. General results

Figure 33 presents the mean marginal mixes for different DSM event durations without compensation of the hydroelectricity reserves. The proportion of hydroelectricity generation was about 44% for perturbations of 30 minutes and decreased when the duration increased, reaching 16% for a duration of one day. For a duration of one week, hydroelectric powerplants were not part of the marginal mix as the model considers hydroelectric energy conservation over a week. As the proportion of the hydroelectricity mix decreased between a duration of one day and one week, the proportion of all the other technologies increased. In (Heggarty et al. 2020), the authors quantified the flexibility contribution of the different generation units of the French power system for annual, weekly and daily timescales for 2018. Their observations are consistent with these results.

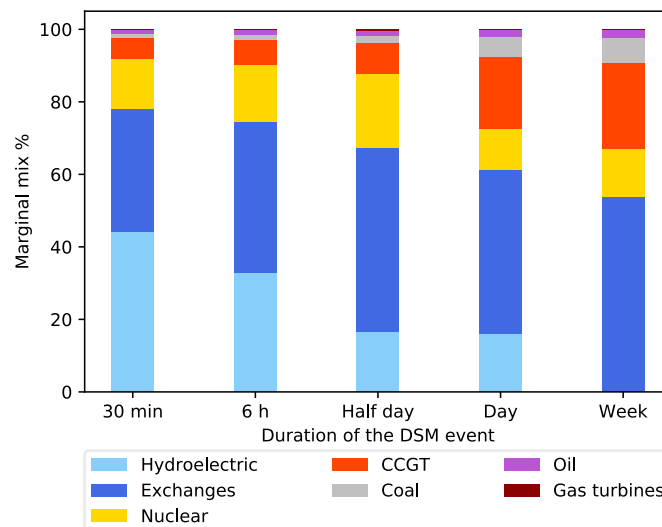


Figure 33: Marginal mix with different durations of DSM events.

Figure 34 presents the mean marginal mixes for different DSM event durations after integration over one week (Equation 22). The hydroelectrical energy production being conserved, this generation does not appear in the incorporated mix. For a decrease of 30 minutes, electricity exchange represented about 62% of the marginal mix, and CCGT power plants about 25%. This marginality decreased with the duration of the perturbation in demand to reach 54% and 14% respectively for a one week-long DSM event. At the same time, the share of national fossil fuel powerplants increased, especially for coal fired powerplants.

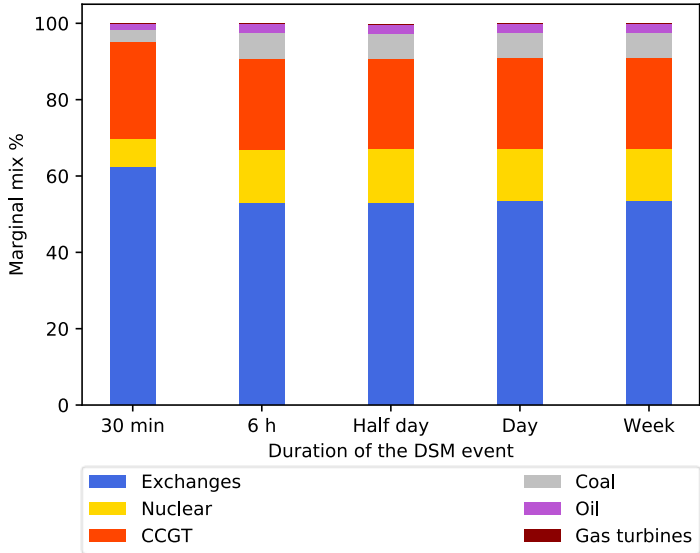


Figure 34: Marginal mix with duration of a DSM event with hydroelectricity compensation

These general results led us to two initial observations:

- Electricity exchange represents a large share of the marginal mix. Identifying the countries responding to the variation in French exchange is therefore crucial to an evaluation of the impact of the change in demand;
- The marginal mix varies with the duration of the DR event. The incorporation of the dynamics of demand is thus important to evaluate the marginal mix.

In the following sections, we analyze in detail the weekly and annual patterns of the marginal mix.

### 3.4.2. Time sensitivity of the marginal mix

We propose a synthetic representation of the results for 30-minute demand response events on a weekly scale. We chose to average the 52 weeks into a typical week with a half-hour resolution. Figure 35 presents this average marginal mix for 2018. The upper graph (a) is the average residual consumption. The middle graph (b) represents the average marginal mix. Technologies responding to a modification in demand are stacked and represented by different colors. The hatched area represents the energy displaced by hydroelectric powerplants, and the technologies balancing the production are detailed using the same colors. The average proportion of hydroelectric powerplants in the marginal mix was around 45% and was quite stable except during off-peak hours, when hydroelectric units are frequently saturated downward. The mix balancing the hydroelectric energy displacement was also quite constant. The influence of the residual consumption level on the marginal

mix is easy to observe by comparing these two graphs (a and b). During peaks of residual consumption, the decrease in demand is frequently addressed by the variation in electricity exchange or a decrease in CCGT generation (except for the compensation of hydroelectric powerplants). The decrease in demand during peaks of residual consumption also generate an increase if nuclear generation during the week through compensation of the hydroelectric generation. During off-peak hours, the presence of electricity exchange in the marginal mix was less common, replaced by nuclear powerplants or CCGT. The lower graph (c) shows in detail the countries adapting their generation when electricity exchange was part of the marginal mix. Most of the marginality of the exchanges was balanced in Germany, which seems logical as it is, together with France, the largest exporter in Europe. Most of the time, France and Germany are competing to export to the same countries. When the French exports increased, German electricity production and exports decreased. The power systems of Portugal also had a significant impact on the French marginal mix. Spain was a net importer most of the time, importing electricity from France and Portugal. Consequently, when French exchanges increased, the model often considered that Portuguese electricity generation and exchanges decreased with the electricity exported to Spain.

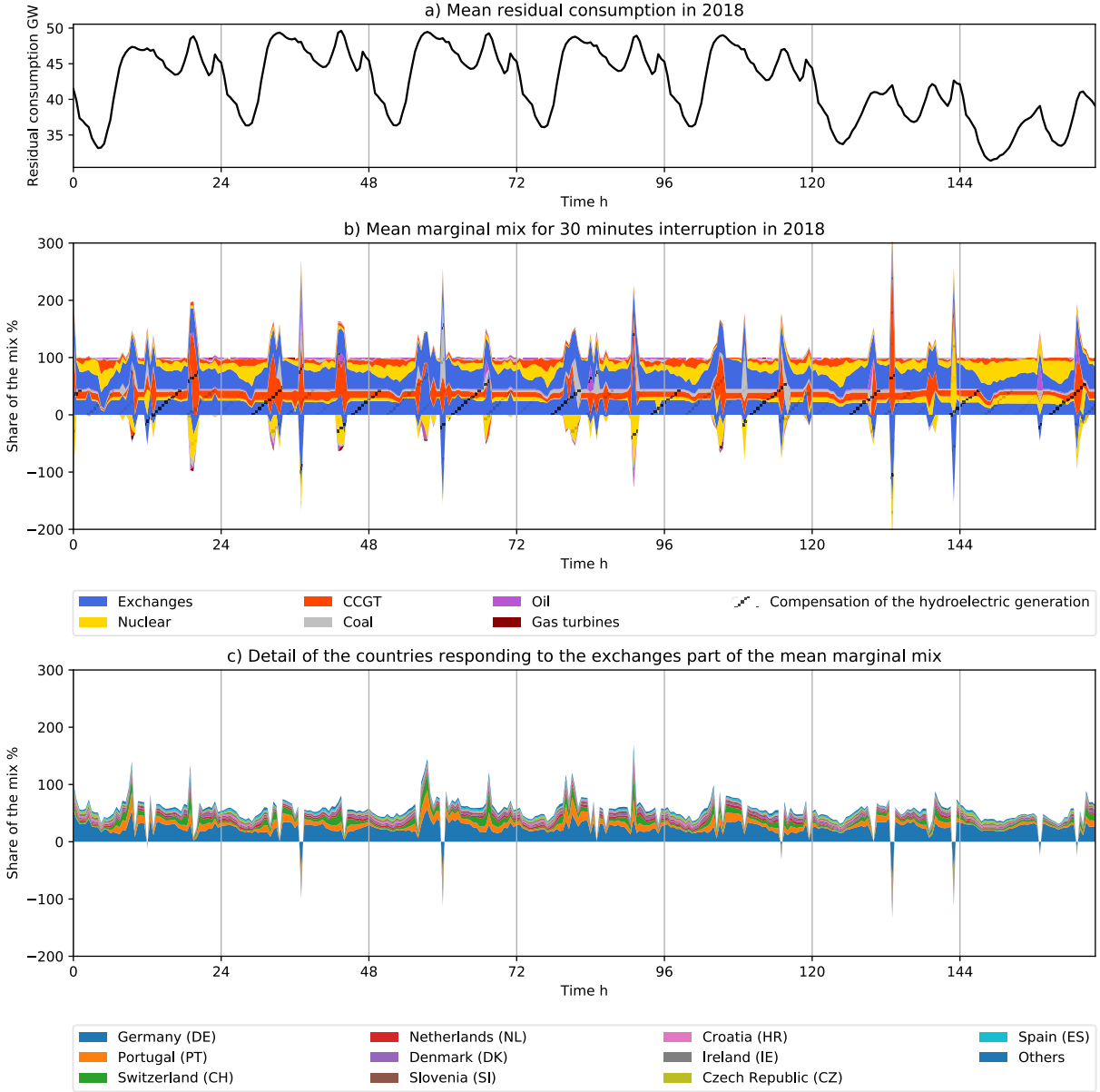


Figure 35: Mean residual consumption and mean marginal mix for 30-minute interruptions in 2018 (half-hour resolution)

### 3.4.3. Seasonal variability of the marginal mix

The previous approach showed the technologies and the countries that are frequently marginal for each time-step of the week. However, it does not highlight the variation in the marginal mix between seasons. We thus propose a complementary approach in Figure 36, where the response over the 52 weeks is averaged. The upper graph represents the average marginal mix. It varies over the months as the share of fossil-fueled power plants during winter is more significant, and the proportion of electricity exchanges is lower.

The graph below represents in detail the countries adapting their generation when electricity exchanges are part of the marginal mix. We observed that the contribution of the different countries to the balance of the marginality of exchanges was highly seasonal. Between April and September, Germany and the Netherlands were partly replaced by Switzerland. The share of Switzerland was especially high during spring. This observation can be explained by the high installed capacity of hydroelectric powerplants in the Swiss power system associated with snow-melting, which increases hydroelectricity generation and decreases the generation cost of Swiss electricity.

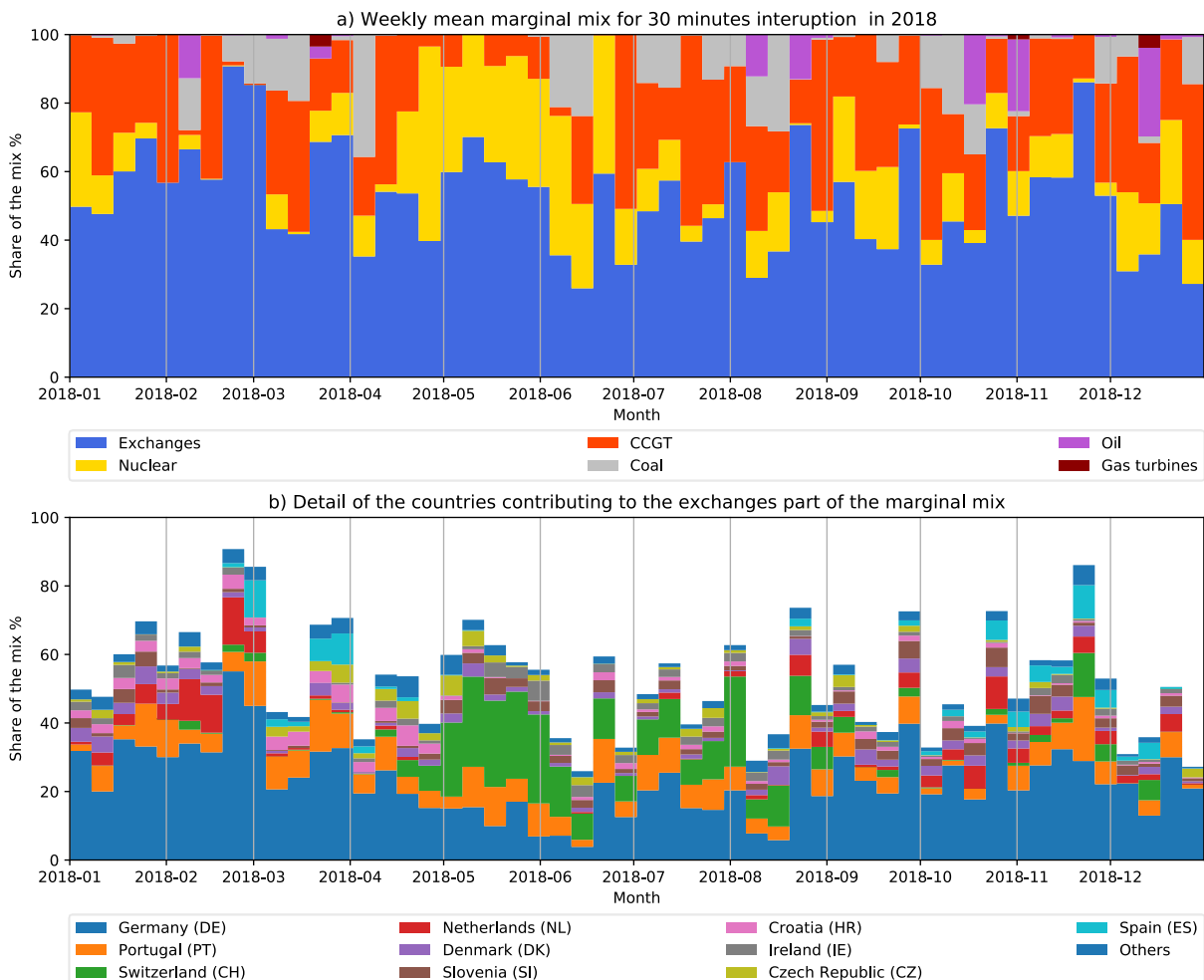


Figure 36: Monthly mean marginal mix for 30-minute interruptions each half-hour in 2018

The graphs in Figure 37 are similar to the one shown previously (Figure 36), but for daily demand response events. In this case, the marginal mix varied more during the year. The share of electricity exchanges in the marginal mix varied between 23% and 97% during the year. Nuclear powerplants are

rarely marginal in February, when they are often saturated. They are more frequently marginal between April and June, which can be explained by the yearly dynamics of the nuclear fleet. Regarding the mix of the countries adapting their generation when electricity exchanges are part of the marginal mix, the observations are similar to the case with 30-minute perturbations.

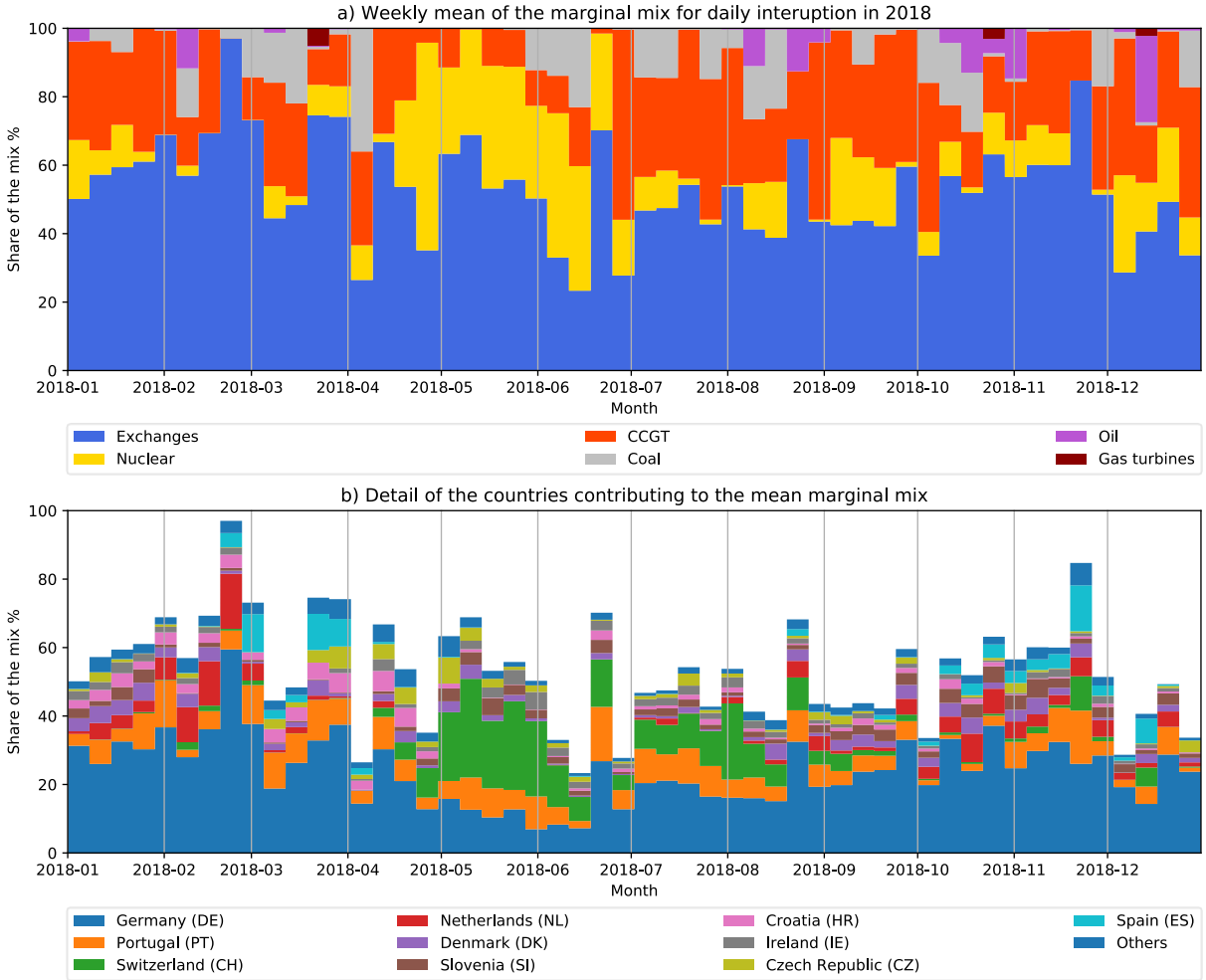


Figure 37: Monthly mean marginal mix for daily interruptions in 2018

3.4.4. Impact of DR strategies on the French power system

In the previous section, the marginal mix was systematically evaluated for each hour of the year. In this last section, three typical demand response (DR) strategies are considered (see Figure 38):

- Peak Clipping: the electricity consumption is decreased during the peak periods in order to reduce the peak demand (e.g. implementation of fuel switch strategies for space heating);
- Valley filling: the electricity consumption is increased during the off-peak periods (e.g. hydrogen production);
- Load shifting: the consumption is displaced from peak periods to off-peak periods, combining the two previous patterns (e.g. electricity storage in batteries or thermal storage in domestic hot water tank).

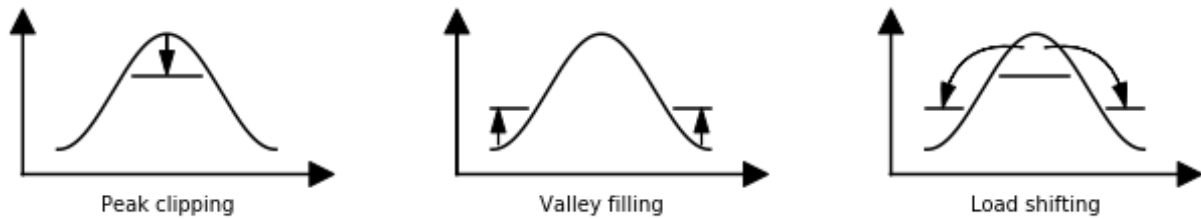


Figure 38: Schematic view of the DR strategies tested.

These DR strategies were then translated into three patterns:

- Peak clipping: daily decrease of the consumption (-100 MW) during three hours applied at the daily maximum of the residual consumption;
- Valley filling: daily increase of the consumption (+100 MW) during three hours applied at the night minimum of the residual consumption;
- Load shifting: addition of the two previous patterns.

Daily peak clipping, valley filling and load shifting were applied for each day of the year 2018, simulating a recurring DR event with an amplitude of 100 MW. Figure 39 represents the overall impact on the French power system of these three DR strategies. The results shown are represented in terms of a net balance and negative values indicate a decrease in production or an increase in exports. Results of the flow tracing method showed that DR applied on the French power system impacted mainly the German, Portuguese, Swiss and Dutch power systems. The details of the impact of DR strategies on the exchanges are detailed in the next paragraphs

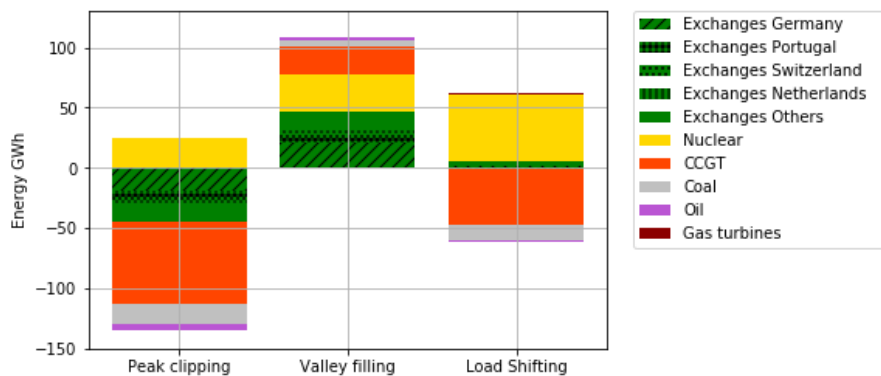


Figure 39: Marginal mixes of the impact of DR on the French Power system in 2018.

The three DR strategies increased the nuclear electricity generation, leading to an increase of the utilization rate of the nuclear fleet. The peak clipping strategy also decreased the energy generated from fossil fuels such as natural gas, coal or oil. Moreover, this strategy increased the total amount of electricity exported and would reinforce France's position as net exporter on the European grid. The valley filling strategy increased the electricity generation from fossil fuels and decreased the total amount of electricity exported. Finally, the load shifting strategy seemed to be the most efficient way to increase the utilization rate of the nuclear fleet while decreasing the electricity generation from fossil fuels. The net balance of the exchanges was only slightly affected. It should be emphasized that this result presents the sum over the year of net imports and net exports occurring at different periods of the year.

The three DR strategies tested previously were applied every day of the year, which might not be an optimal DR strategy. For example, Figure 40 presents the marginal mix consequently to the peak clipping strategy during each quarter of the year. The strategy was the most efficient in improving the utilization rate of the nuclear fleet, reducing the generation from fossil fuels and increasing the exchange balance during the first quarter of the year. The electricity demand was high during this quarter and the power system was often saturated. On the contrary, the demand was lower during the second quarter and the electricity generated by hydroelectric powerplants was high due to snow melting. Consequently, the peak clipping strategy decreased the utilization rate of the nuclear fleet.

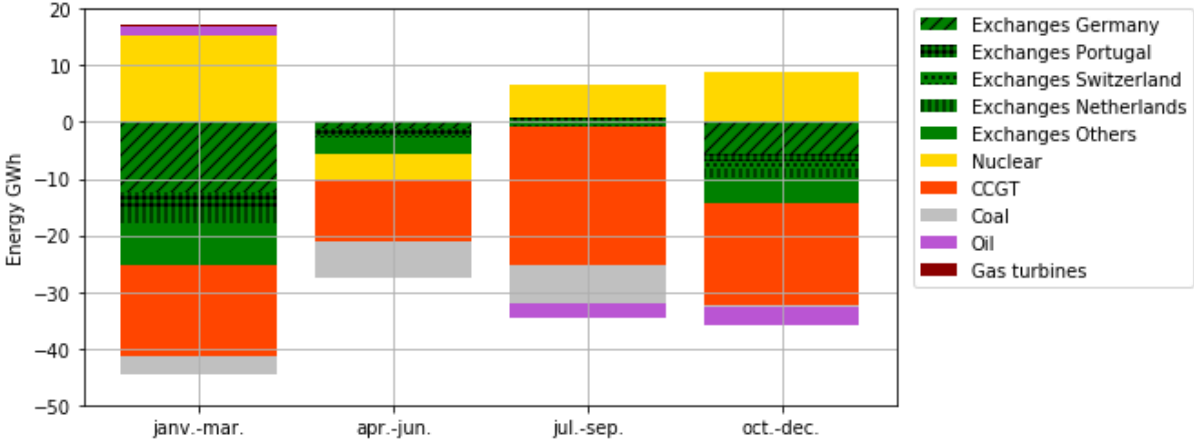


Figure 40: Marginal mix consequently to the peak clipping strategy during each quarter of year 2018.

Figure 41 shows the marginal mix resulting from the peak clipping strategy applied only one day per week. Throughout this example the sensitivity of the marginal mix to the time of the week could be observed. For a similar reason as in the previous example, the peak clipping strategy seemed to be more favorable on weekdays than on weekends.

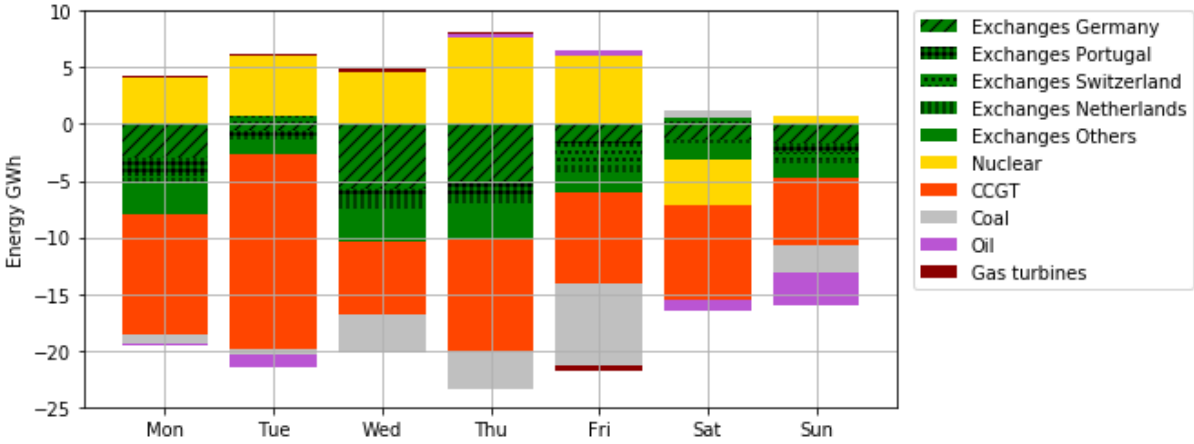


Figure 41: Marginal mix consequently to a peak clipping applied a day per week depending on the day of the week

### 3.5. Conclusions

The objective of this chapter was to assess the marginal mix of electricity consumption in France, using a semi-physical power system model. First, a method to model the UCED problem was developed based on two calibrated merit-orders, the first one representing the unit commitment merit-order, the second one the economic dispatch merit-order. Moreover, the model takes into account the

specificities of hydroelectric production with its energy conservation, the availability of power plants and the electricity exchanges. This allows to reproduce the daily and intra-daily dynamics, which is an essential feature for evaluating various types of DR events. The combination of all these characteristics makes it an original model as the literature shows that single-country models rarely address all these constraints. Moreover, incorporating the “flow-tracing” method, presented in the previous chapter, that allows to identify the origin of the imports and the destination of the exports, adds an essential feature to such models.

The application of the method to France for the year 2018 is validated with historical data for the whole year and for each week. This ensures the validity of the model, an important point to stress in order to analyze the impact of DR events of a few hours. Sub-hourly DR events were not addressed in this thesis, and would require models with a much finer time-step and, given the limited availability of data at sub-hourly time step, a different approach. The validation showed that single-country models, including interconnections, are relevant to model power systems even though countries are increasingly interconnected.

The marginal mix of the French power system was then evaluated for DR events of between 30 minutes and one week and for three specific DR strategies. The results showed that the duration of the marginal demand is important for the evaluation of the associated marginal mix. The marginal mixes obtained were also highly sensitive to the time of the week as well as to the season. The difference between a decrease of 30 minutes and one day highlighted the importance of including dispatch and scheduling as two steps in the model. The results also showed that peak clipping, valley filling or load shifting strategies could increase the utilization rate of the nuclear power plants and decrease the French electricity generation from fossil fuels. Moreover, DR applied in France also affected the interconnected power systems, in particular Germany, Portugal, Switzerland and the Netherlands. This demonstrates the importance to model interconnections and to identify which countries adapt their electricity generation consequently to a change in national exchanges. The limited water reserves also happened to be the key to capturing the displaced energy demand and its overall impact on the marginal mixes.

From this study, it was observed that a large part of the variation in French electricity exchanges is compensated by other countries, where a carbon-intensive marginal mix is expected (e.g. Germany). While the electrification of energy services will be part of the decarbonization process in France, its short-term consequences might lead to higher GHG emissions than expected. Completed with the emission factors for electricity generation in France and the marginal emission factor for electricity exchanges calculated in the previous chapter, this model can be used to evaluate the MEF of the French electricity consumption. The objective of this thesis being the evaluation different control strategies for hybrid heat pumps on GHG emissions, this UCED model has also to be coupled with an energy model including the demand-side and especially the consumption from space heating and domestic hot water.



# 4. Evaluating the space heating and domestic hot water needs of a district

In the previous parts of this thesis, the development of a UCED model of the French power system was presented. Coupled with a model that evaluates the marginal emission factor (MEF) of the electricity exchanged on the European grid, this model can be used to assess the GHG emissions associated to a variation of demand on the French power system. To evaluate the potential contribution of hybrid heating systems to decarbonization, the energy consumption due to space heating and domestic hot water (DHW) production should be known. The aim of this chapter is therefore to present the model developed to evaluate the energy consumption for space heating and DHW for a district and to extrapolate this demand to a national level. Section 4.1 presents the case study of this thesis. Section 4.2 discusses different methods for modelling buildings at district level and scale up the heating demand. Sections 4.3 and 4.4 focus on the model description for space heating and DHW. Finally, Section 4.5 discusses the first results obtained with the models.

## 4.1. Case study

The use case addressed in this thesis is the space heating and DHW demand for multi-family housings. Different heating systems can be used for such a use case (see Figure 42), ranging from decentralized solutions with one heat pump for each room to centralized solutions with one heat pump for the whole building. In this thesis, a centralized hybrid heat pump is installed for 30-35 dwellings. Considering an aggregated scale for the heating demand has multiple advantages: the installation costs can be shared between tenants, avoiding an oversizing, and the heating demand is relatively easy to predict due the coincidence of usages. Indeed, the heating demand of a single dwelling is highly related to both the dwelling characteristics and the behavior of occupants. Due to the variety of load profiles in a building, working at a centralized scale offers a longer uptime than at a dwelling scale. Therefore, the potential of curtailment for one machine is more important at an aggregated scale, and should therefore provide a better cost/benefit ratio than working at the dwelling level.

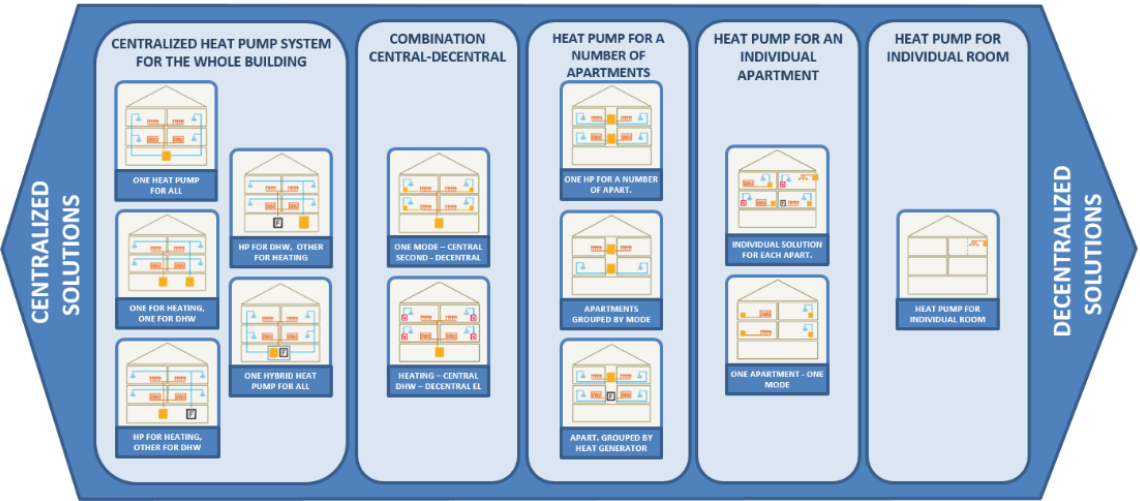


Figure 42: Heat pump systems configurations classified from centralized to decentralized solutions (Annex 50 2023)

Different configurations of hybridization of the heat pump can be identified and are summarized in Figure 43. In the residential sector, heat generation is required to heat spaces and also to produce DHW. If heat can be easily generated with gas boilers for both uses, heat pumps are more limited. They can be classified into two main categories:

- A single hybrid heat pump for space heating and DHW: In this case, the heat pump needs to generate water up to 65°C several times a day. They are more expensive than traditional heat pumps, which typically have a maximum output temperature of around 55°C. In addition, the performance of heat pumps is reduced at high temperatures. Finally, in such configuration, the hybrid heating system has to be carefully designed in order to produce alternatively DHW and space heating without jeopardizing the comfort of occupants.
- Hybrid Heat pump for space-heating only: The heat pump heats the water up to the design temperature for space heating (usually 55°C maximum). Such heat pumps are less expensive but have to be combined with another system to provide DHW. DHW can then be generated:
  - o By a second hybrid heat pump for DHW. With two heat pumps instead of one, this configuration is more expensive than the previous one.
  - o Exclusively by the gas boiler of the hybrid heat pump. This is the most commonly observed configuration for hybrid heat pumps. However, the objective of this thesis is to optimize the GHG emissions. DHW generation exclusively from gas should then be avoided.
  - o By an electric water heater. As heat pumps have better performances than electric water heaters, even in cold conditions, DHW generation exclusively from electric water heater should be avoided considering the objective on GHG emissions.

Finally, a single hybrid heat pump generating both space heating and DHW (first case) was chosen in this thesis for the development of the optimal control strategy.

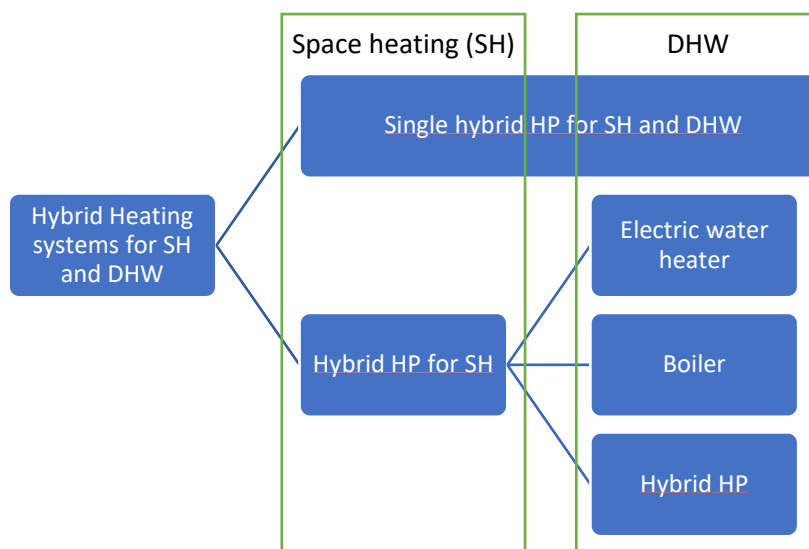


Figure 43: Different configurations of hybrid heat pumps.

Figure 44 presents the general configuration for such hybrid heating systems. In this figure, the topics discussed in the next sections can be identified:

- the modeling of the space heating needs (emission and distribution) (section 4.3);
- the modelling of the DHW needs (section 4.4);
- the modeling and control of the heat generation system (part 5).

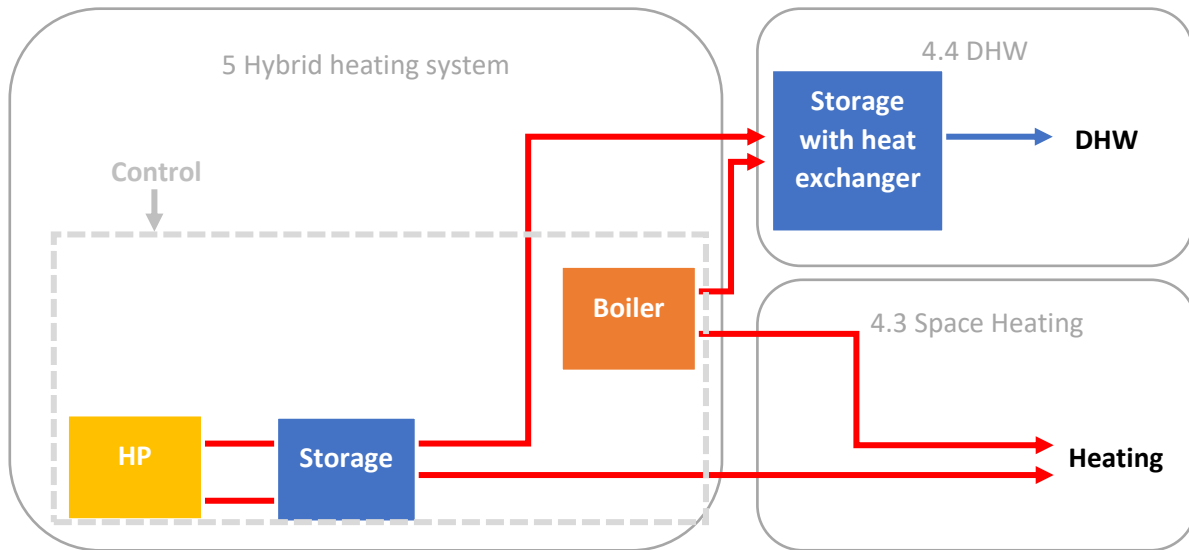
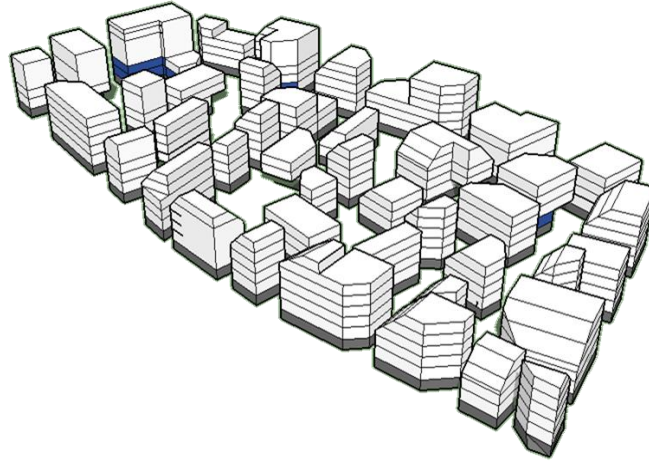


Figure 44: General configuration of hybrid heat pumps providing space heating and DHW

The objective of the modelling work is twofold: to test different sizing and control strategies for a specific hybrid heating system and to evaluate the GHG emissions of such a hybrid system when rolled out at scale in France. The case study should be consistent with the French long-term environmental goal. In “*Energy pathways to 2050*”, the French TSO published different targets for electricity demand reduction potential exceeding one hour in residential heating, which should be partly covered by hybrid heat-pumps. In the different scenarios the required maximum flexibility varies from 0 up to 5.6 GW (RTE 2022c). In this thesis, a fleet of 100 000 dwellings heated by hybrid heat-pumps is modeled. Considering a mean surface of 60 m<sup>2</sup> by dwellings, a peak heating need of around 50 W/m<sup>2</sup> and a minimum COP of 2 for the heat pumps, the maximum flexibility provided by the fleet would be around 0,15 GW which is consistent with the scenario of the French TSO.

Modelling a typical district was then seen as a solution, both to capture the dynamics at the building scale and to extrapolate the results to the national scale. The district archetype modelled in this thesis (see Figure 45 is composed of 337 dwellings in 45 buildings, which was proven to be sufficient to get enough diversity in heating patterns (Martinez, Vellei, and Le Dréau 2021). These dwellings are characterized by a mean floor area of 65 m<sup>2</sup> and occupied in average by 2.2 persons. The space heating is emitted in dwellings through radiators.



*Figure 45: View of the district model*

## 4.2. Method

This part explains the methodology used to model the space heating and DHW demand for a district and to scale up the heating demand to the national level. Subsequently, the choice of the model type and the simulation tool is justified. Finally, the complete modelling procedure from the input data to the evaluation of the heating demand and the associated GHG emissions is presented.

### 4.2.1. Urban Building Energy Modelling tools

In our case-study, a hybrid heat pump is controlled locally to provide heat to 30-35 dwellings. However, the avoided emissions should be evaluated at a national scale to observe the effect of aggregation. The model developed then has to estimate the effect of DR strategies at both national (i.e. 100 000 dwellings) and local (i.e. a few dwellings) scales. An Urban Building Energy Model (UBEM) was developed to assess the heating needs of a district. (Ferrando et al. 2020) reviewed the existing UBEM tools. Figure 46, adapted from this article, shows the different urban modelling approaches.

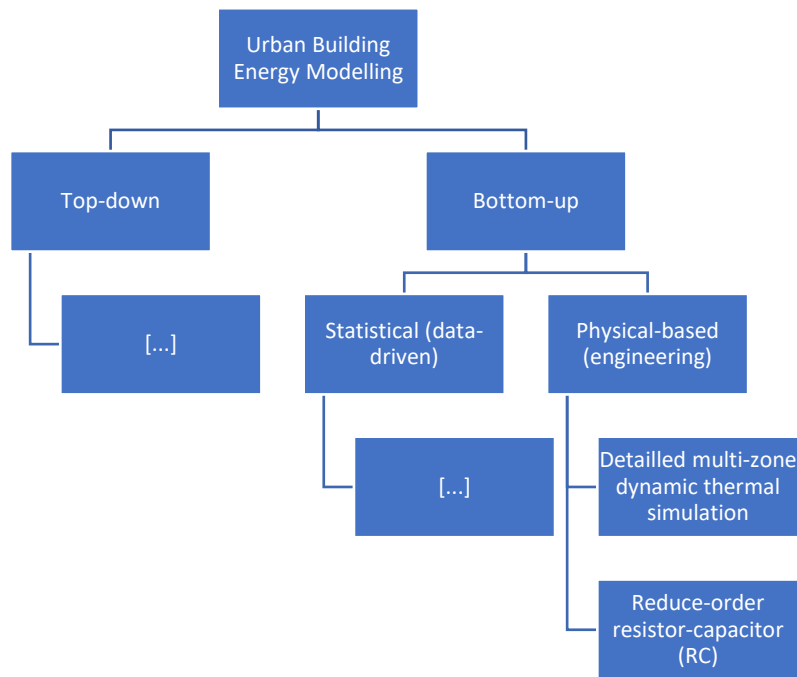


Figure 46: Urban modeling approaches, adapted from (Ferrando et al. 2020)

Two types of models can be used to model a load at a relatively high level of aggregation: top-down and bottom-up models. Top-down models are usually statistical models built from a few explanatory variables (van Vuuren et al. 2009), whereas bottom-up models are the results of summing the behavior of each individual unit and are therefore more explicit. In this work, we decided to use bottom-up models to reproduce the aggregated load in order to model properly the control of hybrid heat pumps.

In bottom-up models, the energy consumption evaluation can be data-driven using machine learning methods (Schneider et al. 2017) or physics-based using explicitly the thermal properties of the buildings (Wang et al. 2018; Perera et al. 2018). Physics-based models need more information for parametrization and can be more computationally intensive. However, they can generate results with different time steps, when data-driven models generally assess the monthly or yearly energy consumption of buildings.

Finally, bottom-up physics-based UBEM comprise physical descriptions with various levels of detail, from multi-zone thermal simulation (Wang et al. 2018) to reduced-order resistor-capacitor approaches (Perera et al. 2018). The computational time is thus a key factor to choose an appropriate modelling approach. Reduced-order resistor-capacitor approach provides a good balance between simulation performance and accuracy at the district level.

In this thesis, a bottom-up physics-based UBEM evaluating the energy demand for space heating and DHW was coupled with a model of the heat generation systems, including the hybrid heat pump, the distribution and the storage.

#### 4.2.2. Dymola libraries for buildings and district simulation

The simulation software *Dymola* (Dynamic Modeling Laboratory) was chosen as the platform for developing the UBEM (Dassault Systèmes 2023). It is based on the *Modelica* language developed within the Modelica Association (Modelica Association 2023). *Dymola* is a multi-physical tool: various kinds

of physical systems can be modelled. *Modelica* is an object-oriented language and various libraries of components, both commercial and non-commercial, are available on the website of the Modelica Association. In this section, only the non-commercial libraries related to buildings and districts modelling available on the Modelica Association website are presented. Some libraries are based on the Modelica-IBPSA library developed in the context of IBPSA Project 1: *AixLib* from RWTH Aachen University (Germany), *Buildings* from LBNL (Berkeley USA), *BuildingSystems* from UdK Berlin (Germany), *FastBuildings* from KU Leuven (Belgium). Other libraries, not based on Modelica-IBPSA, can also be used such as *ATPlus*, *BuildingControlLib* or *BuildSysPro* (EDF).

The objective of this work is to simulate the district archetype with the best achievable accuracy and a reasonable simulation time. The detailed room air model *MixedAir* from the *Buildings* library is the most complex room model of these libraries. The simulation time with such a model for a district of 337 dwellings was evaluated. With a strategic implementation and using the variable step solver *DASSL* with the default configuration, the computation time for the complete district was reasonable to choose this level of modelling. The UBEM model was then based on the *Buildings* library. The heat generation system was modelled using both *Buildings* and *AixLib* libraries.

#### 4.2.3. Large-scale simulation with Dymola

Two main difficulties occur during large-scale simulations with *Dymola*, as discussed in (Casella 2015):

- **Compilation** of *Dymola* models with many components can abort due to memory issues;
- The **simulation performance** and consequently the **simulation time** can be affected by the numerous components in the model.

In this thesis, the detailed model of the *Buildings* library is used to develop a district model, which corresponds to a large-scale simulation problem. However, there are solutions to reduce the impact of the number of components on the simulation time. In the first part of this section, solutions to compile large-scale models will be presented as well as their implementation in the district model. Secondly, the causes of reduced simulation performance are analyzed and solutions are proposed.

##### A) Compilation

The compilation of *Dymola* models begins with flattening, meaning that each component implemented as a vector, each variable and each equation of each loop is explicitly converted to C code and stored in several C files. If there is not enough memory available for flattening, the compilation of the model can abort.

Moreover, it can be observed that the limit on the size of the model that can be compiled with *Dymola* is higher when each component is explicitly instantiated rather than using vectorized components. In the case of a district with 337 dwellings, it would not be realistic to instantiate manually each component. Consequently, in this thesis, the *Modelica* code corresponding to the district model is generated automatically through a *Python* script.

It is important to notice that the number of submodels composing a model also influences the size of the compiled C code. Several libraries for district modeling are available, however most of them generate district models using conventional libraries and none of these two issues (the explicit instantiation and the number of submodels) are considered. The studies addressing the large-scale simulation issues with *Modelica* generally focus on solver issues but often neglect the library

development. Consequently, best practices for the development of libraries designed especially for large-scale problems should also be applied in order to facilitate model compilation.

## B) Slow simulation

Contrary to the compilation problem, which is specific to large-scale simulations, slow simulation problems are largely addressed in the *Dymola* user guide (Dassault Systèmes 2021). Three main causes can explain a long simulation time:

- **Too much time is spent to store results:** By default, all variables of each component are stored during simulation. To reduce the time spent, only useful variables were selected and stored during the simulation using the setup toolbox. In addition, the length of the stored time series was also reduced by disabling the storage of variables at time events and carefully selecting the interval length of the simulation results. The interval length of the district simulation should match the output of the UCED model of the French power system. Therefore, a 30-minute interval was chosen.
- **Too many steps are evaluated due to events:** The events generated by timetables and by changes in “if-conditions” were avoided. The steps corresponding to the time or state events are then no longer evaluated. However, the interval length of the results set for the simulation already ensures accurate results. Consequently, these specific steps are not needed.
- **Too much time is spent for each simulation step:** This can be caused by too many state variables in the model or non-linear algebraic loops, which should to be avoided. This type of problem can also be reduced by applying a higher tolerance for the solver. In this case, it is necessary to check that the results are similar to those obtained with a lower tolerance. Evaluating the parameters during compilation can simplify the systems of equations and reduce the simulation time. However, with this setup, parameters are considered as constant and the model should then be compiled each time a parameter is changed, which is less interesting in the case of a sensitivity analysis or of varying states. Finally, in the case of large-scale simulations, the sparse solver can be activated using the flag “*Advanced.SparseActivate=true*” and the simulation can be parallelized on several cores using the flag “*Advanced.ParallelizeCode = true*”.

In this thesis, the UBEM evaluating the space heating emission and distribution consists of a large non-linear algebraic loop. The heat generation model (i.e. hybrid heat pump model) leads to many state events, which is common for models involving controllers. Coupling these two parts (heating demand and heating generation) in the same model reduces the performance of the model because the two problems are combined. Therefore, the two parts of the model were kept separated to optimize the computation time. The UBEM was then simulated once for one location to generate inputs for the different heating generation models. These inputs are the sum of the mass flow rates flowing through the radiators  $\dot{m}_{SH}$  and the water temperature at the outlet of the radiators  $\theta_{return,SH}$ . In such a configuration, the space heating supply temperature  $\theta_{supply,SH}$  is an input to the urban building model and a setpoint for the control of the heat generation model. It is necessary to ensure that this setpoint is always reached in the heat generation model to avoid a mismatch between the two parts of the model. The coupling of the two models is shown in Figure 47.

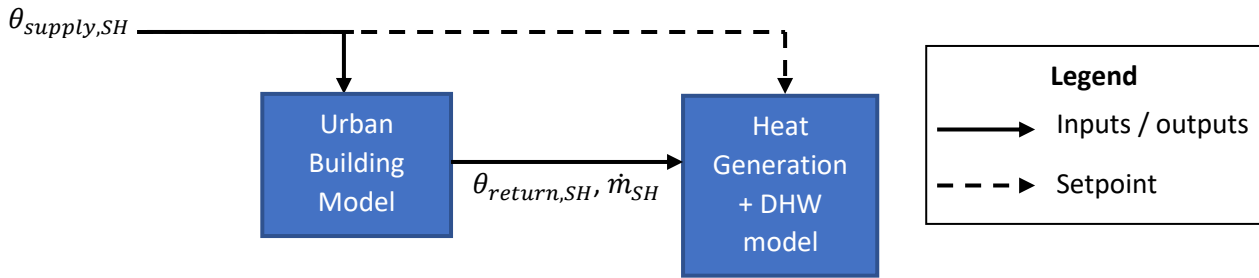


Figure 47: Decoupling strategy applied to the UBEM model

#### 4.2.4. Modelling procedure

The workflow for district modelling can generally be divided into five steps: inputs generation, model development, simulation, output generation and post-process (Ferrando et al. 2020). Figure 48 presents the workflow implemented in this thesis to model the heating demand and the heat generation. Inputs related to buildings, occupant behavior and heat generation were generated based on statistical distributions or fixed values using *Python*. The method to generate these data is described in the following sections. Based on these input data, *Modelica* files corresponding to the models of the buildings and the heat generation were generated using a *Python* script. The simulations were then launched in *Dymola* to generate results. These results were then post-processed with *Python*.

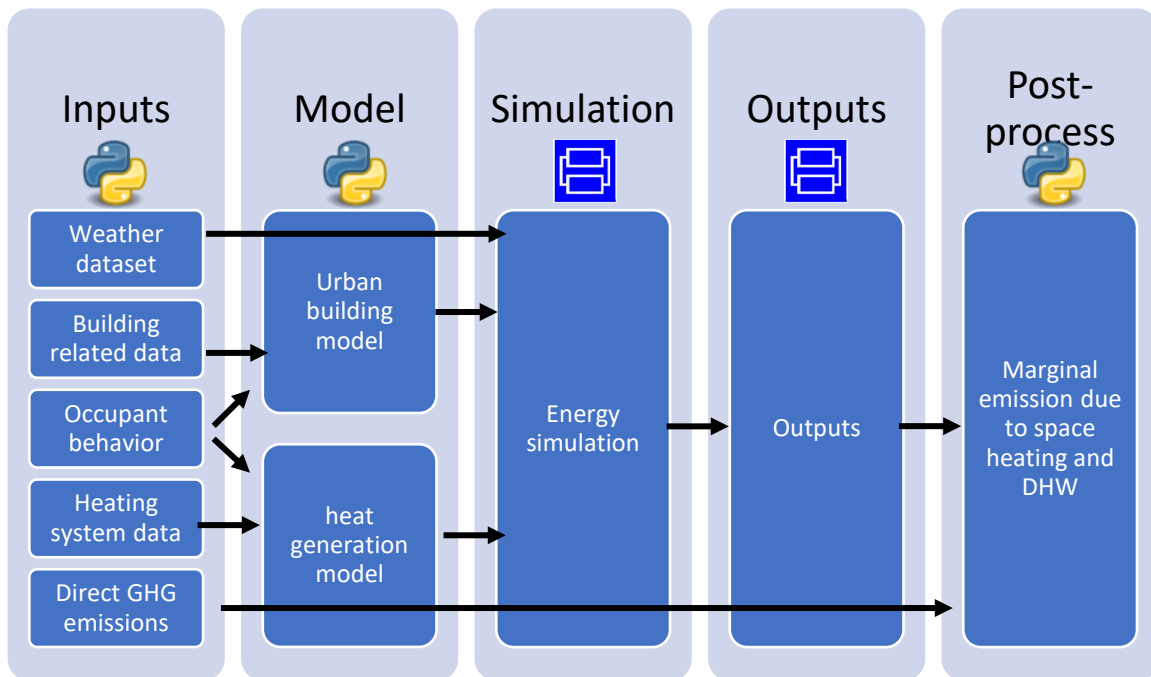


Figure 48 :Workflow for the simulation of the heating demand and heat generation

#### 4.2.5. Scale up from a district to a national heating demand

The scaling up of the heating demand from a district archetype to the national level is presented in this section. The current performance of the UBEM tool is not sufficient to be able to carry out a thorough bottom-up simulation of the national building stock. Therefore, national-level space heating demand is usually evaluated by combining bottom-up methods with grouping techniques. The aim is to identify typical buildings representing the national stock. The UBEM is simulated solely for the building



archetypes, and then the heating demand is scaled up significantly reducing simulation time. (Goy, Coors, and Finn 2021) identified three principal grouping approaches to analyse a country's building stock: supervised, un-supervised, and semi-supervised. In the supervised grouping, building groups are initially defined based on a set of features. The building stock is categorised based on various features. For instance, in (Sasso, Chambers, and Patel 2023), the Swiss building stock was grouped according to their age, district typology (urban, suburban, and rural), Canton, element type (SFH, MHF, offices), heating system, and retrofit period. In contrast, unsupervised methods, also known as clustering, do not have pre-defined groups. Instead, the building stock is divided using an algorithm that relies on graphical and/or numerical criteria such as distance minimization between group members. For example, (Murray et al. 2020) uses a clustering method that defines representative building archetypes based on building area, age, energy demand, climate region and renewable energy potential. Finally, hybrid methods, known as semi-supervised techniques, employ both supervised grouping and clustering on the building stock. For instance, in (Eggimann et al. 2022), grouping is initially based on building type, age, and climate zones. Next, clustering is performed on each group by considering the compactness, density, and size of the buildings. The building archetypes chosen to represent a group are generally the one with the less dissimilarities with the other elements of the group. The previous articles focus on the grouping methods employed on buildings. However, in some studies, the identification of characteristic archetypes for neighbourhoods may be of greater relevance. For instance, (Eggimann et al. 2021) examined the potential for neighbourhood densification in Switzerland and favoured supervised grouping of districts.

In this thesis, only multi-family buildings are considered, which is consistent with the current French building regulation, which no longer allow gas boilers in single-family houses. In terms of years of construction, the case-study will consider the installation of hybrid heat pumps in recent buildings. Heat pumps are indeed rarely installed in old buildings without retrofit as the space heating demand of residential buildings varies greatly with the outdoor temperature. Moreover, the performance of the heat pumps (e.g. COP) is strongly affected by low outdoor temperatures. Consequently, both the average and marginal GHG emissions for space heating and DHW vary in different climatic regions. It is then important to consider the impact of the climate zones in the method to scale up the heating demand.

The methodology used in this thesis is similar to the method presented previously based on districts archetypes (Eggimann et al. 2021). It assumes that the national heat demand can be derived from the heat demand of a district archetype. However, the district archetype was arbitrarily selected and its representativeness for the analysed group of buildings (newly developed residential districts) was not verified. To extrapolate to 100 000 dwellings spread throughout France, the district archetype was simulated with weather data relative to seven cities representative of the seven climatic zones (H2d and H3 were merged). Different weightings were then given to each climatic zone according to the total area of collective housing in the zone (Insee 2021). The distribution of the French climate zones is represented in Figure 49.

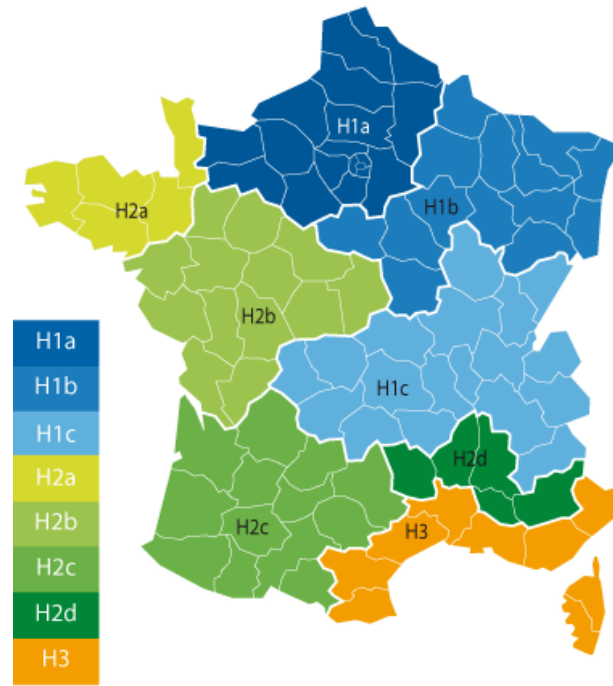


Figure 49: Distribution of the different climate zones in France (Expert Bâti Conseil 2022)

Table 10 summarizes the selected representative cities, the attributed weightings and the design temperatures for heating. The design temperature for space heating  $\theta_{\text{design}}$  is the lowest outdoor temperature observed on at least five days of a year over a 30-year period (AFNOR 2004) and is defined according to the geographical zone and the altitude of the site. This temperature is often used to evaluate the heat losses when sizing a heating system.

Table 10: Weighting and base temperature of the different climatic zones

Climatic Zone	H1a	H1b	H1c	H2a	H2b	H2c	H2d and H3
Representative city	Trappes	Nancy	Lyon	Rennes	La Rochelle	Agen	Nice
Weighting	0.19	0.17	0.20	0.05	0.13	0.14	0.12
Design temperature for heating	-7°C	-15°C	-11°C	-5°C	-4°C	-5°C	-2 °C

The following sections focus on the implementation of this modelling procedure, and more specifically on the modelling of space heating (section 4.3) and of DHW (section 4.4). Both sections contain:

- a description of the input generation;
- a definition of the models for the different components, including their physical description and their parametrization.

### 4.3.Space heating demand

In this section, the different inputs and the model components needed for the evaluation of the space heating demand are presented. This section includes the modeling of the heat emission and distribution.

#### 4.3.1.Inputs definition

The generation of the model inputs related to the space heating demand (thermal properties of dwellings and habits of the occupants) is of main importance to obtain realistic heating demand at district scale. This section describes the definition of the dwelling’s envelope and of the occupant’s scheduling applied in this thesis. These definitions are similar to the one applied in (Martinez, Vellei, and Le Dréau 2021).

### Weather data

The weather data correspond to the measured data of the location of the district (e.g. La Rochelle) for the years 2018-2019. The data used for the simulation are the following: the atmospheric pressure, the dry bulb temperature, the dew point temperature, the black-body sky temperature, the relative humidity, the wind speed and direction, the infrared horizontal radiation, the global, diffuse and direct normal solar radiation, the ceiling height, and the total and opaque sky cover.

### Envelope of the dwellings

The geometry and orientation of dwellings are imported as LOD1 models (user-defined footprint and default height of 3 m). The dwelling is assumed to be a unique thermal zone, all rooms being merged. A distinction is made between internal walls (adiabatic) and external walls. No interzonal heat transfer is considered between dwellings and corridors are ignored. The insulation level of the buildings corresponds to the so-called RT2012, the French Building Regulation for new buildings enforced from 2011 until end of 2021. Each dwelling has thermal properties defined by random draws from distributions based on data of buildings built according to the RT2012 (data.gouv.fr 2020). The air change rate for ventilation and infiltration come from a survey on the indoor environmental quality in French dwellings (Langer et al. 2016). The parameters of the distribution applied for the thermal zones are summarized in Table 11. The envelope and ventilation properties for the district model are presented in Figure 50. The windows are implemented using the double-pane standard model, composed of 3 mm clear glass, 12.7 mm air, and 3 mm clear glass (*Buildings.HeatTransfer.Data.GlazingSystems.DoubleClearAir13Clear*).

Table 11: Envelope and ventilation properties from (Martinez, Vellei, and Le Dréau 2021)

Name	Description	$\mu$	$\sigma$	Units
glazedRatio	Average glazed ration of the dwelling	13.5	3	%
$U_{wall}$	Heat loss coefficient of the walls	0.22	0.035	W/(m <sup>2</sup> .K)
$U_{floor}$	Heat loss coefficient of the floor	0.2	0.055	W/(m <sup>2</sup> .K)
$U_{roof}$	Heat loss coefficient of the roof	0.13	0.042	W/(m <sup>2</sup> .K)
$U_w$	Heat loss coefficient of the window	$\approx 1.4$	-	W/(m <sup>2</sup> .K)
$Q_{ventil}$	Air change rate (ventilation and infiltration)	0.55	0.15	vol/h

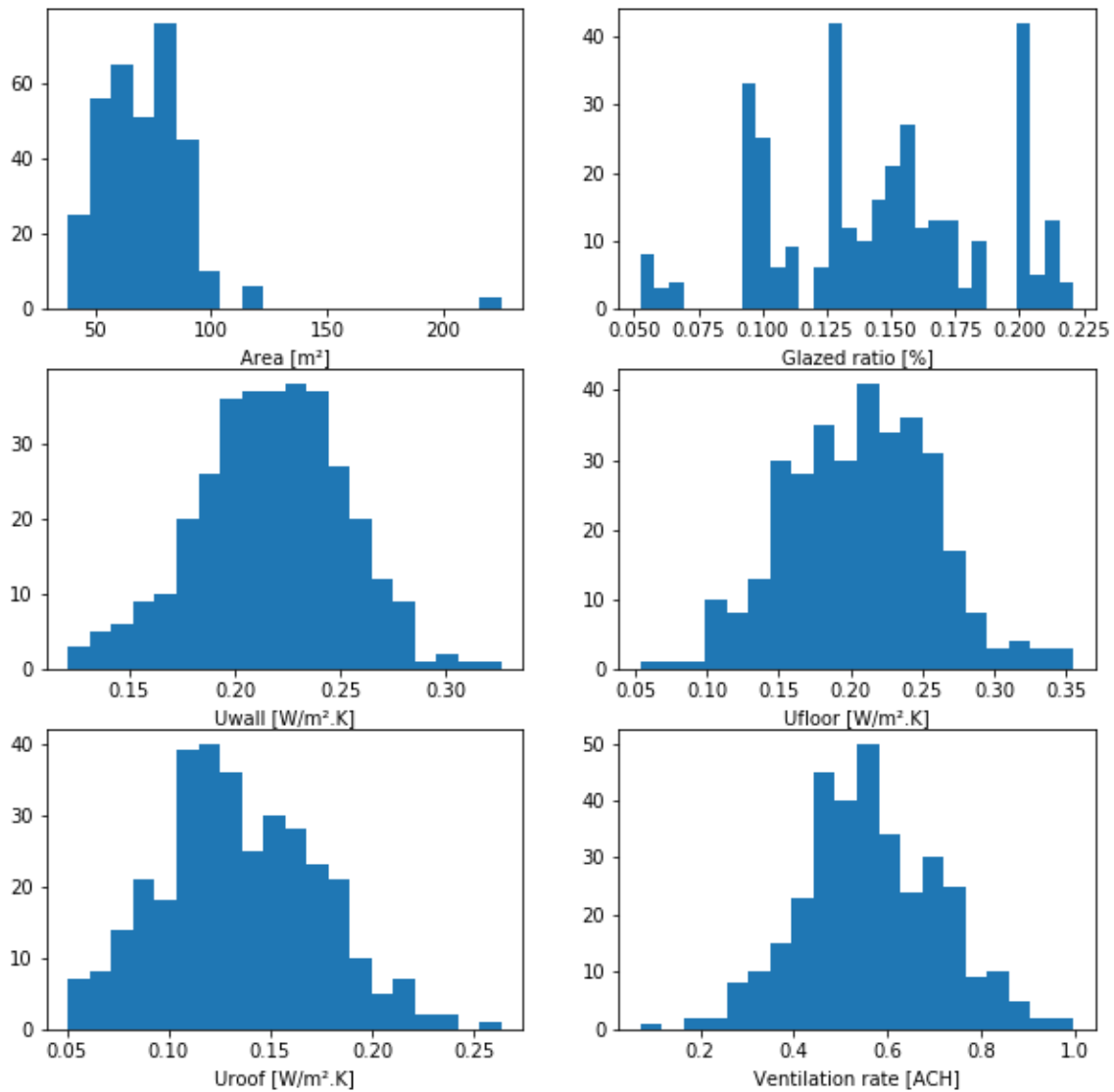


Figure 50: Distribution of the geometric and thermal properties used as input for the district model from (Martinez, Vellei, and Le Dréau 2021)

In addition, to avoid overheating of the dwellings during the shoulder and summer seasons, the air change rates were increased (multiplied by a factor 3 to reproduce the window openings) when the dwelling air temperature reached 24°C.

### Occupant behavior

Families with or without children are living in these dwellings. The number and types of occupants per dwelling were set according to the net floor area and the French census data (INSEE 2010). Figure 51 presents the distribution of the number of occupants per dwelling and the temperature set-points (during occupation) (SDES 2018).

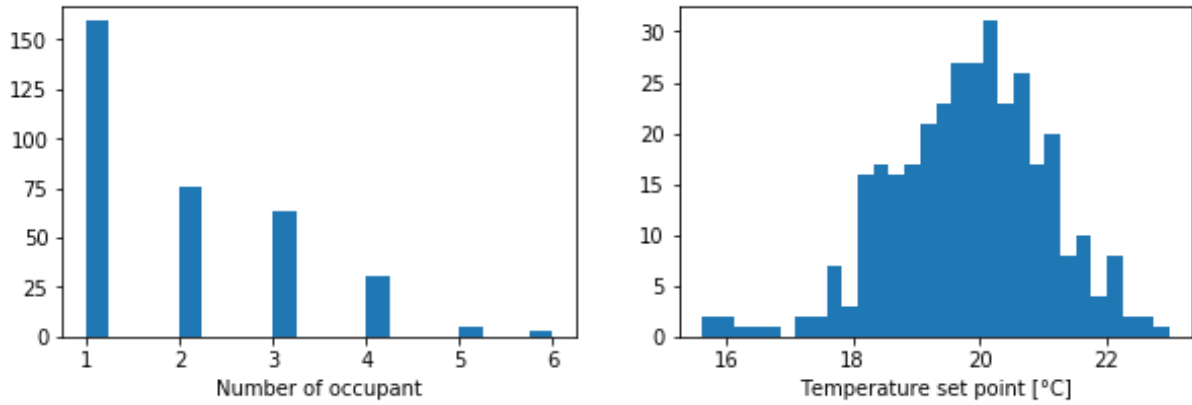


Figure 51: Number of occupants and distribution of the temperature set-points used as input for the district model

Occupants' activities were then simulated for each typology (workers, unemployed, retired, student) based on Time Use Survey (INSEE, 2010) using (Riederer et al. 2015; Garreau et al. 2021). Activities are converted into energy usage based on both national statistics of appliances usage and typical load curves for each appliance. The electricity use is then converted into heat dissipated to the thermal zones based on the types of appliances. Internal loads from occupants are also generated based on activities and accounting for variations in the metabolic rates. Occupants interfere with the heating system by defining both the default set-point (see Figure 51) and the usage of the setback (activated by 60% of dwellings). If the setback is activated, a default weekly occupancy pattern is calculated based on the activities of occupants (active at home, sleeping, or away from home). Figure 52 presents an example of internal load and temperature set-point for a dwelling occupied by a single worker.

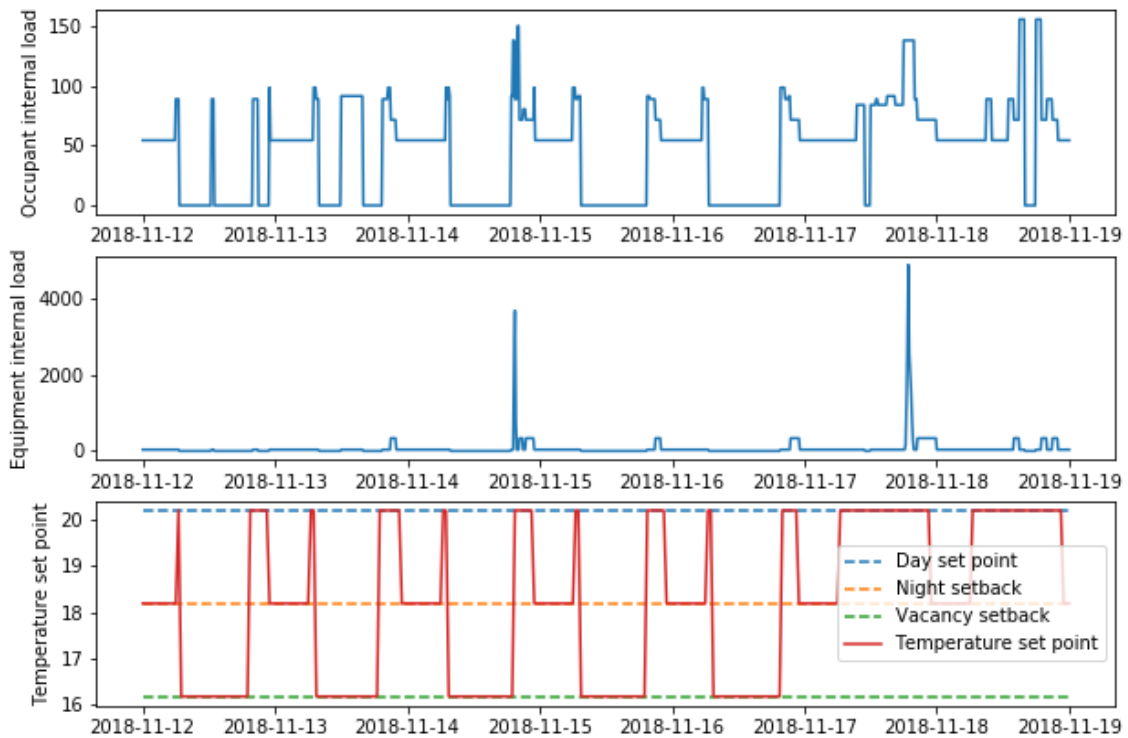


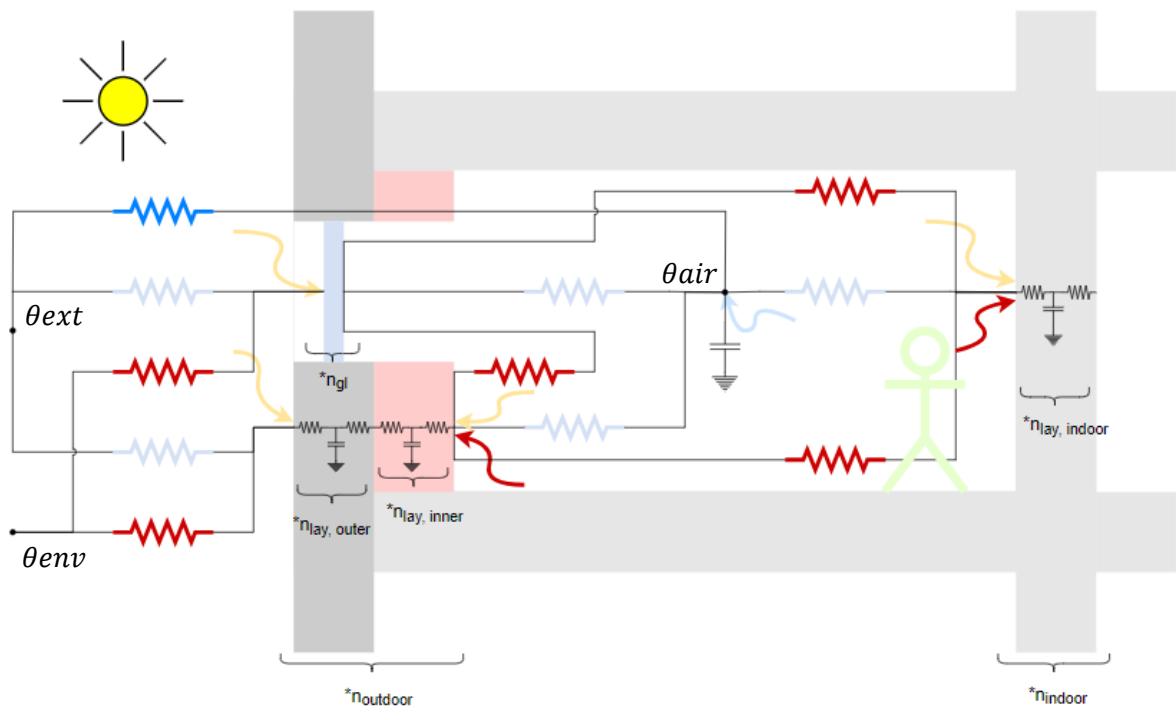
Figure 52: Example of occupant and equipment internal loads (in W) and temperature set-point (in °C) for a dwelling occupied by a single worker (time-step of 30 minutes)

#### 4.3.2.Components description

This section describes the modelling of the thermal zone (a single dwelling) and the radiators.

##### **Thermal zone model**

Each dwelling is modelled by one thermal zone, implemented using the model of the *Buildings* library (*Buildings.ThermalZones.Detailed.MixedAir*). The physical description of the model can be found in (Wetter, Zuo, and Noudui 2011). The air of the room is modelled as one single volume completely mixed. Figure 53 represents the main heat exchanges modelled in the thermal zone. The modelling assumptions for the different heat transfers from Figure 53 are detailed in Table 12. For ease of reading, only one construction of each type (external and internal opaque surfaces and glazing system) is represented. In the implemented model, these constructions as well as the corresponding heat transfers are duplicated by the number of their occurrences (respectively  $n_{outdoor}$ ,  $n_{indoor}$  and  $n_{gl}$ ). The window model implemented in the *Buildings* library is similar to the model used in *Window 6* (Carli 2006) and is validated in (Noudui et al. 2012). This model evaluates the heat balance from the outside to the inside surface of the window. The main difference between the implementation in the *Buildings* library and the *Window 6* model is that the spectrally averaged transmittance and reflectance of the glass are considered instead of the glass properties at different wavelengths. According to (Noudui et al. 2012), the results obtained with the two models are close for multi-layer windows with similar glazings, which was the case in this thesis.



Legend			
	Convective heat transfer		Diffuse and direct solar radiation heat gain
	Infrared radiative exchange		Radiative heat gain
	Air flow		Convective heat gain
	Conduction		Outer material from outdoor opaque constructions
			Glazing system
			Indoor constructions
			Inner material from outdoor opaque constructions
			Thermal capacity

Figure 53: Graphical representation of the heat transfer modelled in the "MixedAir" model

Table 12: Assumptions for the different heat transfers modelled in the room.

	Glazing systems	Outdoor opaque constructions	Indoor constructions
<b>Heat transfer through materials</b>	Heat conduction through glass layers, heat convection through gas between layers and infrared radiation between panes	Transient heat conduction: constructions composed of multi-layered materials, each layer being composed of two resistances and one capacity and solved using a finite volume model	
<b>Convective exchanges</b>	<i>Outer surfaces</i>		
	Constant heat transfer coefficients for exchanges with outside air		Adiabatic surfaces: no exchange with the neighboring dwellings
	<i>Inner surfaces</i>		
	Constant heat transfer coefficient for exchange with the room air		
<b>Infrared radiative exchanges</b>	<i>Outer surfaces</i>		
	Infrared radiation with outside $\theta_{env}$ (being the 4 <sup>th</sup> root of the average of the 4 <sup>th</sup> power of the air temperature and the sky temperature)		
	<i>Inner surfaces</i>		
<ul style="list-style-type: none"> <li>- Radiant heat gains distributed to the room enclosing surfaces based on the product of the area and the infrared emissivity of each surface</li> <li>- Heat exchange (based on radiosity) between the room enclosing surfaces taking into account the absorptivity of the surfaces and the surface area (view factors proportional to the area of the receiving surface, without taking into account the location of the surfaces)</li> </ul>			
<b>Solar radiation exchanges</b>	<i>Outer surfaces</i>		
	Solar direct and diffuse irradiation ( $H_{dir}$ and $H_{diff}$ ) partially absorbed by the glazing and partly transmitted to the floor and walls (computed as a function of the solar incidence)	Solar direct and diffuse irradiation absorbed computed as a function of the solar incidence	No solar radiation
	<i>Inner surfaces</i>		
	<ul style="list-style-type: none"> <li>- Diffuse solar irradiation transmitted through the windows <math>H_{diff}</math> distributed to all surfaces according to Equation 26</li> <li>- Direct solar irradiation transmitted through the windows <math>H_{dir}</math> partially absorbed by the floor according to Equation 27</li> <li>- Rest of the direct solar irradiation distributed to the non-floor areas according to Equation 28</li> <li>- The solar radiative heat gain of each inner surface <i>inner</i> is the sum of the direct and diffuse radiation <math>Q_{sol,inner}</math></li> </ul>		

The diffuse solar radiation  $Q_{diff,inner}$  (in W) absorbed by each inner surface of the dwelling (denoted *inner*) is evaluated by Equation 26.  $\epsilon_{inner}$  and  $T_{inner}$  are respectively the solar absorptivity and the transmittivity (equal to zero, except for windows) of the inner surface.  $A_{inner}$  is the area of the inner surface, and  $L_{inner}$  the list of the inner surfaces of the zone. This equation is applied for both walls with and without windows, which is a simplification.

$$Q_{diff,inner} = \frac{H_{diff} \cdot (\epsilon_{inner} + T_{inner}) \cdot A_{inner}}{\sum_{surf \in L_{inner}} (\epsilon_{surf} + T_{surf}) \cdot A_{surf}} \quad 26$$



It is assumed in the model that the direct solar radiation transmitted through the windows is first received by the floor surfaces. The direct solar radiation  $Q_{dir,inner}$  (in W) absorbed by each floor surface of the dwelling (denoted  $floor$ ) is evaluated by Equation 27.  $L_{floor}$  is the list of the inner surface from a floor construction of the dwelling.

$$Q_{dir,floor} = \frac{H_{dir} \cdot (\varepsilon_{floor} + T_{floor}) \cdot A_{floor}}{\sum_{surf \in L_{floor}} A_{surf}} \quad 27$$

The direct solar radiation absorbed by each non-floor inner surface of the dwelling  $Q_{dir,inner}$  (in W) is evaluated by Equation 28.  $L_{inner} \setminus L_{floor}$  is the list of the non-floor inner surfaces of the room.

$$Q_{dir,inner} = \frac{(H_{dir} - \sum_{surf \in L_{floor}} Q_{dir,floor}) \cdot (\varepsilon_{inner} + T_{inner}) \cdot A_{inner}}{\sum_{surf \in L_{inner} \setminus L_{floor}} A_{surf}} \quad 28$$

The wall composition depends on its function (exterior or internal wall, floor or roof) and is summarized in Table 13. The thickness of the insulation for the exterior walls, floor and roof were adjusted to match the total heat transfer coefficient set for each wall, based on the random draws according to the properties in Table 11. The properties used to describe the materials constituting the walls are summarized in Table 14.

Table 13: Constructions composition

	Model	Inner material		Outer material	
		Material	Thickness (cm)	Material	Thickness (cm)
Exterior walls	Outdoor opaque surfaces	Insulation	Computed value	Concrete	20
Roof		Insulation	Computed value	Concrete	25
Floor		Insulation	Computed value	Concrete	25
Intermediate floor*	Indoor surfaces	Concrete	10		
Internal walls*		Gypsum board	1.3		
Furnitures		Furnitures material	15		
Window	Glazing system (Double pane with 12.7 cm air layer)	Glass	0.3	Glass	0.3

\*symmetric walls, only half of the composition is described

Table 14: Thermal properties of the materials

Material	Thermal conductivity (W/(m.K))	Specific heat capacity (J/(kg.K))	Mass density (g/cm <sup>3</sup> )
Concrete	1.4	840	2240
Insulation	0.03	1200	40
Gypsum	0.16	1090	800
Glass	1	700	2500
Furnitures	0.12	1210	540
Air			

Each wall material  $mat$  is automatically divided into  $n_{lay, mat}$  layers depending on the thermal properties (diffusivity) of the material and the thickness of the layer. The default discretization is three layers for 20 cm of concrete. Such an assumption ensures a similar time rate of change in the different materials despite their different thermal properties (Wetter 2004). The layers being composed of 2 resistances and 1 capacitance, the envelope of each dwelling is modelled with a minimum of 16 resistances and 8 capacitances. The complete dwelling model is then represented with at least 63 resistances and 9 capacitances. The sensitivity of the heating demand to the number of capacitances was tested and the heating demand at the dwelling scale was similar no matter the number of capacitances.

The modelling of internal thermal mass and its impact on the building simulation were reviewed in (Johra and Heiselberg 2017). This article referred to a Danish survey about the building indoor content. In this article, the furniture was modelled as a horizontal partition wall with the same area as the floor with a single layer and thermal properties representative of the building indoor content (see Table 14). According to the building survey, the internal mass varies between 10 and 100 kg by square meter of floor area, which corresponds to a thickness variation of the partition wall between 12.5 and 125 cm by square meter of floor area. The sensitivity of the heating demand to the thickness of the layer representing the furniture was also tested and did not have a significant impact on the heating demand (and pattern) at the dwelling scale.

In the thermal zone model, the heat transfer for convection is constant and does not depend on the tilt of the wall. It is set to 3 W/m<sup>2</sup>.K for heat transfer between the indoor facing surfaces and the room air and to 10 W/m<sup>2</sup>.K for heat transfer between the outdoor facing surfaces and the outdoor air. The infrared absorptivity of the walls is set at 0.9 and the solar absorptivity at 0.5.

In this thesis, shadings between buildings were neglected. The results obtained with the *Dymola* model were compared to a similar model developed in *Dimosim* (Martinez, Vellei, and Le Dréau 2021), in which the shading between buildings was evaluated according to the geometry and to the time of the year. The aggregated demand does not appear to be much affected by the simplification in this model.

In the following,  $\theta_{air}$  refers to the temperature of the room air volume and  $\theta_{rad}$  to the radiant temperature of the room.  $\theta_{rad}$  is calculated as the weighted mean of the temperature of the surfaces using Equation 29 where  $A_{surf}$  are the surface area,  $\varepsilon_{surf}$  the infrared emissivity and  $\theta_{surf}$  the surface temperature.

$$\theta_{rad} = \frac{\sum_{surf} A_{surf} * \varepsilon_{surf} * \theta_{surf}}{\sum_{surf} A_{surf} * \varepsilon_{surf}} \quad 29$$

### Radiator model

The radiator is implemented using the model of the *Buildings* library (*Buildings.Fluid.HeatExchangers.Radiators.RadiatorEN442\_2*), based on the European standard EN 442-2. This model discretizes the radiator into  $N$  elements (5 by default) and computes the heat exchanged by convection (using Equation 30) and by radiation (using Equation 31) between the hot water flowing through each element  $i$  at temperature  $\theta_i$  and the room air volume or the room surfaces, respectively. The convective heat transfer of element  $i$   $Q_{conv,i}$  (in W) is assessed using the room air temperature ( $\theta_{air}$ ) for the air volume, while the radiant temperature  $\theta_r$  is used to assess the radiative heat transfer of element  $i$   $Q_{rad,i}$  (in W).  $Q_{rad,i}$  is then distributed over the different surfaces in a similar way to the radiant heat gains from human activities or equipment. The fraction of radiative heat transfer from the total heat transferred (denoted  $fr$ ) is set to 0.35 and the exponent for heat

transfer calculation  $n$  to 1.24 in the model. These values correspond to typical values for water-based heaters.

$$Q_{conv,i} = \frac{sign(\theta_i - \theta_{air}) * (1 - fr) * UA_{radiator}}{N * |\theta_i - \theta_{air}|^n} \quad 30$$

$$Q_{rad,i} = \frac{sign(\theta_i - \theta_{rad}) * fr * UA_{radiator}}{N * |\theta_i - \theta_{rad}|^n} \quad 31$$

The  $UA$ -value of the radiator  $UA_{radiator}$  is computed from the nominal heating power of the radiator  $\dot{Q}_{radiator}^{nom}$  (in  $W$ ) and the nominal inlet and outlet temperatures ( $\theta_{in radiator}^{nom}$  and  $\theta_{out radiator}^{nom}$ ) using Equation 32.

$$UA_{radiator} = \frac{\dot{Q}_{radiator}^{nom}}{\frac{\theta_{in radiator}^{nom} + \theta_{out radiator}^{nom}}{2} - ((1 - fr) * \theta_{air nom} + fr * \theta_{rad nom})} \quad 32$$

The water volume of the radiator is considered proportional to the nominal heating power of the radiator (equal to  $5,8 * 10^{-6} * \dot{Q}_{radiator}^{nom}$   $m^3$ ). To consider the inertia of the radiator, an additional dry mass (estimated to  $0,0263 * \dot{Q}_{radiator}^{nom}$   $kg$ ) is added to the water capacity. Heat storage is computed using a finite volume approach for the water and the metal mass, which are both assumed to be at the same temperature. The choice of values for  $\dot{Q}_{radiator}^{nom}$ ,  $\theta_{in radiator}^{nom}$  and  $\theta_{out radiator}^{nom}$  is explained later in Section 4.3.4.

#### 4.3.3. Control strategy of the heat distribution and emission

Adjusting the supply temperature for heating avoids over-consumption during shoulder seasons, when the outdoor temperature becomes milder. The supply temperature  $\theta_{in,radiator}$  varies linearly between a maximum temperature set to heat the dwelling when  $-4^\circ C$  is reached and a minimum temperature low enough to control the heat emission with relatively high outdoor temperature. Table 15 summarizes the set-point definition for the variation of the supply temperatures applied in this study. In addition, the temperature set-point for space heating supply is increased by  $10^\circ C$  every day (with a limitation at  $55^\circ C$ ) to ensure that the air temperature in the dwellings warms up quickly after the overnight setback.

Table 15: Set-point for space heating supply temperature depending on the outside temperature

Outside temperature	Supply temperature
$-4^\circ C$	$55^\circ C$
$17^\circ C$	$35^\circ C$

The layout of the heating system for distribution and emission is represented in Figure 54. The radiators are supplied with hot water in parallel. The mass flow rate of the hot water through each radiator is adjusted through a two-way valve placed at the inlet of the radiator. The valve opening is controlled with a proportional controller (proportional band of 2K), comparing the ambient air temperature of the heated dwelling with the set temperature. In such configuration, the rotational

speed of the pump is usually controlled through a PI controller to keep a constant pressure difference  $\Delta P_0$  between each side of the pump. In this model, to reproduce this behavior, the mass flow rate of the pump is set proportional to the valves opening times the nominal mass flow rate of the corresponding radiators.

The temperature of the water flowing through the radiators is controlled by a three-way valve mixing the hot water from the hybrid heating system and the water returning from the radiators. The opening of the three-way valves is controlled by a PID controller that compares the supply temperature for the space heating and the set temperature.

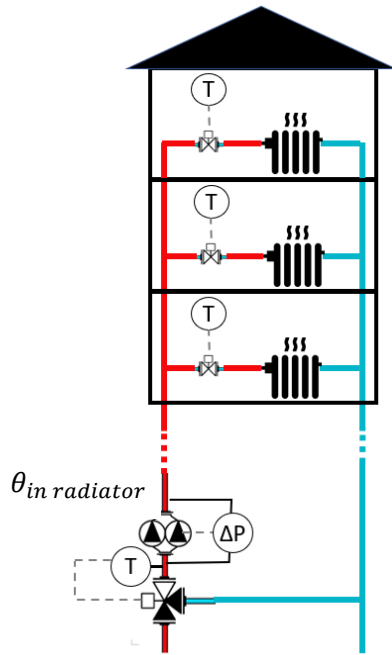


Figure 54: Distribution and emission of the space heating

#### 4.3.4. Sizing of the radiators

For each dwelling, the nominal heating power of the radiator is sized to compensate 120% of the heat losses at the design temperature of the climatic zone, in order to provide enough power for the morning peak. The nominal heat losses  $HL_{dw}^{nom}$  (in W) are assessed using Equation 33.  $Q_{ventil}$  is expressed in vol/h and includes both ventilation and infiltration. Heat losses to the ground and the roof are only considered for the ground floor and the top floor, respectively.

$$HL_{dw}^{nom} = (\theta_{air}(dw) - \theta_{design}) \cdot (0,34 \cdot Q_{ventil}(dw) \cdot 3 \cdot A_{dw} + \sum_{wall \in L_{wall ext}} A_{wall} \cdot (U_{wall}(dw) \cdot (1 - glazedRatio) + U_{window}(dw) \cdot glazedRatio(dw)) + A_{dw} \cdot U_{roof}(dw) + 0,7 \cdot A_{dw} \cdot U_{ground floor}(dw)) \quad 33$$

According to the settings of the supply temperature described previously, water flows through the radiator with an inlet temperature of 55°C under nominal conditions. It is also considered that the temperature difference between the inlet and outlet ( $\theta_{in radiator}^{nom} - \theta_{out radiator}^{nom}$ ) is 10°C. Consequently, a nominal mass flow rate is defined for each radiator according to Equation 34, which corresponds to the mass flow rate through the radiator at nominal power. An oversizing ratio of 20% is chosen to ensure sufficient heating power during the boost phase. The sum of the nominal mass

flow rate  $\dot{m}_{radiator}^{nom}$  of each dwelling is used as the nominal mass flow rate of the primary network of the corresponding building  $\dot{m}_{pump radiator}^{nom}$  in the following section.

$$\dot{m}_{pump radiator}^{nom}(dw) = \frac{1.2 \cdot HL_{dw}^{nom}}{c_p water (\theta_{in radiator}^{nom}) \cdot (\theta_{in radiator}^{nom} - \theta_{out radiator}^{nom})} \quad 34$$

#### 4.4. Domestic Hot Water demand

This section describes the modelling of the DHW needs in the district archetype. The heat for the DHW is supplied by the heat pump or the gas boiler and is transferred to the DHW tank through a heat exchanger. The DHW tank, which supplies around 30-35 dwellings, is a semi-accumulation system providing 3 to 6 hours of storage depending on the sizing and tapping volumes. The water system considered is a loop system, with a secondary return pipe, to ensure a quick delivery of hot water to the different dwellings. In the following section, the generation of inputs for the model (hot water tapping and cold water profile) as well as the components used to model the storage tank are presented. In addition, the sizing of the components and the control strategy for DHW are explained.

##### 4.4.1. Inputs generation

Two inputs are needed to model the DHW demand:

- the tapping profile for each group of 33 dwellings;
- the cold water temperature.

As a simplification, the same monthly cold water temperature  $\theta_{cold,m}$  was considered for all the heating systems independently of their location. The input data for the cold water temperature is presented in Figure 55 and corresponds to monthly means of measurements from 100 locations in France (COSTIC 2016).

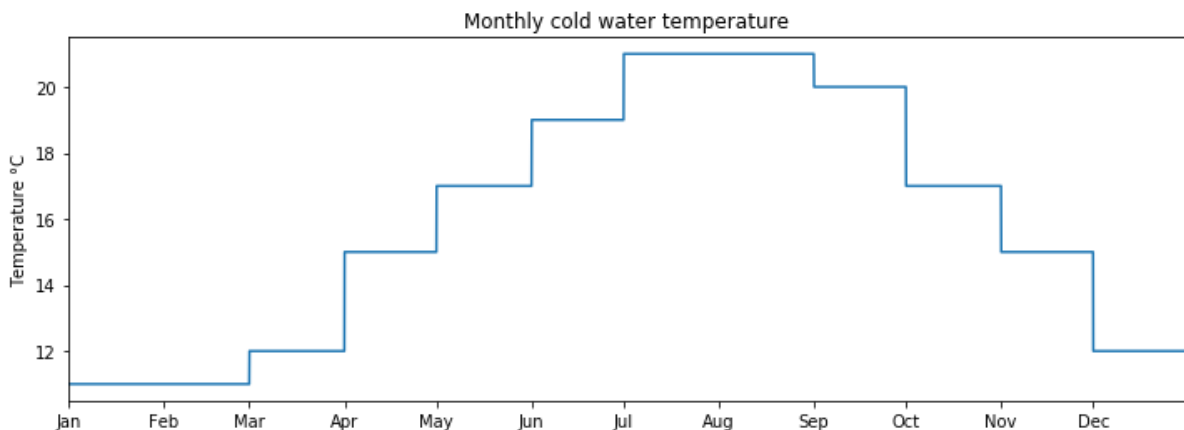


Figure 55: Monthly cold water temperature from (COSTIC 2016)

The tapping profile for the DHW demand of each group of 33 dwellings was modelled with a top-down method based on averaged historical data. Applying such a method to 33 dwellings leads to a decrease of the hourly peak demand and to average the hot water demand throughout the day in comparison with measured data. However, due to the 3 to 6 hours of storage provided by the DHW tank, the heat

generation for DHW is delayed from consumption. Consequently, the top-down model should lead to a similar production pattern of the hybrid heating system as a more detailed model.

The domestic hot water need of the dwellings is assessed using data from (COSTIC 2019). In this study, the average hourly water consumption was evaluated for 290 standard dwellings in social housings in Strasbourg (France). From these data, the monthly, daily and hourly coefficients (respectively  $c_m$ ,  $c_d$ ,  $c_h$ ) were defined to derive the hourly mass flow rate  $\dot{m}_{DHW}(h, d, m)$  from the daily consumption of water at 40°C for a standard dwelling ( $V_{mean}$ ). The same coefficients were calculated for 81 standard dwellings in the Yvelines department and the results were similar. The hourly mass flow rate of domestic hot water  $\dot{m}_{DHW}$  (in kg/h) extracted from the tank at a temperature of 55°C is obtained using Equation 35.

According to the COSTIC guidebook (COSTIC 2016), a standard dwelling corresponds to a dwelling with three rooms and occupied by two inhabitants. The number of standard dwellings  $N_S$  is then defined as the number of inhabitants in the building divided by two. According to the same document, the daily consumption of domestic hot water at 40°C  $V_{mean}$  (in m<sup>3</sup> in the equation) varies between 75 and 175 l, with a mean value of 125 l. In order to generate diversity between the days, a normal distribution  $n_d$  with a standard deviation of 20% was applied on the simulated tapping profile. Figure 56 presents an example of the mass flow rate obtained for a building of 33 standard dwellings.

$$\dot{m}_{DHW}(h, d, m) = n_d \cdot \frac{V_{mean}}{\rho_{water}} \cdot N_S \cdot c_h \cdot c_d \cdot c_m \cdot \frac{(40 - \theta_{cold,m})}{(55 - \theta_{cold,m})} \quad 35$$

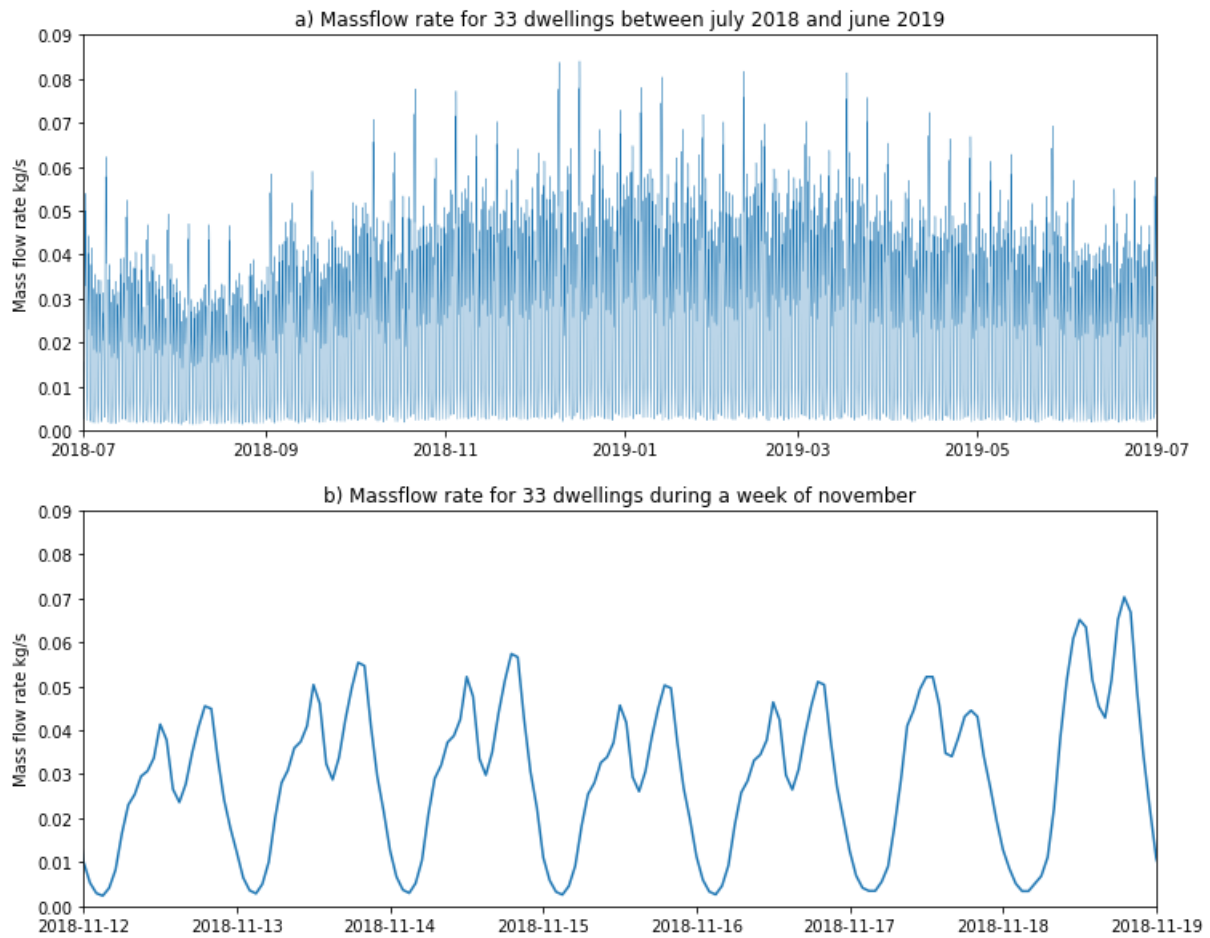


Figure 56: Mass flow rate of water at 55°C extracted for domestic usage in a building with 33 standard dwellings

#### 4.4.2. Component description

The DHW storage tank was implemented using the model *StratifiedEnhancedInternalHex* of the *Buildings* library (*Buildings.Fluid.Storage.StratifiedEnhancedInternalHex*). This stratified storage tank model is composed of  $n_{seg}$  interconnected volumes of the same fixed size. This model implements:

- Convective heat transfers through each segment of water;
- Conductive heat transfer through the tank wall segments, bottom and top;
- Convection between the tank envelope and the ambient air;
- Fluid flow rate from one segment to the other;
- Heat transfer from heated water flowing through a helical coil heat exchanger to stagnant water in the storage tank.

In this work, the DHW storage tanks were discretized in 9 segments. Convection between the tank envelope and the ambient air is modelled considering a constant coefficient of convection ( $3 \text{ W}/(\text{m}^2.\text{K})$ ). The specific heat conductivity of the insulation ( $8 \cdot V_{DHW} + 20.576$  in  $\text{W}/(\text{m}.\text{K})$ ) of the tank depends on the volume of the tank  $V_{DHW}$  in  $\text{m}^3$ . The temperature for the ambient air (of a technical room for example) is the mean between 20°C and the outside temperature.

Figure 57 presents the integration of the input data in the DHW storage tank model. The water volume in the tank being constant, the mass flow rate at the outlet of the tank is the same as the mass flow rate at the inlet.  $\dot{m}_{supply\ DHW}$  corresponds to the constant mass flow rate flowing from

the DHW tank to the dwellings.  $\dot{m}_{supply\ DHW}$  was set to correspond to typical values for hot water circulation systems for such buildings (heat losses of 3.6 kW during distribution considering a temperature decrease of 4°C between the outlet and the inlet of the tank). Consequently, the DHW returning from dwellings is entering the tank with the supply mass flow rate  $\dot{m}_{supply\ DHW}$ , reduced from the extracted water  $\dot{m}_{DHW}$  (see Equation 35). The returning DHW was mixed with cold water (at the monthly cold water temperature  $\theta_{cold,m}$ ), flowing with a mass flow rate corresponding to the hot water consumption  $\dot{m}_{DHW}$ .

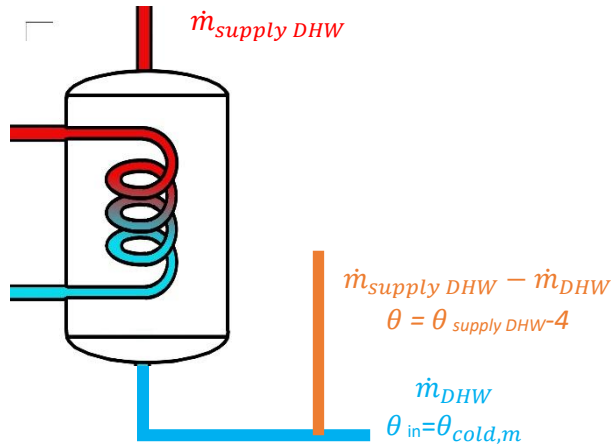


Figure 57: Integration of the DHW consumption in the heating system model

The parameters of the DHW tank models were set using data from a commercial DHW tank (atlantic Guillot 2022). The heat transfer coefficient  $UA_{DHW}$  defining the exchanges between the water flowing through the coil and the stored water is determined according to the heating power, the inlet temperature from the heating system and in the tank under nominal conditions (stored water in the tank  $\theta_{tan\ nom}$  at 45°C, water flowing through the exchanger  $\theta_{coil\ nom}$  at 65°C and heat exchange between the water flowing through the coil and the stored water of 66 kW) using Equation 36. The height of the DHW tank is 2.15 m and the coil is located between 0.45m and 1.215 m from the bottom.

$$UA_{coil} = \frac{P_{DHW}^{nom}}{\theta_{coil\ nom} - \theta_{tan\ nom}} \quad 36$$

#### 4.4.3. Sizing

The sizing of the storage tank for DHW is based on a tradeoff between the volume of the tank and the heating power required to heat the tank. Indeed, for a given number of dwellings, the heating power required for the DHW is lower with a large storage volume. According to (COSTIC 2019), the heating power of a heat pump  $P_{DHW}^{size\ HP}$  required for a tank volume  $V_{DHW}$  and  $N_s$  standard dwellings (higher than 10) can be estimated using Equation 37. Figure 58 represents the minimum heating power of the heat pump for different numbers of standard dwellings and depending on the size of the tank. To optimize the heat pump performance, a large DHW storage is required due to the limited heating power of the heat pump at 65°C. A semi-accumulation DHW storage tank was then chosen for this study. The volume of the DHW storage tank  $V_{DHW}$  was chosen to store about 160l per standard dwelling, which represents about 200% of the daily needs. The tank is charged around four times each day with this sizing.



$$P_{DHW}^{size HP} = (-425 * N_s + 97466) * V_{DHW}^{-1,68+0,213*\ln(N_s)}$$

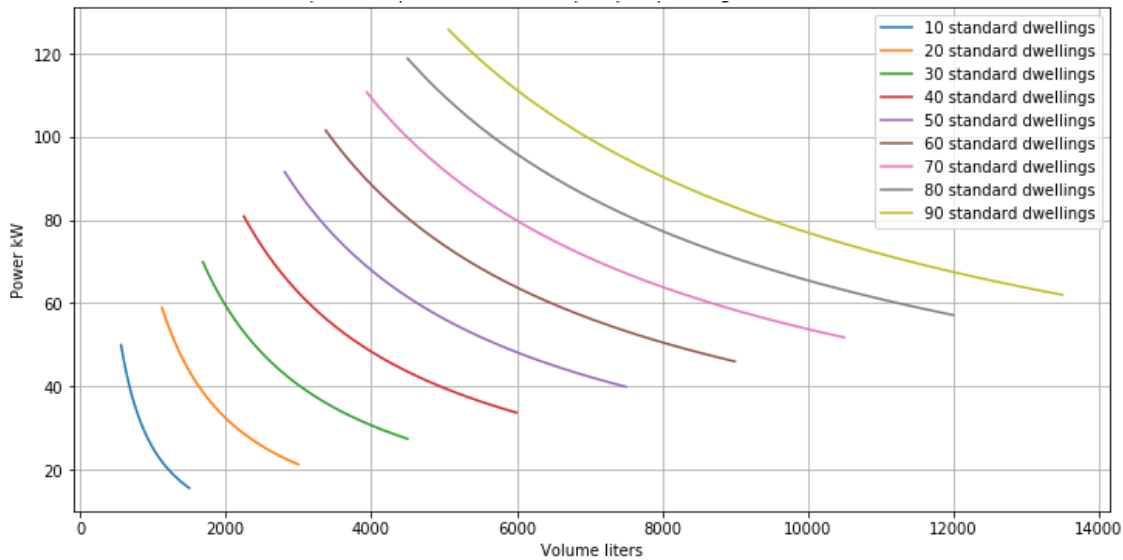


Figure 58: Minimum power required for the heat pump depending on the volume of the tank (COSTIC 2019)

#### 4.4.4. Control of the DHW storage tank

The DHW is stored in the tank at a temperature to ensure that hot water is supplied at 55°C. The storage tank is heated by hot water flowing at 65°C through the heat exchanger at a constant mass flow rate. The control of the stored water temperature is performed with a sensor placed in the second segment (out of ten) from the top of the tank. When the measured temperature is lower than 55°C, the reheating of the tank is activated until the sensor measures a value above 58°C. A larger temperature difference for the hysteresis would ensure a lower number of charge and discharge cycles of the tank. However, the maximum outlet temperature of the heat pump being 65°C, a minimum set-point of 58°C in the tank avoids a too long reheat time of the tank. In addition, the DHW is heated daily between 4 am and 6 am to avoid the activation of the DHW production at 6 am when the space heating peak demand occurs by increasing the set-point temperature by 10°C.

### 4.5. First results

In this section, the results obtained with the models described previously are shown. The results for the space heating demand and for the DHW demand for a single heating system located in La Rochelle are discussed in the first two parts. Finally, the influence of scaling up the space heating and DHW demand to the national scale is presented in the third part of this section.

#### 4.5.1. Space heating demand for one heating system

In this section, some results of the heating demand for one heating system (33 dwellings) in La Rochelle are presented. The heat losses for this building at the design temperature ( $-4^{\circ}\text{C}$ ) are equal to 57 kW. According to the sizing rules described previously (+20% oversizing), the sizing of all the radiators to heat the 33 dwellings correspond to a heat generation of 69 kW. Figure 59 shows the heating demand, the mass flow rate, the inlet and outlet temperature through the radiators and the outdoor temperature in La Rochelle between October 2018 and April 2019. It should be noted that the outdoor temperature never reached the design temperature ( $-4^{\circ}\text{C}$ ) during the heating season. Consequently, the maximum heat demand and the maximum mass flow rate during the year are lower than the sizing.

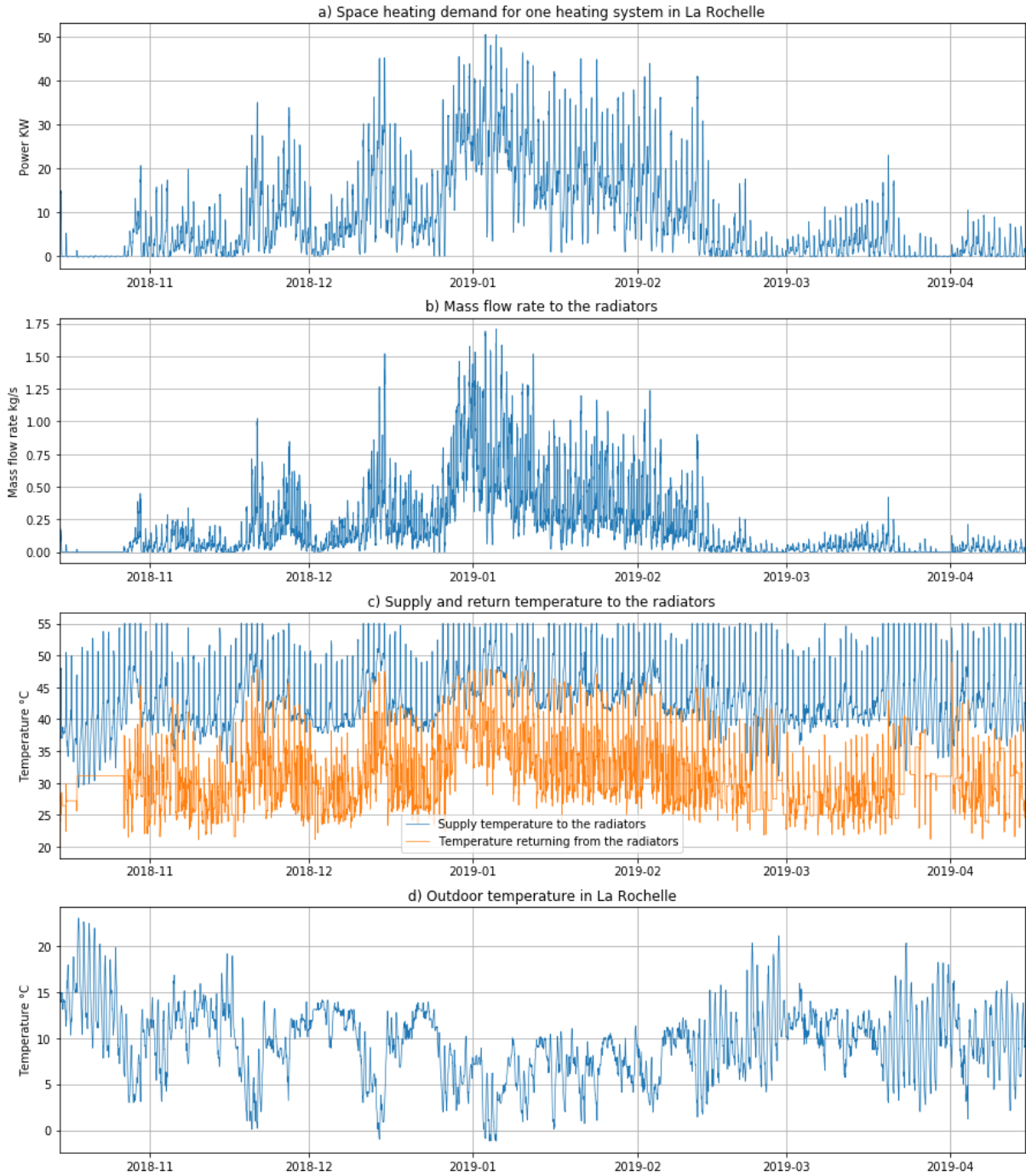


Figure 59: Space heating generation, mass flow rate, supply and return temperature to the radiator and outdoor temperature in La Rochelle, for one heating system during the heating period 2018-2019 with a half-hourly resolution

Figure 60 shows the set-point and dwelling temperatures and the space heating demand in one dwelling during one mild and one cold week of the 2018-2019 heating season in La Rochelle. A temperature set-back is applied in this household during the night and during the time of low occupancy. Due to this temperature set-back during the week, the radiator is turned on a few hours in the morning and in the evening during the weekdays and for the whole day during the week-ends.

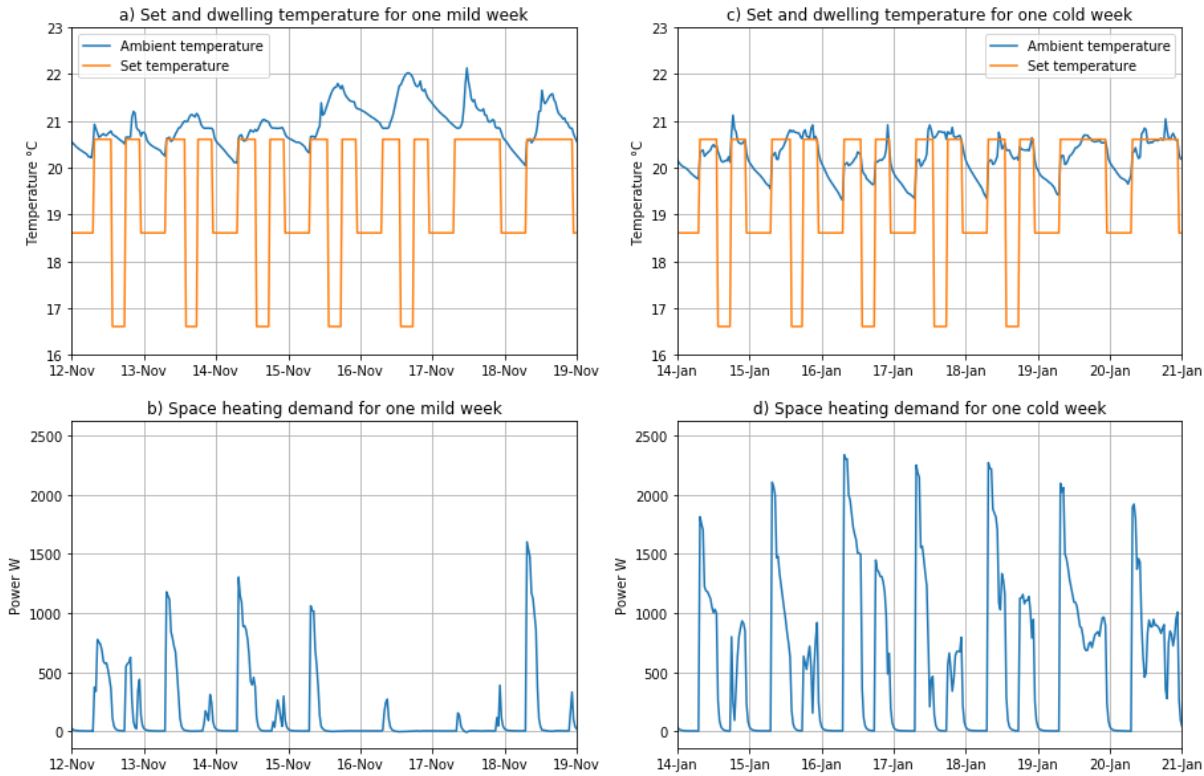


Figure 60: Set point and ambient temperature and space heating generation for one dwelling in La Rochelle for a mild and a cold week with a half- hourly resolution

Figure 61 shows the distribution of the difference between the ambient temperature and the set-point for the 33 dwellings during occupied hours. Positive values mean that the indoor temperature is lower than the set-point. The orange lines depict the median of the difference, whereas the boxes display the range of the data between the first and third quartiles. The whiskers illustrate the 5<sup>th</sup> and 95<sup>th</sup> percentiles.

The annex D of the standard EN 16798-2-2019 (BSI 2019) suggests for the evaluation of the comfort of a building to calculate the percentage of the occupied hours outside of a range. We assume that the difference between the indoor temperature and the set point should not exceed 1°C for more than 5% of the occupancy time. This condition is not met in only one dwelling out of the 33 dwellings displayed in the Figure 61 (dwelling n°8). The discomfort in this dwelling may be due to a lack of synchronization between the occupancy of this dwelling and the morning temperature boost. In this dwelling, the temperature setbacks are applied during the away-periods, and the occupancy periods are outside the temperature set-point boost (between 6 am and 9 am).

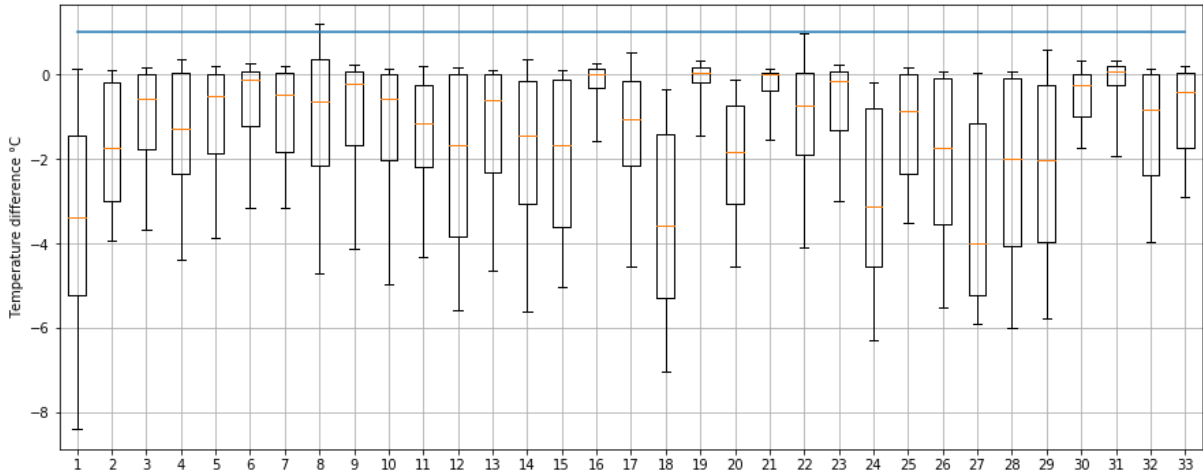


Figure 61: Distribution of the difference between the setpoint and the ambient temperature when the dwellings are occupied (blue line is the 1°C threshold).

#### 4.5.2. Domestic hot water

In this section, the results regarding the DHW generation for 33 dwellings are presented. 74 occupants are living in these dwellings. The capacity of the water storage tank is 5920 liters. The power required to produce hot water was estimated to be around 32 kW. Figure 62-a and -d show the space heating and DHW demand for a cold and a mild week during the 2018-2019 heating season. Thanks to the scheduled heating of the water storage tank between 4 am and 6 am, the heating of the water storage tank is avoided during the period of high demand for space heating.

Figure 62-b and -e show the state of charge of the water storage tank for a cold and a mild week. The state of charge of the water storage tank was assessed using Equation 38, with  $\theta_{DHW,i}$  the temperature of the water in the section  $i$  (out of ten) of the tank. The tank is then considered fully charged (i.e. the SOC is 100%) when the average temperature of the water reaches 60°C. The tank is completely discharged when the average temperature of the tank is lower than 45°C.

$$SOC = \frac{100}{10} * \sum_{i=1}^{10} \frac{60 - \theta_{DHW,i}}{60 - 45} \quad 38$$

Figure 62-c and -f show the outlet temperature of the water storage tank for a cold and a mild week during the 2018-2019 heating season. The daily forced heating of the tank between 4 am and 6 am can be observed in the figures below, showing the state of charge of the tank and the outlet temperature.

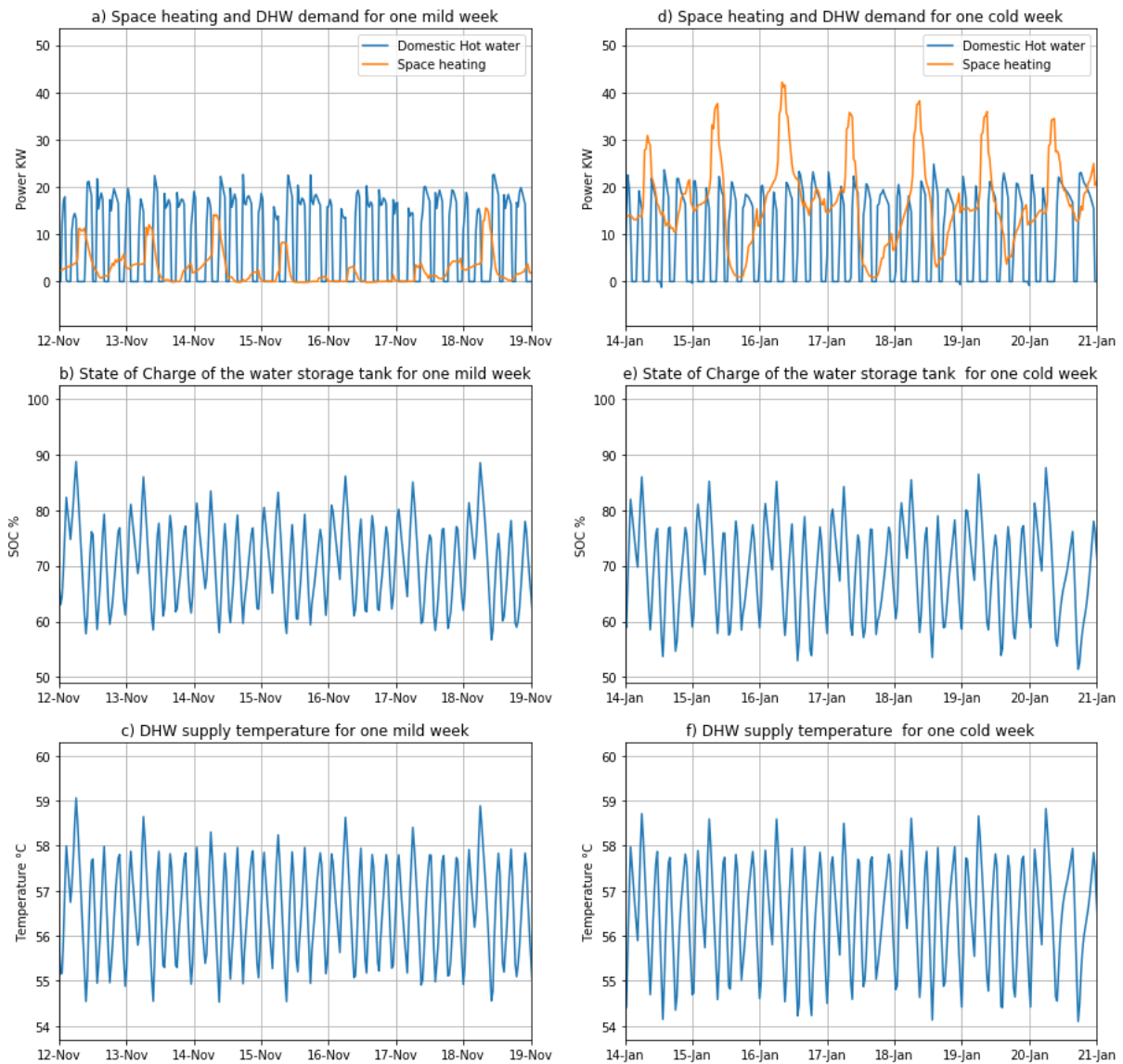


Figure 62: Space heating and DHW demand, state of charge of the water storage tank and DHW supply temperature for one heating system in La Rochelle for one mild week and one cold week of the 2018-2019 heating season

#### 4.5.3. Space heating and domestic hot water at the national level

The heating demand models described in this chapter were then simulated for each representative city. The annual space heating and DHW demand per square meter for each representative city are summarized in Table 16.

Table 16: Yearly space heating and DHW demand for each representative city

Representative city	Trappes	Nancy	Lyon	Rennes	La Rochelle	Agen	Nice
Heating+DHW need (kWh/m <sup>2</sup> .yr)	70	77	67	64	52	55	45

Figure 63-a and -b show for a winter and a summer week the space heating and DHW demand for the different climate zones after scaling up the simulation results at the national level using the method described in Section 4.2.5. During the summer week, the heating demand appears to be synchronised across all heating systems. This is a bias in the simulation due to the identical sizing of the storage water tank and the same schedule for heating the tank and space heating boost in the morning. These settings could have been changed outside the heating season to allow for more varied patterns.

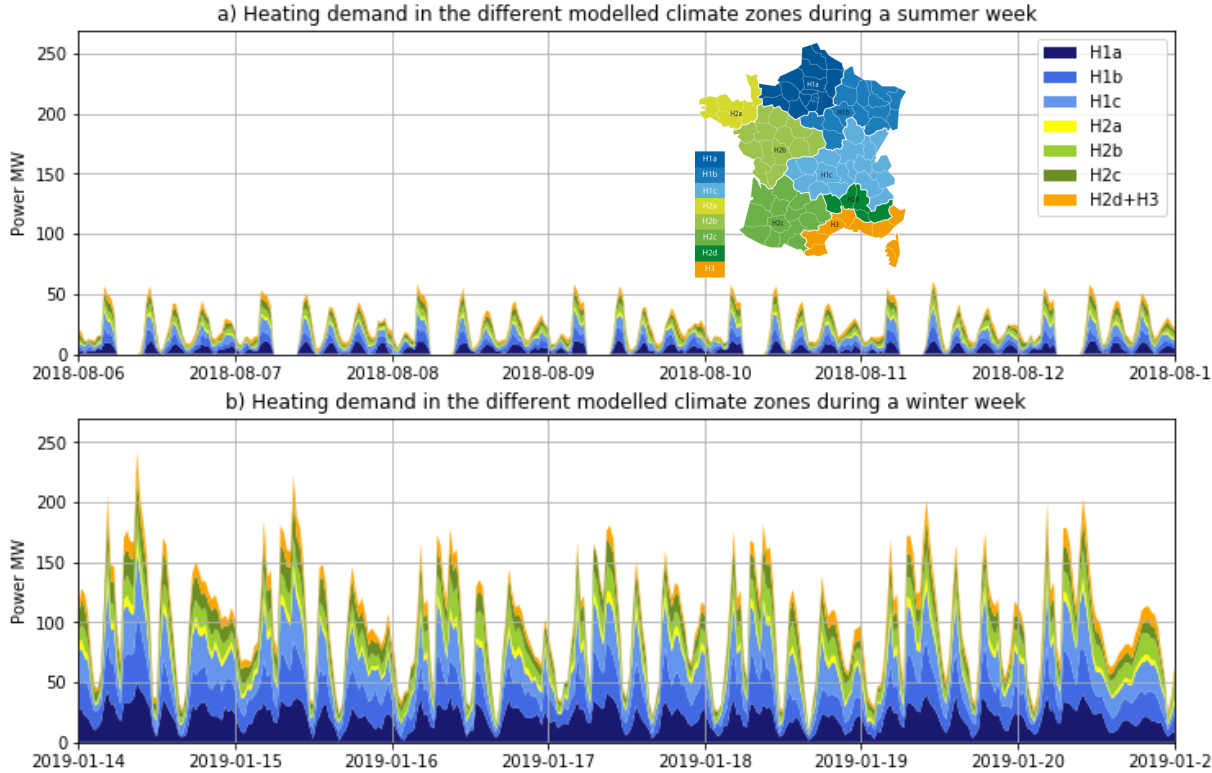


Figure 63: Heating demand in the different climate zone during a summer and a winter week

### 4.6. Conclusion

The first part of this chapter discussed the case-study addressed by this thesis. The Atlantech district in La Rochelle was chosen as the archetype for the simulation of the heating demand. In terms of hybrid heating system, both the heat pump and the gas boiler provide heat for DHW production and space heating. In a second part, the development of an urban energy model in *Dymola* and the scaling up of the heating demand to a national level were presented. In a third and fourth parts, the development of the building and the DHW models were discussed. These two sections focused on the physical description of these models as well as the constraints on the control strategy for each component and their sizing. Finally, the fifth section discusses the simulation results obtained with the models previously described. The aim of this thesis is to develop a control strategy that decrease the GHG emissions for a national fleet of hybrid heat pumps. To this end, the heating demand models developed in this section will be coupled with a detailed hybrid heating system model, including the different control systems.

## 5. Evaluation of control strategies for a fleet of hybrid heat pumps

In the second and third chapters of this thesis, a model to evaluate the Marginal Emission Factor (MEF) of the electricity consumption in France was developed and validated. In the fourth chapter, the UBEM tool based on a district archetype with more than 300 dwellings was developed to evaluate the space heating and DHW demand. The objective of this last chapter is the evaluation of different sizing and control strategies for hybrid heat pumps. To evaluate the potential contribution to decarbonization, the GHG emissions due to the heating of 100 000 additional dwellings with hybrid heat pumps is estimated. In Section 5.1, the models for the heat generation system with a hybrid heat pump are developed. Section 5.2 summarizes the different control strategies and sizing of the hybrid heat pump considered in this thesis. Then, in Sections 5.3, 5.4 and 5.5, the reference heating system and two control strategies are presented. Finally, in Section 5.6, the different scenarios and sizing for the hybrid heat pumps are successively evaluated and compared.

### 5.1. Model of the heat generation system

In this section, the hybrid heating system providing both space heating and DHW is presented. This system coordinates a gas boiler with a heat pump coupled with a hydraulic separator. Figure 64 presents the general configuration for such hybrid heat pumps. As mentioned previously, the heat pump and the gas boiler provide both space heating and DHW. The following components are then necessary to provide these two energy services:

- An air-to-water heat pump ensuring a significant part of the heating needs;
- A hydraulic separator to decouple the heat pump from the primary network and avoid short cycles;
- A gas boiler.

In the following sections, we focus on the general configuration, the control strategies and the sizing of the systems.

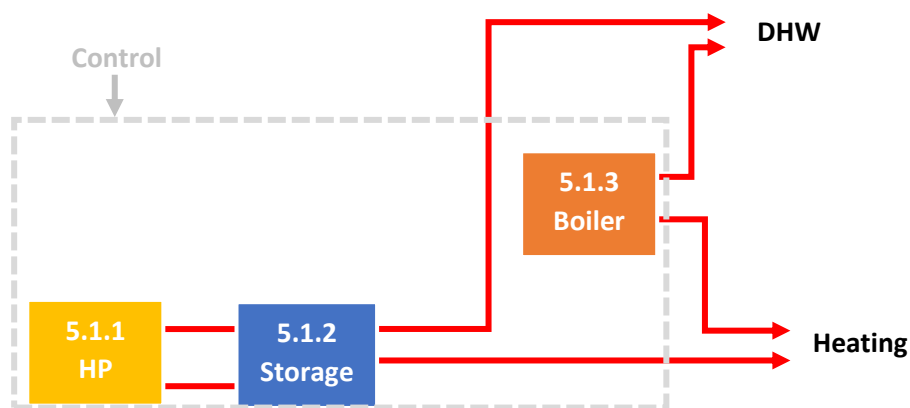


Figure 64: General configuration of hybrid heat pumps

### 5.1.1. Air-to-water heat pump

#### Component description

The heat pump is implemented using the heat pump model of the *AixLib* library (*AixLib.Fluid.HeatPumps.HeatPump*). The air-to-water heat pump model is controlled using a variable-speed compressor, whose speed  $\gamma_{HP}$  is normalized between 0 and 1. The heat flow rate generated by the heat pump and the electric power consumption are calculated with the heat pump performance matrix using as input the evaporator inlet temperature (outside air) and the condenser outlet temperature. The heat flow rate generated by the heat pump is then transferred to the water flowing through the condenser of the heat pump, the temperature of the water at outlet of the condenser varying then according to the water mass flow rate for a given heat flow rate.

In this thesis, the heat pump performance was modelled based on specific manufacturer data (atlantic 2022). The electrical power as well as the COP of the heat pump are given for an evaporator inlet temperature of both 7°C and -7°C and for some condenser outlet temperatures. Under non-nominal conditions, the heat pump matrix of performance is adjusted using the method from EN 15316-4-2. The obtained performance matrix used in the model is presented in Figure 65. The maximum water temperature on the condenser side is set to 65°C. To avoid too high temperatures in the condenser outlet, a COP of 0 and an electrical power of 0 W were added in the performance matrix for a condenser outlet temperature above 68°C. For other sizing of the heat pump, a scaling factor is applied on the electrical power to adapt this matrix.

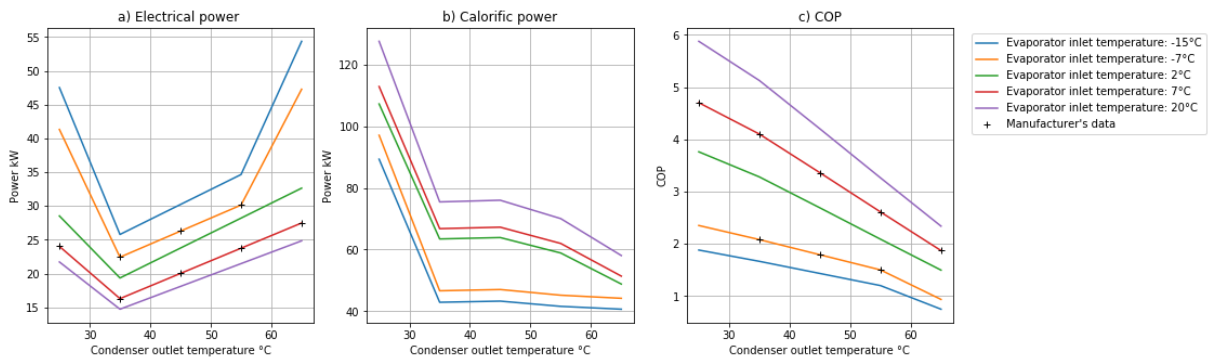


Figure 65: Heat pump performance matrix (atlantic 2022) with the following nominal characteristics (7/35°C): COP of 4.1, calorific power of 67 kW

The nominal mass flow rate at condenser was calculated using Equation 39. According to EN 14511, the nominal temperature difference between inlet and outlet was set at 5K (at the condenser) to calculate the nominal mass flow rate.

$$\dot{m}_{nom} = \frac{\dot{Q}_{nom}}{c_{p\ water} * \Delta\theta_{nom}} \quad 39$$

In the model used, the performance of the heat pump does not depend on the mass flow rate and does not consider eventual defrosting.



## Sizing

Regarding the sizing of heat pumps, the design heat losses correspond to the heating power of the heat pump in the worst-case conditions, or a lower value if combined with a gas boiler. Consequently, the generated heat flow used for sizing was evaluated for the evaporator inlet temperature at  $\theta_{design}$  and the condenser outlet temperature at 55°C or 65°C, respectively for space heating or DHW.

### 5.1.2. Hydraulic separator

#### Component description

The hydraulic separator is implemented using the fluid storage model of the *Buildings* library (*Buildings.Fluid.Storage.Stratified*), which is similar to the model used for the DHW storage tank without heat exchanger.

#### Sizing

The hydraulic separator was integrated into the heating system to decouple the heat pump from the primary network and prevent short cycles from the heat pump. The heat pump can only be activated 7 minutes after it has been switched off. The hydraulic separator should then be sufficient to ensure the demand during  $t_{HP\ off}$  (7 minutes or 420 seconds). According to DTU 65.16, the increase by  $\Delta\theta$  of the hydraulic separator temperature should compensate this shut down. For space heating with radiators, the value of  $\Delta\theta$  is set to 4K. After a shutdown, the water volume should last at least the minimum operating time of the heat pump to be recharged. The volume of the hydraulic storage  $V_{\tan HP}^{size\ HP}$  should then correspond to the volume that can be overheated by  $\Delta\theta = 4K$  with a heat pump working at the minimum power  $0,3 * P_{7/35}^{y_{HP}=1}$  during the minimum time  $t_{HP\ off}$ . This volume was calculated using Equation 40.

$$V_{HP}^{dim} = \frac{0,3 * P_{7/35}^{y_{HP}=1} * t_{HP\ off} * 1000}{\rho_{water} * C_{p\ water} * 4} \quad 40$$

### 5.1.3. Gas boiler model

The gas boiler is implemented using the boiler model with the efficiency based on tabulated data from the *Buildings* library (*Buildings.Fluid.Boilers.BoilerTable*). The boiler model is controlled with a firing rate signal varying between 0 and 1. For a firing rate  $y_{boiler}$ , the heat generated by the natural gas combustion  $Q_f$  (higher heating value) is calculated from the nominal heating power  $Q_{boiler}^{nom}$  and the nominal efficiency  $\eta_{boiler}^{nom}$  using Equation 41. The nominal heating power and efficiency correspond to the values for a boiler at full-load ( $y_{boiler}=1$ ) and an inlet temperature of 50°C.

$$Q_f = y_{boiler} * \frac{Q_{boiler}^{nom}}{\eta_{boiler}^{nom}} \quad 41$$

The heat transferred to the water in the boiler is then calculated using Equation 42.

$$Q_{boiler} = \eta_{boiler}(\gamma_{boiler}, \theta_{in\ boiler}) * Q_f$$

In this work, the efficiency curves of the condensing gas boiler were parametrized based on manufacturer data (Lochinvar 2023). The efficiency of the boiler  $\eta_{boiler}$  is estimated using a performance matrix with as input the inlet temperature in the boiler ( $\theta_{in\ boiler}$ ) and the firing rate ( $\gamma_{boiler}$ ). Figure 66 presents an example of the efficiency variation according to the inlet temperature for three different values of firing rate. The implementation of the gas boiler model was adapted for the different sizing by changing the value of the nominal heating power. The volume of water ( $1.5 * 10^{-6} * Q_{boiler}^{nom}$  m<sup>3</sup> with  $Q_{boiler}^{nom}$  in W) and the dry mass ( $1.5 * 10^{-3} * Q_{boiler}^{nom}$  kg with  $Q_{boiler}^{nom}$  in W) of the boiler were set proportional to the nominal heating power of the boiler and were also adapted to the sizing of the boiler.

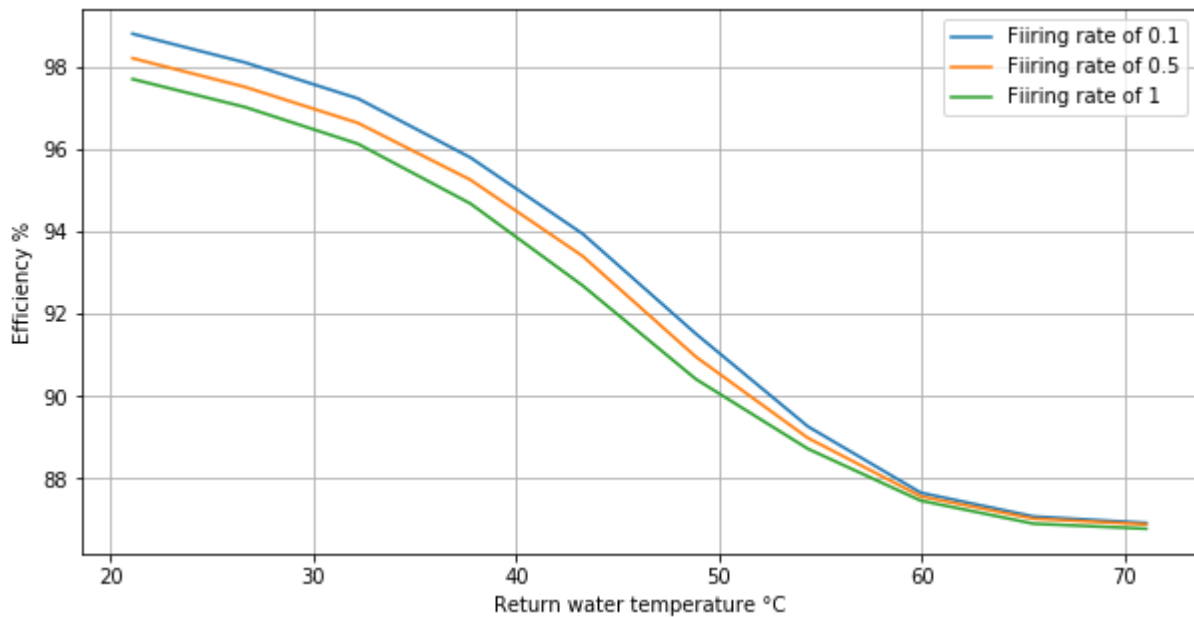


Figure 66: Gas boiler efficiency (given for the higher heating value) depending on the return water temperature (Lochinvar 2023) (nominal efficiency of 90% for a temperature of 50°C and a firing rate of 1)

The heat losses between the boiler envelope and the ambient air were neglected.

## 5.2. Overview of the heating system configurations

The aim of this thesis is to provide a detailed assessment of the performance of hybrid heating systems, taking into account the influence of both design and control strategy. Two control strategies, summarized in Figure 70, were implemented and compared with a reference heating system (stand-alone heat pumps):

- **Prioritizing the heat pump (boiler backup):** This control strategy aims to maximize the energy generation from the heat pump. In such control strategies, the heat pump is usually undersized compared to the estimated heat losses. The sum of the installed capacity of the gas boiler and the heat pump should however correspond to 120% of the estimated heat losses. Figure 67 schematically represents the activation band of the gas boiler (in red) and of the heat pump (in blue) according to the MEF of the heat pump for this control strategy. The boundary between the two activation bands depends on the sizing of the heat pump. For a given sizing

value, the limit varies according to the outdoor temperature and the outlet temperature of the heat pump.

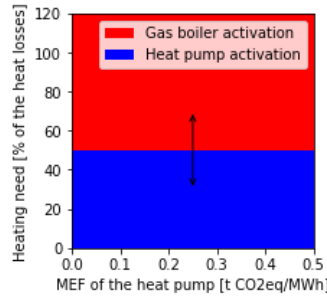


Figure 67: Schematic representation of the activation bands for the heat pump and the gas boiler in the control strategy prioritizing the heat pump

- **MEF-based fuel switch:** the MEF of the electricity consumption is used as an indicator to switch between the heat pump and the gas boiler in order to minimize the GHG emission of the heating system. It should be noted that indicators other than the GHG emissions have also been considered in the literature for switching fuel: the electricity cost, the primary energy, the outside temperature, the coefficient of performance of the heat pump, the national consumption... In general, with such control strategies, the capacity of both the heat pump and the gas boiler corresponds to 120% of the estimated heat losses. Figure 68 schematically represents the activation band for the gas boiler (in red) and for the heat pump (in blue). The boundary between the two activation bands corresponds to the emission factor of the gas boiler  $EF_{GB}$  considering the actual efficiency  $\eta_{boiler}$ . To evaluate this emission factor, a value for a reference boiler is calculated using the *ecoinvent* database ( $EF_{GB}^{ecoinvent} = 0.251$  t<sub>CO2eq</sub>/MWh) (Ecoinvent 2013). The efficiency of the gas boiler varying with its firing rate, the emission factor is then adapted using Equation 45, considering an efficiency of 95% for the EF from ecoinvent.

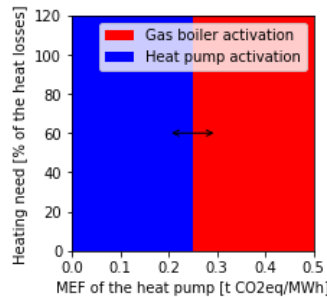


Figure 68: Schematic representation of the activation bands for the heat pump and the gas boiler in the MEF-based fuel switch strategy

$$EF_{GB}(t) = \frac{EF_{GB}^{ecoinvent} \cdot 95}{\eta_{boiler}(t)}$$

43

The impact of the sizing of the heat pump is also investigated (decreasing the sizing of the heat pump from 120% down to 20%). Figure 69 schematically represents the activation bands for the gas boiler (in red) and for the heat pump (in blue) for this control strategy. Similarly to the previous figures, the boundary between the two activation bands can vary with the sizing of the heat pumps and the changing performance of both heating systems.

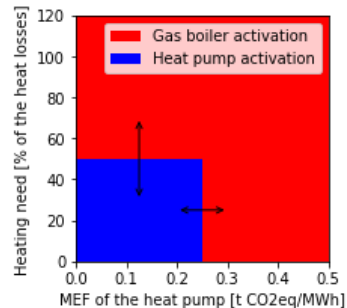


Figure 69: Schematic representation of the activation bands for the heat pump and the gas boiler in the MEF-based fuel switch strategy with an undersized heat pump

For these two control strategies, three different sizing of the heat pump (50, 35 and 20% of the heat losses) are considered. This is an arbitrary choice as there is currently no recommendation in France or in Europe for the sizing of hybrid heat pumps for apartment blocks. For hybrid heat pumps in single-family houses, (Ministère de la Transition Énergétique 2022) specifies that the heat pump capacity should provide between 40% and 80% of the heating need evaluated for an outdoor temperature of 0°C and a supply temperature of 50°C. In addition, a hybrid system can be called as such if at least 70% of the required heat is generated by the electric heat pump. Consequently, the different control strategies and sizing should also be compared according to the share of the heat demand provided by the electric heat pump.

Heating systems are generally sized in order to supply at least 120% of the heat losses. This should be sufficient to quickly return dwellings to the set temperature after a period without heating. From the simulations, it was observed that such a sizing (based solely on the space heating need) was sufficient to provide heat for both space heating and DHW. Indeed, the heating power for DHW is avoided during the peak load for space heating and is limited in comparison with the space heating demand thanks to the relatively large DHW storage tank.

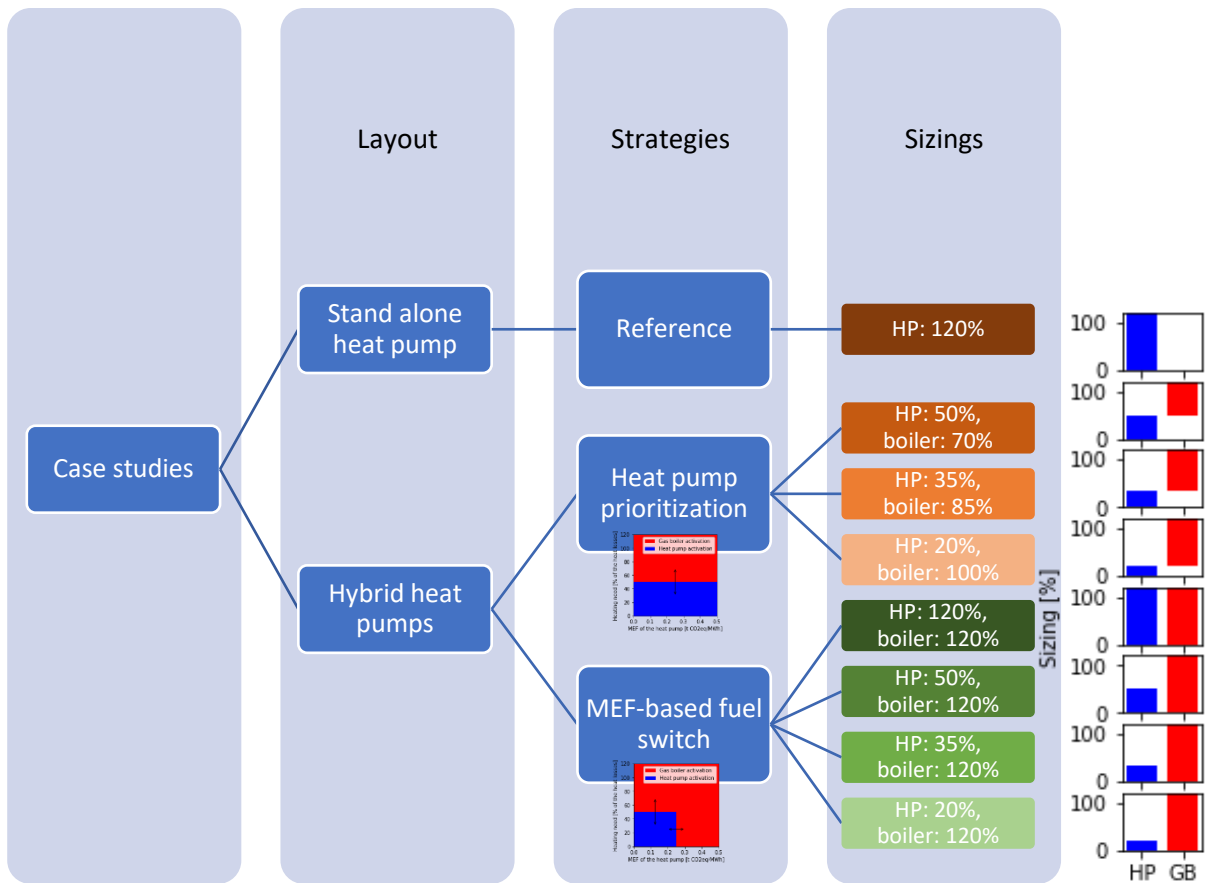


Figure 70: Summary of the evaluated control strategies and sizing of the hybrid heat pumps

## 5.3. Reference heating system

### 5.3.1. Configuration of the heating system

In this section, the control strategy applied to the components of the reference heating system is described. Figure 71 shows the configuration for the reference heating system considered in this work. The location of the different sensors required to control the heating system is also represented in Figure 72 (circled letter T). The grey dotted lines indicate the relationship between the sensors and the actuators. The corresponding control strategies are described in the next paragraph.

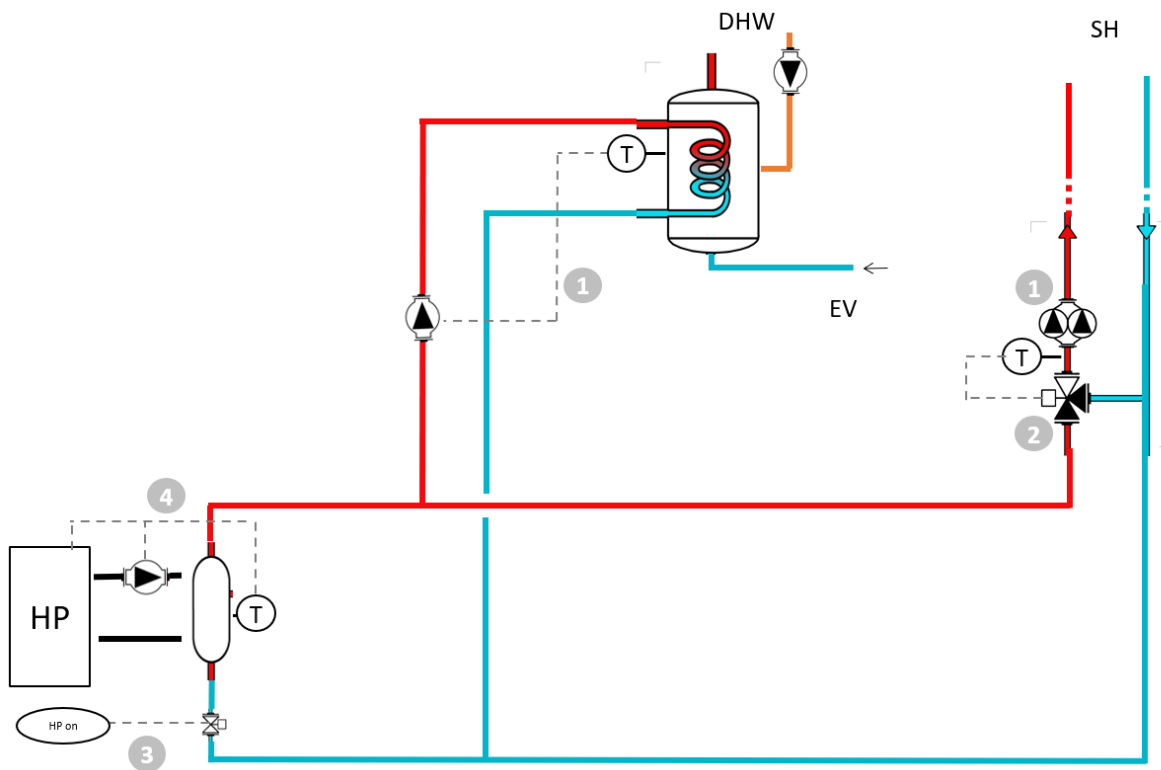


Figure 71: Configuration of the reference heating system

### 5.3.2. Control strategy of the standalone heat pumps

The general control process is described in Figure 72. The numbers on the figure refer to the sensors and components numbered in Figure 71.

- 1) Space heating is activated when at least one radiator valve is opened. The detailed control strategy for space heating distribution and emission was explained in Section 4.3.3. The activation of the DHW production depends on the temperature of the water stored in the tank and was detailed in Section 4.4.4. When DHW is activated, the pump dedicated to the DHW storage is activated with a constant mass flow rate. In this case, the space heating demand is still met as the pump dedicated to space heating continues to operate (both running in parallel).
- 2) When space heating is activated, the temperature supplied by the heating system is adjusted according to the outside temperature (as explained in Section 4.3.3). In addition, the temperature set point of the water supplied to the radiators is increased by 10°C (with a saturation of the set point at 55°C) between 6 am and 9 am, to ensure that the dwellings heat up quickly after the night setback. When the hybrid system is used for DHW production, the temperature supplied by the heating system is set to 65°C. As explained in Section 4.3.3, the temperature of the water flowing through the radiators is controlled using a three-ways valve mixing the hot water from the hybrid heating system and the water returning from the radiators. The opening of the three-way valve is controlled by a PID controller comparing the supply temperature for space heating with the set point.
- 3) When either DHW or space heating is activated, the two-way valve is opened and the heat pump may be activated.

- 4) The heat pump is combined with a hydraulic separator to prevent cycles from being too short. Indeed, after each shutdown, the heat pump has to stay off for at least 7 minutes. The temperature set-point for the heat pump is thus increased by 4°C when space heating is activated to meet the demand during these 7 minutes. In addition, the normalized compressor speed  $y_{HP}$  varies in a range between 0.2 and 1 to avoid working at very low part load. Consequently, the input signal for the normalized compressor speed of the heat pump is set using a PI controller to adjust the water temperature in the hydraulic separator. The temperature sensor is located in the 2<sup>nd</sup> section of the hydraulic separator out of 9 sections (from the top).

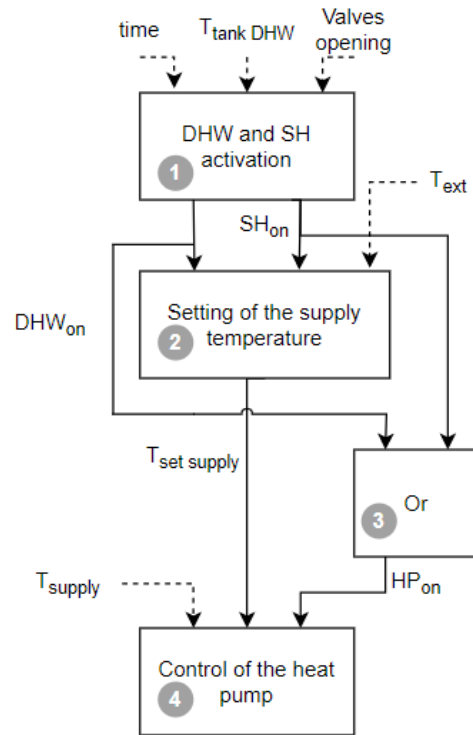


Figure 72: Control strategy of the reference heating system

### 5.3.3. Results

In this section, some results on the performance of a standalone heat pump in La Rochelle are presented. 33 dwellings with a total of 74 occupants are heated by this heat pump. The heat losses for this building at the base temperature (-4°C) are equal to 57 kW. According to the sizing rules described previously (+20% oversizing), the heat pump should produce 69 kW of heat at an outlet water temperature of the condenser of 55°C. The heat pump was then chosen with a nominal power of 92 kW under nominal conditions (7/35°C). The necessary heat for the DHW production was estimated to be around 32 kW. Figure 73 shows the power consumption, the normalized compressor speed, the COP and the outdoor temperature in La Rochelle from July 2018 to June 2019. The heat pump was sized considering a base temperature of -4°C. However, this outdoor temperature was never reached during the heating season. Consequently, the maximum generated heat during the year is lower than the sizing of the heat pump. In winter, the average COP of the heat pump is lower than during the rest of the year mainly due to the decrease of the outdoor temperature. However, during the heating season, the COP can be higher than during the rest of the year. It can be explained by observing the outlet temperature of the heat pump shown in Figure 74.

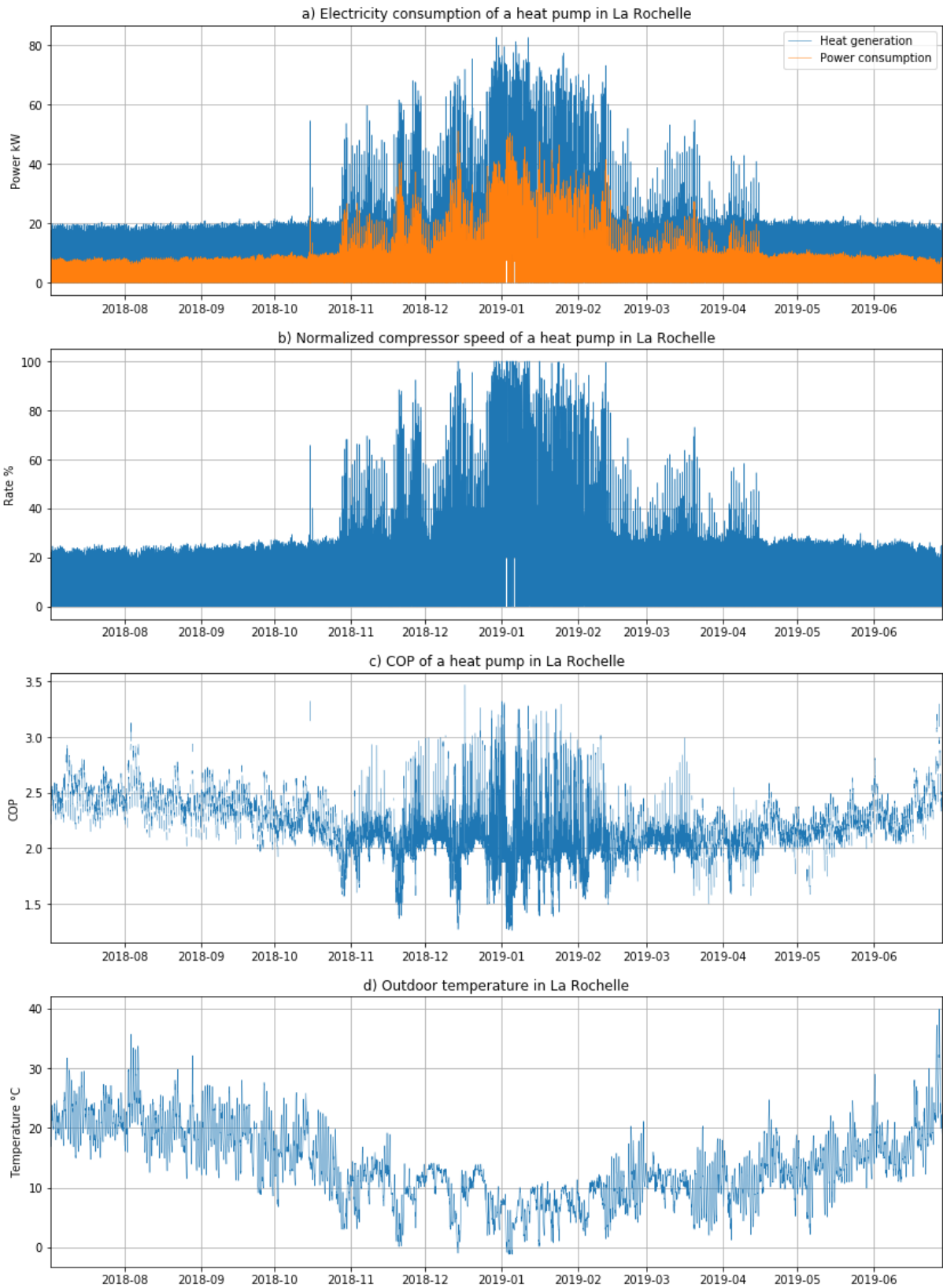


Figure 73: Results for a stand alone heat pump in La Rochelle



For most of the year, the temperature set-point for heating is 65°C for heating up the DHW tank. When the heat pump is generating heat only for space heating, the set temperature is lower and consequently, the heat pump has better performances.

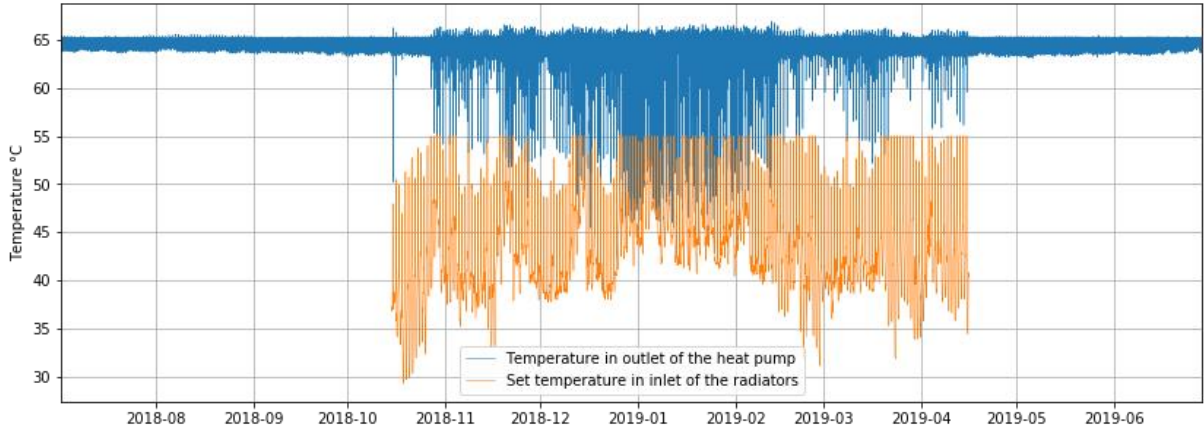


Figure 74: Outlet temperature of the heat pump and temperature set-point of the water supplied to the radiators

Figure 75 shows the temperature at the top, middle and bottom of the hydraulic separator and the temperature set-point for the radiators for one week in January. It can be observed that the temperature at the top of the hydraulic separator is rarely close to the set temperature for the space heating. This means that due to the frequent reheating of the DHW tank, the water for space heating demand is mostly produced at a set temperature of 65°C for the heat pump. As a result, the performance of the heating system is lower than with a system that only provides space heating.

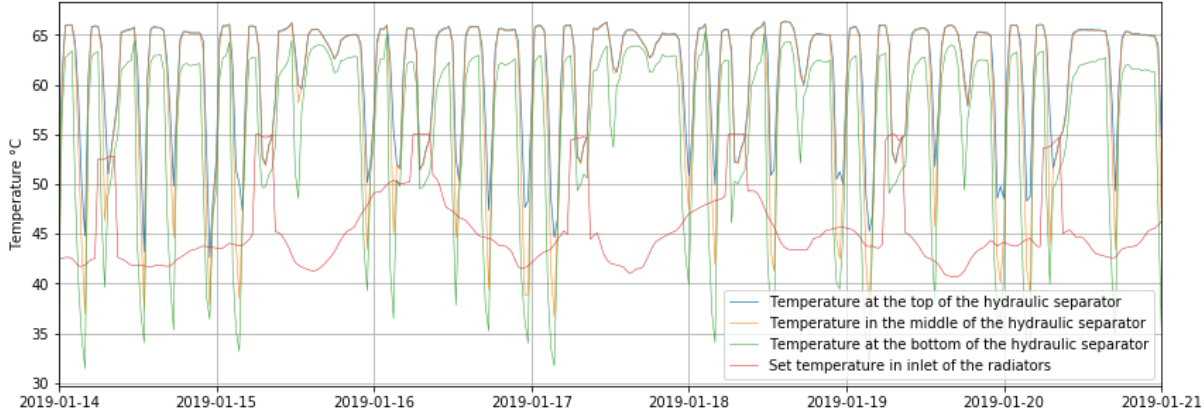


Figure 75: Temperatures in the hydraulic separator and temperature set-point for the radiators for a week in January

Figure 76 presents a heat map of the state-wide activation pattern of the heat pumps (around 3000 heat pumps). The x-axis represents each step of 30 minutes during a week and the y-axis represents the 52 weeks between July 2018 and June 2019. The activation level of the heat pumps depends mainly on the outdoor temperature. The coldest weeks of the year can easily be identified on the heat map. During weeks without space heating (between spring and autumn), the pattern of heating of the DHW storage tank can be clearly identified, especially the forced heating up of the tank between 4 am and 6 am before the space heating peak demand. During the heating season, the morning boost for space

heating can also be observed (from 6am to 9am). In general, a synchronization of the activation pattern can be observed between the different heat pumps, mainly due to these two morning boosts occurring in a synchronized way in the pool. This synchronization tends to fade out at the end of each day.

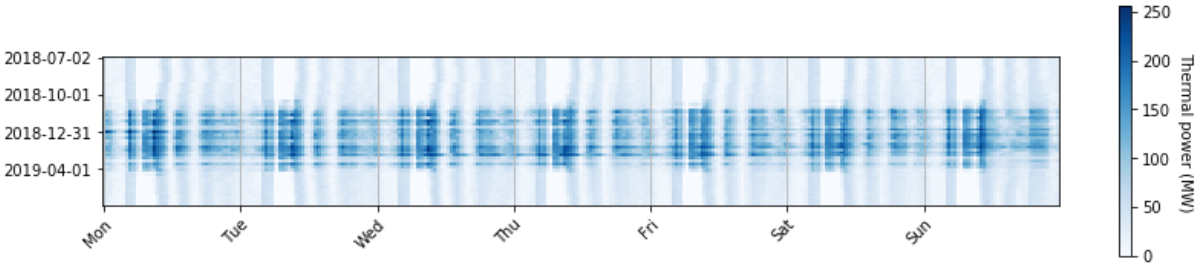


Figure 76: Activation pattern of a national fleet of standalone heat pumps (July 2018 to June 2019)

The marginal mix and the corresponding marginal emissions can be evaluated from the electricity use of heat pumps using the UCED model of the French power system described in Chapter 3 and the MEF of the electricity exchanges at the French border described in Chapter 2. The calculation of the electricity use and of the marginal mix and emissions are performed for the same year (from July 2018 to June 2019). For the evaluation of the marginal mix using the UCED model, the only change compared to Chapter 3 is the updating of the order in the two merit-orders to better fit the 2018-2019 period. The merit-orders are calibrated for the whole year 2018 (respectively 2019) for the simulation times occurring during the last half of 2018 (respectively 2019). As explained in Section 2.2.2, the marginal mix corresponding to the electricity used by the heat pumps was obtained by running the UCED model on two cases, one with and one without the 100 000 additional heated dwellings. The corresponding marginal emissions are evaluated using Equation 23. The emission factors used for the calculation of the marginal emissions are presented in Table 4 for the electricity generation and the time series assessed in Section 2.3.3 for the electricity exchanges.

Figure 77 shows the marginal electricity mix and emissions corresponding to the 100 000 additional heated dwellings between July 2018 and June 2019. The different colors show the technology, which would need to be activated to supply the additional electricity consumption (30-minute interval). 60% of the marginality was attributed to the electricity exchanges with neighboring countries (shown in green in the figure). Consequently, the activation pattern of the gas boiler highly depends on the MEF of the electricity exchanges. 31% of the marginality was attributed to fossil-fired power plants, including 22% for CCGT, 6% for coal-fired power plants and 3% for oil-fired power plants. Nuclear power plants, which provide 9% of the yearly marginality, were mainly marginal during low electricity consumption periods: in order to compensate for the additional consumption, nuclear power plants decrease less when they are adjusting downward. Hydroelectric power plants are supplied with rainwater and runoff water whose reserves are limited and used entirely. Consequently, the yearly share of the marginality of hydroelectric powerplants is zero.

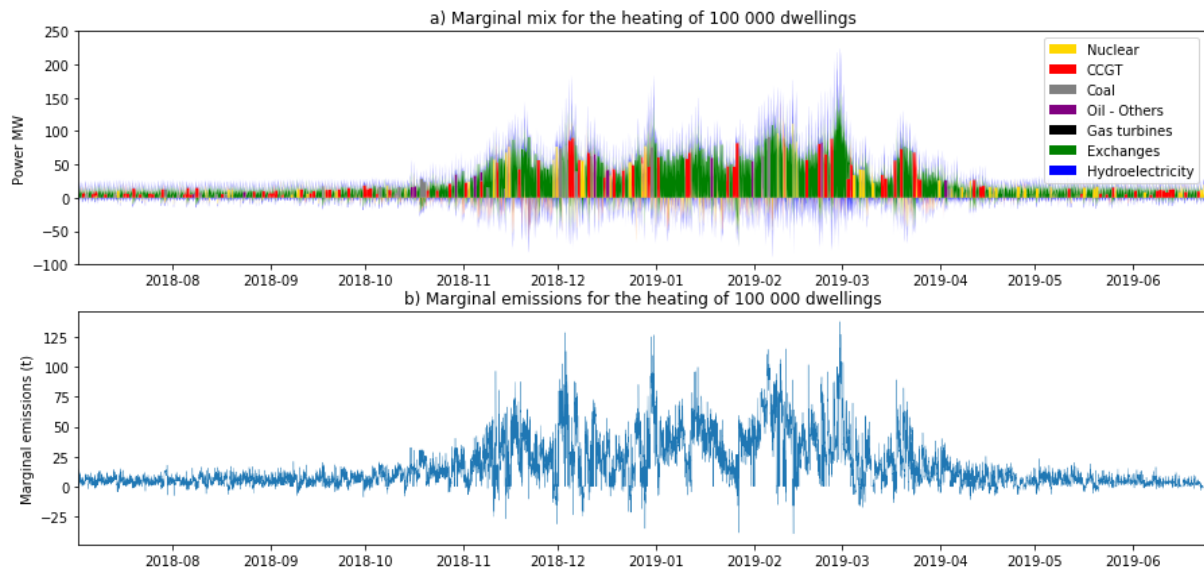


Figure 77: Marginal mix and emissions for the heating of 100 000 dwellings with heat pumps between July 2018 and June 2019 (30-minute resolution)

## 5.4. Control strategy 1: Prioritizing the heat pump

### 5.4.1. Configuration of the hybrid heating system

In this section the control strategy applied to the components of the reference heating system is described. Figure 78 shows the configuration for the hybrid heating system (similar configuration for control strategies 1 and 2). The location of the different sensors needed to control the heating system is also represented in Figure 78. The corresponding control strategies are described in the next paragraph.

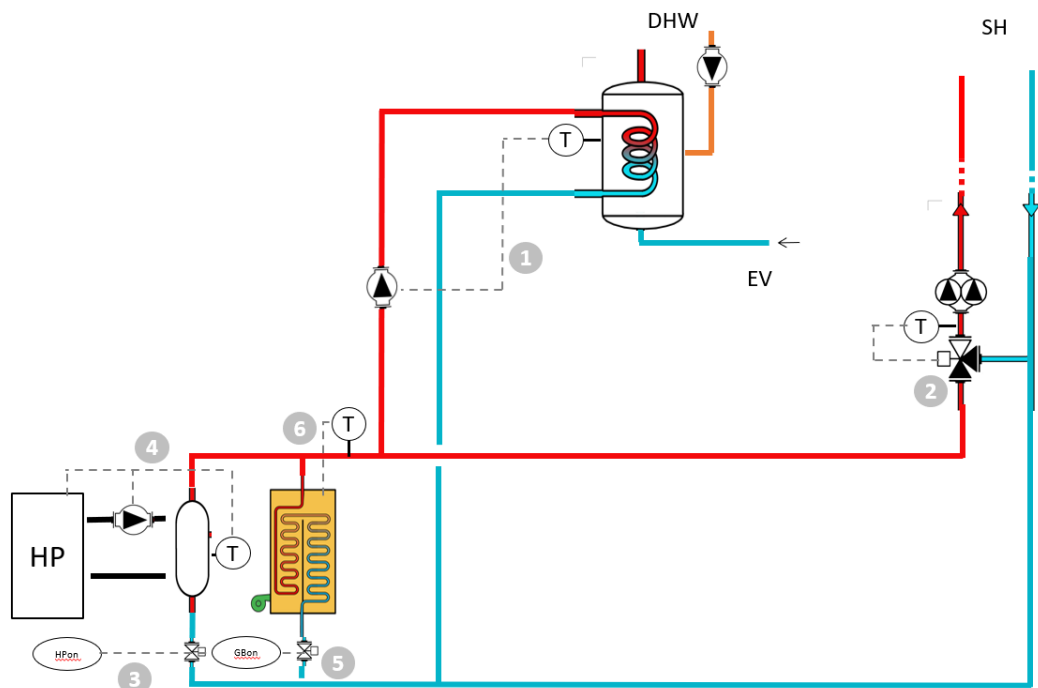


Figure 78: Configuration of the hybrid heating system

### 5.4.2. Control strategy to prioritize the heat pump

The general control process is described in Figure 79. The numbers on the figure refer to the sensors and the components numbered in Figure 78.

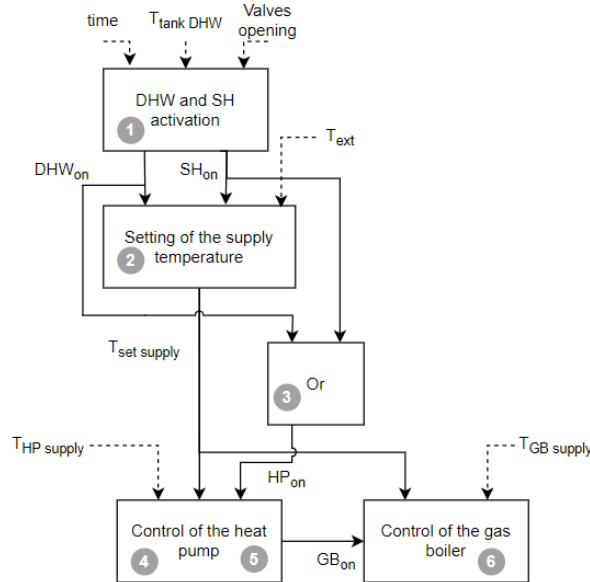


Figure 79: Control strategy 1 (prioritizing the heat pump) for the hybrid heating system

- 1-4) Steps 1 to 4 are similar to the reference case.
- 5) To maximize the use of the heat pump, the boiler is only activated when the heat pump cannot provide the required heat. In practice, the heat pump generates heat by default. The gas boiler is only activated if the temperature set-point for heating has not been reached after 20 minutes of full-load heat generation by the heat pump. Finally, the gas boiler is switched off again when the heat pump is no longer producing at full load.
- 6) The firing rate of the boiler is controlled according to the supply temperature set for the heating system using a PI controller. The firing rate of the boiler varies in a range between 10% and 100%. The gas boiler is only activated for a mass flow rate greater than 20% of the nominal value to avoid overheating of the gas boiler.

### 5.4.3. Results

Figure 80 represents the heat produced by the heat pump in blue and by the gas boiler in red when the heat pump is sized to supply 50% of the heat losses at the base temperature. The gas boiler is only activated during a few days of the year. The heat pump is sufficient to provide DHW in summer. Such a control strategy helps to reduce the peak demand during winter caused by the electrification of space heating on the power system. The gas boiler is activated around 5% of the working time of the heating system.

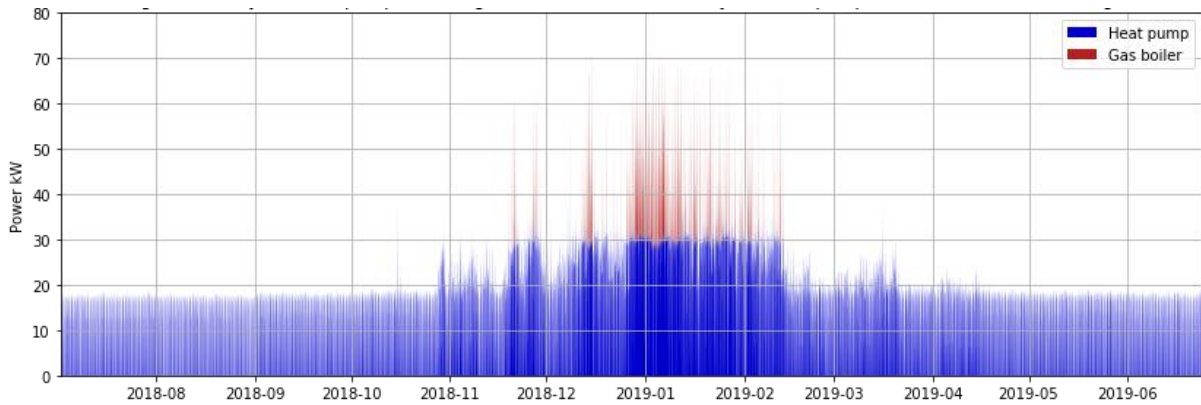


Figure 80: Heat generation for a hybrid heat pump in La Rochelle with a control strategy prioritizing the heat pump (sizing at 50% of the design heat losses: 29 kW)

Figure 81 shows a heat map of the state-wide activation pattern of the gas boilers and the heat pumps. With such a control strategy, the activation of the gas boiler depends mainly on the level of the heating demand, which is directly related to the outdoor temperature and the DHW demand. Consequently, the gas boiler is mostly activated between 6 am and 9 am (when space heating starts again after the night setback) during the coldest days of the year. The gas boilers are also activated sometimes in the evening, to help heat up the DHW storage tanks and the dwellings after the set back in the middle of the day. At the national scale, around 32% of the working time of the heating systems, gas boilers are activated in at least one of the climate zone.

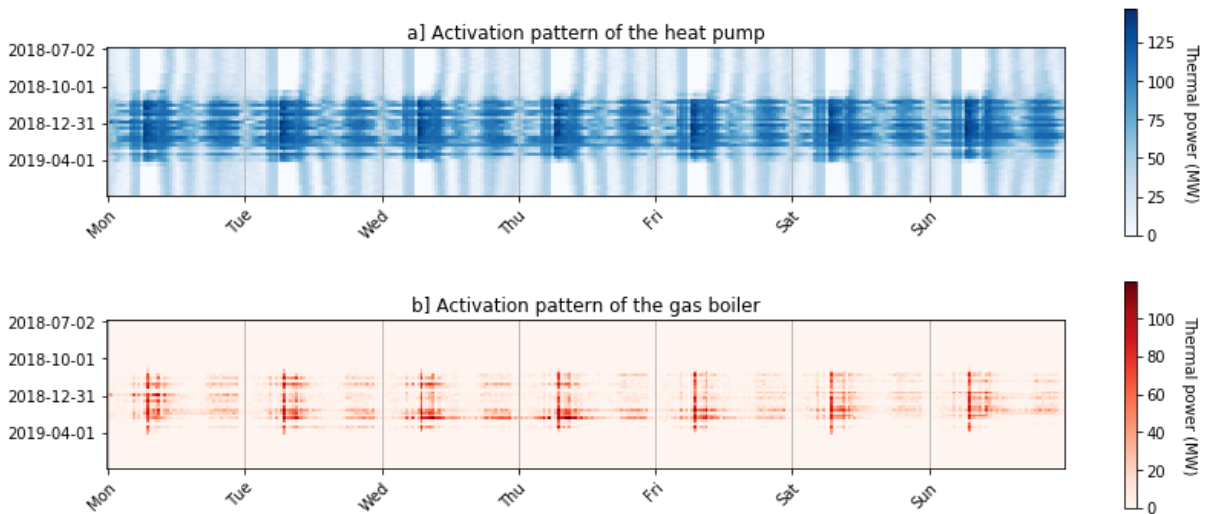


Figure 81: Activation pattern of the heat pumps and gas boilers for the national fleet of hybrid heat pumps controlled to maximize the heat pump use (sizing at 50% of the design heat losses)

## 5.5. Control strategy 2: MEF-based fuel switch

In this section, the control strategy to minimize GHG emissions is presented. In a first subsection, the ideal activation pattern of the gas boiler is evaluated in the case with a heat pump and a gas boiler sized to supply 120% of the heat losses using the results from section 5.3.3. In a second subsection, the detailed control strategy is presented. Finally, first simulation results are presented.

### 5.5.1. Ideal activation pattern of the gas boiler

After evaluating the GHG emissions factor for heating the 100 000 dwellings with heat pumps (see Section 5.3.3, an ideal activation pattern for the gas boiler can be assessed by comparing the marginal emissions of the heat pump with that of the gas boiler. Figure 82a represents the marginal emissions of the fleet of heat pumps as well as the corresponding emissions for heating with a gas boiler in December 2018. For this potential study, the emissions from the gas boiler were calculated using the emission factor of a gas boiler ( $0.251 \text{ t}_{\text{CO}_2\text{eq}}/\text{MWh}$ ) multiplied by the heat generated by the heat pumps for each time step. This is an oversimplification as the generation pattern will be different with a hybrid system and the efficiency of the gas boiler will vary over time. The activation pattern is derived considering that the gas boilers are activated when their emissions are lower than the emissions of the heat pumps. Figure 82b represents the ideal activation pattern for the gas boilers in La Rochelle in December 2018. Considering these preliminary results for La Rochelle, the gas boiler would be activated 3951 hours (51% of the working time of the heating systems).

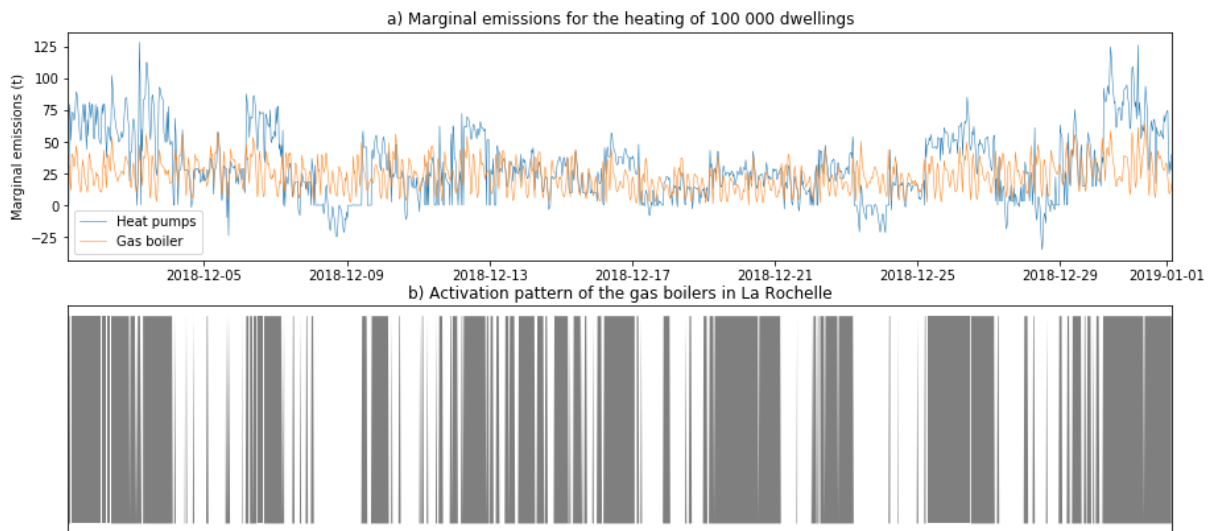


Figure 82: Marginal emissions for the heating of 100 000 dwellings with heat pumps or gas boilers and derived activation pattern for the heat pumps in La Rochelle

Table 17 summarizes some simulation results (heating demand, average COP, annual activation time and potential activation ratio of the gas boiler) for the seven French representative cities. The average COP presented in this table corresponds to the ratio between the annual heat generated and the consumed electricity. French climate is characterized by a high territorial diversity. Consequently, the space heating demand and duration varies greatly from one climate zone to another. The DHW demand being poorly correlated with the outside temperature, only the variability of the space heating demand can be observed between the cities. The COP of the heat pumps decreasing with the outdoor temperature, the COP and the activation time of the gas boiler vary between the climate zones. As for the activation time of the heating system, the variability of these results from one city to another would be more visible for a system only providing space heating, as these results aggregate space heating and DHW.

Table 17: Characteristics of the heating demand for each French representative city

Representative city	Trappes	Nancy	Lyon	Rennes	La Rochelle	Agen	Nice
Heating+DHW need (kWh/m <sup>2</sup> .yr)	70	77	67	64	52	55	45
Average COP	1.89	1.81	1.94	1.99	2.09	2.04	2.22
Activation time of the heating system (h)	7750	7632	7664	7770	7717	7683	7701
Potential activation ratio of the gas boiler (%)	53	54	52	52	51	51	48

These results confirm the interest of hybrid technologies to decarbonize the heating demand. However, this first evaluation corresponds to an ideal activation time and does not take into account the real behavior of hybrid heating systems.

#### 5.5.2. Control strategy to minimize the GHG emissions

In this section, the configuration of the heating system is the same as in the previous section (see Figure 78). With this control strategy, the MEF of the electricity consumption is used as an indicator to switch between the heat pump and the gas boiler to minimize the GHG emissions. This MEF is evaluated using the reference case (standalone heat pump). The general control process is described in Figure 83 for a heat pump and a gas boiler sized both to 120% of the heat losses. The numbers in the figure refer to the sensors and components numbered in Figure 78. Equation 44 corresponds to the condition for the activation of the heat pump.  $P_{HP}^{elec}(t)$  is the electricity consumption of the heat pump and  $P_{HP}^{th}(t)$  is the thermal power generated by the heat pump.

$$\frac{MEF(t) \cdot P_{HP}^{elec}(t)}{P_{HP}^{th}(t)} < EF_{GB}(t)$$

44

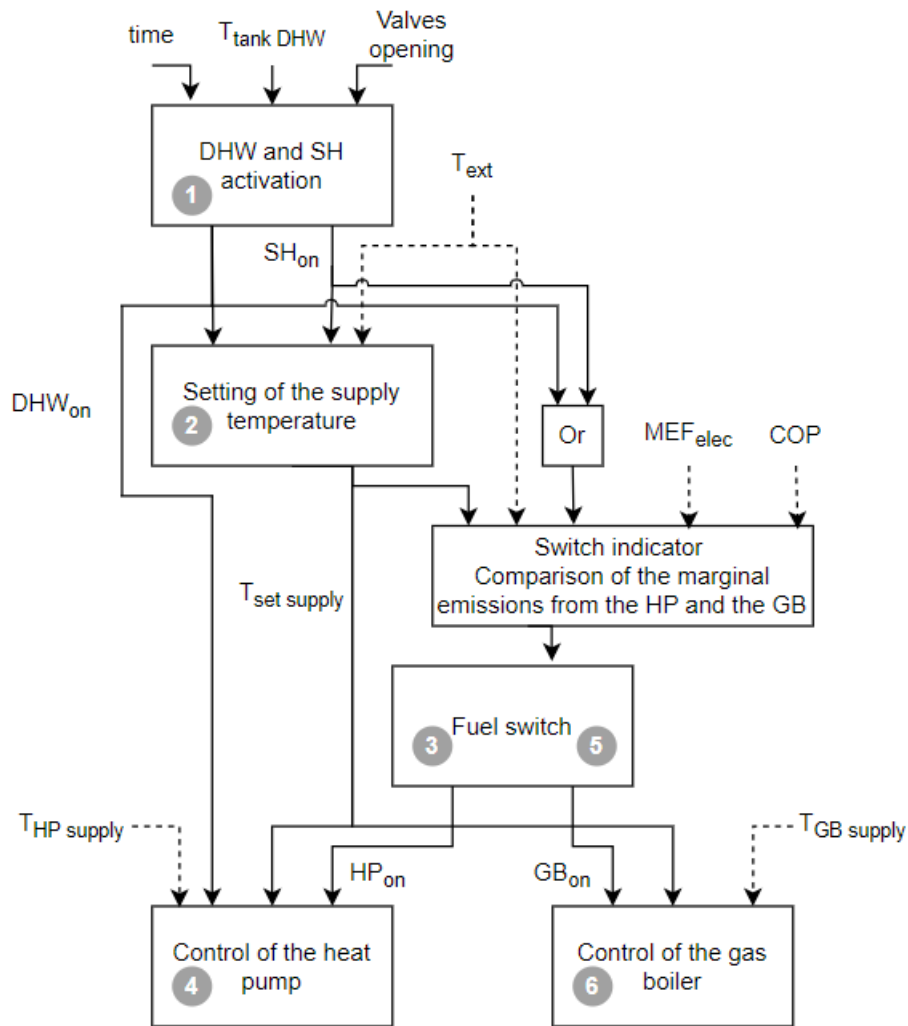


Figure 83: Control strategy 2 (MEF-based fuel switch) for the hybrid system

- 1-2) Steps 1 and 2 are similar to the reference case.
- 3) When either DHW or space heating is activated, the heat pump or the boiler may be activated. The heat pump is activated when the condition of Equation 44 is *true* and the boiler is thus turned off.
- 4) Step 4 is similar to the reference case.
- 5) When the condition of Equation 44 is *false*, the gas boiler is activated and the heat pump is turned off.
- 6) Step 6 is similar to the case prioritizing the gas boiler (control strategy 1).

Variants with undersized heat pumps are also modelled (50%, 35% and 20%). If the heat pump cannot supply the required heat, the gas boiler can also be activated. In this case, the control of the gas boiler is similar to control strategy 1. When the condition of Equation 44 is *false*, the gas boiler provides heat and the heat pump is turned off. When the heat pump is undersized, the MEF evaluated using the control strategy prioritizing the heat pump corresponding to the actual heat pump sizing is used as input of the controller.

### 5.5.3. Results



Figure 84 represents the heat produced by the heat pump in blue and by the gas boiler in red when the heat pump is sized to supply 120% of the heat losses at the base temperature. The gas boiler is activated during the entire year with this control strategy, corresponding to around 29% of the working time for the single hybrid system.

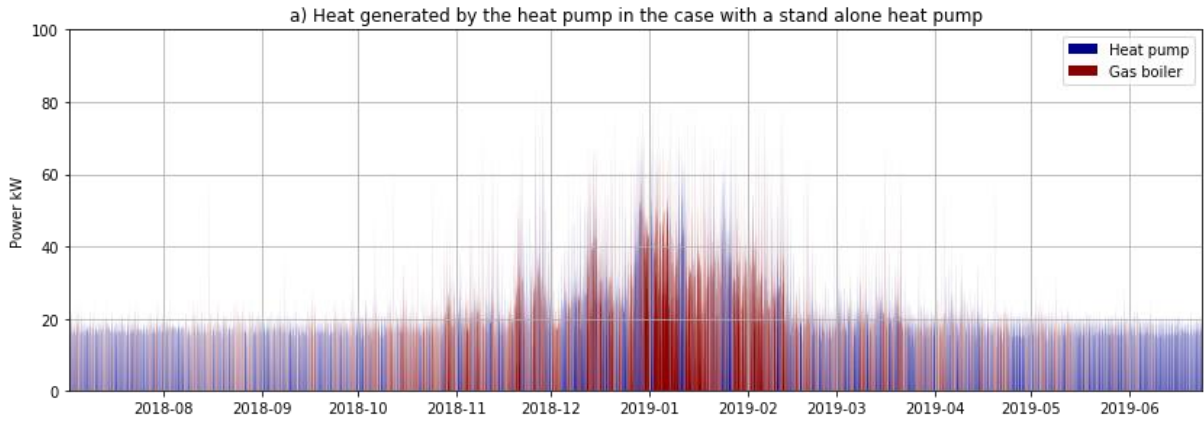


Figure 84: Heat generation for a hybrid heat pump in La Rochelle with a control strategy to minimize the GHG emissions (sizing at 120% of the design heat losses for both systems)

Figure 85 presents a heat map of the activation pattern of the gas boilers and the heat pumps with the control strategy 2 (MEF-based fuel switch). With such a control strategy, the activation of the gas boiler depends on the MEF of the French power system and on the COP of the heat pump. Consequently, the gas boiler is often activated during the coldest days of the year, when the COP of the heat pump is low and the national power demand is high. However, more parameters influence the activation of the gas boiler with this control strategy, and a temporal activation pattern seems more difficult to identify. It would be discussed in the next section. At the national scale, around 55% of the working time of the heating systems gas boilers are activated in at least one of the climate zone, which corresponds to the estimation of Section 5.1.

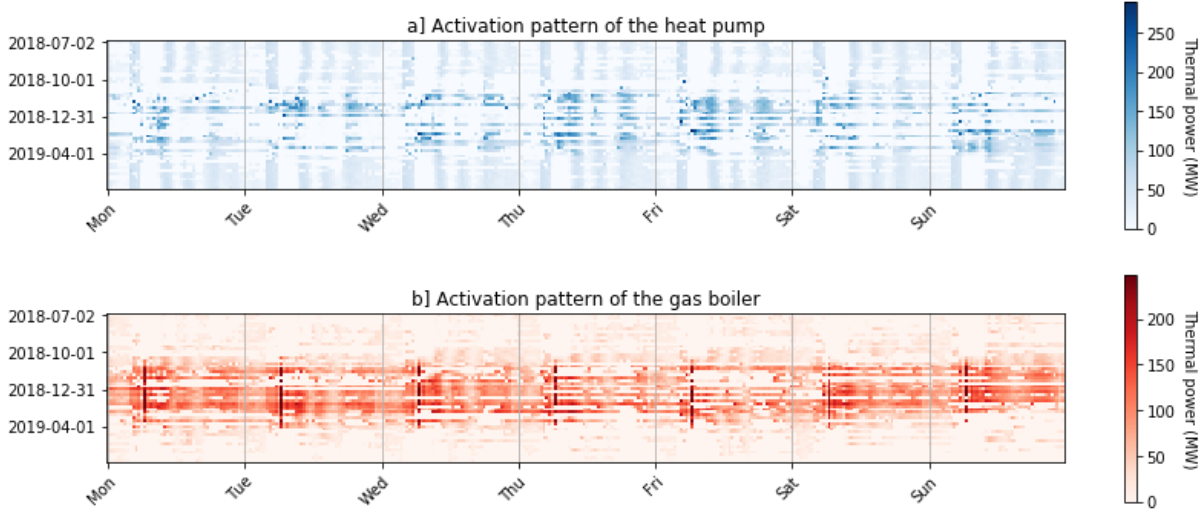


Figure 85: Activation pattern of the heat pumps and the gas boilers for the national fleet of hybrid heat pumps controlled to minimize the GHG emissions (sizing at 120% of the design heat losses for both systems)

## 5.6. Evaluation of the impact of the control strategies and heat pump sizing

In this section, the different control strategies and sizing of the heating systems are compared with the reference case (standalone heat pump), with the objective to evaluate the influence on GHG emissions. The avoided emissions during the off-time of the heat pumps and the additional emissions due to the gas boiler are assessed. To explain the variation in the GHG emissions between the different cases, the average COP of the heating system and the average MEF of the consumed electricity are presented for the case-studies. As a reminder, the average COP of the heating systems refers to the ratio between the yearly heat generation from the heat pumps and their yearly electricity consumption. Similarly, the average MEF of electricity refers to the ratio between the yearly marginal emissions related to the heat pumps and the yearly electricity consumption.

### 5.6.1. Comparison of the two control strategies

In this section, the impact of the control strategy is evaluated. Consequently, the marginal emissions of the control strategy 1 (prioritizing the heat pump) and control strategy 2 (switching fuel based on MEF) are compared to the reference case. In this section, only the sizing of the heat pump at 50% is shown for control strategy 1, and a sizing of 120% for control strategy 2.

Figure 86 represents the heat generated by the gas boilers and the heat pumps in each case. With the MEF-based fuel switch strategy, the use of the heat pump is around 45%, while in the case of the strategy prioritizing the heat pump, most of the heat is produced by the heat pump (93%).

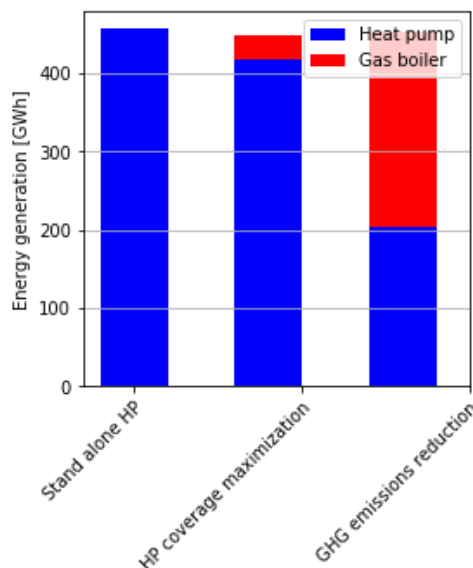


Figure 86: Heat generated by the heat pump and the gas boiler for each control strategy

Figure 87 shows the GHG emissions avoided by the decrease in the heat pump generation (whole grey area, hatched and unhatched) and the GHG emissions by the gas boiler (hatched area). The total GHG emissions avoided with the hybrid systems corresponds thus to the grey area that is not hatched. The control strategy prioritizing the heat pump and MEF-based fuel switch would have avoided respectively the emission of 8 000 tons of CO<sub>2eq</sub> and 38 000 tons of CO<sub>2eq</sub>. This represents an average decrease in GHG emissions of 0.08 and 0.38 t<sub>CO<sub>2eq</sub></sub> per dwelling, respectively. For comparison, in 2019, the

electricity generation in France and Germany generated respectively 19 Mt and 227 Mt of CO<sub>2eq</sub> (RTE 2019c; Umwelt Bundesamt 2020).

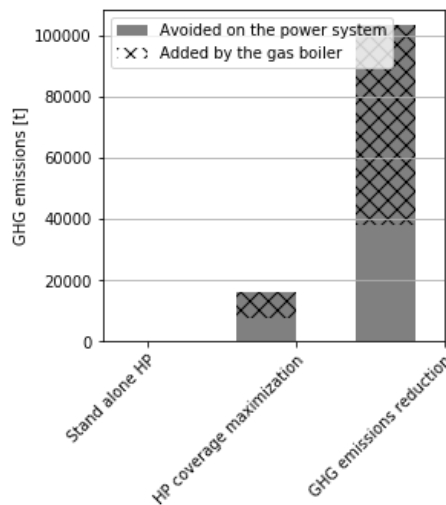


Figure 87: Balance of the GHG emissions for each control strategy

Table 18 summarizes the GHG emissions avoided by the hybrid systems, the average COP of the heat pumps and the average MEF of the electricity consumption for the two control strategies and the reference case. These results show the interest in hybrid heat pumps with both control strategies to decrease the GHG emissions and improve the performance of the heat pumps. The improvement in heat pump performance means that they are generally switched off when operating at reduced performance.

The control strategy 2 (MEF-based fuel switch) would have been the most efficient to avoid GHG emissions. This emissions reduction is mainly explained by the reduction of the average MEF of the electricity consumption due to the activation of the boiler. The electricity consumption is avoided when the marginal emissions are high. The decrease in GHG emissions is lower with control strategy 2 (prioritizing the heat pump). The amount of electricity consumed being close to the reference case (only a 7% of decrease), the MEF of the electricity consumption remains close to the reference case. The avoided emissions are mainly explained by the improved performance of the heat pumps. In this case, the heat pump is assisted by the gas boiler when the heating demand is the highest, which corresponds to the coldest days. It means that during these periods, the supplied temperature of the heat pumps is lower than in the reference case and the performance of the heat pumps is improved.

Table 18: Avoided GHG emissions, COP of the heat pump and MEF of the electricity consumption for the reference case and the two control strategies

	Standalone heat pump	Heat pump prioritisation	MEF-based fuel switch
GHG emissions avoided	- (Reference)	7859 t <sub>CO2eq</sub>	38188 t <sub>CO2eq</sub>
COP of the heat pump	1.95	1.99	2.03
MEF of the consumed electricity	0.607 t <sub>CO2eq</sub> /MWh	0.603 t <sub>CO2eq</sub> /MWh	0.378 t <sub>CO2eq</sub> /MWh

Figure 88 presents the marginal mix corresponding to the electricity consumption of the heat pumps fleet in the reference case and with the two hybrid systems. Figure 89 summarizes the marginal mix avoided through the activation of the gas boiler in comparison with the reference case for the two control strategies and considering the transport and distribution losses. In both cases, most of the avoided electricity consumption influenced the electricity exchanges. In the case of the MEF-based fuel

switch control strategy, the generation of electricity through coal- and oil-fired powerplants was also avoided.

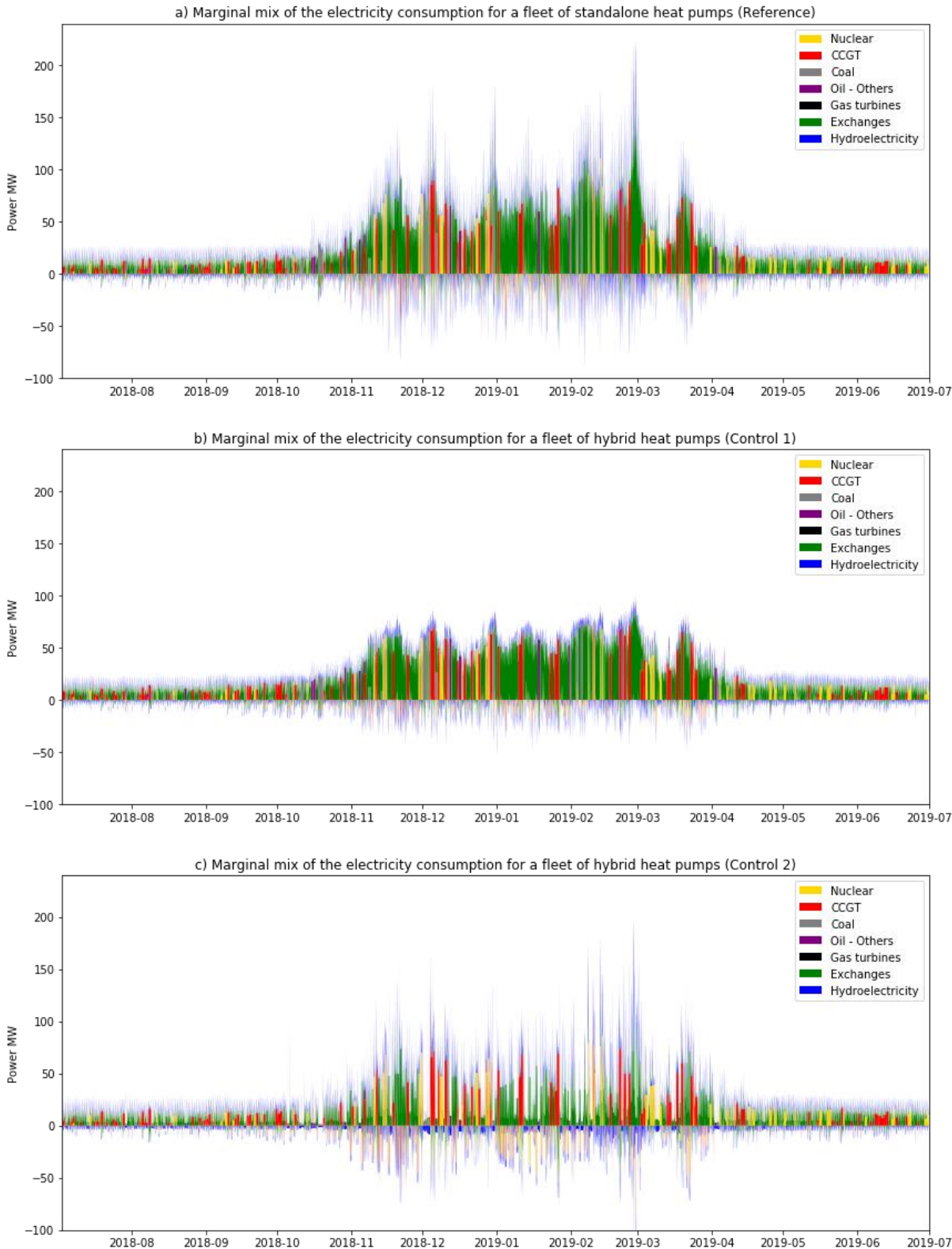


Figure 88: Half-hourly marginal mix of the electricity consumption for the reference case and the two control strategies

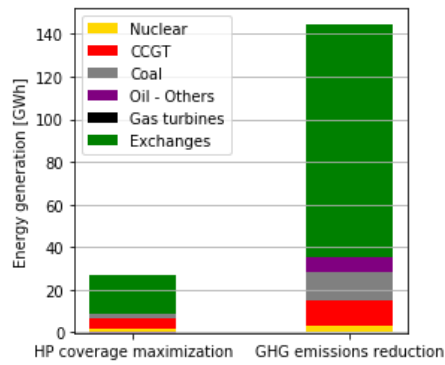


Figure 89: Yearly marginal mix of the avoided electricity consumption through the activation of the gas boilers for the two control strategies in comparison to the reference case

A limitation to this study is the complexity to implement in practice such a control strategy minimizing the GHG emissions. The signal for the activation of the gas boiler is assessed considering the MEF of the electricity consumed by the equivalent system without fuel switch. This type of control would be easier to implement with simplified indicators, such as the outdoor temperature, the COP of the heat pump or the time of the day. It is therefore of interest to observe the activation patterns of hybrid systems based on these indicators.

Figure 90 represents the heat generated by a heating system in La Rochelle as a function of the outdoor temperature for the standalone heat pump (left) and for the hybrid heat pumps (middle and right). Blue and red data points represent the operating points of the heat pump and the gas boiler respectively. It can be seen that the heating demand is generally higher (meaning that the space heating is activated) for outdoor temperatures below 12°C. The minimum firing rate of the heat pump (20% of the nominal power) can also be observed on these figures. Figure 90-c (related to the control strategy 2, MEF-based fuel switch) shows that it is not possible to define an activation pattern for the gas boiler only considering the outdoor temperature. Similarly, other indicators were investigated (COP of the heat pump, temperature set-point in output of the heating system, load of the power system) and none of them on their own seemed to be sufficient to generate a simplified indicator.

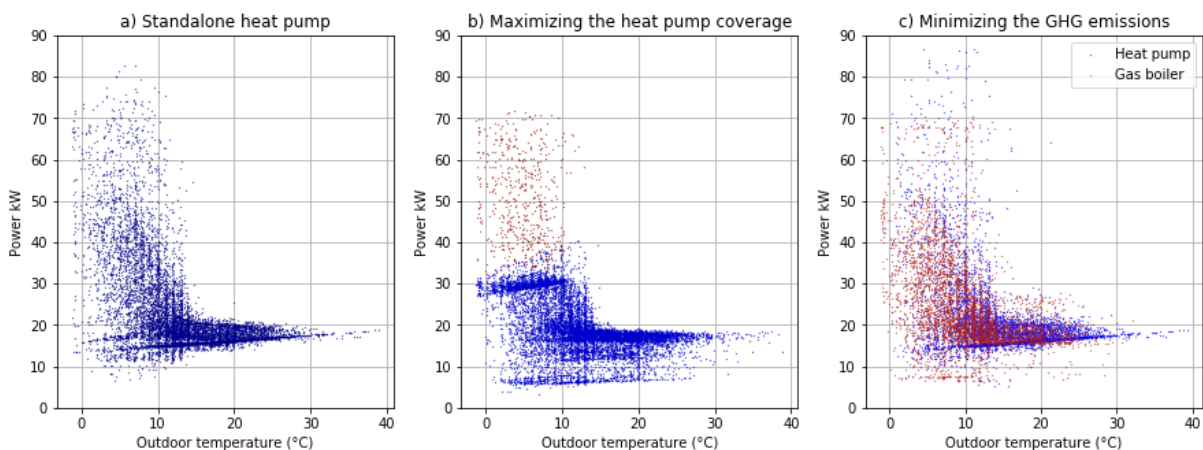


Figure 90: Heat generated by the heat pump and the gas boiler depending on the outdoor temperature for the reference case and the two control strategies (for one building in La Rochelle)

In conclusion, both control strategies avoid GHG emissions and improve the average performance of the heat pumps. Control strategy 2 avoids more GHG emissions but is more complex to implement than the control strategy prioritizing the heat pump.

5.6.2.Sensitivity of the results to the sizing of the heat pumps

In this section, the sensitivity to the sizing of the heat pumps is assessed. The marginal emissions of the hybrid heat pump fleet were then assessed for each control strategy for three different sizing of the heat pumps corresponding to 50%, 35% and 20% of the heat losses.

Figure 91 presents the share of the heating demand met by the heat pump for different heat pump sizing and the two control strategies. For the two control strategies, the proportion of the heating demand met by the heat pump decreases as the size of the heat pump decreases. The hybrid systems were sized to supply 120% of the heat losses considering the design temperature of the city, as well as the worst-case conditions for the performance of the heat pumps. However, such harsh conditions do not usually occur in a typical year and the heat pump can meet a large proportion of the heating demand, even if it is undersized. Indeed, its heating capacity increases with increased outdoor temperature. Consequently, the share of heating need met by the heat pump decreases only slightly between sizing to cover 120% and 50% of the heat losses. The decrease in the heat pump ratio is stronger for a sizing decreasing from 35% to 20%, as in this case the sizing is not enough to supply all the DHW demand. Such a tight sizing then affects the activation pattern throughout the year, not just during the coldest weeks of the year.

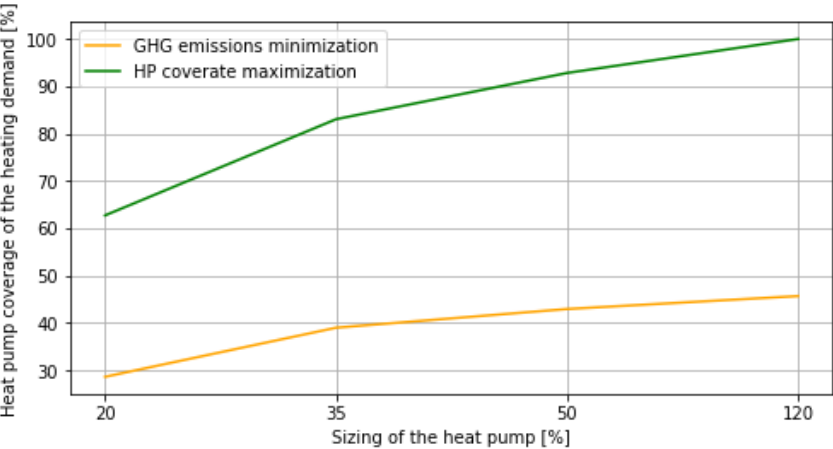


Figure 91: Share of the heating demand met by the heat pump for the two control strategies and depending on the sizing of the heat pump

Figure 92 presents the variation of the COP of the heat pumps for the two control strategies and the different heat pumps sizing. For both control strategies, the COP of the heat pump increases when the sizing of the heat pump decreases because the supply temperature of the heat pump is lower in case of saturation.

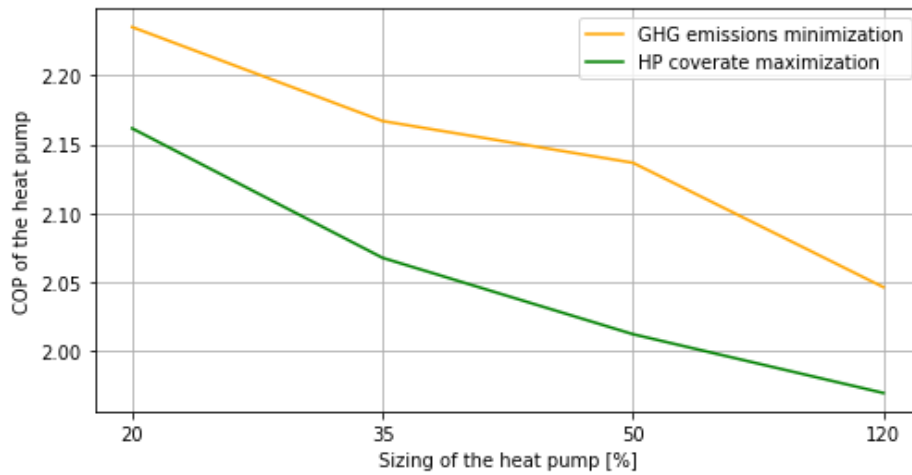


Figure 92: COP of the heat pump for the two control strategies and depending on the sizing of the heat pump

Figure 93 shows the variation of the MEF of the heat pump electricity consumption for the two control strategies and the different heat pumps sizing. For both control strategies, the MEF of the electricity consumption decreases when the sizing of the heat pump decreases.

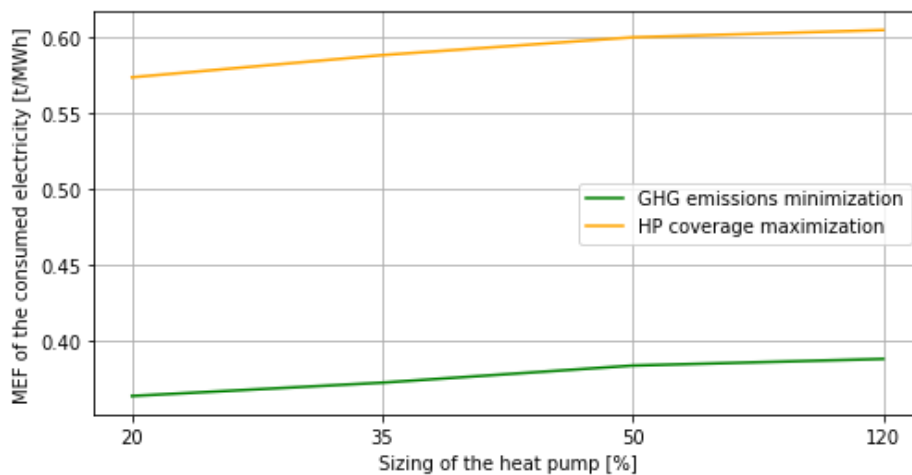


Figure 93: MEF of the consumed electricity by the heating system for the two control strategies and depending on the sizing of the heat pump

Figure 94 represents the emissions avoided by the decrease in the heat pump generation and the GHG emitted by the gas boiler for the two control strategies and the different heat pumps sizing. As in the previous part, the balance corresponds to the grey area that is not hatched. For the control strategy prioritizing the heat pump, the decrease of the sizing of the heat pumps increases the avoided GHG emissions. This can be explained by the decrease of the MEF of the electricity consumption and the improvement of the heat pump performances. For the MEF-based fuel switch, the GHG emissions avoided on the power system and the additional emissions from the gas boiler increase by a similar amount as the heat pump sizing decreases. Consequently, the change in the avoided emissions is not significant between the different sizing of heat pumps. It means that when the heat pump is undersized, the gas boiler is activated more often to help the heat pump, despite higher GHG emissions from the gas boiler. However, this is compensated by an improvement of the heat pump performance.

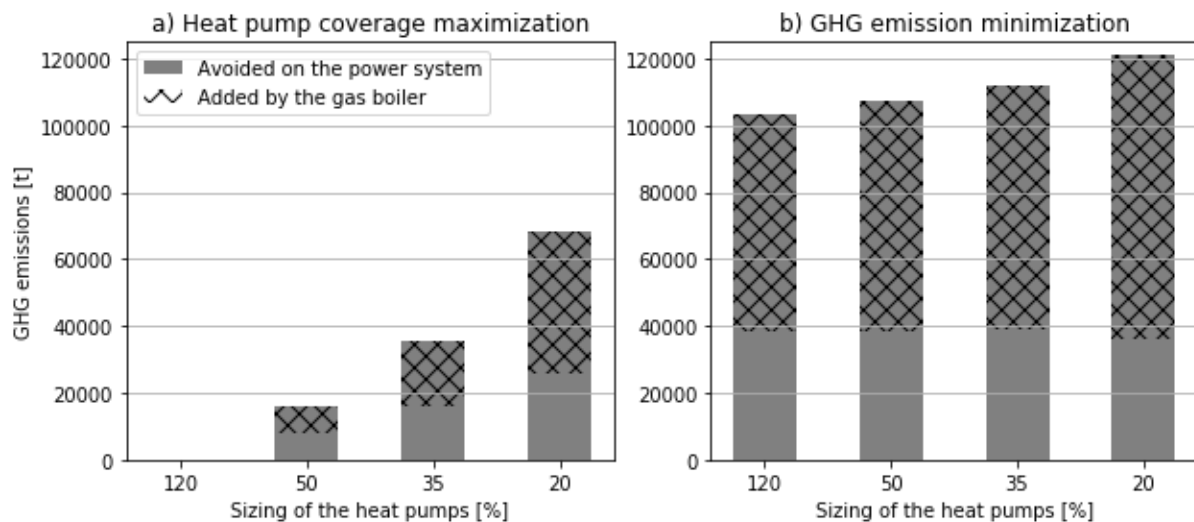


Figure 94: Balance of the GHG emissions for the two control strategies and the different sizing of the heat pumps

In conclusion, in case of a control strategy prioritizing the heat pump, the undersizing of the heat pumps increases the GHG emissions reductions. In case of the MEF-based fuel switch strategy, the sizing of the heat pumps has a limited impact on the avoided GHG emissions. In both cases, it can be interesting to undersize the heat pumps in terms of GHG emissions, but also to improve the performance of the heat pumps and reduce the installation costs.

### 5.6.3. Sensitivity of the results to the marginal emission factor of the electricity exchanges

In the previous sections, the evaluation of the impact of the control strategies based on the heat pump prioritization and on the MEF-based fuel switch showed a positive impact of the hybrid heat pumps. In this part, a parametric analysis is carried out on the MEF of the electricity exchanges. The service life of a heat pump is in the region of 15 years. This thesis should then investigate the interest of such control strategies for hybrid heat pumps until 2040.

The results of Section 5.6.1 (cf. Figure 88 and Figure 89) showed that the MEF of the electricity consumption in France is highly related to the MEF of the electricity exchanges. Currently, the flexibility of the interconnected power system is mainly provided by coal-fired power plants and OCGT located in other European countries. The installed capacity of such power plants should decrease rapidly over the next 15 years. Figure 95 shows the evolution of the mix for electricity generation in the French neighboring countries (ADEME 2018b). These results accounts for the following 13 European countries: Belgium, Germany, Luxembourg, the Netherlands, Austria, Czech Republic, Slovakia, Slovenia, Switzerland, Italy, Spain, Portugal and the UK. Until 2030, the installed capacities are based on the European Climate Foundation's technical and economic study on the future European power system (European Climate Foundation 2017). Beyond 2030, the expansion of the renewable electricity generation is based on the TYNDP 2018 Sustainable Transition scenario from ENTSO-E, assuming a quick development of renewable energy in Europe and thus optimistic regarding the decommitment of the fossil powerplants. From this figure, it can be observed that the share of fossil-fuel power plants is expected to decrease from 45% down to 15% by 2040.



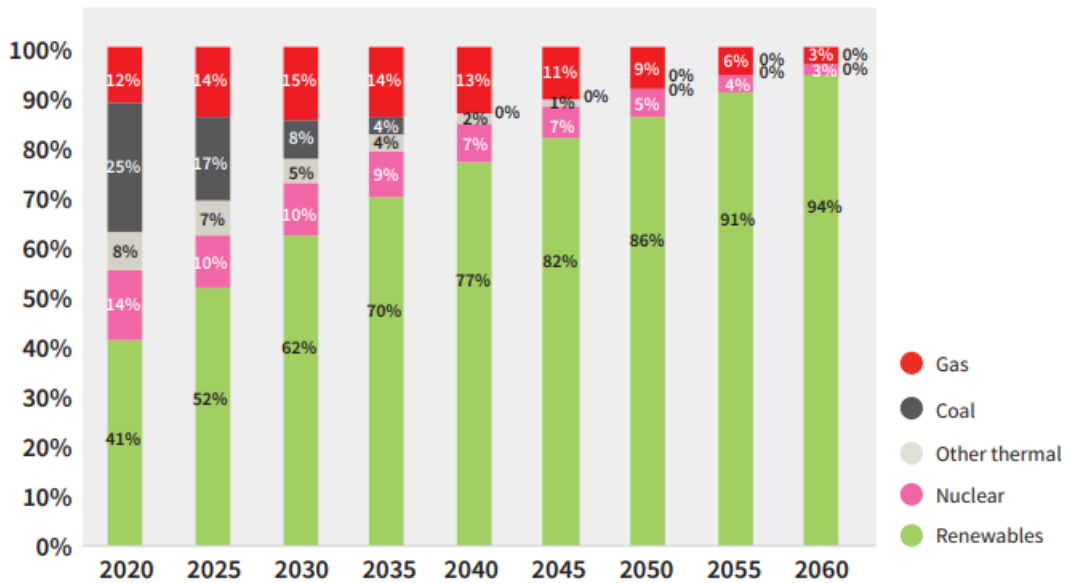


Figure 95: European production mix (outside of France) - CSC Scenario, from (ADEME 2018b)

In order to account for such changes in the electricity generation in Europe, the sensitivity of the hybrid heating system potential to the MEF of the electricity exchanges should be evaluated. In the next set of results, a parametric analysis is carried out on the MEF of the electricity exchanges:

- The original MEF for electricity exchanges, as calculated in Chapter 2;
- The modified MEF for electricity exchanges, reduced by 25% compared to the original MEF;
- The modified MEF for electricity exchanges, reduced by 50% compared to the original MEF.

Figure 96 presents the three time series considered for the MEF of the electricity exchanges. The reduction by 50% of the MEF of the exchanged electricity would correspond to the decommissioning of the OCGT, the coal- and oil-fired power plants, which is consistent with the electricity mixes for 2040 from Figure 95.

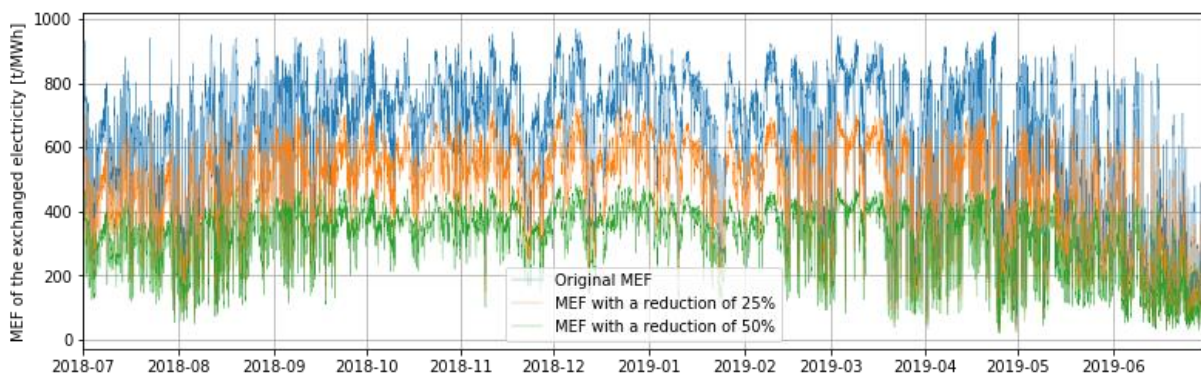


Figure 96: Scenarios for the MEF of the electricity exchange

Figure 97 represents the avoided emissions for the two control strategies, the four sizing of the heat pumps and three different time series for the MEF of the exchanged electricity. By applying a reduction by 25% on the MEF of the electricity exchange, all the evaluated configurations of hybrid heating

systems remain interesting. For a reduction by 50% on the MEF of the electricity exchanges, the avoided GHG emissions are strongly reduced and hybrid heating systems with heat pumps sized below 20% of the heat losses will emit more than the reference case. Considering such a decrease of the MEF in the interconnected countries, the interest of hybrid heating system is low regarding GHG emissions. Control strategies to provide more flexibility to the power grid would then be more useful. Therefore, although the previous section highlighted the interest of undersizing the heat pumps in hybrid systems, it could reduce the benefit in GHG emissions for future evolution of the European power system.

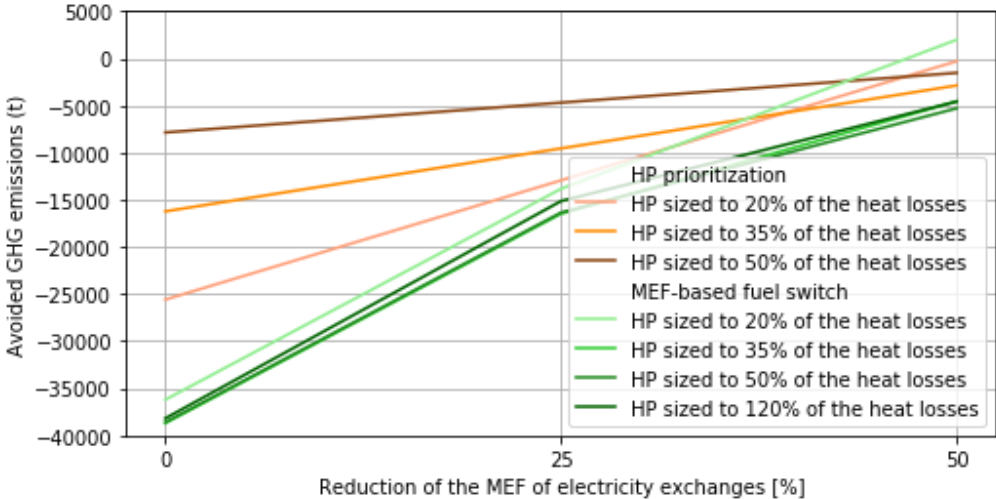


Figure 97: Avoided GHG emissions in comparison with the reference case for the two control strategies, the different sizing of the hybrid heat pumps and depending on the applied reduction of the MEF of the electricity exchanges

#### 5.6.4. Results for hybrid heat pumps installed in typical existing buildings

The installation costs of heat pumps are directly proportional to their size. Additionally, heat pumps experience degraded performance at lower loads. Hence, it is advisable to refrain from installing standalone heat pumps prior to retrofitting buildings with inefficient thermal envelopes. However, in the case of buildings heated with a gas boiler, a heat pump of appropriate size based on the anticipated thermal envelope resulting from the future retrofit can be incorporated into the existing heating system. Such a heating system should produce comparable results to the cases with undersized heat pumps. However, prior to retrofitting, the space heating demand should be higher than in a recent building, while the DHW demand should remain similar. This implies that the average COP of the heat pump and consequently the MEF of the space heating using the heat pump should be better than that of a new house.

### 5.7. Conclusion

Two control strategies were developed for the hybrid heating systems. In the traditional control strategy (prioritizing the heat pump), the boiler is activated only when the heat pump cannot meet the demand. An alternative strategy (MEF-based fuel switch) consists of switching between the heat pump and the gas boiler based on the MEF of the heating system. The influence of these control strategies on the GHG emissions was evaluated for different sizing of the heat pump and of the gas boiler using the models previously presented. For the comparison, a reference heating systems with standalone heat pumps was also evaluated. Between July 2018 and June 2019, 3 000 hybrid heating systems

providing heat for 100 000 dwellings would have avoided 38 000 tons of CO<sub>2eq</sub> with heat pumps sized to 120% of design losses. The avoided emissions remain similar in the case of a heat pump sized to 50% of the heat losses, which reduces the installation cost such system. The traditional control strategy with heat pumps sized to supply 50% of the heat losses would have avoided 8 000 tons of CO<sub>2eq</sub>. However, the avoided emissions are highly correlated with the MEF of the electricity exchanges, which could strongly decrease in the coming years. Considering a MEF for the exchanges reduced by 50%, the avoided emissions in the case of a heat pump sized to 120% of design losses falls down to 5 000 tons of CO<sub>2eq</sub>. In the future, hybrid heating systems with heat pumps sized below 20% of the heat losses could emit more GHG than standalone heat pumps. It should be noted that these results are based on the technical data available for the actual commercial heat pumps. In the future, the performance of heat pumps might improve and lead to a reduction of the GHG emissions of these systems.

## 6. Conclusion

### 6.1. Summary

In France, space heating emits 75 million tons of CO<sub>2eq</sub> annually, accounting for approximately 15% of total emissions. By providing demand-side flexibility without any service interruption, hybrid heating systems can foster the integration of non-dispatchable renewable energies into the power grid and avoid greenhouse gas (GHG) emissions from carbonized electricity production. In this thesis, the control of hybrid heat pumps (heat pumps coupled with gas boilers) supplied alternatively with electricity or with gas was considered. The main application for these systems has usually been the undersizing of the heat pump to improve the performance and reduce the installation costs. Alternative control strategies can be developed based on indicators related to the power system. The aim of this thesis was to develop a control strategy to minimize the GHG emissions from the heating demand of residential buildings.

First, a model of the French power system was developed to evaluate the impact of different demand-side management strategies on the GHG emissions by deriving a marginal emission factor. A unit-commitment and economic dispatch model was developed based on two calibrated merit-orders to reproduce the daily and intra-day dynamics, including the conservation of hydroelectric energy and the electricity exchanges with the European grid. A simplified approach based on linear regressions between the GHG emissions and the variation of the dispatchable electricity generation was developed to evaluate the marginal emission factor of the electricity generation in the other European countries. Finally, the French power system model coupled with the marginal emission factor of the electricity exchanges and of the national power plants provided a tool to assess the GHG emissions resulting from different electricity demand patterns. A first evaluation showed that the marginal mix responding to demand response events was strongly depending on the season and the time of the week on which the time event is occurring as well as the duration of the event.

Secondly, a model was developed for a fleet of hybrid heat pumps installed in France to evaluate different control strategies at the building and aggregated levels. To simulate the electricity and gas consumption of such a fleet, an urban energy model was developed to generate the space heating and domestic hot water demand of 100 000 dwellings throughout France. A district archetype of 300+ dwellings was modelled using Dymola. In addition, the hybrid production, storage and distribution systems were modelled at the building level, including the variation of the production efficiency and the low-level controllers. The district archetype was simulated in seven cities representative of the French climate zones to obtain a representative heating demand on a national scale.

Finally, two control strategies and three sizing cases were developed for the hybrid heating systems. In the traditional control strategy (prioritizing the heat pump), the boiler is only activated when the heat pump cannot provide the required heat. An alternative strategy (switching fuel based on the GHG emissions of electricity) consists of alternating between the heat pump and the gas boiler based on the marginal emission factor of the heating system. The influence of these control strategies on the GHG emissions was evaluated for different sizing of the heat pumps and the gas boilers using the models presented previously. For the comparison, a reference heating system with standalone heat pumps was also evaluated. Between July 2018 and June 2019, 30 000 hybrid heating systems providing heat for 100 000 dwellings would have avoided 38 000 tons of CO<sub>2eq</sub> with heat pumps sized to supply the total demand (corresponding to a reduction of 0.38 tons of CO<sub>2eq</sub> per dwelling). The avoided emissions remain similar in the case of a heat pump sized to supply 50% of the heat losses, which is an interesting solution to reduce the installation cost of the system. The traditional control strategy with

heat pumps sized to supply 50% of the heat losses would avoid 8 000 tons of CO<sub>2eq</sub>. However, it should be noted that the avoided emissions of hybrid systems are highly correlated with the marginal emission factor of the electricity exchanges with the European grid, which could decrease significantly in the coming years. If the marginal emission factor of the exchanges is reduced by 50%, the avoided emissions in the case of a heat pump sized to supply the total demand drops down to 5 000 tons of CO<sub>2eq</sub>. Hybrid heating systems with heat pumps sized below 35% of the heat losses would even emit more GHG than standalone heat pumps. As a conclusion, the results show the interest of hybrid heating systems to participate in the energy transition and alternative control strategies can be proposed for hybrid systems to reduce GHG emissions.

## 6.2. Thesis contribution

The thesis mainly contributed to two research topics, namely the evaluation of Marginal Emission Factors (MEF) of power systems and the evaluation of innovative control strategies for a fleet of hybrid heating systems.

To evaluate marginal technologies, a new method was developed and validated to model the Unit-Commitment and Economic Dispatch (UCED) problem based on two calibrated merit-orders and including hydroelectric energy conservation, the availability of power plants, realistic daily and intra-day dynamics and electricity exchanges. In the literature, few national models incorporate electricity exchanges. Moreover, the validation of such models is rarely addressed. The validation showed that the national scale, including interconnections, remains relevant for modelling power systems even though they are increasingly interconnected. Specific developments have also been carried out to improve the evaluation of the MEF of the electricity exchanges with interconnected countries. An existing model has been extended to include water reserve conservation for hydropower generation, improving the accuracy of the results. Many studies evaluate MEF, but often neglect some of the power system constraints mentioned above. In future work, the methodologies presented in this thesis could be used for other countries and other case-studies.

Regarding the control of hybrid heating systems, the literature review performed in the introduction to this thesis highlighted a gap in the studies. The few studies evaluating the GHG emissions from hybrid heat pumps are generally not considering the impact of the control strategies and are often evaluating a single hybrid system. Moreover, such systems are rarely controlled by a signal providing the marginal GHG emissions of the avoided electricity production and few studies have investigated this point in details. By assessing the impact of the control of a state-wide fleet of hybrid heat pumps, this thesis addresses this gap and highlighted the influence of the sizing and control of such systems. Moreover, the UBEM model developed can be adapted to analyze other heating systems, other DSM strategies, or assess other indicators (such as flexibility, cost, acceptance).

## 6.3. Future work

Additional work could improve the different models developed in this thesis:

- In this work, the MEF of the electricity generation in France is assessed based on a UCED model, but this is not the case for the MEF of the interconnected power systems. Such an approximation is accurate enough for the purposes of this thesis. However, the model could be improved by developing semi-physical models for the interconnected countries, which was not feasible for this work. For this purpose, the preprocessing steps of the model development

(e.g. clustering of the technologies groups) could be automated and applied for each power system in Europe.

- With regard to the modelling of the heating demand, further work can be considered to avoid the synchronization effect at the national scale, especially outside the heating season. This artefact of simulation can be explained by the synchronization of the heating up of the DHW tank and of the dwellings in the morning. The synchronization of the space heating and DHW production could be solved by shifting the schedules between the heating systems and by more diversity in the sizing. Regarding the DHW model, different settings could also be tested in the temperature set points for the hysteresis controlling the DHW tank to evaluate its effect on both the synchronization and the overall performance of the heat pump. In summary, most of the efforts to generate diversity were focused on the demand-side of the model and not on the heat generation.
- In this thesis, the marginal emissions of hybrid heating systems providing both space heating and DHW were evaluated. However, it could have been interesting to evaluate other configurations such as a heat pump sized for DHW combined with an additional heat pump providing heat for space heating only. Such a configuration would probably be more expensive, but would improve the performance of the heating system by limiting the space heating generation at 55°C.

Other research directions can also be identified in the evaluation of hybrid heating systems. The impact of the control strategies was only evaluated for a year with one configuration of the French and interconnected power systems and only considering interactions between the domestic heating demand and the power system. This thesis demonstrated the benefit of hybrid heating systems for the decarbonization of the heating demand, however complementary analysis should be considered before the integration of hybrid heating systems in the French energy system:

- To consider the future change in the European grid (decarbonization of the electricity generation), the sensitivity of the results to the MEF of the electricity exchanges was evaluated. This parametric analysis of the MEF of the electricity exchanges indicated that such systems should remain useful during the entire lifetime of hybrid systems. Further work can be considered to evaluate more accurately the evolution of the French and European power systems within the two next decades. With the increase of the share of the non-dispatchable electricity generation in Europe, the power systems interconnected with France might become less flexible. In such a scenario, the French power system will probably rely on a larger part on the national flexibility and hybrid heating systems will probably be more interesting for providing flexibility rather than for reducing GHG emissions.
- Such an analysis should be completed with 15 years multi-energy scenario considering hybrid heating systems and alternative solutions (e.g. thermal storage, batteries, thermal solar systems...). The benefit of hybrid systems regarding other criteria (cost, system autonomy, flexibility needs, social acceptance...) could then be assessed and compared with other solutions providing flexibility. Such an analysis would require the development of a capacity expansion model to analyze the impact of the installation of such systems on the planning of the French power system (installation and decommitment of units, change on the grid, need for flexibility).
- This thesis focused on the GHG emissions of the heating system, in collective heating controlled by an activation signal coming from an aggregator. Business models are missing to ensure the profitability and consequently the acceptance of such systems. Further development is also needed to develop a reliable and transparent GHG signal, that could be transmitted to such decentralized devices.

- This thesis focused on the benefit of hybrid heating systems for multi-family residential buildings. A similar study could be conducted regarding the industrial heating demand. Hybridization in industry could be a major advantage in an energy system where flexibility is essential and where industrial processes are difficult to stop and restart.

As a general conclusion of the thesis, many discussions are taking place in France as well as in other European countries about the future energy mix. In addition to the reduction of the GHG emissions, hybrid heating systems provide a quick and efficient solution to provide flexibility to the power system as gas boiler can be activated within a minute. Moreover, the infrastructure for the distribution of the natural gas already exists and does not entail any infrastructure costs compared to the power grid that needs to be reinforced to face the electrification of many energy uses. This thesis brought tools and preliminary answers regarding GHG emissions, and further work should investigate these questions related to the cost effectiveness, the robustness of the solution, the social acceptance, etc.

## References

- ADEME. 2018a. *Climat Air et Energie Chiffres-Clés*.
- . 2018b. 'Evolution Trajectories French Electricity Mix 2020-2060 Study Summary'.
- . 2020. 'Centre de Ressources Sur Les Bilans de Gaz à Effet de Serre'. 2020. <https://www.bilans-ges.ademe.fr/>.
- . 2021. 'Transition(s) 2050'.
- Aditya, Gregorius Riyan, and Guillermo A. Narsilio. 2020. 'Environmental Assessment of Hybrid Ground Source Heat Pump Systems'. *Geothermics* 87 (May): 101868. <https://doi.org/10.1016/j.geothermics.2020.101868>.
- AFNOR. 2004. *NF EN 12831 Systèmes de Chauffage Dans Les Bâtiments - Méthode de Calcul Des Déperditions Calorifiques de Base*. France.
- Annex 50. 2023. 'Solution Matrix'. 2023. <https://heatpumpingtechnologies.org/annex50/solution-matrix/>.
- atlantic. 2022. 'Guide de Saisie RE 2020 de La Solution Chaufferie Hybride Par Usage EFFIPAC Chauffage Hybride'.
- atlantic Guillot. 2022. 'Ballons Stockage Primaire, Production et Stockage d'eau Chaude Sanitaire et Enr'.
- Beccali, Marco, Marina Bonomolo, Francesca Martorana, Pietro Catrini, and Alessandro Buscemi. 2022. 'Electrical Hybrid Heat Pumps Assisted by Natural Gas Boilers: A Review'. *Applied Energy* 322 (July): 119466. <https://doi.org/10.1016/j.apenergy.2022.119466>.
- Bennett, George, Stephen Watson, Grant Wilson, and Tadj Oreszczyn. 2022. 'Domestic Heating with Compact Combination Hybrids (Gas Boiler and Heat Pump): A Simple English Stock Model of Different Heating System Scenarios'. *Building Services Engineering Research and Technology* 43 (2): 143–59. <https://doi.org/10.1177/01436244211040449>.
- Bettle, R, C H Pout, and E R Hitchin. 2006. 'Interactions between Electricity-Saving Measures and Carbon Emissions from Power Generation in England and Wales'. *Energy Policy* 34: 3434–46. <https://doi.org/10.1016/j.enpol.2005.07.014>.
- Bialek, J. 1996. 'Tracing the Flow of Electricity'. *IEE Proceedings: Generation, Transmission and Distribution* 143 (4): 313–20. <https://doi.org/10.1049/ip-gtd:19960461>.
- Boesten, Stef. 2018. 'Business Models for Fuel-Shift Technology in Heat and Electricity Smart Grids', no. September.
- Braeuer, Fritz, Rafael Finck, and Russell McKenna. 2020. 'Comparing Empirical and Model-Based Approaches for Calculating Dynamic Grid Emission Factors: An Application to CO2-Minimizing Storage Dispatch in Germany'. *Journal of Cleaner Production* 266: 121588. <https://doi.org/10.1016/j.jclepro.2020.121588>.
- Broekhoff, Derik. 2005. 'The Greehhouse Gas Protocol Guidelines for Quantifying GHG Reductions from Grid-Connected Electricity Projects'. <http://www.wri.org/publication/guidelines-quantifying-ghg-reductions-grid-connected-electricity-projects>.
- BSI. 2019. 'BSI Standards Publication Energy Performance of Buildings — Ventilation for Buildings'. *British Standards Institution*. <https://doi.org/10.3403/BSEN16798>.



- Cany, C, C Mansilla, G Mathonni, and P da Costa. 2018. 'Nuclear Power Supply : Going against the Misconceptions . Evidence of Nuclear Flexibility from the French Experience' 151: 289–96. <https://doi.org/10.1016/j.energy.2018.03.064>.
- Cany, Camille. 2017. 'Interactions Entre Énergie Nucléaire et Énergies Renouvelables Variables Dans La Transition Énergétique En France : Adaptations Du Parc Électrique Vers plus de Flexibilité, Doctoral Thesis'. Université Paris-Saclay. <https://tel.archives-ouvertes.fr/tel-01509918/>.
- Carli, Inc. 2006. 'TARCOG: Mathematical Models for Calculation of Thermal Performance of Glazing Systems with or without Shading Devices'.
- Casella, Francesco. 2015. 'Simulation of Large-Scale Models in Modelica: State of the Art and Future Perspectives'. *Proceedings of the 11th International Modelica Conference, Versailles, France, September 21-23, 2015* 118: 459–68. <https://doi.org/10.3384/ecp15118459>.
- Cebulla, F, and T Fichter. 2017. 'Merit Order or Unit-Commitment : How Does Thermal Power Plant Modeling Affect Storage Demand in Energy System Models ?' *Renewable Energy* 105: 117–32. <https://doi.org/10.1016/j.renene.2016.12.043>.
- Clauß, John, Sebastian Stinner, Christian Solli, Karen Byskov Lindberg, Henrik Madsen, and Laurent Georges. 2019. 'Evaluation Method for the Hourly Average CO<sub>2</sub>eq. Intensity of the Electricity Mix and Its Application to the Demand Response of Residential Heating'. *Energies* 12 (7): 1–25. <https://doi.org/10.3390/en12071345>.
- Clegg, Stephen, and Pierluigi Mancarella. 2019. 'Integrated Electricity-Heat-Gas Modelling and Assessment, with Applications to the Great Britain System. Part II: Transmission Network Analysis and Low Carbon Technology and Resilience Case Studies'. *Energy* 184: 191–203. <https://doi.org/10.1016/j.energy.2018.02.078>.
- Connolly, D., H. Lund, B. V. Mathiesen, and M. Leahy. 2010. 'A Review of Computer Tools for Analysing the Integration of Renewable Energy into Various Energy Systems'. *Applied Energy* 87 (4): 1059–82. <https://doi.org/10.1016/j.apenergy.2009.09.026>.
- Corradi, Olivier. 2018. 'Estimating the Marginal Carbon Intensity of Electricity with Machine Learning'. <https://www.Tmrow.Com/Blog/Marginal-Carbon-Intensity-of-Electricity-with-Machine-Learning/>. 2018.
- COSTIC. 2016. 'Guide Technique Les Besoins d'eau Chaude Sanitaire En Habitat Individuel et Collectif'.
- . 2019. 'Le Dimensionnement Des Systèmes de Production d'eau Chaude Sanitaire En Habitat Individuel et Collectif'.
- D'Ettorre, Francesco, Mattia De Rosa, P. Conti, Daniele Testi, and D. Finn. 2019. 'Mapping the Energy Flexibility Potential of Single Buildings Equipped with Optimally-Controlled Heat Pump, Gas Boilers and Thermal Storage'. *Sustainable Cities and Society* 50 (December 2018): 101689. <https://doi.org/10.1016/j.scs.2019.101689>.
- Dassault Systèmes. 2021. 'Dymola Dynamic Modeling Laboratory Full User Manual'.
- . 2023. 'Dymola'. 2023. <https://www.3ds.com/fr/produits-et-services/catia/produits/dymola/>.
- data.gouv.fr. 2020. 'Observatoire Des Performances Énergétiques (OPE)'. 2020. <https://www.data.gouv.fr/fr/datasets/observatoire-des-performances-energetiques/>.
- Delarue, E, D Cattrysse, and W D'Haeseleer. 2013. 'Enhanced Priority List Unit Commitment Method for Power Systems with a High Share of Renewables'.

- Delarue, Erik. 2009. 'Modeling Electricity Generation Systems Development and Application of Electricity Generation Optimization and Simulation Models, with Particular Focus on CO2 Emissions, Doctoral Thesis'. Katholieke Universiteit Leuven. [http://www.mech.kuleuven.be/en/tme/research/energy\\_environment/Pdf/WPEN2009-014](http://www.mech.kuleuven.be/en/tme/research/energy_environment/Pdf/WPEN2009-014).
- Delarue, Erik, and William D'haeseleer. 2008. 'Adaptive Mixed-Integer Programming Unit Commitment Strategy for Determining the Value of Forecasting'. *Applied Energy* 85: 171–81. <https://doi.org/10.1016/j.apenergy.2007.07.007>.
- Department of Development and Planning Aalborg University. 2022. 'EnergyPLAN'. 2022. <https://www.energyplan.eu/>.
- Ecoinvent. 2013. 'Ecoinvent Database 3.0'. 2013. <https://ecoinvent.org/the-ecoinvent-database/data-releases/ecoinvent-3-0/>.
- Eggimann, Sven, Natasa Vulic, Martin Rüdüsüli, Robin Mutschler, Kristina Orehounig, and Matthias Sulzer. 2022. 'Spatiotemporal Upscaling Errors of Building Stock Clustering for Energy Demand Simulation'. *Energy and Buildings* 258: 111844. <https://doi.org/10.1016/j.enbuild.2022.111844>.
- Eggimann, Sven, Michael Wagner, Yoo Na Ho, Mirjam Züger, Ute Schneider, and Kristina Orehounig. 2021. 'Geospatial Simulation of Urban Neighbourhood Densification Potentials'. *Sustainable Cities and Society* 72 (April): 103068. <https://doi.org/10.1016/j.scs.2021.103068>.
- Ekvall, Thomas. 2019. 'Attributional and Consequential Life Cycle Assessment'. In *Sustainability Assessment at the 21st Century*. IntechOpen. <https://doi.org/10.5772/intechopen.89202>.
- Elkraft System, Risø National Laboratory, AKF Institute of Local Government Studies, Stockholm Environment Institute, Institute of Physical Energetics, Lithuanian Energy Institute, PSE International, and Kaliningrad State University. 2001. 'Balmorel: A Model for Analyses of the Electricity and CHP Markets in the Baltic Sea Region'. <http://www.balmorel.com/>.
- Enedis. 2019. 'Bilan Electrique Enedis 2018'.
- ENEDIS. 2020. 'Données de Température et de Pseudo-Rayonnement En J+2'. 2020. <https://data.enedis.fr/explore/dataset/donnees-de-temperature-et-de-pseudo-rayonnement/information/>.
- Energy, Advanced, Systems Analysis, and Computer Model. 2019. 'EnergyPLAN'.
- Entchev, Evgueniy, Libing Yang, Mohamed Ghorab, Antonio Rosato, and Sergio Sibilio. 2018. 'Energy, Economic and Environmental Performance Simulation of a Hybrid Renewable Microgeneration System with Neural Network Predictive Control'. *Alexandria Engineering Journal* 57 (1): 455–73. <https://doi.org/10.1016/j.aej.2016.09.001>.
- ENTSOE. 2020. 'Transparency Platform'. 2020. <https://transparency.entsoe.eu/>.
- . 2022. 'Transparency Platform'. 2022. <https://transparency.entsoe.eu/>.
- European Climate Foundation. 2017. 'CLEANER , SMARTER , CHEAPER Responding to Opportunities in Europe's Changing Energy System'.
- Expert Bâti Conseil. 2022. 'Les Zones Climatiques En France- H1, H2 Ou H3'. 2022. <https://expert-bati-conseil.fr/rt-2012-re-2020/les-zones-climatiques-en-france-h1-h2-ou-h3/>.
- Ferrando, Martina, Francesco Causone, Tianzhen Hong, and Yixing Chen. 2020. 'Urban Building Energy Modeling ( UBE M ) Tools : A State-of-the-Art Review of Bottom-up Physics-Based Approaches'. *Sustainable Cities and Society* 62 (June): 102408. <https://doi.org/10.1016/j.scs.2020.102408>.

- Flatabø, Nils, Arne Haugstad, Birger Mo, and Olav B Fosso. 1998. 'Short-Term and Medium-Term Generation Scheduling in the Norwegian Hydro System under a Competitive Power Market Structure'. In *VIII SEPOPE, Brazilia, 2002*, 1–18.
- Fleschutz, Markus, Markus Bohlayer, Marco Braun, Gregor Henze, and Michael D. Murphy. 2021. 'The Effect of Price-Based Demand Response on Carbon Emissions in European Electricity Markets: The Importance of Adequate Carbon Prices'. *Applied Energy* 295 (November 2020): 117040. <https://doi.org/10.1016/j.apenergy.2021.117040>.
- Frapin, Marie, Charlotte Roux, Edi Assoumou, and Bruno Peuportier. 2021. 'Modelling Long-Term and Short-Term Temporal Variation and Uncertainty of Electricity Production in the Life Cycle Assessment of Buildings'. *Applied Energy*, no. February: 118141. <https://doi.org/10.1016/j.apenergy.2021.118141>.
- Fraunhofer ISE. 2021. 'Wege Zu Einem Klimaneutralen Energiesystem: Update Klimaneutralität 2045'.
- Garreau, Enora, Yassine Abdelouadoud, Eunice Herrera, Werner Keilholz, G. E. Kyriakodis, Vincent Partenay, and Peter Riederer. 2021. 'District MODeller and SIMulator (DIMOSIM) – A Dynamic Simulation Platform Based on a Bottom-up Approach for District and Territory Energetic Assessment'. *Energy and Buildings* 251: 111354. <https://doi.org/10.1016/j.enbuild.2021.111354>.
- Goy, Solène, Volker Coors, and Donal Finn. 2021. 'Grouping Techniques for Building Stock Analysis: A Comparative Case Study'. *Energy and Buildings* 236. <https://doi.org/10.1016/j.enbuild.2021.110754>.
- Gupta, Ankit, Matthew Davis, and Amit Kumar. 2021. 'An Integrated Assessment Framework for the Decarbonization of the Electricity Generation Sector'. *Applied Energy* 288 (August 2020): 116634. <https://doi.org/10.1016/j.apenergy.2021.116634>.
- Hawkes, A D. 2010. 'Estimating Marginal CO<sub>2</sub> Emissions Rates for National Electricity Systems'. *Energy Policy* 38 (10): 5977–87. <https://doi.org/10.1016/j.enpol.2010.05.053>.
- Heggarty, Thomas. 2021. 'Techno-Economic Optimisation of the Mix of Power System Flexibility Solutions'. Université Paris sciences et lettres.
- Heggarty, Thomas, Jean Yves Bourmaud, Robin Girard, and Georges Kariniotakis. 2020. 'Quantifying Power System Flexibility Provision'. *Applied Energy* 279 (August): 115852. <https://doi.org/10.1016/j.apenergy.2020.115852>.
- Heinen, Steve, Daniel Burke, and Mark O'Malley. 2016. 'Electricity, Gas, Heat Integration via Residential Hybrid Heating Technologies - An Investment Model Assessment'. *Energy* 109: 906–19. <https://doi.org/10.1016/j.energy.2016.04.126>.
- Heinen, Steve, and Mark O'Malley. 2015. 'Power System Planning Benefits of Hybrid Heating Technologies'. *2015 IEEE Eindhoven PowerTech, PowerTech 2015*. <https://doi.org/10.1109/PTC.2015.7232421>.
- Huang, Jiangyi, and Arturs Purvins. 2020. 'Validation of a Europe-Wide Electricity System Model for Techno-Economic Analysis'. *Electrical Power and Energy Systems* 123 (June): 106292. <https://doi.org/10.1016/j.ijepes.2020.106292>.
- Huber, Julian, Kai Lohmann, Marc Schmidt, and Christof Weinhardt. 2021. 'Carbon Efficient Smart Charging Using Forecasts of Marginal Emission Factors'. *Journal of Cleaner Production* 284: 124766. <https://doi.org/10.1016/j.jclepro.2020.124766>.
- Huo, Yuchong, François Bouffard, and Géza Joós. 2022. 'Integrating Learning and Explicit Model

- Predictive Control for Unit Commitment in Microgrids'. *Applied Energy* 306 (PA): 118026. <https://doi.org/10.1016/j.apenergy.2021.118026>.
- IAEA. 2018. 'Non-Baseload Operation in Nuclear Power Plants: Load Following and Frequency Control Modes of Flexible Operation'. *IAEA Nuclear Energy Series*, 1–190. <http://www.iaea.org/Publications/index.html>.
- . 2020. 'Operational & Long-Term Shutdown Reactors'. 2020. <https://pris.iaea.org/PRIS/WorldStatistics/OperationalReactorsByType.aspx>.
- Insee. 2021. 'Logement En 2018'. 2021. <https://www.insee.fr/fr/statistiques/5650749>.
- INSEE. 2010. 'Enquête Emploi Du Temps. 2009-2010 / Enquête Couples - Familles – Ménages.'
- Johra, Hicham, and Per Heiselberg. 2017. 'Influence of Internal Thermal Mass on the Indoor Thermal Dynamics and Integration of Phase Change Materials in Furniture for Building Energy Storage : A Review'. *Renewable and Sustainable Energy Reviews* 69 (September 2015): 19–32. <https://doi.org/10.1016/j.rser.2016.11.145>.
- Klein, K, K Huchtemann, and D Müller. 2014. 'Numerical Study on Hybrid Heat Pump Systems in Existing Buildings'. *Energy & Buildings* 69: 193–201. <https://doi.org/10.1016/j.enbuild.2013.10.032>.
- Künle, Eglantine. 2018. 'Incentives to Value the Dispatchable Fleet's Operational Flexibility across Energy Markets, Doctoral Thesis'. Clausthal University of Technology.
- Langer, Sarka, Olivier Ramalho, Mickaël Derbez, Jacques Ribéron, Severine Kirchner, and Corinne Mandin. 2016. 'Indoor Environmental Quality in French Dwellings and Building Characteristics'. *Atmospheric Environment* 128: 82–91. <https://doi.org/10.1016/j.atmosenv.2015.12.060>.
- Li, Gang, and Yuqing Du. 2018. 'Performance Investigation and Economic Benefits of New Control Strategies for Heat Pump-Gas Fired Water Heater Hybrid System'. *Applied Energy* 232 (September): 101–18. <https://doi.org/10.1016/j.apenergy.2018.09.065>.
- Lochinvar. 2023. 'KNIGHT XL Efficiency Curves'. 2023.
- Martinez, S., M. Vellei, and J. Le Dréau. 2021. 'Demand-Side Flexibility in a Residential District: What Are the Main Sources of Uncertainty?' *Energy and Buildings*, no. xxxx: 111595. <https://doi.org/10.1016/j.enbuild.2021.111595>.
- Masson-Delmotte, V., P. Zhai, A. Pirani, S.L., J.B.R. Connors, C. Péan, S. Berger, N. Caud, Y. Chen, L. Goldfarb, M.I. Gomis, M. Huang, K. Leitzell, E. Lonnoy, and and B. Zhou (eds.) Matthews, T.K. Maycock, T. Waterfield, O. Yelekçi, R. Yu. 2021. 'IPCC, 2021: Climate Change 2021: The Physical Science Basis. Contribution of Working Group I to the Sixth Assessment Report of the Intergovernmental Panel on Climate Change'. <https://doi.org/10.1017/9781009157896>.
- Mckenna, Eoghan, and Sarah J Darby. 2017. 'How Much Could Domestic Demand Response Technologies Reduce CO2 Emissions ?' *ECEEE on Consumption, Efficiency and Limits*, no. January 2017: 337–47. <http://proceedings.eceee.org/visabstrakt.php?event=7&doc=2-107-17%0Ahttps://ora.ox.ac.uk/objects/uuid:21036010-5422-4de9-9650-e8759f6825b5>.
- Ministère de la transition écologique et solidaire. 2019. 'Synthèse Stratégie Française Pour l'énergie et Le Climat Programmation Pluriannuelle de l'énergie'.
- Ministère de la Transition Energétique. 2022. *Arrêté Du 20 Juillet 2022 Modifiant Certaines Dispositions Relatives Aux Contrôles Dans Le Cadre Du Dispositif Des Certificats d'économies d'énergie et La Fiche d'opération Standardisée BAR-TH-159*. <https://www.legifrance.gouv.fr/download/file/5gAfOAZyNglh7Fm->

Ar17lqv2XwHvYu92ldliBeWQ\_tw=/JOE\_TEXTE.

- Ministère de la transition énergétique. 2023. 'Bilan Énergétique de La France 2021'.
- Ministry for the ecological and solidarity transition. 2020. 'National Low Carbon Strategy', no. March.
- Modelica Association. 2023. 'Modelica.Org'. 2023. <https://modelica.org/>.
- Moradi, Saeed, Sohrab Khanmohammadi, Mehrdad Tarafdar Hagh, and Behnam Mohammadi-ivatloo. 2015. 'A Semi-Analytical Non-Iterative Primary Approach Based on Priority List to Solve Unit Commitment Problem'. *Energy* 88: 244–59. <https://doi.org/10.1016/j.energy.2015.04.102>.
- Morales-España, Germán, Rafael Martínez-Gordón, and Jos Sijm. 2022. 'Classifying and Modelling Demand Response in Power Systems'. *Energy* 242 (January 2022): 122544. <https://doi.org/10.1016/j.energy.2021.122544>.
- Morilhat, Patrick, Stéphane Feutry, Christelle Le Maitre, and Jean-Melaine Favennac. 2019. 'Nuclear Power Plant Flexibility at EDF'.
- Murray, Portia, Julien Marquant, Mathias Niffeler, Georgios Mavromatidis, and Kristina Orehoung. 2020. 'Optimal Transformation Strategies for Buildings, Neighbourhoods and Districts to Reach CO2 Emission Reduction Targets'. *Energy and Buildings* 207: 109569. <https://doi.org/10.1016/j.enbuild.2019.109569>.
- Nouidui, Thierry Stephane, Kaustubh Phalak, Wangda Zuo, and Michael Wetter. 2012. 'Validation and Application of the Room Model of the Modelica Buildings Library'. *Proceedings of the 9th International MODELICA Conference, September 3-5, 2012, Munich, Germany* 76 (January 2019): 727–36. <https://doi.org/10.3384/ecp12076727>.
- Patteeuw, Dieter, Kenneth Bruninx, Alessia Arteconi, Erik Delarue, William D'haeseleer, and Lieve Helsen. 2015. 'Integrated Modeling of Active Demand Response with Electric Heating Systems Coupled to Thermal Energy Storage Systems'. *Applied Energy* 151: 306–19. <https://doi.org/10.1016/j.apenergy.2015.04.014>.
- Péan, Thibault, Ramon Costa-castelló, Jaume Salom, Institut De Recerca, De Catalunya Irec, Jardins De, Dones De Negre, Sant Adrià, and De Besòs Barcelona. 2019. 'Price and Carbon-Based Energy Flexibility of Residential Heating and Cooling Loads Using Model Predictive Control'. *Sustainable Cities and Society* 50 (April): 101579. <https://doi.org/10.1016/j.scs.2019.101579>.
- Péan, Thibault Q, Jaume Salom, and Joana Ortiz. 2018. 'Environmental and Economic Impact of Demand Response Strategies for Energy Flexible Buildings'. In *BSO 2018*, 277–83.
- Perera, A. T.D., Silvia Coccolo, Jean Louis Scartezzini, and Dasaraden Mauree. 2018. 'Quantifying the Impact of Urban Climate by Extending the Boundaries of Urban Energy System Modeling'. *Applied Energy* 222 (December 2017): 847–60. <https://doi.org/10.1016/j.apenergy.2018.04.004>.
- Riederer, Peter, Vincent Partenay, Nicolas Perez, Christophe Nocito, Romain Trigance, and Thierry Guiot. 2015. 'Development of a Simulation Platform for the Evaluation of District Energy System Performances'. *14th International Conference of IBPSA - India*, no. December: 2499–2506. <https://doi.org/10.13140/RG.2.1.4668.8401/1>.
- Roccatello, Erica, Alessandro Prada, Paolo Baggio, Cristian Zambrelli, and Marco Baratieri. 2021. 'Simulation Of Efficiency Of Different Configurations Of Residential Hybrid Heating Systems Combining Boiler And Heat Pump'. In *International High Performance Buildings Conference*.
- Rogers, Michelle M, Yang Wang, Caisheng Wang, Shawn P Mcelmurry, and Carol J Miller. 2013. 'Evaluation of a Rapid LMP-Based Approach for Calculating Marginal Unit Emissions'. *Applied*

- Energy* 111: 812–20. <https://doi.org/10.1016/j.apenergy.2013.05.057>.
- Roux, Charlotte. 2017. 'Analyse de Cycle de Vie Conséquentielle Appliquée Aux Ensembles Bâtis'.
- Roux, Charlotte, Patrick Schalbart, and Bruno Peuportier. 2017. 'Development of an Electricity System Model Allowing Dynamic and Marginal Approaches in LCA—Tested in the French Context of Space Heating in Buildings'. *International Journal of Life Cycle Assessment* 22 (8): 1177–90. <https://doi.org/10.1007/s11367-016-1229-z>.
- RTE. 2015. 'Registre Des Installations de Production Raccordées Au Réseau Public de Transport d'électricité'.
- . 2017. 'ANTARES OPTIMIZATION PROBLEMS FORMULATION'.
- . 2018. 'Bilan Électrique 2018'. *RTE Bilan Électrique 2018*. <https://bilan-electrique-2018.rte-france.com/reseau-de-transport-qualite-deelectricite/#>.
- . 2019a. 'Bilan Électrique 2019'.
- . 2019b. 'Bilan Prévisionnel de l'équilibre Offre Demande d'électricité En France - Principaux Résultats'.
- . 2019c. 'Synthèse Bilan Électrique 2019' 2018.
- . 2020a. 'Antares Simulator'. 2020. <https://antares-simulator.org/>.
- . 2020b. 'Indisponibilités Des Moyens de Production'. 2020. <https://www.services-rte.com/fr/visualisez-les-donnees-publiees-par-rte/indisponibilites-des-moyens-de-production.html>.
- . 2020c. 'Téléchargement de Données'. 2020. <https://www.rte-france.com/fr/eco2mix/eco2mix-telechargement>.
- . 2021. 'Energy Pathways to 2050 Key Results'.
- . 2022a. 'Download Data Published by RTE'. 2022. <https://www.services-rte.com/en/download-data-published-by-rte.html>.
- . 2022b. 'Download ECO2mix Indicators'. 2022. <https://www.rte-france.com/en/eco2mix/download-indicators>.
- . 2022c. 'Futurs Énergétiques 2050'.
- RTE ADEME. 2020. 'Rapport Complet: Réduction Des Émissions de CO<sub>2</sub>, Impact Sur Le Système Électrique : Quelle Contribution Du Chauffage Dans Les Bâtiments à l'horizon 2035?'
- Ryan, Nicole A., Jeremiah X. Johnson, and Gregory A. Keoleian. 2016. 'Comparative Assessment of Models and Methods to Calculate Grid Electricity Emissions'. *Environmental Science and Technology* 50 (17): 8937–53. <https://doi.org/10.1021/acs.est.5b05216>.
- Sahraoui, Youcef, Pascale Bendotti, and Claudia D'Ambrosio. 2019. 'Real-World Hydro-Power Unit-Commitment: Dealing with Numerical Errors and Feasibility Issues'. *Energy* 184: 91–104. <https://doi.org/10.1016/j.energy.2017.11.064>.
- Sasso, Francesco, Jonathan Chambers, and Martin K. Patel. 2023. 'Space Heating Demand in the Office Building Stock: Element-Based Bottom-up Archetype Model'. *Energy and Buildings* 295 (February): 113264. <https://doi.org/10.1016/j.enbuild.2023.113264>.
- Schneider, Stefan, Pierre Hollmuller, Pascale Le Strat, Jad Khoury, Martin Patel, and Bernard Lachal. 2017. 'Spatial–Temporal Analysis of the Heat and Electricity Demand of the Swiss Building

- Stock'. *Frontiers in Built Environment* 3 (August): 1–17.  
<https://doi.org/10.3389/fbuil.2017.00053>.
- SDES. 2018. 'Enquête Performance de l'Habitat, Équipements, Besoins et Usages de l'énergie (Phébus), Données et Études Statistiques.' <https://www.statistiques.developpement-durable.gouv.fr/enquete-performance-de-lhabitat-equipements-besoins-et-usages-de-lenergie-pherbus#:~:text=L'enquête Phébus vise à,de leurs consommations d'énergie>.
- Secrétariat général à la planification Écologique. 2023. 'Tableau de Bord de La Planification Écologique'. *Encyclopédie Du Management Public*. <https://doi.org/10.4000/books.igpde.16786>.
- Senjyu, Tomonobu, Tsukasa Miyagi, Ahmed Yousuf Saber, Naomitsu Urasaki, and Toshihisa Funabashi. 2006. 'Emerging Solution of Large-Scale Unit Commitment Problem by Stochastic Priority List'. *Electric Power Systems Research* 76 (5): 283–92.  
<https://doi.org/10.1016/j.epsr.2005.07.002>.
- Staffell, Iain, and Richard Green. 2016. 'Is There Still Merit in the Merit Order Stack? The Impact of Dynamic Constraints on Optimal Plant Mix'. *IEEE Transactions on Power Systems* 31 (1): 43–53.  
<https://doi.org/10.1109/TPWRS.2015.2407613>.
- Tseng, Chung-li, Shmuel S Oren, Alva J Svoboda, and Raymond B Johnson. 1997. 'A Unit Decommitment Method in Power System Scheduling'. *Electrical Power & Energy Systems* 19 (6): 357–65.
- Umwelt Bundesamt. 2020. 'Bilanz 2019: CO2-Emissionen pro Kilowattstunde Strom Sinken Weiter Deutschland Verkauft Mehr Strom Ins Ausland Als Es Importiert'. 2020.  
<https://www.umweltbundesamt.de/presse/pressemitteilungen/bilanz-2019-co2-emissionen-pro-kilowattstunde-strom>.
- Voorspools, Kris R., William D. D'Haeseleer, D D William, Saeed Moradi, Sohrab Khanmohammadi, Mehrdad Tarafdar Hagh, Behnam Mohammadi-ivatloo, et al. 2000. 'The Influence of the Instantaneous Fuel Mix for Electricity Generation on the Corresponding Emissions'. *Energy* 25 (11): 1119–38. [https://doi.org/10.1016/S0360-5442\(00\)00029-3](https://doi.org/10.1016/S0360-5442(00)00029-3).
- Voorspools, Kris R, and D D William. 2003. 'Long-Term Unit Commitment Optimisation for Large Power Systems : Unit Decommitment versus Advanced Priority Listing'. *Applied Energy* 76: 157–67. [https://doi.org/10.1016/S0306-2619\(03\)00057-6](https://doi.org/10.1016/S0306-2619(03)00057-6).
- Vuillecqard, Cyril, Charles Emile Hubert, Régis Contreau, Anthony mazzenga, Pascal Stabat, and Jerome Adnot. 2011. 'Small Scale Impact of Gas Technologies on Electric Load Management - MCHP & Hybrid Heat Pump'. *Energy* 36 (5): 2912–23. <https://doi.org/10.1016/j.energy.2011.02.034>.
- Vuuren, Detlef P. van, Monique Hoogwijk, Terry Barker, Keywan Riahi, Stefan Boeters, Jean Chateau, Serban Scriciu, et al. 2009. 'Comparison of Top-down and Bottom-up Estimates of Sectoral and Regional Greenhouse Gas Emission Reduction Potentials'. *Energy Policy* 37 (12): 5125–39.  
<https://doi.org/10.1016/j.enpol.2009.07.024>.
- Wang, Danhong, Jonas Landolt, Georgios Mavromatidis, Kristina Orehounig, and Jan Carmeliet. 2018. 'CESAR: A Bottom-up Building Stock Modelling Tool for Switzerland to Address Sustainable Energy Transformation Strategies'. *Energy and Buildings* 169: 9–26.  
<https://doi.org/10.1016/j.enbuild.2018.03.020>.
- Wetter, Michael. 2004. 'Simulation-Based Building Energy Optimization'. University of California, Berkeley. [http://biblioteca.usac.edu.gt/tesis/08/08\\_2469\\_C.pdf](http://biblioteca.usac.edu.gt/tesis/08/08_2469_C.pdf).
- Wetter, Michael, Wangda Zuo, and Thierry Stephane Noudui. 2011. 'Modeling of Heat Transfer in Rooms in the Modelica "Buildings" Library'. In *Proceedings of Building Simulation 2011: 12th*

*Conference of International Building Performance Simulation Association*, 1096–1103.

Yang, Linfeng, Wei Li, Yan Xu, Cuo Zhang, and Shifei Chen. 2021. 'Two Novel Locally Ideal Three-Period Unit Commitment Formulations in Power Systems'. *Applied Energy* 284 (October 2020): 116081. <https://doi.org/10.1016/j.apenergy.2020.116081>.

Zheng, Zhanghua, Fengxia Han, Furong Li, and Jiahui Zhu. 2015. 'Assessment of Marginal Emissions Factor in Power Systems Under Ramp-Rate Constraints'. *CSEE JOURNAL OF POWER AND ENERGY SYSTEMS* 1 (4): 37–49.

Zhou, Bo, Xiaomeng Ai, Jiakun Fang, Wei Yao, Wenping Zuo, Zhe Chen, and Jinyu Wen. 2019. 'Data-Adaptive Robust Unit Commitment in the Hybrid AC / DC Power System'. *Applied Energy* 254 (May): 113784. <https://doi.org/10.1016/j.apenergy.2019.113784>.



# Appendix A: Description and analysis of the French power system

In the following sections, the specific electricity generation processes, the causes and frequency of the planned and unplanned unavailability and the power modulation capacities will be presented for the different types of generation units. Then the current and future (2035) French fleet and the usage of these technologies with a focus on the French fleet will be detailed. For every type of generation, the relevant inputs and parameters for the model will be deduced from the literature review and the historical data observation.

The nuclear powerplants supply most of the electricity produced in France. Furthermore, these units have strong technical constraints but low cost. Consequently, the dynamics of the French electricity system for both electricity production and exchanges are strongly affected by the constraints on the nuclear fleet. This is why this technology has to be analyzed first. The other technologies will be then successively evaluated in decreasing order of volumes adjusted upward on the ancillary services. These values are indeed a good representation of the flexibility of the technology on the system.

## A) Nuclear electricity generation

### Description of the nuclear power plants

The pressurized water reactor is the most widespread nuclear technology in the world (IAEA 2020). The powerplants using this technology are constituted of:

- A primary system (reactor) where uranium fission and neutron absorption reactions are performed in order to transfer heat to the water,
- A secondary system where water is changed in steam through a steam generator,
- A turbine which is set in motion by the generated steam,
- A generator which is driven by the turbine generates electricity.

In (Morilhat et al. 2019) two strategies are described to control electricity generation in a nuclear power plant:

- The fission reactions are modulated, as it is in French nuclear units for example,
- The reactor core thermal power remains constant while the generated steam is diverted away from the turbine, as it is in Canadian units for example.

Nuclear powerplants able to proceed flexible operations have specific designs (safety margins, auxiliary equipment) and the operators have to be trained to perform these operations.

Some unavailability of the nuclear units have to be planned and are scheduled during low electrical consumption periods if possible. The reasons for the planned unavailability are:

- Ten-year visits, which is an inspection of the complete reactor that lasts in average 60 days,
- Refuelling performed every 12 or 18 months for a duration of about one month,
- Maintenance works,
- Low electricity consumption,
- Grid unavailability.

The duration of the planned unavailability is foreseen depending on the complexity of the intervention but can be adjusted during the shut-down. The generation of the nuclear plants can also be affected by unplanned unavailability:

- for a breakdown,
- for local unavailability of the transmission network,
- for weather or environmental conditions (for example by limited thermal discharge into water during summer),
- because of the unplanned extension of a planned shutdown.

Nuclear power plants worldwide are mostly operated in base-load mode and flexibility is provided by other generating units. This operational mode is often more profitable because of the high fixed costs and low marginal costs of the nuclear plants (see Table 2). While it is more complex to implement, flexibility of nuclear power plants is sometimes necessary. For example, the nuclear power plants cover a large part of the overall generation in France. The nuclear units have therefore to participate in the balancing mechanism. In Slovakia nuclear units constitute about 50% of the fleet and are also partially operated flexibly (IAEA 2018). In Germany nuclear powerplants are operated in flexible mode because of the high penetration of renewable energy in the electrical production system. Other reasons for flexible operation of nuclear power plants can be the presence of large nuclear power plants in regions with few connections to the grid, transmission system constraints, lack of flexibility of the non-nuclear units or market rules.

### **Current and future (2035) French fleet**

In France 58 nuclear units (34 of 900 MW, 20 of 1300 MW and 4 of 1500 MW) based on pressurized water reactors were commissioned over 19 plants between 1977 and 2002 (RTE 2015). The installed capacity constitutes 63 130 MW which corresponds to 47.5% of the total production capacity. Nuclear generation is the predominant form of electricity supply in France: in 2018 71.7% of the electricity generation came from nuclear powerplants (RTE 2018). Because of the large nominal power of the nuclear units large security reserves are needed in case of outages.

According to the multi-annual energy-plan the share of nuclear generation in the French electricity supply should decrease to 50% until 2035 with the decommissioning of 14 units. Between 4 and 6 units (including the 2 880 MW of Fessenheim in 2020) will be shut down between 2019 and 2028. These units will be shut down independently of the plant after the fifth ten-year visit (Ministère de la transition écologique et solidaire 2019). The opening of a new EPR (European Pressurised Water Reactor) of a nominal power of 1 650 MW in the plant of Flamanville is planned during the year 2024 (RTE 2019b).

Figure 98 presents the planned and unplanned unavailability of the French nuclear fleet between August 2018 and July 2019. Prolongation of the planned unavailability occurred more frequently than normal during the past years and the unavailability planned or not of the nuclear increased. Given this trend and the coming ten-year visits RTE plans a decrease of the availability of the French nuclear fleet during the coming years (RTE 2019b).

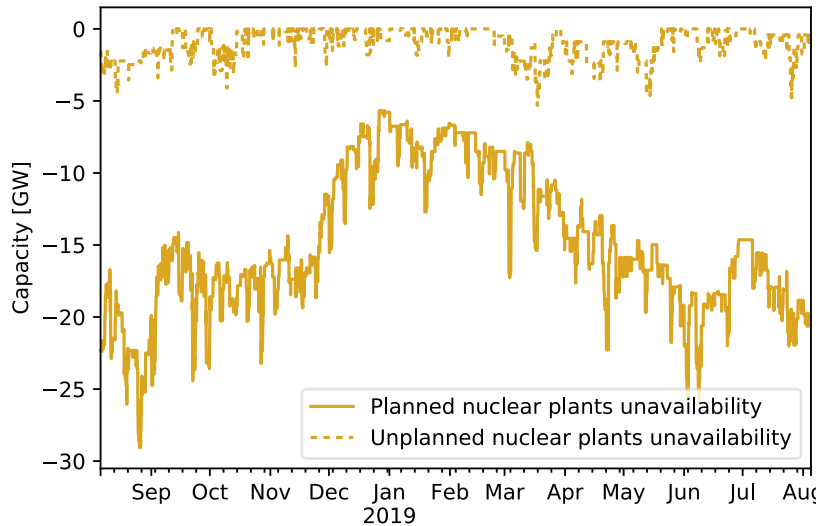


Figure 98: Unavailability of the French nuclear fleet between August 2018 and July 2019, Data: (ENTSOE 2020)

### Seasonal, weekly and daily flexibility in France

Weekly and seasonal flexibilities are performed by scheduling the planned unit unavailability during low demand periods. Figure 99 presents the French electricity consumption, the nuclear supply and the nuclear fleet availability in 2018. The seasonal flexibility can be noticed in Figure 99: the electricity consumption and the nuclear generation are strongly correlated. As the nuclear fleet provides a large part of the generated electricity in France, the weekly variations of nuclear generation follow the consumption variation apart during high consumption period where the nuclear fleet is saturated. Even when the nuclear fleet is not saturated, a correlation between the availability variation and the generation variation within the months can be observed. The coverage rate ranged between 53% and 128% in 2018. During the consumption peak the nuclear fleet still provides half of the electricity consumed and during lower consumption periods the nuclear generation exceeds the electricity consumption which allows export of electricity to the neighbouring countries.

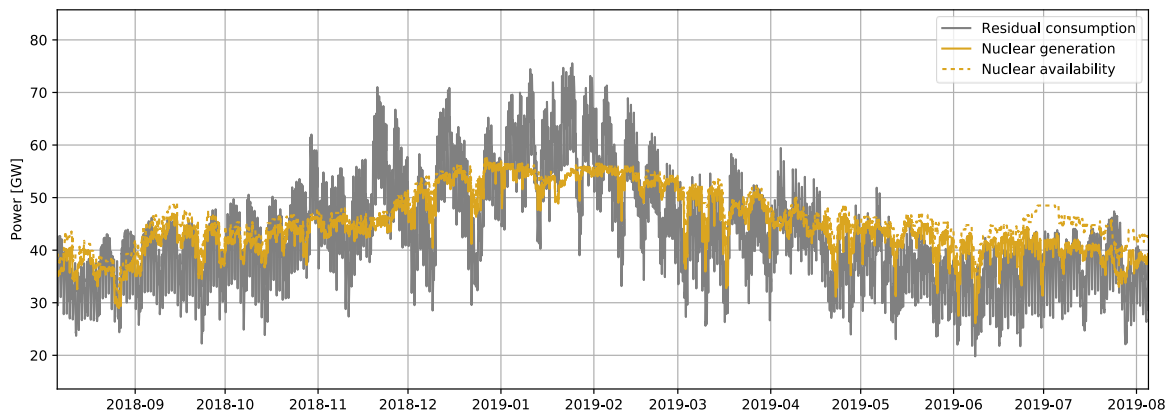


Figure 99: French electricity consumption, nuclear generation and availability between August 2018 and July 2019 on a half-hourly basis, data: (RTE 2020c; 2020b)

Besides seasonal and weekly generation variations, two modes of flexibility (load following and frequency control) are used in France in order to adapt within a day the nuclear electricity generation depending on the residual consumption. These generation variations can be observed in Figure 100 and will be analyzed after a presentation of the nuclear power plant operational flexibility. The different modes of nuclear power plant flexibility in the French context are described in Table 19.

Table 19: Flexibility of the nuclear power plants in France (Morilhat et al. 2019; IAEA 2018)

Timescale	Flexibility	Setting	Power range for flexibility
Day	Planned load following: variation programs corresponding to the foreseen electrical demand planned in advance between the grid operator and the plant operator	Manually by the plant operator	Ramp up or down between the nominal unit's power and 20% of the nominal unit's power in half an hour and again after at least two hours, twice a day
	Unplanned load following: response to requests or instructions from the grid system operator as part of the balancing mechanism		
	Primary frequency control	Automatically	± 2% of the nominal unit's power
	Secondary frequency control	Automatically	± 5% of the nominal unit's power
Week	Shifting routine tests to meet electricity consumption variations within the week	Planned by the plant operator	Nominal unit's power in test
Season	Planning refueling and maintenance for the nuclear power plant in order to meet the seasonal variations, Management of the fuel reserve in the core	Planned by the plant operator	+/- 100 TWh between summer and winter

According to EDF, nuclear flexibility has no impact on lifetime of the primary system components and a limited impact on the secondary systems components (mainly on joints, pipes and heat exchangers) as long as the amplitude and the frequency of the flexible operations performed respect the allowed limits of the plant design. The load factor unavailability capability of the nuclear powerplants of EDF is about 2-2,5%, which 0,5% is attributed to flexible operation (Morilhat et al. 2019).

In (C Cany et al. 2018) the production of every reactor of the French nuclear fleet was analyzed between 2012 and 2016 in order to quantify the flexibility of the fleet. According to the observations, the French nuclear powerplants do not follow the theoretical ramping profiles (ramp-down, constant intermediate level or outage, ramp-up) but adapts continuously the power level to the requirements and the constraints. These constraints (maximum power ramp, minimum power, number and duration of shut-downs/start-ups as well as duration at intermediate power level) depends of the time span since the last refueling outage and until the next one. This analysis also showed that in 2016 about 40% of the nuclear fleet was significantly involved in load following operations. Furthermore, the number of load following operations performed by every reactor is below the European Utility Requirements (at least 200 load-following operations between two refueling outages, twice a day and five a week). It seems therefore that load-following operations of the nuclear powerplants are not significantly technically limited. An economical criterion could better explain the frequency and amplitude of the operations. Indeed the main economic impact of the nuclear flexibility is to decrease the load factor of the nuclear fleet and consequently decrease the profitability of the nuclear power plants.

## Input and parameter selection for the model

Figure 100 shows the residual consumption, the available capacity of the nuclear fleet and the nuclear generation over a complete week for four different weeks between August 2018 and July 2019. The two different colors in backgrounds of the figures differentiate week days and weekends.

During the week days of the chosen winter week (*b*) the nuclear fleet is saturated. During these days the nuclear generation depends mostly of the nuclear available capacity. In the three other weeks, it seems that a constant margin is kept between the availability and the production. During weekend and the residual consumption decreases. In weeks *b* and *d* downward adjustments of the nuclear generation occur during the lowest consumption hours of the weekend and sometime also during the night. In the weeks *a* and *c* the electricity exports and pumping are high enough during the weekend to maintain the total electricity generation to a level that avoids nuclear load following. Although the nuclear availability and the generation variations within larger period seem to be correlated, this correlation is not discernible at this scale. Load following operations occur more often during week *d* than during the week *c* when the nuclear plants supply most of the dispatchable electricity generated. Even if the nuclear fleet is no more saturated, the nuclear load following occurs only for high nuclear coverage of the dispatchable electricity generation. In all seasons small and fast generation variations interpretable as frequency control occur. This phenomenon is out of the scope of the developed model.

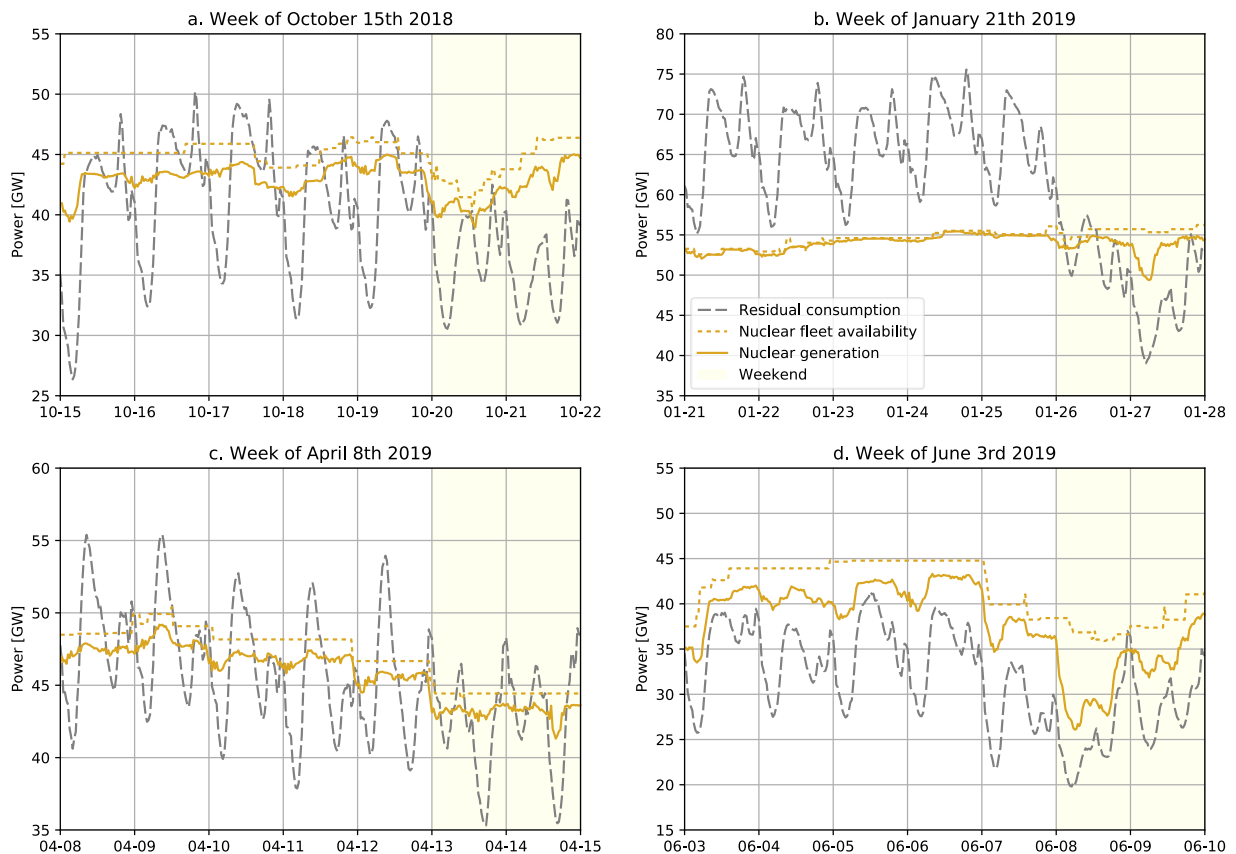


Figure 100: Residual consumption, nuclear fleet availability and nuclear generation for four different weeks between August 2018 and July 2019, data:(RTE 2020c; ENTSOE 2020)

To summarize, relevant inputs and parameters for a model of the French nuclear fleet are:

- as boundaries : the available capacity (saturation of the fleet) from which is subtracted a margin (for the frequency control and relative to the load following operating units)
- Ramping limits: There is a technical limitation that can be modelled but this parameter doesn't seem to significantly constrain the variation of the nuclear generation considering the variations each 30 minutes (see Table 1). Consideration of start-up or ramping costs could be more relevant for the model of the variations.
- Variations within a day: Total dispatchable generation and nuclear coverage
- Variations for a longer time scale: Consumption and availability

## B) Hydroelectric powerplants

### i. Storage

The pumped storage hydroelectric units are fitted with reversible turbines located between two water tanks at different levels. The reversible turbines operate alternatively in pumping or running a turbine. The performance of such units is around 80%. These units are nowadays the most employed electricity storage system but other solutions are under development such as batteries or power-to-gas-to-power solutions. The pumped storage hydroelectric powerplants can be mainly unavailable because of maintenance works, or breakdown or for local unavailability of the transmission network.

During off peak hours, when the marginal price of electricity is the lower of the day, water is pumped from the downstream basin to the upstream one. The pumped water is used during peak hours, when the marginal price of electricity is the highest, in order to generate electricity through the turbine. Highly reactive, these units are a significant mean of flexibility for the electrical systems. Depending on the size of the storage, the running of the turbine/pumping cycles allows flexibility at the scale of the day, week or season.

### Current and future (2035) French fleet

There are three types of pumping units in France:

- The pure pumped storage units are closed and the generated energy during a time period is correlated with the energy used for pumping during this period and with the efficiency factor.
- The mixed pumped storage units also store natural water inputs that increase the generated electricity. These units are coupled with non-reversible units in order to turbine melted ice in spring that can damage reversible turbines.
- Non-reversible pumps can also be used to pump water to reservoirs fitted with non-reversible turbines.

The Table 20 summarizes the pumping and the generation capacities of the French hydraulic fleet in 2018. The installed capacity for electricity production constitutes 5029 MW which corresponds to 3,8% of the total production capacity (RTE 2018).

Table 20: Installed capacity of pumped storage units and pumps in France in 2018 (RTE 2015)

	Number of units	Pumping power (MW)	Generation power (MW)	Additional turbines (MW)
Pure Pumped Storage units	2	1584	1728	0

Mixed Pumped Storage units	6	2831	2455	846
Input Pumps	16	371	0	0
Total	24	4785	5029	

According to the French Multi Annual Energy Plan (Ministère de la transition écologique et solidaire 2019) additional Pumped Storage units representing 1,5 GW of electricity production should be installed between 2030 and 2035. Electricity storage per batteries should also be developed across the country.

Only data about available electricity generation capacity for the pumped storage units are published. No information concerning the available pumping capacity and the availability of the additional turbines are published. This is while the available pumping power has to be deduced from the available generation capacity. Figure 101 presents the planned and unplanned unavailability of the French pumped storage units between August 2018 and July 2019.

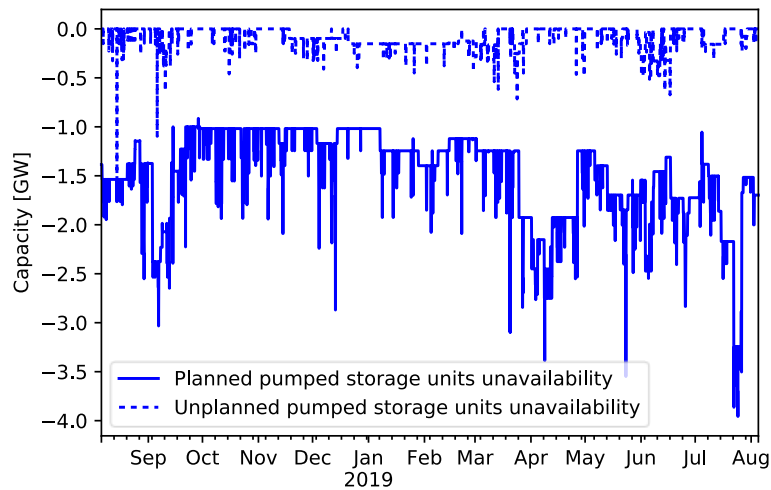


Figure 101: Unavailability of the French pumped storage units between August 2018 and July 2019, data:(ENTSOE 2020)

### Seasonal, weekly and daily flexibility in France

In this part only the organization of the pumping will be discussed as the pumped water will be turbined in relation with the other hydroelectric plants. The electricity production from pumped storage units will be therefore discussed section ii. In France pumped storage units enable a daily and weekly flexibility. Figure 102 represents the available pumping capacity and the pumping in France between August 2018 and August 2019. The amplitude of the pumping is directly correlated with the availability of the pumps. The pumping power seems to vary between zero (no pumping) and the pumping capacity every day (or less).

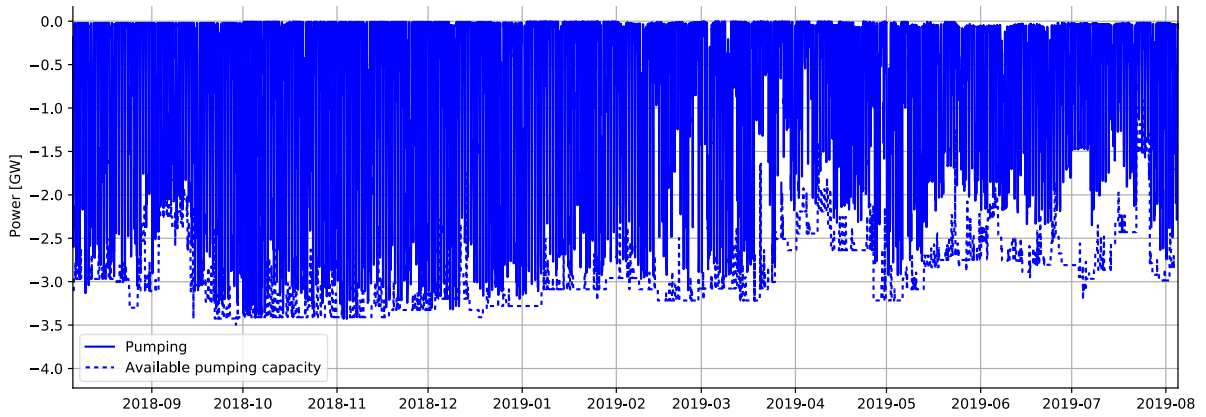


Figure 102: Available pumping capacity and pumping in France between August 2018 and August 2019, data:(RTE 2020c; ENTSOE 2020)

Figure 103 compares the pumped power with the residual consumption to which is subtracted the weekly mean of the residual consumption. Pumping mostly occurs when the residual consumption is above this weekly mean.

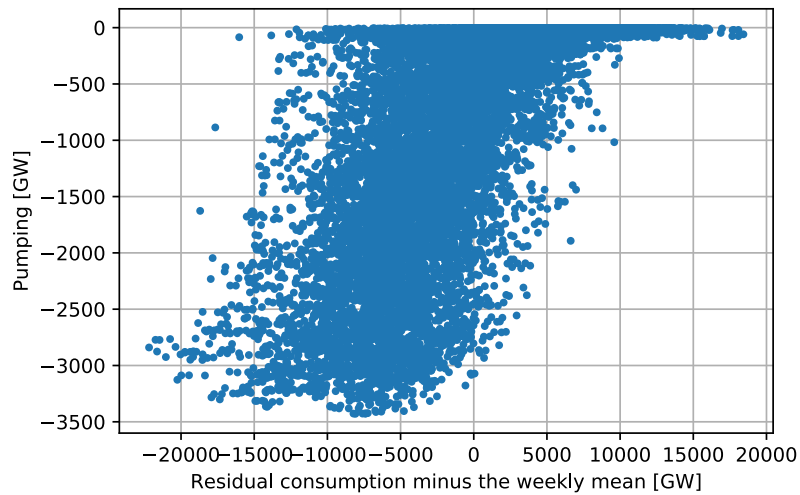


Figure 103: Comparison of the pumped power and the residual consumption minus its weekly mean

Figure 104 represents the available pumping capacity, the pumping and the residual consumption to which is subtracted the weekly mean for four different weeks. Activating the pumping when the residual consumption is above the weekly mean value seems to be a sufficient criteria for modelling pumping during weekdays. However, a second criteria need to be defined for weekends. As the storages have a limited capacity, it is logical to define a maximal energy that can be pumped every day.



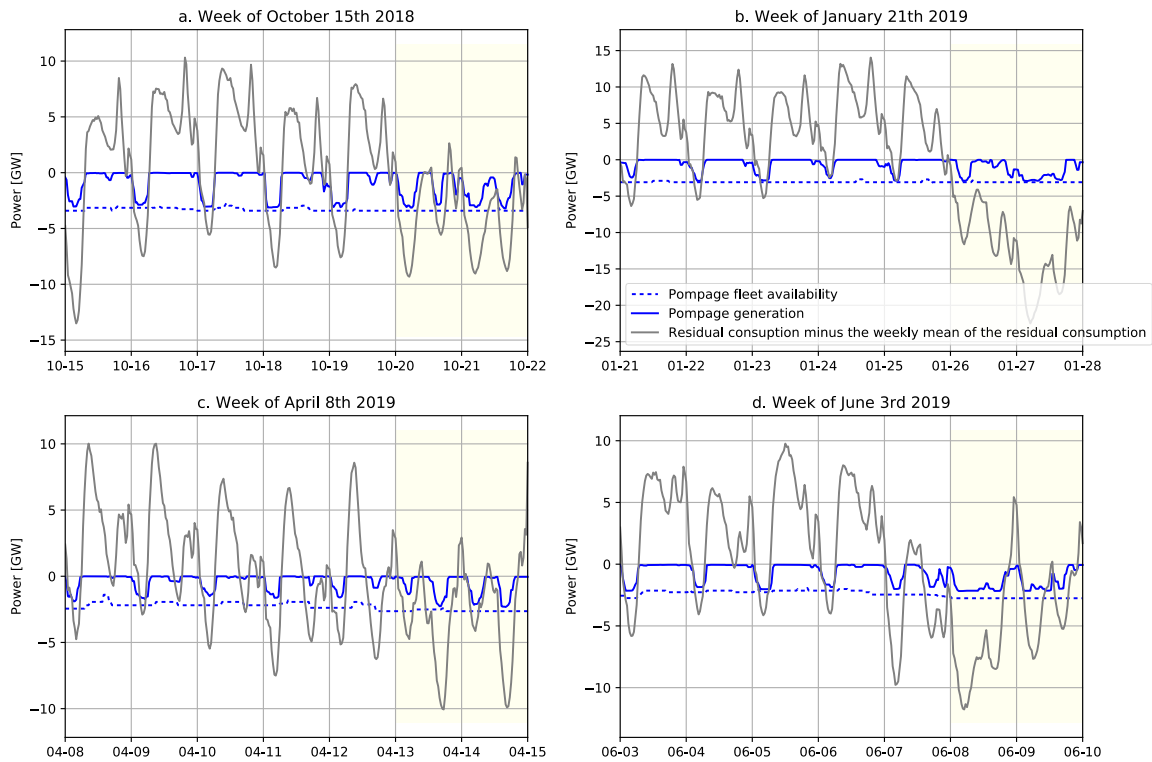


Figure 104: Available pumping capacity, pumping and residual consumption minus his weekly mean for four different weeks between august 2018 and July 2019, data:(RTE 2020c; ENTSOE 2020)

Figure 105 presents the energy used to pump water every day in France between August 2018 and August 2019. According to the observations a limit of 45 GWh (represented in orange on the figure) of energy used for pumping in the pumped storage units for every day could be used.

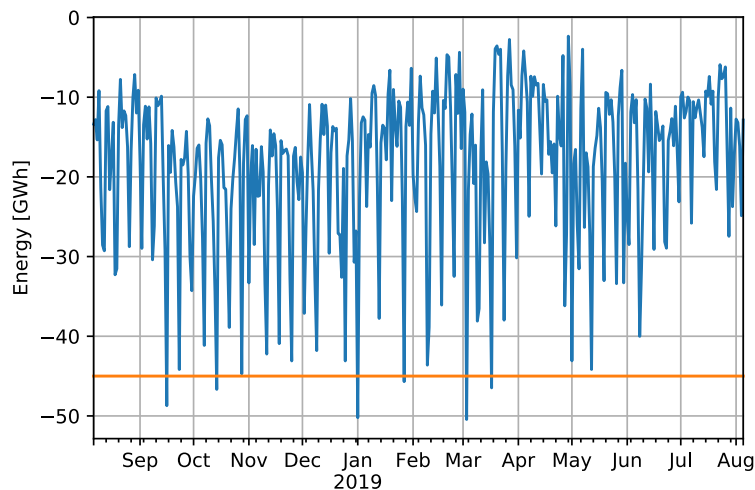


Figure 105: Daily pumped energy in France, data: (RTE 2020c)

### Input and parameter selection for the model

To summarize, the relevant inputs and parameters for a model of the French pumped storage hydroelectric fleet are:

- Boundaries : the availability of the pumped storage hydroelectric units and the maximal amount of energy that can be used for pumping every day;
- Ramping limits: these units are highly reactive and don't have ramping limits;
- Variations within a day: The variations within a day are highly related to the residual consumption and to the level of these residual consumption in comparison to the weekly mean value;
- Variations for a longer time scale: The running the turbine / pumping cycles are only controlled at daily and weekly time scale.

## ii. Electricity generation

### Description of the process for electricity generation

Besides run-of-river power plants, three types of hydraulic power plants - more or less dispatchable- are used to generate electricity:

- The hydropeaking units are located in the lakes downstream of medium-altitude mountains. These plants can store water for electricity generation from 2 up to 400 hours. Therefore, these units are used to follow the daily consumption peak or for modulation between working and non-working days.
- The storage hydroelectric plants stand downstream of medium- or high altitude mountains. The capacity of their storage is over 400 hours and consequently provides a seasonal storage.
- The pumped storage hydroelectric plants mentioned in the previous section can produce electricity with their reversible turbine when there are not used to pump or with additional non-reversible turbines.

### Unavailability

The hydroelectric powerplants can be unavailable because of maintenance works, breakdown or for local unavailability of the transmission network. Environmental constraints or water unavailability can also result in powerplant unavailability. However, the electricity generation of the hydroelectric powerplants is moderately impacted by the unavailability of the generation units and is mainly related to the management strategy of the water resources.

### Operation modes

The hydroelectric powerplants have a very low marginal cost (see Table 2) and have high ramping rate. Hydropower is therefore the most valuable power source but its capacity is limited (as the water resources are limited). The cost of hydroelectricity is not calculated according to its marginal cost but according to its usage cost. The usage cost of the hydroelectric plants is the cost of the plant that would be used instead of the hydroelectric unit. The usage of the hydraulic reserve has to be optimized during the day, the week and the year depending on the size of the different storages. The totality of the water reserves has to be used during the period of the optimization of the water reserves. The water level of reservoirs depends on the rainfalls, the season and the runoff water. The water level also depends on the electrical consumption, so varying over the year for the larger reservoirs and with the day of the week for the smaller. . As a result, it usually decreases in winter when the electricity consumption is high and increases during spring due to melting snow.

### Current and future (2035) French fleet

In Europa the hydroelectricity represented 17.6% of the consumed electricity in 2018. The hydroelectric capacity of a country mainly depends on its geography. In Europa the main producers of hydroelectricity are Norway, Iceland, Swiss and Austria. The French installed capacity constitutes 25 510 MW which corresponds to 19.2% of the total production capacity. Table 20 summarizes the French hydroelectric fleet in 2018. The hydroelectric fleet is mainly installed in mountainous regions. As the run-of-river plants are almost not dispatchable only the resting 17 443 MW can be used in load following mode. Hydroelectric generation is the predominant form of renewable electricity supply in France: in 2018 68.3 TWh were generated by hydroelectric plants, which corresponds to 11.5% of the overall French generation (RTE 2018).

Table 21: Installed capacity of hydroelectric powerplants in France in 2018 (RTE 2015)

Type of units	Run-of-river	Hydropeaking	Storage hydroelectric plants	Pumped storage hydroelectric plants
Number of units	189	121	97	7
Installed capacity (MW)	6 218	3 719	9 542	4 183

According to the multi-annual energy-plan the hydroelectric installed capacity should vary little because the territory is already saturated. In addition to the installation of new pumped storage units (1.5 GW), the existing plants should be renovated or optimized and a few new projects developed. To summarize, the installed hydroelectric capacity should increase to 25.7 GW by 2023 and between 26.4 and 26.7 GW by 2028 (Ministère de la transition écologique et solidaire 2019).

Figure 106 presents the variation of the reservoir level for 2018 and 2019. This variation follows every year a similar pattern which depends on the climatic conditions. The reservoirs level reaches usually its maximum in July and stays nearly constant until the end of summer. A too high usage of these reserves during summer is avoided in order to keep water for winter, when the electricity demand is higher, but also in respect of the environmental and touristic constraints. The reserves are then used by fall and mostly winter and reach its minimum at the beginning of the spring. The reservoirs are then refilled by spring melt-water and the important rainfalls that can occur at this time of the year.

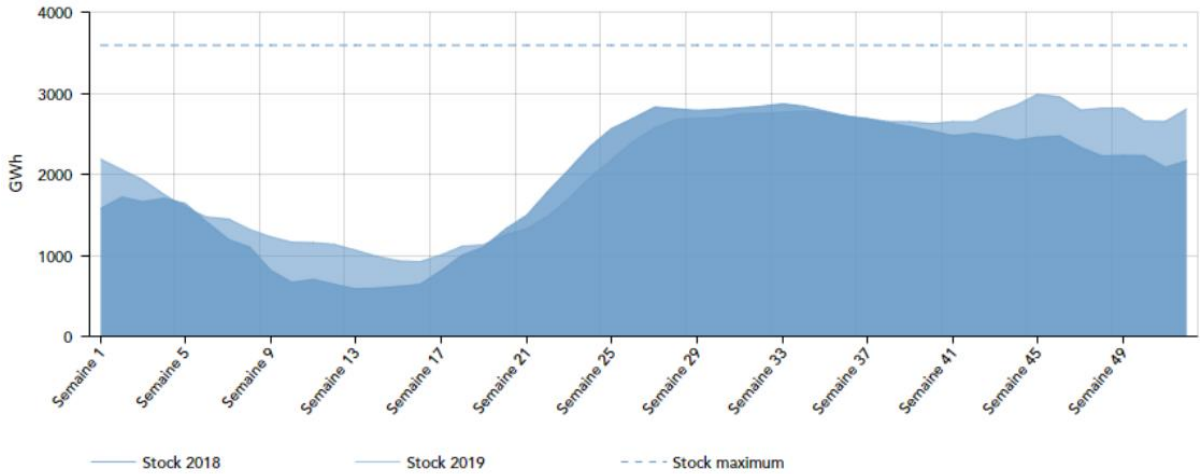


Figure 106: Weekly variation of the level of the hydraulic reservoirs in 2018 and 2019 (RTE 2019a)

### Seasonal, weekly and daily flexibility in France

In the published data from RTE electricity generation of the hydropeaking and run-of-river units are merged. The hydropeaking reservoirs have a storage capacity from 2 up to 400 hours and are only partially dispatchable. For these reasons, we will consider in the following than run-of-river and hydropeaking units are non-dispatchable technologies although part of them is dispatchable on short durations. Only pumped storage units and storage hydroelectric plants are considered dispatchable and will consequently be discussed in this part.

Figure 107 presents the availability and the electricity generation of the storage hydroelectric powerplants in France between August 2018 and August 2019. The water reserve management seems to be a more influential parameter than powerplants availability in the electricity generation of these plants. The electricity generation of these plants seem indeed saturated only a few days, mostly in winter. The storage hydroelectric plants produce also more electricity in winter.

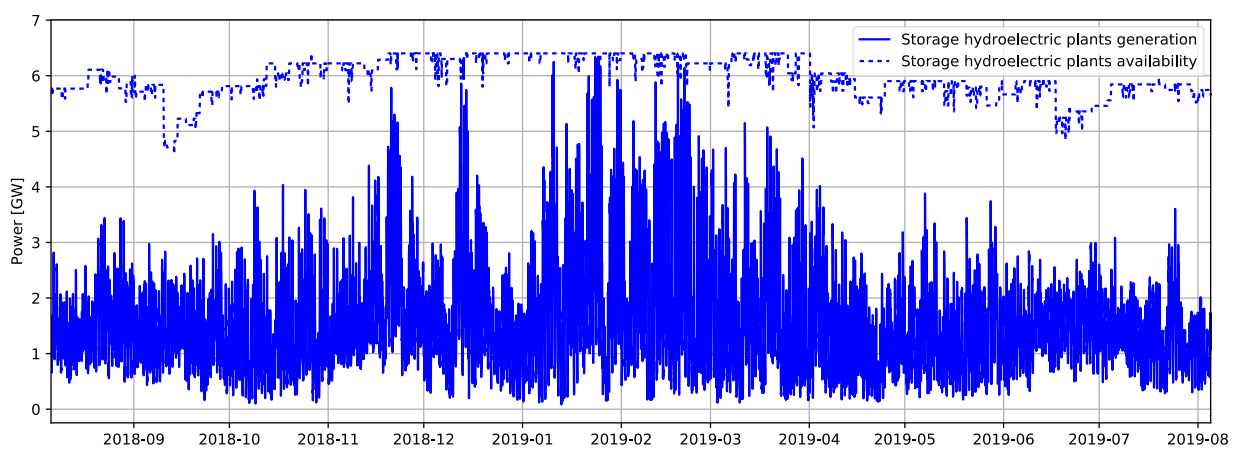


Figure 107: Available capacity and generation of the storage hydroelectric plants in France between August 2018 and August 2019, data:(RTE 2020c; ENTSOE 2020)

Figure 108 presents the availability and the electricity generation of the pumped storage hydroelectric powerplants in France between August 2018 and August 2019. The electricity generation of the pumped storage hydroelectric powerplants are more correlated with their availability. As for the pumping, the electricity generation varies every day between zero and a maximal value, which varies from day to day.

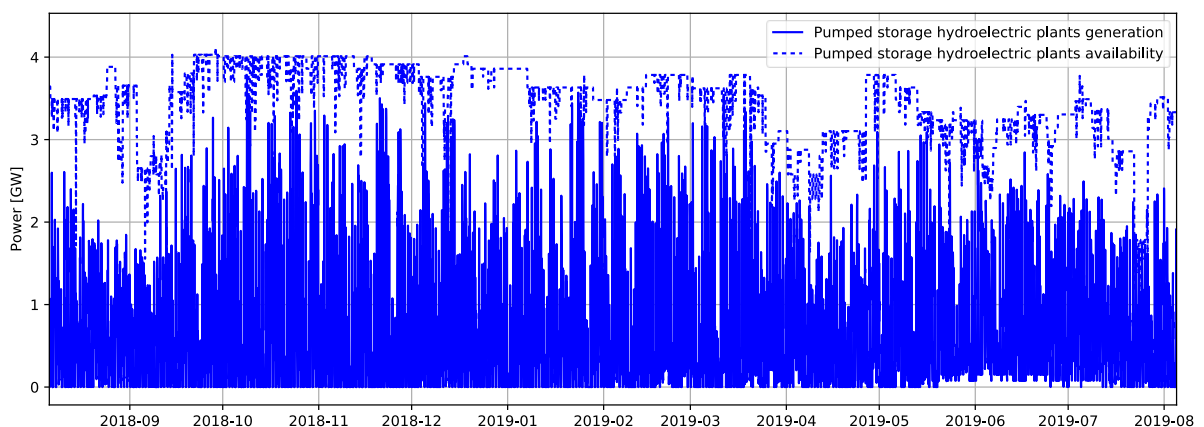


Figure 108: Available capacity and generation of the pumped storage hydroelectric plants in France between August 2018 and August 2019, data:(RTE 2020; ENTSOE 2020)

Figure 109 presents the weekly ratio between the energy produced and the pumped energy in the pumped storage hydroelectric plants. It seems difficult to deduce a correlation between the energy used for pumping and the electricity generation. Although, most of the water turbined in the pumped storage hydroelectric plants comes from the pumping of the reversible turbines, the water in the mixed pumped storage units also comes from rainfalls and runoffs.

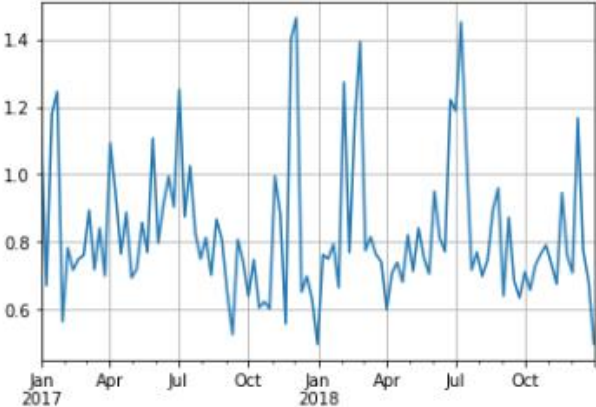


Figure 109: Weekly ratio between the energy produced and the pumped energy in the pumped storage hydroelectric plants in 2017 and 2018, data :(RTE 2020c)

**Input and parameter selection for the model**

The hydroelectric units can follow important load variations. Figure 110 presents the storage hydroelectric plants generation for four different weeks between august 2018 and July 2019. The electricity generation is highly flexible. Every day two generation peaks can be observed, corresponding to the daily consumption peaks. Except of the week b, there is no significant difference between the week days and the weekend.

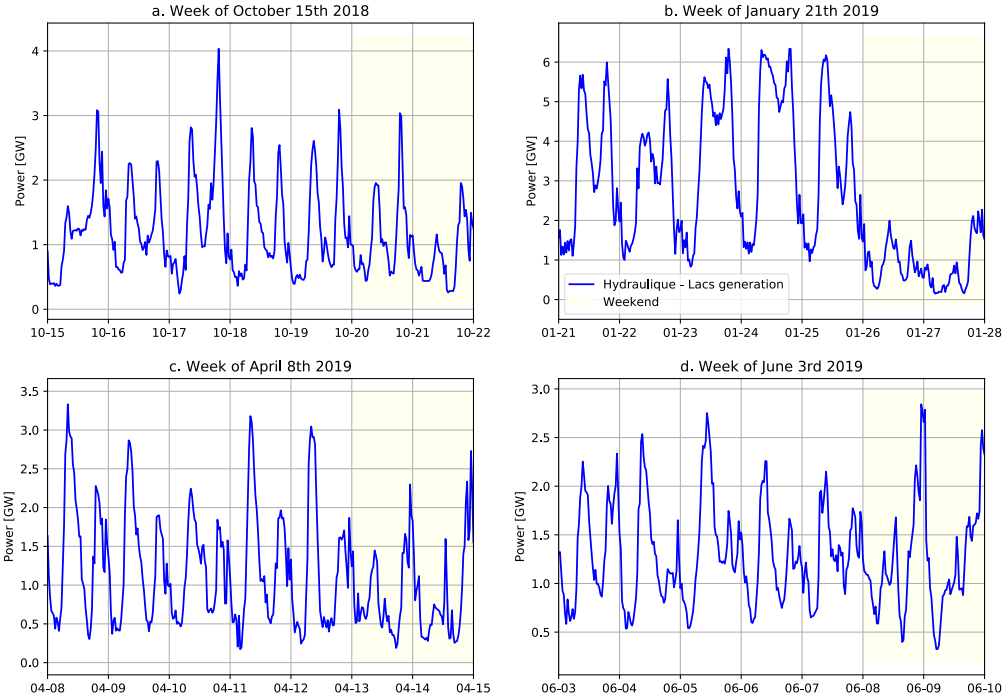


Figure 110: Storage hydroelectric plants generation for four different weeks between august 2018 and July 2019, data:(RTE 2020; ENTSOE 2020)

Figure 111 presents the pumped storage hydroelectric plants generation and availability for four different weeks between august 2018 and July 2019. As for the storage hydropower plants, the electricity generation is highly flexible and the two daily peaks can be observed. However, every night there is no electricity generation for a few hours, during pumping. During weeks a, b and d, the electricity generation is lower during the weekend.

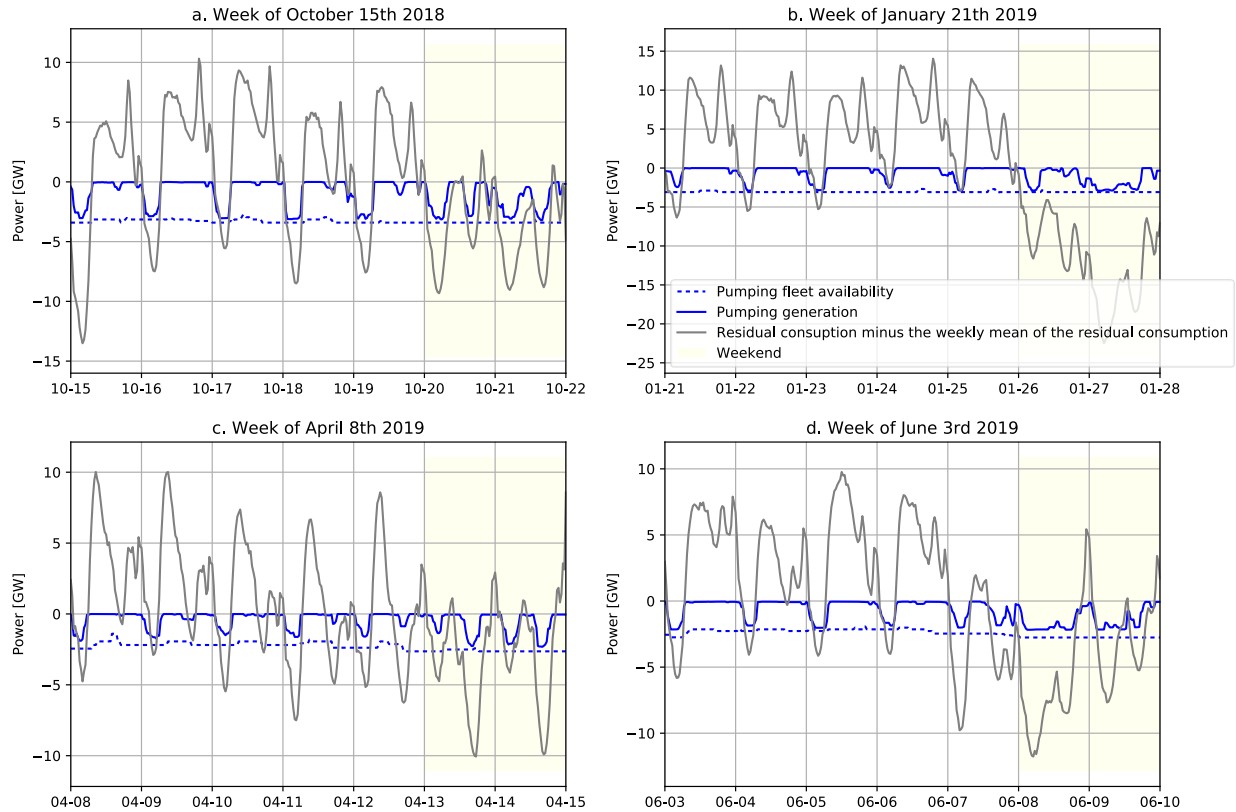


Figure 111: Pumped storage hydroelectric plants generation and availability for four different weeks between august 2018 and July 2019, data:(RTE 2020; ENTSOE 2020)

To summarize, relevant inputs and parameters for a model of the French dispatchable hydraulic fleet are:

- as boundaries : The fleet availability for the pumped storage hydroelectric plants. For the storage hydroelectric plants the optimization of the usage of the water reservoirs is performed over a year, between July and June.
- Ramping limits: Hydroelectric powerplants are highly reactive.
- Variations within a day: Load following
- Variations for a longer time scale: Storage hydroelectric plants generate more electricity in winter. There is no seasonal variation for the pumped storage hydroelectric plants.

As the water reservoirs levels varies during the year but the balance between input and output over the year is null or very low. It means that the energy produced over the year depends highly on the rainfalls and that rainfalls could also influence the yearly produced energy pf the fossil powerplants or the volume exchanged.

### C) Interconnections

#### Description of the process for electricity exchanges at a border

The different price areas of the European electrical system are coupled according to their respective market prices in order to improve the economic efficiency of the overall system within the physical constraints of the grid. The electricity exchanges between countries also improve the integration of the non-dispatchable renewable electricity generation. The prices of the electricity for the different interconnected countries change continuously and are estimated a day-ahead in order to forecast the electricity exchanges, which can be then continuously adjusted during the day. The electricity flow at a border is oriented according to the price difference between the two countries. When the interconnection doesn't restrict the electricity exchange, the marginal price of the electricity of the both countries became identical. Identical market prices between neighboring countries means then that the exchanges between them are not constrained by interconnection capacity or that their marginal generation units have similar properties. In this case, the marginal generation unit is not anymore to identify at the scale of a country and should be defined at the scale of the different interconnected countries. Consequently, in the future, the electrical system will probably have to be modeled considering a continent (or part of) and not anymore a single country as the interconnections between countries are growing all over the world.

The "Total Transfer Capacity" (TTC) between two countries is the maximal allowed electricity power that can be exchanged on this interconnection according to the availability of the grid and the consumption level of the country. A security margin called "Transmission Reliability Margin" (TRM) is subtracted to the TTC in order to ensure the exchanges despite the uncertainties on the TTC calculations due to:

- The frequency grid regulation,
- The emergency exchanges between the TSOs,
- The uncertainties on the data and measurements.

The Net Transfer Capacity (NTC), corresponding to the difference between the TTC and the TRM, is defined for both directions (import and export) and was historically used to calculate the interconnection constraints to couple the different countries. The NTC only reflects an agreement between two neighboring countries on the possible electricity exchanges.

Since 2015 the five countries of the Central West Europe (CWE) region are coupled with a flow-based method. The flow-based market coupling method is a new dynamic method for cross-border capacity calculation jointly developed by TSOs in Central Western Europe (CWE). A dynamic calculation for the cross-border capacity is needed for the integration of the non-dispatchable electricity generation, which their volume will be significantly increased in the coming years. This method considers more information than the NTC calculation and rely consequently on the increased sharing of information between TSOs. The flow-based method optimizes the electricity exchanges inside the entire CWE area taking account of :

- The dependencies between the countries of the CWE area
- The situation of the cross-border interconnections of every country,
- The situation of the national grid,
- The situation of the fleet,
- The prediction of the national dispatchable as-non dispatchable electricity generation.

During the last years the number of hours with one price for all the CWE countries increased to reach 42% in 2019 (RTE 2019a).

There are three main reasons for a country to import electricity:

- His own production fleet is already saturated, electricity import is necessary in order to avoid blackout.
- The electricity is cheaper on a neighboring country and some dispatchable units can be stopped or adjusted downward. In this case it is economically more interesting to import electricity rather than produce.
- A neighboring country produces too much solar or wind electricity and sells it with a negative price. It happens when it is too expensive or not possible to stop or adjust downward the production level of the fleet. This occurs relatively rarely (27 hours for France in 2019) but the frequency of the time steps with negative prices is increasing as the implantation of the non-dispatchable renewable energy is growing. Negative step time prices are indeed mostly caused by too high wind or solar electricity generation. In Europe, it mainly occurs in Germany (RTE 2019a).

Physical electricity flows and commercial exchanges have to be distinguished. Physical flows correspond to the electricity that is really exchanged between two countries via the interconnection at the border. The commercial exchanges define the electricity that is bought by a country to another one, but the corresponding electricity can transit via other countries. However, the sum for a country of all the commercial exchanges and the physical flows are always equal. For example for a commercial exchange between France and Germany, the electricity could be split between the Belgian, Swiss and Italian borders.

### Current and future (2035) interconnections in France

The French electricity system was originally sized to cover the consumption peak in winter. With the increase of the unavailability of the French powerplants and the decommissioning of thermal fossil powerplants the last years, the electricity import is nowadays essential in order to supply the electricity demand during the colder weeks of winter. It allows France to export electricity when the electricity consumption is lower. France is the European country exporting the most. 84 TWh of electricity were exported in 2018 and 28.3 TWh were imported. France is currently connected with Swiss, Italy, Spain, Great-Britain, Belgium and Germany. The electricity exchanges for 2019 between France and these six countries are summarized in Figure 112.

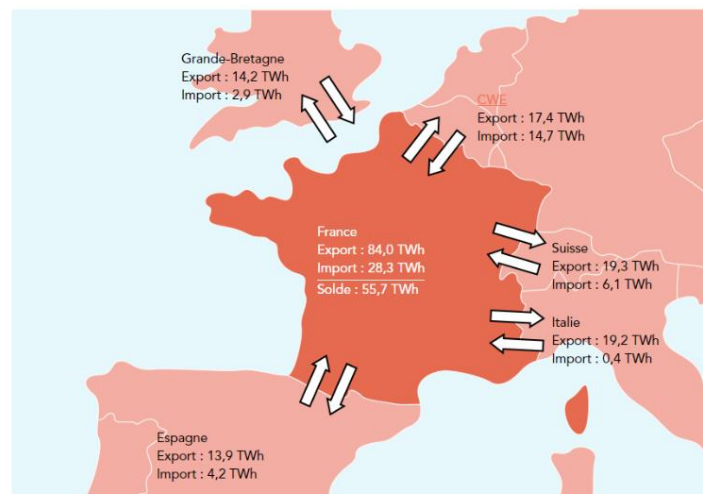


Figure 112: Exchanges between France and the neighboring countries in 2019 (RTE 2019a)

The Celtic Interconnector Project plans to directly connect France and Ireland with a capacity of 700 MW between Britain and the south of the Ireland. The Gulf of Gasconne Project foresees the installation of a new interconnection of 5 GW between France and Spain. A future connection of 1 GW



between France and England should help to securize the electricity exchanges between the two countries. Since Spring 2015 a new interconnection between France and Italy is being build in order to increase their transmission capacity by 60%.

After 2022 the marginal cost of electricity in France should decrease due to the growing share of the renewable powerplants in the fleet. In the same time most of the carbonated powerplants in Europe should be stopped. These plants constitute nowadays the base part of the electricity production for several countries. The interconnection in Europe should also be enhanced. This explains why the export of French electricity from France should grow from 2022. Figure 113 presents the evolution (historical data and forecast) of the balance for the French electricity exchanges from 2014 until 2026.

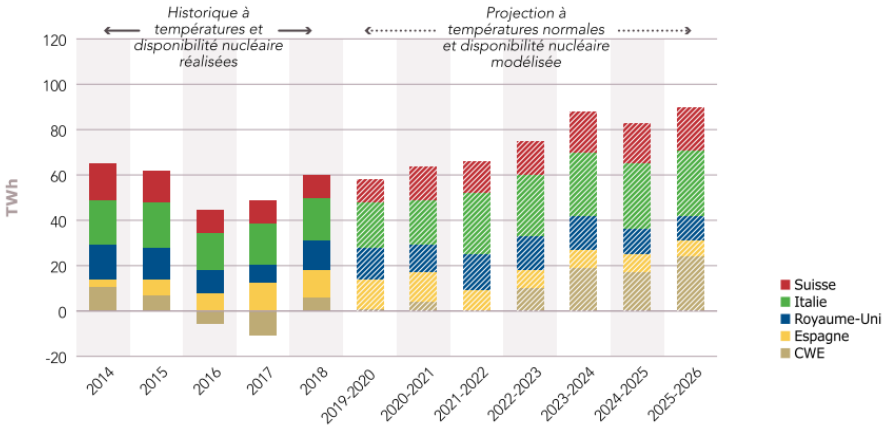


Figure 113: Variation of the balance of the electricity exchanges between 2014 and 2026

**Seasonal, weekly and daily flexibility of the electricity exchanges with France**

Figure 114 presents the residual consumption, which is subtracted the nuclear availability, the total net Transfer Capacity and the electricity exchanges between France and its neighboring countries between August 2018 and August 2019. The two time series of the Figure 114 are strongly correlated: the variable cost of nuclear electricity is cheaper that the marginal cost of the neighboring countries. Thanks to the interconnections, the load factor of the nuclear plants can be maintained in summer and less electricity is exported in winter when the nuclear fleet is saturated. France is mainly importing electricity in November, December and January when the temperature is lower than the normal seasonal level. The electricity exchanges vary a lot during the whole year. During the year 2018/2019 the highest level of export was 8.7 GW at 23:30 on the 20<sup>th</sup> of November 2018 and the highest level of import was 19.9 GW at 17:00 on the 22<sup>nd</sup> of February 2019. That means that interconnections allowed an additional flexibility of 28.6 GW for the French grid during the year 2018/2019. These variations are constrained between the NTC for import and for export, with addition of an extra capacity for several days, which probably corresponds to the TRM.

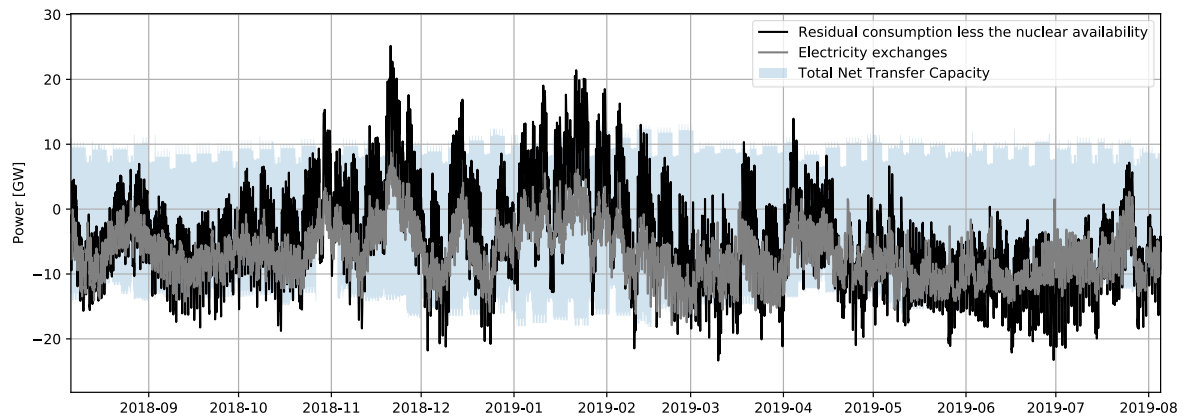


Figure 114: Total Net Transfer Capacity for import and export between France and its neighboring countries and electricity exchanges between August 2018 and August 2019, data:(RTE 2020)

Figure 115 presents the Net Transfer Capacity for import and export and the commercial exchanges between France and the CWE countries. The exchanges on these borders corresponds to most of the variability of the exchanges, which can be explained with the flow-based calculations, that optimizes the transfer capacity. The commercial exchanges exceed the NTC for import in winter, and the NTC for export in summer. The exceedance is higher than the TRM. It means that a share of the electricity sold between France and the CWE countries is transported through other borders. These exceedances should then be reflected in the exchanges between France and Swiss and between France and Italy.

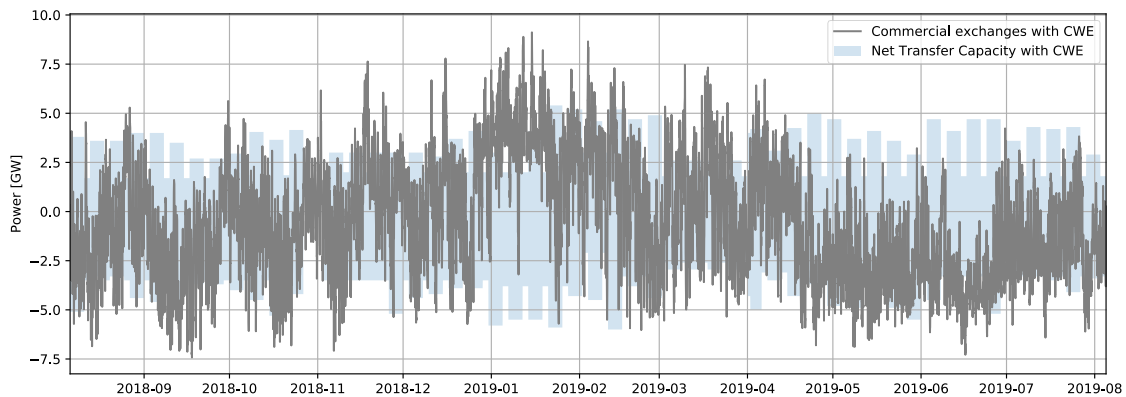


Figure 115: Net Transfer Capacity for import and export and electricity exchanges between France and CWE countries between August 2018 and August 2019, data:(RTE 2020)

Figure 116 presents the Net Transfer Capacity for import and export and the commercial exchanges between France and Swiss. The variations of the level of exchanges between France and Swiss are quick and over a large range (most of the time between the NTC for import and for export). However, the Commercial exchanges between France and CWE countries can limit the range of variation of the exchanges with Swiss.

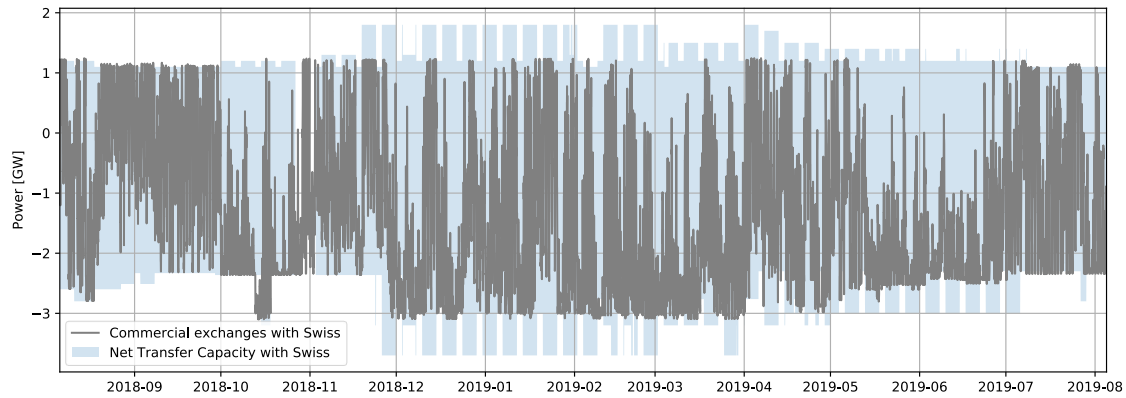


Figure 116: Net Transfer Capacity for import and export and electricity exchanges between France and Swiss between August 2018 and August 2019, data:(RTE 2020)

Figure 117, Figure 118 and Figure 119 present the Net Transfer Capacity for import and export and the commercial exchanges between France and Spain, England and Italy respectively. For each of the three time series, export at the NTC level seems to be the default state and the export is decreased or electricity is imported when the residual consumption is higher in France. The NTC for imports can be limited during weekend, when the electricity demand is lower, especially in Summer or during days with a large photovoltaic or wind electricity production. This can be notices in the time-series concerning Italy (Figure 119). Symmetrical NTC variations between imports and exports are probably caused by an unavailability of the interconnection.

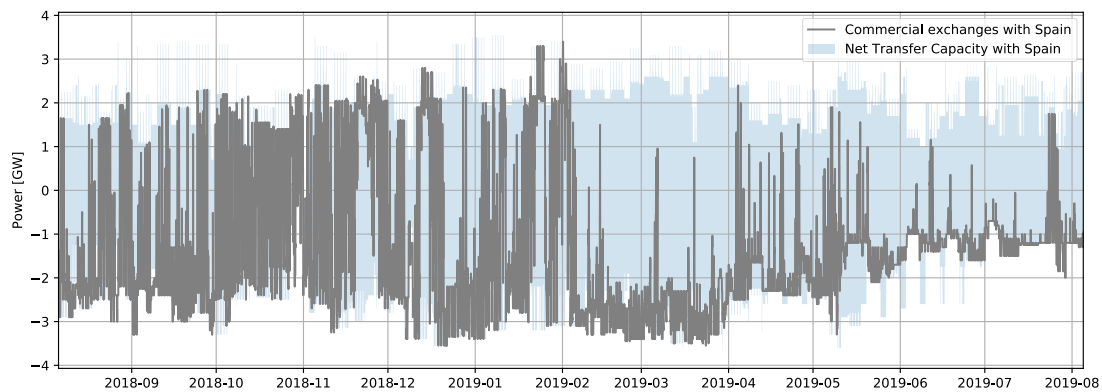


Figure 117: Net Transfer Capacity for import and export and electricity exchanges between France and Spain between August 2018 and August 2019, data:(RTE 2020)

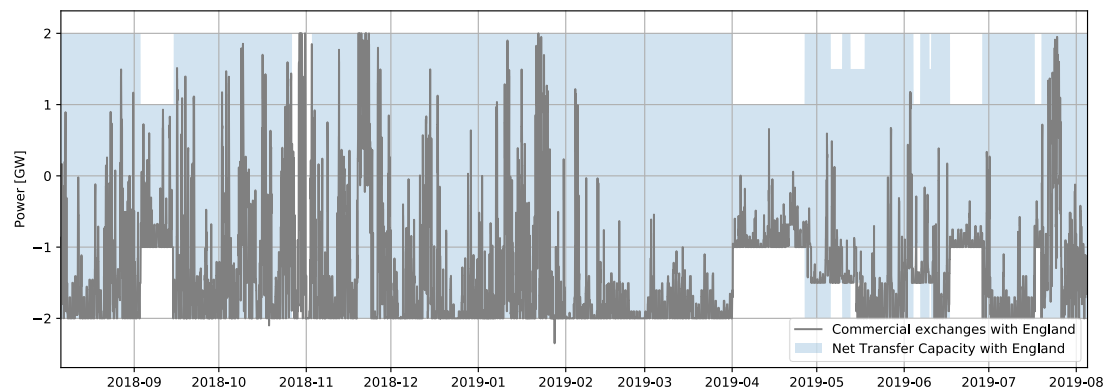


Figure 118: Net Transfer Capacity for import and export and electricity exchanges between France and England between August 2018 and August 2019, data:(RTE 2020)

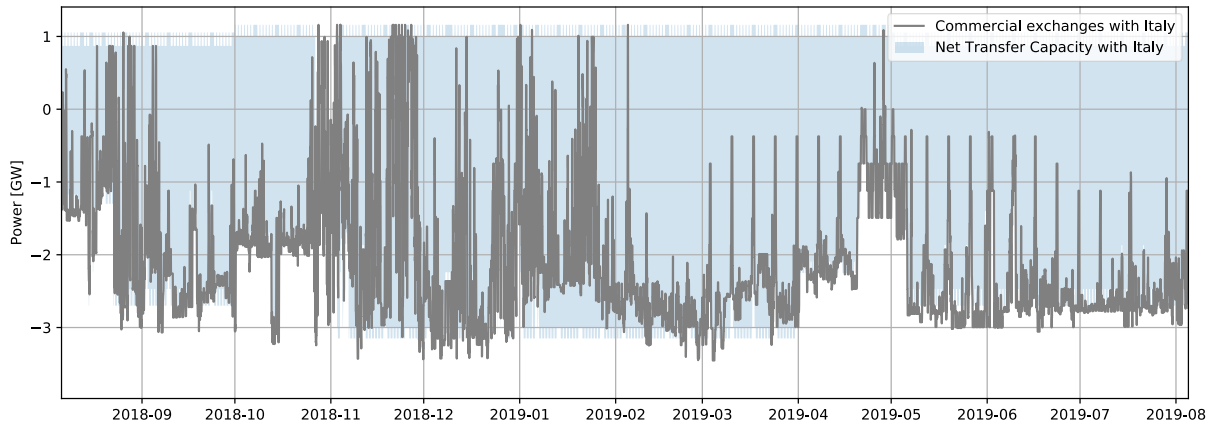


Figure 119: Net Transfer Capacity for import and export and electricity exchanges between France and Italy between August 2018 and August 2019, data:(RTE 2020)

Figure 120 presents the residual consumption which is subtracted the nuclear availability, the total net Transfer Capacity and the electricity exchanges between France and its neighboring countries for four weeks between August 2018 and August 2019. The global trend of the Residual variation which is subtracted the nuclear availability is observable in the variations of physical exchanges, especially during the night and weekends. During the week b, when the electricity demand is the higher during the observed period, the time-series seems to be distorted during the day. It is probably to fit the constraints related to the several thermal units activated, when the electricity demand is high.

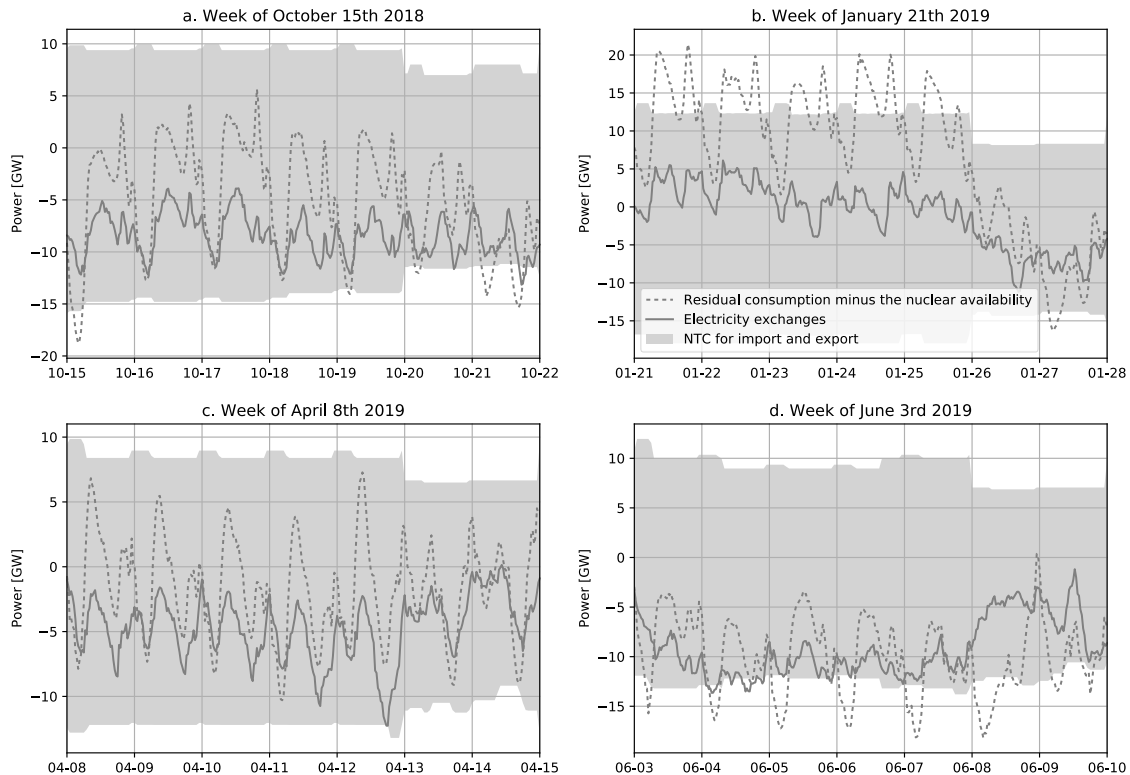


Figure 120: NTC for import and export, electricity exchanges and residual consumption minus the nuclear availability for four different weeks between august 2018 and July 2019, data:(RTE 2020; ENTSOE 2020)

### Input and parameter selection for the model

To summarize, relevant inputs and parameters for a model of the interconnections of the French electric system with the neighboring countries are:

- as boundaries: The NTC for Spain, Great-Britain, Italy and Swiss. The NTC, the availability of the fleet and the residual consumption for the CWE region.
- Ramping limits: The ramping is limited by the ramping of the fleet of the interconnected countries. As for France, these ramping limits cannot be noticed with a time step of 30 minutes.
- Variations within a day: Constraints due to the thermal powerplants and residual consumption.
- Variations for a longer time scale: The level of the physical exchanges is strongly linked to the residual consumption and to the availability of the French nuclear fleet.

## D) Electricity generation from fossil fuels

### i. Technologies and combustibles

Several electricity generation technologies are supplied with fossil fuel. These technologies are differentiated from each other by their efficiency and their combustible. The different combustible can be summarized in three main categories: natural gas, oil and coal. However, these three categories group several fuels with different prices and emission factors. In addition to the distinction according to the combustible, four main technologies are used to generate electricity from fossil fuels:

- The combustion turbine, called open cycle gas turbine (OCGT) in the case of gas, is the simplest technology fueled with gas or oil. The gas or the oil are mixed with water, pressurized and led to a turbine where the mix will be burn. The startup time of this type of units is quick (less than 30 minutes) but their efficiency is low (around 35-40%). A solution to improve the efficiency of these turbine is to use the heat from the exhaust gas, that is completely unused in these plants.
- In the combined cycle plants, called CCGT in the case of gas turbines, the combustion turbine is coupled with a secondary turbine. The heat from the exhaust gas of the combustion turbine is used to boil water and the steam turbine is set in motion with the steam to produce electricity. Gas and oil can directly be used in these plants. Coal can also be used in plants integrating a gasification. These plants are more expensive to install and need a few hours to start electricity production but their efficiency is around 55%.
- In the combined heat and power (CHP) units, the heat from exhaust gas can also directly be used for another purpose (heating network, greenhouses heating, ...). The combustible of these plants can be gas or oil but also biomass. As discussed in section 21 this technology is in some countries such as France not driven by the electricity demand but rather by heat demand. This technology is then considered non-dispatchable and these units will consequently not be discussed in this part.
- In the coal-fired plants coal is burned to heat up water. A turbine is set in motion by the produced steam and generates electricity. This is the most used process to generate electricity from coal. Due to the emission factor of coal and the low efficiency of the process, this is the most polluting electricity generation technology. The coal-fired plant efficiency can vary between 30 and 50%.

The thermal units have to be located near to a water source as their systems need to be cooled. The thermal discharge into water during summer can be limited for some locations causing unplanned unavailability of the powerplant. Other reasons for unplanned unavailability are breakdown or local unavailability of the network. Unavailability can also be planned for maintenance work or in case of a lower electricity consumption forecast. In countries where the difference of electricity consumption

between summer and winter is important and where the variable cost of such plants is higher than the base generation units, a part of the fossil generation fleet can be cocooned in summer in order to spare the fixed costs of the plants.

Fossil plants are highly flexible (see Table 1). In contrast to the nuclear plants the complete fleet can be controlled in load following mode and the dynamics of the different plants are mostly due to their comparative fixed and variable costs. The fixed costs are mainly related to the technology and are considered constant for a technology and a fuel type. The variable cost of fossil units is related to:

- the efficiency of the plant (dependent on the technology);
- the market price of the combustible (dependent on the combustible and time-varying);
- the price of the GHG emission certificate (dependent on the emission factor of the combustible and time-varying);
- the exchange rate between the euro and the dollar (only for coal and dependent on the country): as coal can be bought in dollar and electricity is sold in Europe in euros, the exchange rate can also influence the variable cost of coal plants in European countries importing coal (RTE 2019a).

CCGT and coal-fired powerplants have high start-up times and lower ramping limitations in comparison to combustion turbines but are more profitable. This explains why in France CCGT and coal-fired powerplants are generally used as semi-base technologies and combustion turbines as peak technologies. The fossil semi-base technologies will be discussed in the following section and the peak units in the next one.

## ii. Semi-base units

### **Current and future (2035) French fleet**

CCGT and coal-fired plants constitute nowadays the semi-base part of the French electrical system and are necessary in order to comply with the energy supply security criterion. In this section, the technology registered as “Fioul – Autres” in the data from RTE will also be presented as these units also seem behave as semi-base.

In 2018 CCGT units represented 6,2 GW which corresponds to 4,8% of the French fleet (RTE 2019b). 18 TWh of electricity were produced from this technology representing 3,3% of the annual production. During the last years gas prices decreased occurring a decrease of the variable cost of these units. Additionally, the increase of the price for GHG emission certificate and the remuneration for the availability of the capacity since 2017 in France are making CCGT enough profitable (its variable cost is the lower among the fossil plants) to ensure its viability in long term. This explains why the current CCGT fleet should be maintained in the coming years and a new CCGT unit of 0,5 GW should be installed in Landivisiau by the end of 2021 (RTE 2019b).

In 2018 coal-fired powerplants were still producing electricity in France representing 2,93 GW which corresponds to 2,3% of the total installed capacity. 5,8 TWh were produced with coal fired plants which is 1,1% of the annual production (RTE 2018). In 2017 France planned to close the coal-fired powerplants between 2020 and 2022 (Ministère de la transition écologique et solidaire 2019). However, there is still uncertainty on the future of the power plant of Cordemais: due to the delay in the start-up of the Flamanville nuclear unit and in the new interconnections availability, so that the electricity supply security criterion may not be fulfilled without this coal-fired plant. The powerplant

of Cordemais is the largest coal-fired unit still producing electricity in France and combines two units representing each a capacity of 580 MW. Two alternative projects to the complete closure of the powerplant have been proposed. The first proposal would be to maintain the powerplant with a limited number of generation hours per year. According to the “energy and climate” law from November 2019, the units emitting more than 0,55 tCO<sub>2</sub>eq/MWh will be limited in the annual amount of energy that can be generated. The limitation on coal units would be set to 0,7 ktCO<sub>2</sub>eq/year for every installed MW corresponding to 700h of electricity generation per year (this value is not definitive). The other proposal would be to convert this unit to biomass with a reduction of its nominal capacity within the context of the Ecocombust project.

Figure 121 and Figure 122 present the planned and unplanned unavailability for respectively the CCGT and the coal-fired units in France between August 2018 and August 2019. For the two fleet the planned unavailability is mainly explained by maintenance work and cocooning and are primarily scheduled during summer when the electricity consumption is lower.

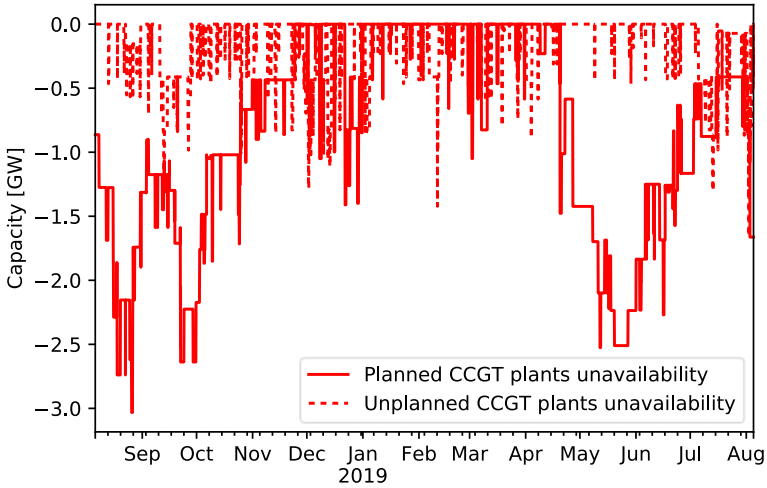


Figure 121: Planned and unplanned unavailability of the French CCGT plants between August 2018 and August 2019, data: (ENTSOE 2020)

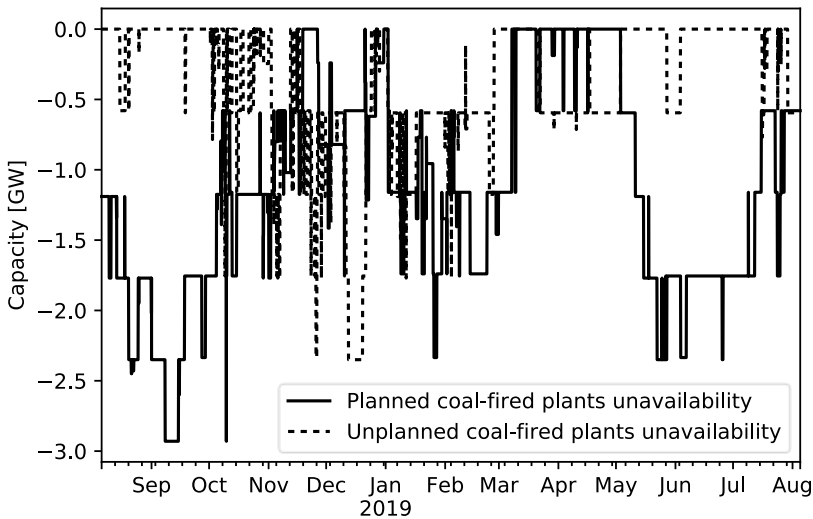


Figure 122: Planned and unplanned unavailability of the French coal-fired plants between August 2018 and August 2019, data: (ENTSOE 2020)

**Seasonal, weekly and daily flexibility in France**

Figure 123 presents the evolution of the electricity generation from French CCGT and coal-fired units, the evolution of the variable cost of these two technologies and the evolution of the price of the GHG emission certification in 2018 and 2019. The electricity generated by coal-fired plants has decreased in 2019 (1,6 TWh). This trend can be explained with the large decrease of the gas price and to the increase of the GHG emission taxes (around 5 €/ton in June 2017 to 29,8 €/ton in July 2019). Indeed coal-fired powerplants having the highest GHG emission factor in the French fleet (three times higher than CCGT) (RTE 2019a). The coal-fired powerplants are mainly used during the colder months of the year but can also produce electricity during summer consumption peak (in case of heatwave for example) or to compensate the unavailability of nuclear plant. The CCGT units currently profit from the decrease of the coal-fired powerplants electricity generation. The low fossil electricity generation in 2018 in comparison to 2019 is explained by the high hydroelectric generation in 2018.

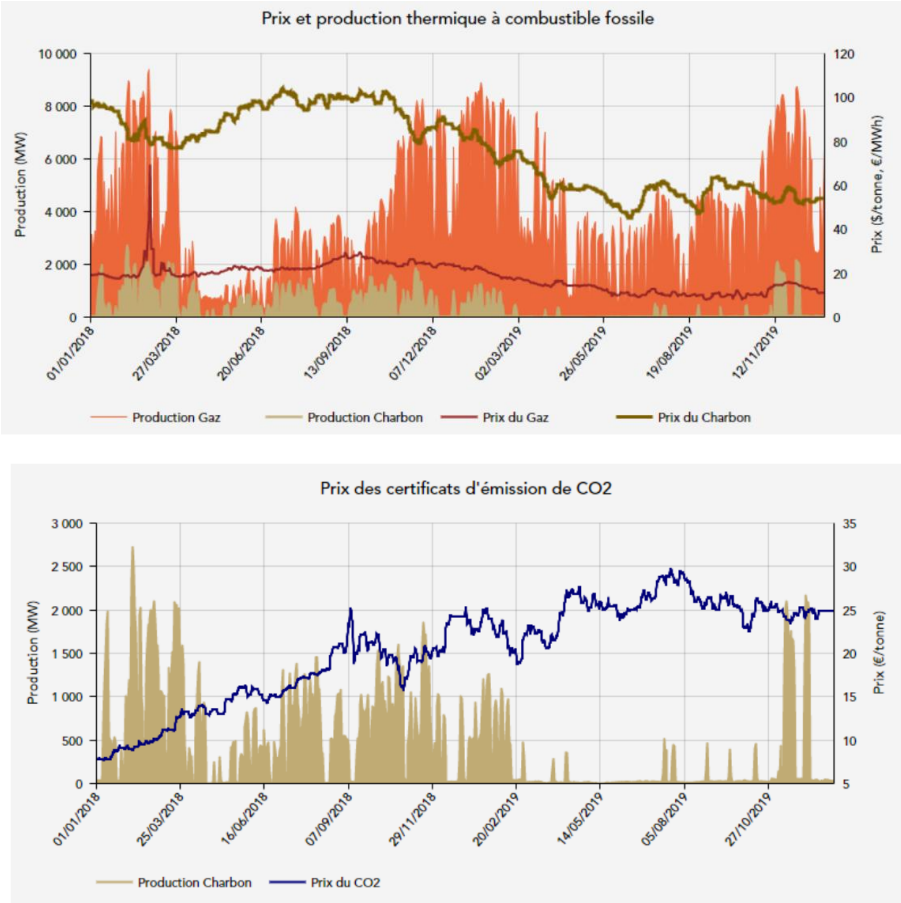


Figure 123: Evolution of the electricity generation from French CCGT and coal-fired units, evolution of the variable cost of these two technologies and evolution of the price of the GHG emission certification in 2018 and 2019 (RTE 2019a)

Figure 124 presents the French CCGT units generation and availability between August 2018 and August 2019. The CCGT fleet is rarely saturated: a part of the generation capacity seems to be kept as a reserve. They also always produce a minimum level of electricity.



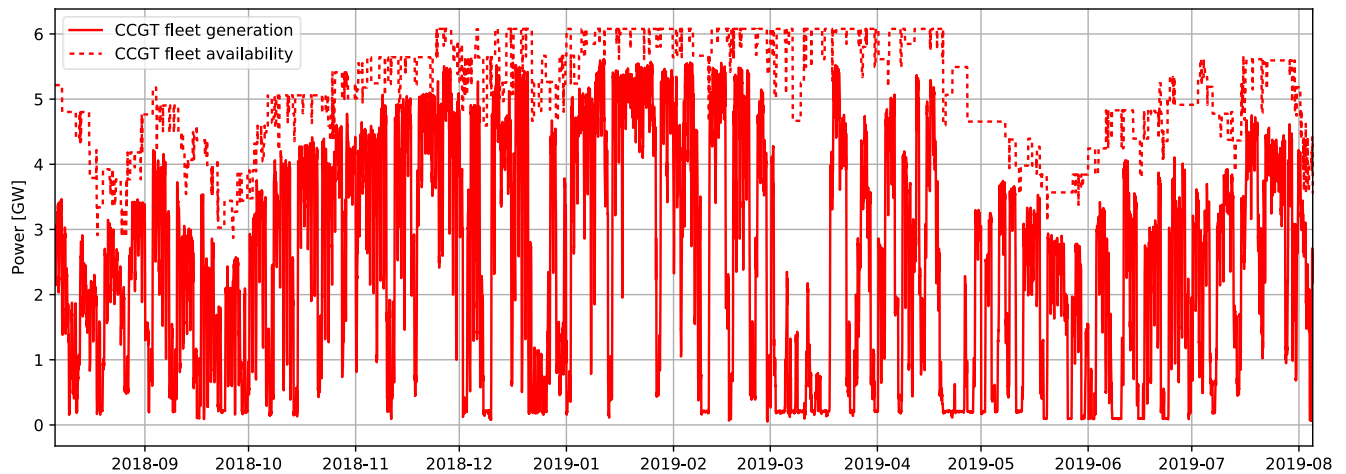


Figure 124: Available capacity and generation of the CCGT units in France between August 2018 and August 2019, data:(RTE 2020; ENTSOE 2020)

Figure 125 presents electricity generation and the available capacity of the coal-fired French powerplants between August 2018 and 2019. As there are only 5 coal-fired powerplants with similar nominal power (around 0,6 GW) in the French fleet during this period, the number of activated plants for every day can be easily observed with these time-series. Unlike CCGT plants no reserve capacity or minimum power generation can be identified. It can probably be explained by the shorter start-up time of the coal-fired powerplants. However, during the days for which only one coal-fired powerplant are activated, a minimum generated power can be observed probably due to the high start-up cost of this technology.

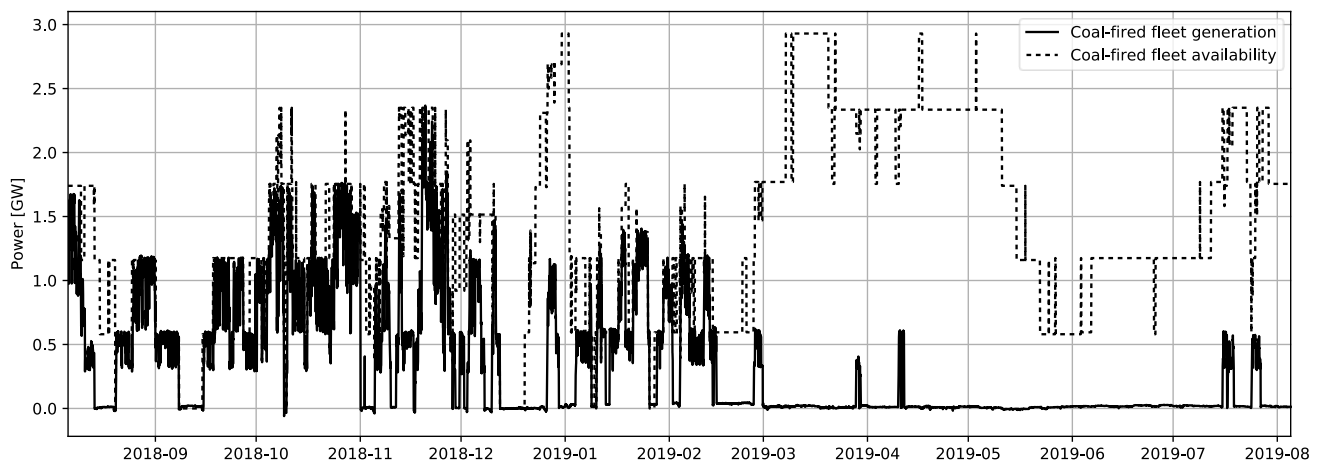


Figure 125: Available capacity and generation of the coal-fired units in France between August 2018 and August 2019, data:(RTE 2020; ENTSOE 2020)

Figure 126 presents the French oil-fired ( called “Fioul – Autres”) units generation between August 2018 and August 2019. This generation unit is producing electricity most of the year with a maximal power of around 0,4 GW. These units seem to have a minimum power output to generate when the unit is committed.

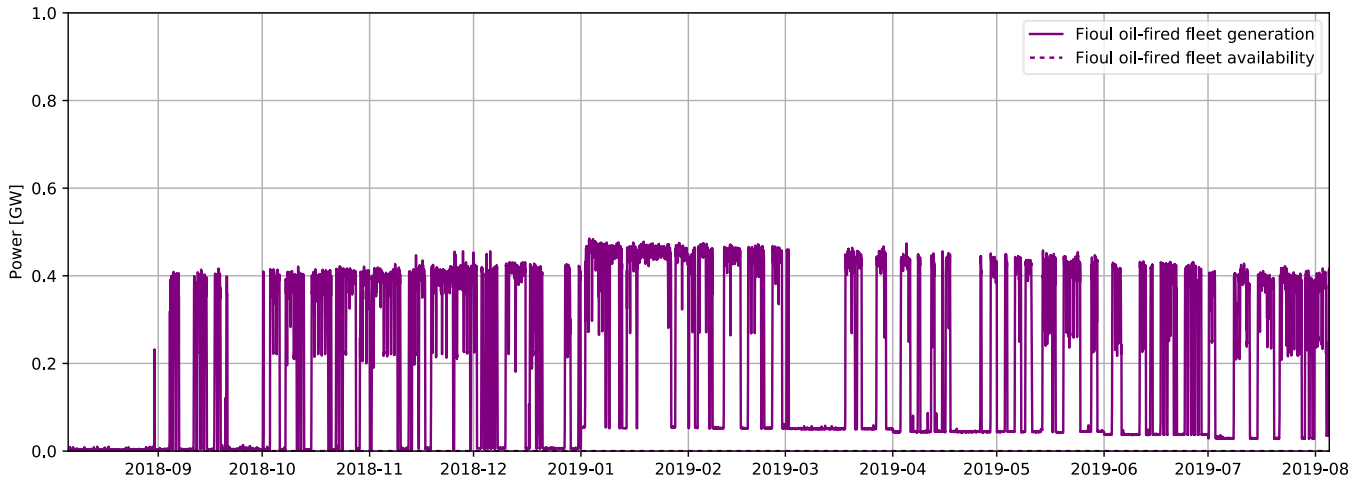


Figure 126: Available capacity and generation of the oil-fired units in France between August 2018 and August 2019, data:(RTE 2020; ENTSOE 2020)

### Input and parameter selection for the model

Figure 127 presents the generation and the availability of the French CCGT units for four different weeks between August 2018 and August 2019. During the week of October 15<sup>th</sup> the reserve capacity of CCGT units seems to be around 0,5 GW while the reserve capacity is around 1 GW during the other three weeks. It is not surprising to see a lower reserve during the weeks with high electricity consumption in order to be able to provide the demand. During the four observed weeks the power supplied by the CCGT is continuously adjusted on a wide range of power in order to follow the residual electricity consumption, especially during week-ends when the electricity demand is lower.

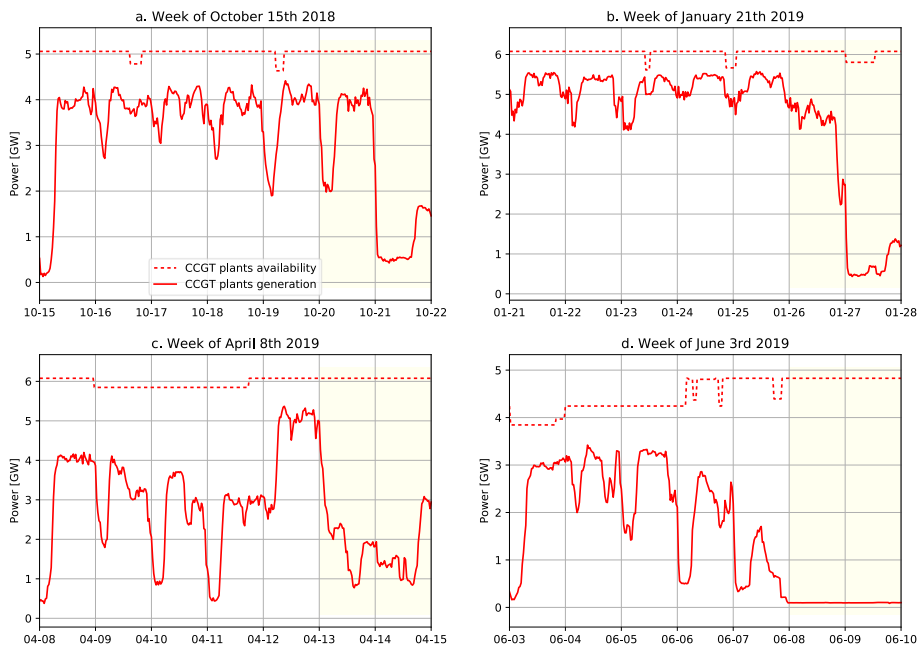


Figure 127: CCGT units generation and availability for four different weeks between august 2018 and July 2019, data:(RTE 2020; ENTSOE 2020)

Figure 128 presents the generation and the availability of the French coal-fired powerplants for four different weeks between August 2018 and August 2019. During the weeks of October 15 and of

January 21 the maximum number of available powerplants is committed every day. However, during the week of April 8, the units are activated only two days out of fourteen despite the availability of four units. During the week of June 3 no coal-fired powerplants are committed. These differences are due to the economical context explained previously. Unlike the CCGT, the coal-fired units don't adjust as much their output power, probably because of economical constraints. When more than one coal-fired powerplant is committed, the power variation is restricted in a range similar to the nominal power of one powerplant (around 0,6 GW).

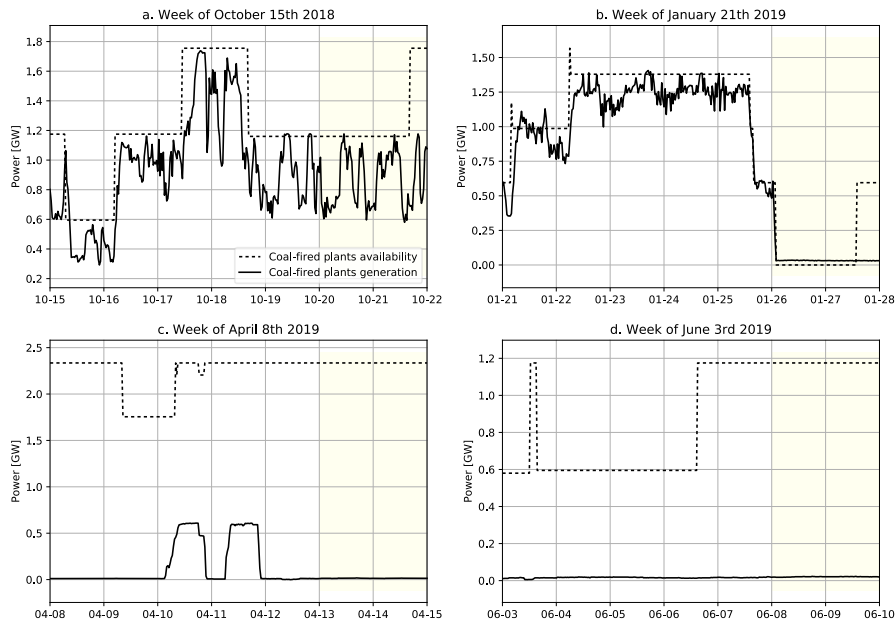


Figure 128: Coal-fired powerplants units generation and availability for four different weeks between august 2018 and July 2019, data:(RTE 2020; ENTSOE 2020)

Figure 129 presents the generation and the availability of the French oil-fired registered under “Fioul-Autres” in the RTE data powerplants for four different weeks between August 2018 and August 2019. The oil-fired units are activated every day except Sunday during the weeks of the October 15 and of the January 21. These units are less activated during the weeks of the of April 8 and of the June 3 when the residual consumption is lower. Similar observations to those done for coal-fired units can be made about the flexibility of this unit.

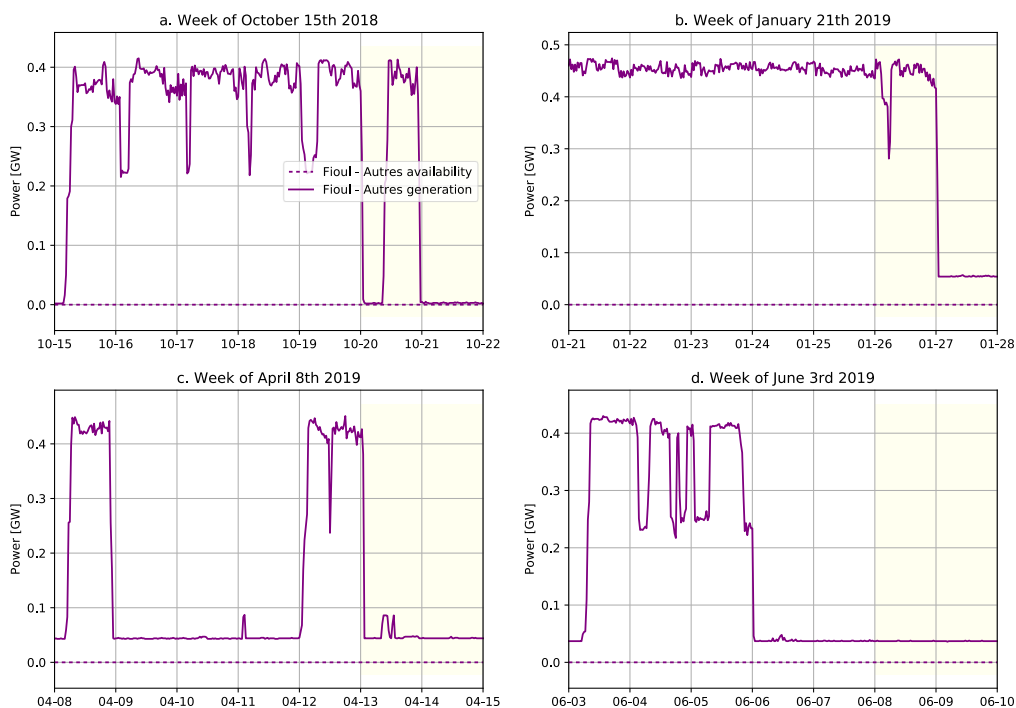


Figure 129: Oil-fired powerplants units generation and availability for four different weeks between august 2018 and July 2019, data:(RTE 2020; ENTSOE 2020)

To summarize, relevant inputs and parameters for a model of the French semi-base units fleet are:

- as boundaries : the installed capacity of these units and their availability. CCGT units also presents a minimum power output value and a reserve. Coal-fired and oil-fired units have a minimum output power value only when one unit is committed.
- Ramping limits: CCGT, coal-fired and oil-fired plants don't have ramping limits that could be visible at a half-hour time step. The daily and intra-day variations of the coal-fired and oil-fired powerplants power generation are only constrained by their high fixed costs.
- Variations within a day: The CCGT units are reactive and can adjust their generation level during the day. However, their generation level is never zero certainly in order to compensate their start-up time. The power variation of coal-fired plants is limited in an interval corresponding the nominal power of one plant.
- Variations for a longer time scale: As the start-up cost and time of the coal-fired units are significant these units are started for more than a day.

### iii. Peak units

OCGT and oil-fired combustion turbines constitute the fossil part of the peak technologies of the French electrical system. In 2018 the installed OCGT units capacity represented 0,7 GW corresponding to 0,5% of the French fleet. 0,1 TWh (0,02% of the annual production) of electricity were produced from this technology. The same year the installed oil-fired combustion turbines represented 1,4 GW or 1,1% of the French fleet. 0,3 TWh (0,1% of the annual production) of electricity were produced from this technology. The last big fuel unit closed in march 2018 (RTE 2018).

With the increase of the GHG emission certificate price combustion turbines are less activated in France and hydroelectric electricity or import are preferred as peak technologies. Figure 130 and Figure

131 present the available capacity and the generation respectively of the OCGT and oil-fired combustion turbines in France between August 2018 and August 2019. Combustion turbines produce mostly electricity in winter when the other peak technologies are saturated. There are highly reactive and generally activated just for a few hours.

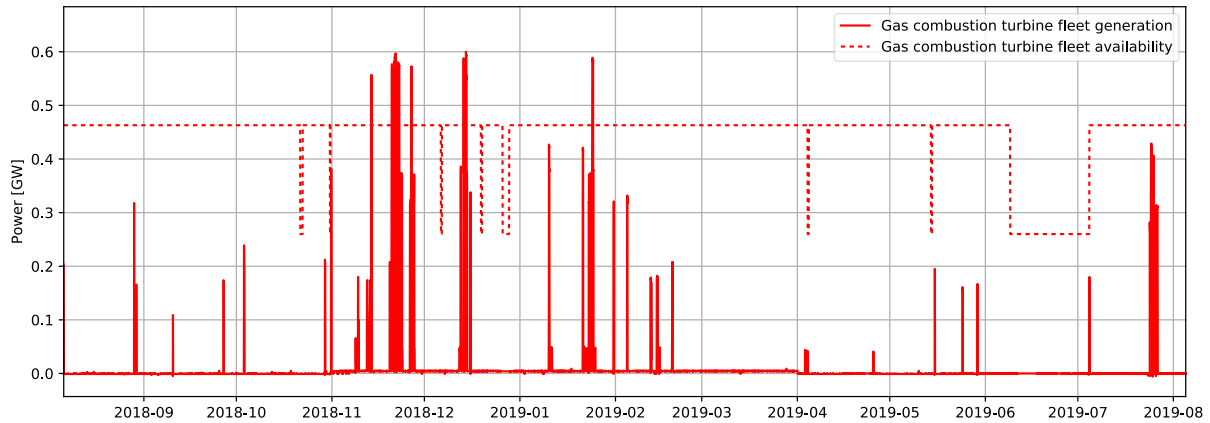


Figure 130: Available capacity and generation of the OCGT units in France between August 2018 and August 2019, data:(RTE 2020; ENTSOE 2020)

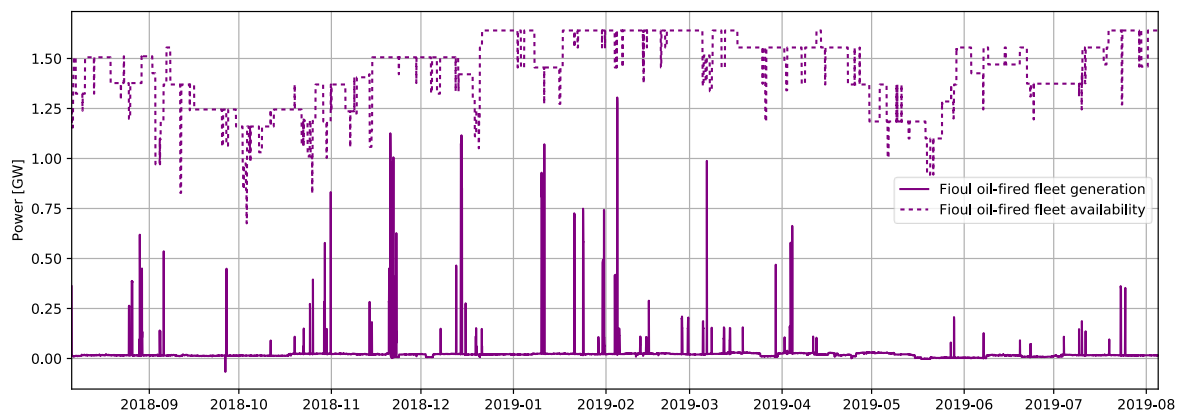


Figure 131: Available capacity and generation of the oil-fired combustion turbines in France between August 2018 and August 2019, data:(RTE 2020; ENTSOE 2020)

To summarize, relevant inputs and parameters for a model of the French combustion turbines are:

- as boundaries : the availability of the units
- Ramping limits: these plants are highly reactive and are used as peak units. The ramp of these plants are consequently not limited.
- Variations within a day: These units are activated for a few hours.
- Variations for a longer time scale: These units are activated mostly in winter.

## List of publications

- Marianne Biéron, Jérôme Le Dreau, Benjamin Haas , Assessment of the Marginal Technologies Reacting to Demand Response Events: A French Case-Study. Energy 275, 127415, 2023
- Marianne Biéron, Jérôme Le Dréau, Benjamin Haas. Control of a state-wide pool of hybrid heating systems to decrease the GHG emissions of heating, BS2021 conference, September 2021, Bruges, Belgium.
- Marianne Biéron, Jérôme Le Dréau, Benjamin Haas. Peut-on éviter des émissions de CO2 en pilotant l'appoint gaz de pompes à chaleur hybrides ?, Conférence IBPSA France, November 2020, Reims, France.